LEAF ANATOMICAL TRAIT VARIATION AND PLASTITICY IN CULTIVATED AND WILD SUNFLOWER (*HELIANTHUS ANNUUS* L.*)*

by

ASHLEY MARIE EARLEY

(Under the Direction of John M. Burke)

ABSTRACT

Drought is major agricultural stress that reduces crop productivity and is predicted to increase in frequency and severity due to climate change. As such, we need crops that can withstand drought to feed a growing population. In this dissertation, I explore variation in leaf anatomy across cultivated and wild sunflower (*Helianthus annuus* L.). Stomatal and vein traits are important for plant-water relations, influencing both gas exchange and water transport. I quantified trait variation across the cultivated sunflower gene pool and associated it with genomic regions, finding associations for numerous traits but limited colocalization between traits despite pervasive trait-trait correlations. However, I was able to map major axes containing traits relating to gas exchange and leaf construction. Next, I used a subset of lines to investigate trait variation and plasticity under multiple levels of drought stress. I again found substantial variation in traits and that trait plasticity increased with increasing drought stress, along with the same major axes of trait variation. This suggests the existence of persistent functional relationships among traits. I also found that four key leaf traits (leaf mass per area, vein length per area, stomatal density, and stomatal size) were strongly predictive of plant performance.

Finally, I analyzed leaf trait variation and its relationship with environmental variables and performance in wild sunflower in a common garden setting. Once again, I found substantial variation across traits, with significant population effects indicating the existence of genetic variation for most of these traits across the wild sunflower range. Growth/biomass-related traits showed much stronger environmental associations compared to finer-scale leaf traits. I also found that many of the same traits that exhibited predictive power in cultivated sunflower could be used to predict plant performance in wild sunflower. Taken together, my results show that there is variation in leaf anatomical traits that are important for plant-water relations in both cultivated and wild sunflower, and that these traits exhibit substantial plasticity under drought. This sort of information on the extent and nature of trait variation and covariation has the potential to influence breeding strategies aimed at modifying leaf traits in response to looming environmental challenges.

INDEX WORDS: *Helianthus annuus*, sunflower, leaf anatomy, stomata, veins, GWA, drought, cultivated, wilds

# LEAF ANATOMICAL TRAIT VARIATION AND PLASTITICY IN CULTIVATED AND WILD SUNFLOWER (*HELIANTHUS ANNUUS* L.*)*

by

ASHLEY MARIE EARLEY

AB, Washington University in Saint Louis, 2015

A Dissertation Submitted to the Graduate Faculty of The University of Georgia in Partial Fulfillment of the Requirements for the Degree

DOCTOR OF PHILOSPOHHY

ATHENS, GEORGIA

2022

# LEAF ANATOMICAL TRAIT VARIATION AND PLASTITICY IN CULTIVATED AND WILD SUNFLOWER (*HELIANTHUS ANNUUS L.)*

by

ASHLEY EARLEY

| | |
|---|---|
| Major Professor: | John M. Burke |
| Committee: | Lisa Donovan |
| | Andrea Sweigart |
| | Katrien Devos |
| | Marc van Iersel |

Electronic Version Approved:

Ron Walcott
Vice Provost for Graduate Education and Dean of the Graduate School
The University of Georgia
December 2022

# DEDICATION

To my dad - I wish you were here to see me finish my PhD. You would be so proud and would be telling everyone you met that you had a daughter who was a doctor!

To my mom - you are my best friend and I really appreciate you always being there to support and love me! Our Thursday night phone calls and my visits to Rock Hill helped keep me going throughout this PhD.

Lastly, to my kitties, Abby and Ziva, who were great company as I wrote this dissertation and great nap companions in between writing.

# ACKNOWLEDGEMENTS

I would like to thank my advisor, John Burke, without your support and guidance I would not have been able to finish this degree especially the final push to get it submitted! Thank you for supporting me through all the challenges in grad school including surgeries, a pandemic, and more! Thank you to all my committee members, Lisa Donovan, Andrea Sweigart, Katrien Devos, and Marc van Iersel for all your guidance and feedback over the last few years.

Huge thanks to the entire Sunflower Mafia who have helped with brainstorming, feedback, greenhouse work, images analysis and so much more! - Andries Temme, Vivian Tran, Kelly Bettinger, Emily Dittmar, Kristen Nolting, Max Barnhart, Summerlin Courchaine, Niki Padgett, Brian Park, Garrett Janzen, Rishi Masalia, Nichole Reisinger, Nadia Krigger and probably many others throughout the years that I am forgetting to mention. I cannot express how grateful I am for all your help root washing and harvests, and manuscript and presentation feedback!

Particular thanks to Summerlin, Niki, Nicole, and Nadia for endless hours of counting and measuring stomata and to Max, Niki, and Summerlin who helped weigh heavy pots full of sand in the hot greenhouse for my second chapter. Without you guys I would never have finished my first chapter or gotten the drought data for my second. Thank you also to Sasha for stomata measurements for the second and third chapters!

Thank you to all the greenhouse staff including Kevin Tanner, Mike Boyd, Greg Cousins for pot filling, keeping pests off my plants and watering them when needed (except during the drought experiment!). Thank you also to everyone in the PBIO office for constantly being there to answer questions, fill out paperwork, and generally make sure all of us grad students are on track! Thank you to the sources of funding for this dissertation including NSF and the International Consortium on Sunflower Genomics.

I am extremely grateful to my cohort Vivian Tran, Callie Oldfield, Patrick Smallwood, and Kyle Swentowsky for being on this journey alongside me! It was nice to have others to talk to who were at the same stage! Also, thanks to everyone in PBIO who has been there to study, write, and hang out together and generally support me throughout grad school!

Last but definitely not least, to my PSC family for being a community of belonging. I will never forget how welcome you all always made me feel from my first week at UGA!

TABLE OF CONTENTS

Page

LIST OF TABLES

Page

LIST OF FIGURES

Page

LIST OF METHODS

# CHAPTER 1

# INTRODUCTION AND LITERATURE REVIEW

Climate change is expected to worsen in the coming years, resulting in increased frequency and severity of droughts (Foley *et al.*, 2011; Munns, 2011; IPCC, 2014). Drought is a major challenge in agriculture as it limits plant growth and yield worldwide (NOAA; Munns, 2011; IPCC, 2014). By 2050 the world's population is expected to increase from the current nearly 7.8 billion to 9.8 billion (United Nations, 2017). As these challenges mount, the human population will continue to increase in size, thereby increasing food demand and threatening food security. Currently nearly 10% of the world population lives in areas with severe to critical water stress, which includes areas affected by drought (FAO, 2021). In addition, as of 2022, a quarter of the agricultural lands in the United States are experiencing drought (NOAA and NIDIS 2022). Therefore, to continue to feed the world, we need to develop crop plants that are better able to withstand environmental challenges such as drought while continuing to produce a high yield. This effort will require an increased understanding of the genetic basis of traits relevant to drought as well as trait responses to such challenges.

Leaf anatomical traits such as stomatal and vein are central to plant-water relations. Leaf veins distribute water from the petiole throughout the leaf. In the intercellular space, water then moves through the mesophyll to stomata – the ultimate site

of transpiration. Thus, stomata control the rate of transpiration in the leaf while veins distribute water (Sack and Scoffoni, 2013). The relationship between stomatal size/density and vein density (estimated as vein length per area; VLA) is important for optimization of water transport, transpiration, and carbon acquisition (Fiorin *et al.*, 2016; Bertolino *et al.*, 2019). In particular, a shorter distance from the veins to the stomata is thought to improve gas exchange and photosynthetic performance. This distance is affected by traits such as stomatal density, VLA, leaf thickness, and cell shape (Brodribb *et al.*, 2007; de Boer *et al.*, 2012). Stomatal conductance ($g_s$), a measure of the conductance of water vapor through the stomata, is determined by the physiological control of stomatal opening and closing as well as the size and distribution of stomata (Faralli *et al.*, 2019). Similarly, vein length per area (VLA) affects leaf hydraulic conductance ($K_{leaf}$), or the ratio of water flow rate to the water potential gradient across the leaf, and thus greatly affects how long stomata can remain open without drying out the leaf (Sack and Scoffoni, 2012). Plant performance under drought conditions is known to be influenced by both stomatal and vein traits (Scoffoni *et al.*, 2011; Lei *et al.*, 2018; Buckley, 2019); thus, these traits are widely regarded as being important to plant adaptation to drought stress (Sack and Scoffoni, 2013; Bertolino *et al.*, 2019).

While leaf mass per area (LMA) is recognized as a key trait for determining plant ecological strategies, finer-scale aspects of leaf anatomy are known to play a key role in leaf hydraulics and plant photosynthetic water use efficiency (WUE; i.e., the ratio of water used in photosynthesis to water lost by transpiration; (Franks *et al.*, 2015). Investigating the variation present in both finer-scale aspects of leaves as well as whole

leaf traits promises to broaden our understanding of the evolution of correlated suites of leaf traits. In particular, vein and stomatal traits tend to be highly correlated with one another both within (Carins Murphy *et al.*, 2014) and across (Zhang *et al.*, 2012) species. For instance, vein density and stomatal density are known to be positively correlated (Sack and Scoffoni, 2013), while stomatal density and size are negatively correlated (Shahinnia *et al.*, 2016; Doheny-Adams *et al.*, 2012). However, most studies looking at intraspecific variation in leaf anatomy have used relatively small sample sizes or focused on stomata to the exclusion of vein traits (e.g., Khan *et al.*, 2003; Ries *et al.*, 2012; Shi *et al.*, 2021; Haworth *et al.*, 2021). The general dearth of studies that explicitly examine the variability and genetic basis of stomatal and vein traits, particularly together, is likely due to the time constraints associated with large scale phenotyping. Across species, stomatal size varies widely, from ca. 10 to 80 µm, and stomatal density can vary from ca. 5 to 1000 stomata/mm$^2$ (Shahinnia *et al.*, 2016). Plant species from increasingly dry habitats tend to have smaller and more dense stomata (Xie *et al.*, 2022; Dunlap and Stettler, 2001). A higher stomatal density in dry environments allows for higher photosynthetic capacity and cooler leaves than a lower density in the same environment (Carlson *et al.*, 2016).

Researchers have also found a connection between these traits and environmental variables within species, particularly for stomatal traits. Interestingly, these patterns have been largely concordant with the cross-species observations. For example, across 19 *Protea repens* populations, stomatal density was found to correlate negatively with summer rainfall levels when grown in a common garden (Carlson *et al.*, 2016; but see

Wu *et al.*, 2010)). In addition to differences seen between populations, these traits also exhibit plastic responses when exposed to varying levels of watering. Plants often shift towards increased vein and stomata densities and smaller stomata under drought vs well-watered conditions (Sack and Scoffoni, 2013; Sun *et al.*, 2014). These changes under drought conditions are thought to improve gas exchange by decreasing the distance from veins to stomata, improving photosynthetic efficiency while limiting water loss (Brodribb *et al.*, 2007; Bertolino *et al.*, 2019). Smaller stomata also have faster ion fluxes and can thus close more quickly than larger stomata. This results in faster changes in stomatal conductance (Bertolino *et al.*, 2019; Drake *et al.*, 2013) which allows plants to reduce transpiration in response to dry conditions while still allowing them to rapidly re-open when water is available (Sack and Scoffoni, 2013).

The severity of drought stress is also known to affect the magnitude of leaf trait plasticity with studies that investigate multiple drought levels generally finding increased trait plasticity in response to more severe stress. As drought severity increases, stomatal size in newly developed leaves tends to decrease, while stomatal and vein densities increase (Lei *et al.*, 2018; Wang *et al.*, 2018; Stojnić *et al.*, 2015; Bresta *et al.*, 2018). For instance, there was an increase in stomatal and vein density with worsening drought in cotton (Lei *et al.*, 2018). Similarly, more severe drought resulted in increased stomatal and vein density and decreased stomatal size in barley (Bresta *et al.*, 2018). In addition to water availability, leaf anatomical traits also interact strongly with temperature. Transpiration of water from the stomata allows for evaporative cooling while stomatal closure helps to maintain water but, at the same time, restricts the ability of the plants to

cool (Buckley, 2019). As temperatures increase, more water needs to be released to cool the plant, but the amount of water vapor needed to saturate the air increases exponentially with increasing temperature. This can result in more water loss from the plant (Moore *et al.*, 2021). Relative humidity, the ratio of the water vapor pressure in the air compared to the water vapor pressure at saturation, is predicted to decrease as global temperatures are predicted to increase in the coming years due to climate change (Driesen *et al.*, 2020)**.** Given the importance of these traits, leaf trait plasticity, along with the possibility of breeding plants with novel leaf trait combinations, both have a potential role to play in mitigating the increasingly deleterious effects of drought. However, there are few studies that explicitly explore the role of both stomata and veins as it relates to trait variation, plasticity, and overall plant performance. Here, I investigate these and related issues in cultivated sunflower (*Helianthus annuus* L.) and its wild progenitor (also *H. annuus*).

Cultivated sunflower is one of the world's most important oilseed crops (FAO, 2018) and also an important source of confectionery seeds and ornamental flowers. The available evidence points to a single origin of domestication in east-central North America from the wild, common sunflower ca. 4,000 years ago (Blackman *et al.*, 2011; Rieseberg and Seiler, 1990; Harter *et al.*, 2004; Wills and Burke, 2006). This single origin of domestication resulted in a population bottleneck that reduced genetic diversity in the crop gene pool to ca. two-thirds the level in its wild progenitor, and subsequent breeding efforts have further reduced genetic variation within the gene pool (Liu and Burke, 2006; Chapman *et al.*, 2008; Mandel *et al.*, 2011). This loss of genetic diversity potentially limits our ability to adapt sunflower to emerging environmental challenges

including increased temperatures and increasingly variable precipitation patterns (Godfray *et al.*, 2010). In the USA, sunflower is cultivated across a relatively broad range where it is often rainfed and therefore dependent on natural patterns of precipitation (Meyer, 1999). While sunflower is generally regarded as being drought resistant due to its ability to root deeply (Connor and Sadras, 1992), drought is frequently a major yield-limiting factor across the range of production (Lambrides and Chapman, 2001; Rauf, 2008). There is thus considerable interest in identifying traits that might contribute to improved drought tolerance in sunflower, and wild populations represent a possible source of additional genetic variation that can be leveraged to develop more tolerant crop varieties (e.g., Dempewolf *et al.*, 2017).

Excellent genetic and genomic resources are available for sunflower research. This includes a reference genome for cultivated sunflower (Badouin *et al.*, 2017) and an extensive germplasm collection maintained by the US National Plant Germplasm System (NPGS). This collection was used to assemble the so-called sunflower association mapping (SAM) population (Mandel *et al.*, 2011), which is a diversity panel containing 288 inbred lines of cultivated *Helianthus annuus* that is estimated to capture ca. 90% of the allelic diversity in the crop gene pool (Mandel *et al.*, 2013). This population has since been subjected to extensive genomic characterization which has enabled the identification of a genome-wide collection of single nucleotide polymorphisms (SNPs) from the full set of lines (Hübner *et al.*, 2019). The NPGS also provides access to seeds from wild populations of *H. annuus* collected from across much of its native range, along with detailed locale information.

Prior work on sunflower has shown substantial variability and plasticity in leaf anatomical traits (Wang *et al.*, 2020). Previous genomic analyses have, however, been largely limited to higher level traits such as leaf mass, leaf area, LMA, and leaf mass fraction (Temme *et al.*, 2020; Masalia *et al.*, 2018). The overall goal of this dissertation is to investigate patterns of phenotypic and genetic variation in leaf traits and their significance in cultivated sunflower and its wild progenitor, the common sunflower. This work focuses primarily on leaf vein and stomatal traits, along with higher-level growth and allocation traits, and involves analyses of: (1) the genetic architecture of these traits within the cultivated sunflower gene pool; (2) the response of these traits to water limitation and the degree to which observed variation can predict performance under such stress in cultivated sunflower; and (3) the range of variation of these traits across the natural range of common sunflower and its association with relevant environmental variables. The results of this work shed light on the potential role of leaf trait variation in response to water limitation in cultivated and wild sunflower.

REFERENCES

**Badouin, H., Gouzy, J., Grassa, C.J., et al.** (2017) The sunflower genome provides insights into oil metabolism, flowering and Asterid evolution. *Nature*, **546**, 148–152.

**Bertolino, L.T., Caine, R.S. and Gray, J.E.** (2019) Impact of stomatal density and morphology on water-use efficiency in a changing world. *Front. Plant Sci.*, **10**, 225.

**Blackman, B.K., Scascitelli, M., Kane, N.C., Luton, H.H., Rasmussen, D.A., Bye, R.A., Lentz, D.L. and Rieseberg, L.H.** (2011) Sunflower domestication alleles support single domestication center in eastern North America. *Proc. Natl. Acad. Sci. U. S. A.*, **108**, 14360–14365.

**Boer, H.J. de, Eppinga, M.B., Wassen, M.J. and Dekker, S.C.** (2012) A critical transition in leaf evolution facilitated the Cretaceous angiosperm revolution. *Nat. Commun.*, **3**, 1221.

**Bresta, P., Nikolopoulos, D., Stavroulaki, V., Vahamidis, P., Economou, G. and Karabourniotis, G.** (2018) How does long-term drought acclimation modify structure-function relationships? A quantitative approach to leaf phenotypic plasticity of barley. *Funct. Plant Biol.*, **45**, 1181–1194.

**Brodribb, T.J., Feild, T.S. and Jordan, G.J.** (2007) Leaf maximum photosynthetic rate and venation are linked by hydraulics. *Plant Physiol.*, **144**, 1890–1898.

**Buckley, T.N.** (2019) How do stomata respond to water status? *New Phytol.*, **224**, 21–36.

**Carins Murphy, M.R., Jordan, G.J. and Brodribb, T.J.** (2014) Acclimation to humidity modifies the link between leaf size and the density of veins and stomata. *Plant Cell Environ.*, **37**, 124–131.

**Carlson, J.E., Adams, C.A. and Holsinger, K.E.** (2016) Intraspecific variation in stomatal traits, leaf traits and physiology reflects adaptation along aridity gradients in a South African shrub. *Ann. Bot.*, **117**, 195–207.

**Chapman, M.A., Pashley, C.H., Wenzler, J., Hvala, J., Tang, S., Knapp, S.J. and Burke, J.M.** (2008) A genomic scan for selection reveals candidates for genes involved in the evolution of cultivated sunflower (*Helianthus annuus*). *Plant Cell*, **20**, 2931–2945.

**Connor, D.J. and Sadras, V.O.** (1992) Physiology of yield expression in sunflower. *Field Crops Research*, **30**, 333–389.

**Dempewolf, H., Baute, G., Anderson, J., Kilian, B., Smith, C. and Guarino, L.** (2017) Past and Future Use of Wild Relatives in Crop Breeding. *Crop Sci.*, **57**, 1070–1082.

**Doheny-Adams, T., Hunt, L., Franks, P.J., Beerling, D.J. and Gray, J.E.** (2012) Genetic manipulation of stomatal density influences stomatal size, plant growth and tolerance to restricted water supply across a growth carbon dioxide gradient. *Philosophical Transactions of the Royal Society of London. Series B, Biological sciences*, **367**, 547–555.

**Drake, P.L., Froend, R.H. and Franks, P.J.** (2013) Smaller, faster stomata: scaling of stomatal size, rate of response, and stomatal conductance. *J. Exp. Bot.*, **64**, 495–505.

**Driesen, E., Van den Ende, W., De Proft, M. and Saeys, W.** (2020) Influence of Environmental Factors Light, CO2, Temperature, and Relative Humidity on Stomatal Opening and Development: A Review. *Agronomy*, **10**, 1975. Available at: [Accessed July 5, 2022].

**Dunlap, J.M. and Stettler, R.F.** (2001) Variation in leaf epidermal and stomatal traits of *Populus trichocarpa* from two transects across the Washington Cascades. *Can. J. Bot.*, **79**, 528–536.

**FAO** (2018) Food Outlook - Oilcrops. *United Nations*. Available at: http://www.fao.org/fileadmin/templates/est/COMM_MARKETS_MONITORING/Oilcrops/Documents/Food_outlook_oilseeds/FO_Oilcrops.pdf [Accessed March 25, 2019].

**FAO** (2021) The State of the World's Land and Water Resources for Food and Agriculture: Systems at breaking point. Available at: https://www.fao.org/3/cb7654en/cb7654en.pdf [Accessed August 22, 2022].

**Faralli, M., Matthews, J. and Lawson, T.** (2019) Exploiting natural variation and genetic manipulation of stomatal conductance for crop improvement. *Curr. Opin. Plant Biol.*, **49**, 1–7.

**Fiorin, L., Brodribb, T.J. and Anfodillo, T.** (2016) Transport efficiency through uniformity: organization of veins and stomata in angiosperm leaves. *New Phytol.*, **209**, 216–227.

**Foley, J.A., Ramankutty, N., Brauman, K.A., et al.** (2011) Solutions for a cultivated planet. *Nature*, **478**, 337–342.

**Franks, P.J., W Doheny-Adams, T., Britton-Harper, Z.J. and Gray, J.E.** (2015) Increasing water-use efficiency directly through genetic manipulation of stomatal density. *New Phytol.*, **207**, 188–195.

**Godfray, H.C.J., Beddington, J.R., Crute, I.R., et al.** (2010) Food security: the challenge of feeding 9 billion people. *Science*, **327**, 812–818.

**Harter, A.V., Gardner, K.A., Falush, D., Lentz, D.L., Bye, R.A. and Rieseberg, L.H.** (2004) Origin of extant domesticated sunflowers in eastern North America. *Nature*, **430**, 201–205.

**Haworth, M., Marino, G., Loreto, F. and Centritto, M.** (2021) Integrating stomatal physiology and morphology: evolution of stomatal control and development of future crops. *Oecologia*, **197**, 867–883.

**Hübner, S., Bercovich, N., Todesco, M., et al.** (2019) Sunflower pan-genome analysis shows that hybridization altered gene content and disease resistance. *Nat Plants*, **5**, 54–62.

**IPCC** (2014) Climate Change 2014: Synthesis Report. Contribution of Working Groups I, II and III to the Fifth Assessment Report of the Intergovernmental Panel on Climate Change. *Intergovernmental Panel on Climate Change*.

**Khan, M.U., Chowdhry, M.A., Khaliq, I. and Ahmad, R.** (2003) Morphological response of various genotypes to drought conditions. *Asian J. Plant Sci.*, **2**, 392–394.

**Lambrides and Chapman** (2001) Breeding Sunflower for Improved Drought Tolerance in Australia. *13th Australian*. Available at: http://www.australianoilseeds.com/__data/assets/pdf_file/0009/4959/Breeding_drought_tolerant_sunflowers.pdf.

**Lei, Z.Y., Han, J.M., Yi, X.P., Zhang, W.F. and Zhang, Y.L.** (2018) Coordinated variation between veins and stomata in cotton and its relationship with water-use efficiency under drought stress. *Photosynthetica*, **56**, 1326–1335.

**Liu, A. and Burke, J.M.** (2006) Patterns of nucleotide diversity in wild and cultivated sunflower. *Genetics*, **173**, 321–330.

**Mandel, J.R., Dechaine, J.M., Marek, L.F. and Burke, J.M.** (2011) Genetic diversity and population structure in cultivated sunflower and a comparison to its wild progenitor, *Helianthus annuus* L. *Theor. Appl. Genet.*, **123**, 693–704.

**Mandel, J.R., Nambeesan, S., Bowers, J.E., Marek, L.F., Ebert, D., Rieseberg, L.H., Knapp, S.J. and Burke, J.M.** (2013) Association mapping and the genomic consequences of selection in sunflower. *PLoS Genet.*, **9**, e1003378.

**Masalia, R.R., Temme, A.A., Torralba, N. de L. and Burke, J.M.** (2018) Multiple genomic regions influence root morphology and seedling growth in cultivated sunflower (*Helianthus annuus* L.) under well-watered and water-limited conditions. *PLoS One*, **13**, e0204279.

**Meyer, R.** (1999) High plains sunflower production handbook. Available at: https://agris.fao.org/agris-search/search.do?recordID=US201300051629 [Accessed August 1, 2022].

**Moore, C.E., Meacham-Hensold, K., Lemonnier, P., Slattery, R.A., Benjamin, C., Bernacchi, C.J., Lawson, T. and Cavanagh, A.P.** (2021) The effect of increasing temperature on crop photosynthesis: from enzymes to ecosystems. *J. Exp. Bot.*, **72**, 2822–2844.

**Munns, R.** (2011) Chapter 1 - Plant Adaptations to Salt and Water Stress: Differences and Commonalities. In I. Turkan, ed. *Advances in Botanical Research*. Academic Press, pp. 1–32.

**NOAA** Drought: Monitoring Economic, Environmental, and Social Impacts. *NOAA: National Centers for Environmental Information*. Available at: https://www.ncdc.noaa.gov/news/drought-monitoring-economic-environmental-and-social-impacts [Accessed May 11, 2021].

**NOAA and NIDIS** (2022) US Crops and Livestock in Drought. *National Integrated Drought Information System*. Available at: https://www.drought.gov/sectors/agriculture [Accessed August 22, 2022].

**Rauf, S.** (2008) Breeding sunflower (*Helianthus annuus* L.) for drought tolerance. *Communications in Biometry and Crop Science*, **3**, 29–44.

**Rieseberg, L.H. and Seiler, G.J.** (1990) Molecular Evidence and the Origin and Development of the Domesticated Sunflower (*Helianthus annus*, Asteraceae). *Econ. Bot.*, **44**, 79–91.

**Ries, L.L., Purcell, L.C., Carter, T.E., Edwards, J.T. and King, C.A.** (2012) Physiological Traits Contributing to Differential Canopy Wilting in Soybean under Drought. *Crop Sci.*, **52**, 272–281.

**Sack, L. and Scoffoni, C.** (2013) Leaf venation: structure, function, development, evolution, ecology and applications in the past, present and future. *New Phytologist*, **198**, 983–1000.

**Sack, L. and Scoffoni, C.** (2012) Measurement of leaf hydraulic conductance and stomatal conductance and their responses to irradiance and dehydration using the Evaporative Flux Method (EFM). *Journal of Visualized Experiments*, e4179.

**Scoffoni, C., Rawls, M., McKown, A., Cochard, H. and Sack, L.** (2011) Decline of leaf hydraulic conductance with dehydration: relationship to leaf size and venation architecture. *Plant Physiol.*, **156**, 832–843.

**Shahinnia, F., Le Roy, J., Laborde, B., Sznajder, B., Kalambettu, P., Mahjourimajd, S., Tilbrook, J. and Fleury, D.** (2016) Genetic association of stomatal traits and yield in wheat grown in low rainfall environments. *BMC Plant Biology*, **16**, 150.

**Shi, P., Jiao, Y., Diggle, P.J., Turner, R., Wang, R. and Niinemets, Ü.** (2021) Spatial distribution characteristics of stomata at the areole level in *Michelia cavaleriei* var. platypetala (Magnoliaceae). *Ann. Bot.*, **128**, 875–886.

**Stojnić, S., Orlović, S., Trudić, B., Živković, U., Wuehlisch, G. von and Miljković, D.** (2015) Phenotypic plasticity of European beech (Fagus sylvatica L.) stomatal features under water deficit assessed in provenance trial. *Dendrobiology*, **73**, 163–173.

**Sun, Y., Yan, F., Cui, X. and Liu, F.** (2014) Plasticity in stomatal size and density of potato leaves under different irrigation and phosphorus regimes. *J. Plant Physiol.*, **171**, 1248–1255.

**Temme, A.A., Kerr, K.L., Masalia, R.R., Burke, J.M. and Donovan, L.A.** (2020) Key Traits and Genes Associate with Salinity Tolerance Independent from Vigor in Cultivated Sunflower. *Plant Physiol.*, **184**, 865–880.

**United Nations** (2017) World Population Prospects. *Department of Economics and Social Affairs*. Available at: https://population.un.org/wpp/Publications/Files/WPP2017_KeyFindings.pdf.

**Wang, X., Du, T., Huang, J., Peng, S. and Xiong, D.** (2018) Leaf hydraulic vulnerability triggers the decline in stomatal and mesophyll conductance during drought in rice. *J. Exp. Bot.*, **69**, 4033–4045.

**Wang, Y., Donovan, L.A. and Temme, A.A.** (2020) Plasticity and the role of mass-scaling in allocation, morphology, and anatomical trait responses to above- and belowground resource limitation in cultivated sunflower (*Helianthus annuus* L.). *Plant Direct*, **4**, e02924.

**Wills, D.M. and Burke, J.M.** (2006) Chloroplast DNA variation confirms a single origin of domesticated sunflower (*Helianthus annuus* L.). *J. Hered.*, **97**, 403–408.

**Wu, C.A., Lowry, D.B., Nutter, L.I. and Willis, J.H.** (2010) Natural variation for drought-response traits in the *Mimulus guttatus* species complex. *Oecologia*, **162**, 23–33.

**Xie, J., Wang, Z. and Li, Y.** (2022) Stomatal opening ratio mediates trait coordinating network adaptation to environmental gradients. *New Phytol.*, **235**, 907–922.

**Zhang, S.-B., Guan, Z.-J., Sun, M., Zhang, J.-J., Cao, K.-F. and Hu, H.** (2012) Evolutionary association of stomatal traits with leaf vein density in *Paphiopedilum*, rchidaceae. *PLoS One*, **7**, e40080.

# CHAPTER 2

# GENOMIC REGIONS ASSOCIATE WITH MAJOR AXES OF VARIATION DRIVEN BY GAS EXCHANGE AND LEAF CONTRUCTION TRAITS IN CULTIVATED SUNFLOWER (*HELIANTHUS ANNUUS* L.)[1]

[1] Earley, Ashley M., Andries A. Temme, Christopher R. Cotter, and John M. Burke. 2022. *The Plant Journal*. https://doi.org/10.1111/tpj.15900.Reprinted here with permission of publisher

ABSTRACT

Stomata and leaf veins play an essential role in transpiration and the movement of water throughout leaves. These traits are thus thought to play a key role in the adaptation of plants to drought and a better understanding of the genetic basis of their variation and coordination could inform efforts to improve drought tolerance. Here, we explore patterns of variation and covariation in leaf anatomical traits and analyze their genetic architecture via genome-wide association (GWA) analyses in cultivated sunflower (*Helianthus annuus* L.*)*. Traits related to stomatal density and morphology as well as lower order veins were manually measured from digital images while the density of minor veins was estimated using a novel deep learning approach. Leaf, stomatal, and vein traits exhibited numerous significant correlations that generally followed expectations based on functional relationships. Correlated suites of traits could further be separated along three major principal component (PC) axes that were heavily influenced by variation in traits related to gas exchange, leaf hydraulics, and leaf construction. While there was limited evidence of colocalization when individual traits were subjected to GWA analyses, major multivariate PC axes that were most strongly influenced by several traits related to gas exchange or leaf construction did exhibit significant genomic associations. These results provide insight into the genetic basis of leaf trait covariation and showcase potential targets for future efforts aimed at modifying leaf anatomical traits in sunflower.

## INTRODUCTION

Stomata and leaf veins are central players in plant water relations. Veins distribute water throughout the leaf and stomata control the rate of transpiration (Sack and Scoffoni, 2013). As such, these traits are generally thought to play a key role in the adaptation of plants to drought (e.g., Bertolino *et al.*, 2019; Sack and Scoffoni, 2013), a major agricultural stress that limits plant growth and productivity worldwide (NOAA, n.d.; IPCC, 2014). Plant performance in water-limited conditions is known to be influenced by stomatal and vein traits (Lei *et al.*, 2018; Scoffoni *et al.*, 2011; Buckley, 2019). Stomatal conductance ($g_s$), a measure of the conductance of water vapor through the stomata, is determined by the physiological control of stomatal opening and closing as well as the size and distribution of stomata (Faralli *et al.*, 2019). Similarly, vein length per area (VLA) affects leaf hydraulic conductance ($K_{leaf}$), or the ratio of water flow rate to the water potential gradient across the leaf, and thus greatly affects how long stomata can remain open without drying out the leaf (Sack and Scoffoni, 2012). While substantial work has been done on the developmental and regulatory pathways determining stomatal density and morphology (e.g., Gudesblat *et al.*, 2012; Bergmann and Sack, 2007) less is known about the genetic basis of the observed relationships between stomatal and leaf vein traits.

Leaf veins distribute water from the petiole throughout the leaf. In the intercellular space, water then moves through the mesophyll to the ultimate site of transpiration, the stomata. It is important to note here that stomata can be distributed on

both the top (adaxial) and bottom (abaxial) sides of the leaf, and that species with stomata on both sides (i.e., amphistomatous) tend to have greater gas exchange capacity than species with stomata on a single side (Xiong and Flexas, 2020). An increase in the number of stomata on the upper side leads to increased maximum photosynthetic rates and to increased rates of transpiration due to increased $CO_2$ diffusion (Muir, 2018; Xiong and Flexas, 2020). Due to these effects on water supply and loss, a close relationship between vein density and stomatal size/density is expected to be important for the optimization of water transport and transpiration (Fiorin *et al.*, 2016; Bertolino *et al.*, 2019). In particular, a shorter vein-to-stomata distance is thought to improve gas exchange and photosynthetic performance (Brodribb *et al.*, 2007; de Boer *et al.*, 2012). This distance is affected by traits such as stomatal density, vein density (estimated as vein length per area; VLA), leaf thickness, and cell shape (Brodribb *et al.*, 2007; de Boer *et al.*, 2012). As a general rule, vein and stomatal density are positively correlated (Sack and Scoffoni, 2013) while stomatal size and density are negatively correlated (Shahinnia *et al.*, 2016; Doheny-Adams *et al.*, 2012). Smaller epidermal cell size is also known to correlate with increases in stomatal and vein densities (Simonin and Roddy, 2018; Brodribb *et al.*, 2013) Such correlations are observed within (Carins Murphy *et al.*, 2014) and across species (Zhang *et al.*, 2012), though the extent to which these trait correlations are conditioned by genetic correlations (i.e., linkage or pleiotropy of major effect loci) remains an open question.

At the whole leaf level, plant species exhibit a range of strategies related to the cost of leaf construction. Traits such as leaf mass per area (LMA) and VLA play a role in

leaf construction in addition to affecting leaf hydraulics (Xing *et al.*, 2021; Poorter *et al.*, 2009; John *et al.*, 2017). These strategies occur along a major axis of leaf trait variation (the Leaf Economics Spectrum, LES), which ranges from resource conservative (i.e., 'slow') with a greater investment in leaf construction to resource acquisitive (i.e., 'fast') with a smaller investment in leaf construction (Wright *et al.*, 2004; Reich, 2014; Díaz *et al.*, 2016). A key indicator trait for the location of species along this spectrum is LMA, with leaf hydraulic traits (allocation to major vs. minor veins in particular) accounting for a portion of the observed variation in LMA (John *et al.*, 2017). Investigating the variation present in both finer scale aspects of leaves as well as whole leaf traits promises to broaden our understanding of the evolution of correlated suites of leaf traits.

To date, most studies focusing on within species variation in leaf anatomy have either relied on relatively small sample sizes or have largely focused on stomatal traits to the exclusion of vein traits (e.g., Khan *et al.*, 2003; Ries *et al.*, 2012; Shi *et al.*, 2021; Haworth *et al.*, 2021). The general dearth of studies that explicitly examine the genetic basis of stomatal and vein traits, particularly in tandem, is likely due to challenges associated with the large-scale phenotyping of such traits. One study on wild tomato found that strongly correlated leaf traits were not controlled by the same QTL, suggesting that natural selection had favored particular trait combinations (Muir *et al.*, 2014). However, another study on wild *Arabidopsis* accessions found that stomatal density correlated with various other leaf traits, including stomatal index and pavement cell density, and that they seemed to share a common genetic basis (Delgado *et al.*, 2011).

The lack of a clear pattern across species leaves as an open question the extent to which variation in such traits can be decoupled, thereby allowing them to vary independently.

Here, we describe patterns of phenotypic variation in leaf traits in cultivated sunflower (*Helianthus annuus* L.) and investigate their genetic architecture via genome-wide association (GWA) analyses. Domesticated from the common sunflower *(*also *H. annuus*; Wills and Burke, 2006; Blackman *et al.*, 2011), cultivated sunflower is one of the world's most important oilseed crops (FAO, 2018). Often grown in rainfed regions, sunflower productivity is frequently dependent on natural patterns of precipitation. While sunflower is generally regarded as being drought resistant due to its ability to root deeply (Connor and Sadras, 1992), drought is considered to be a major yield-limiting factor across the range of production (Hussain *et al.*, 2018), making traits underlying plant-water relations a vital avenue of research. Prior work on sunflower has shown substantial variability and plasticity in leaf anatomical traits (Wang *et al.*, 2020). Previous genomic analyses, however, have been largely limited to higher level traits such as leaf mass, leaf area, LMA, and leaf mass fraction (Temme *et al.*, 2020; Masalia *et al.*, 2018). To overcome limitations in the analysis of vein traits, we developed a neural network deep learning approach to increase phenotyping efficiency from digital images (see Xu *et al.*, 2020 for a similar approach), enabling an investigation of the genomic basis on finer scale leaf anatomical traits.

In this study, we sought to: (1) quantify phenotypic variation in stomatal and leaf vein traits and test for trait correlations in sunflower, (2) identify genomic regions

underlying these traits using genome-wide association analyses, and (3) determine the extent to which observed trait correlations are due to a shared genetic basis. Our results provide insight into the genetic complexity of these traits and the degree to which observed trait correlations are constrained by linkage or pleiotropy of major effect loci and serve as a valuable first step toward optimizing leaf trait combinations via breeding.

## RESULTS

We sampled leaves from a diversity panel of 239 cultivated sunflower genotypes from the Sunflower Association Mapping (SAM) population (Mandel *et al.*, 2011) grown under greenhouse conditions. These leaves were then used to collect measurements for a variety of leaf anatomical traits (Figure 2.1). Traits of interest included stomatal density and size and vein length per area (VLA) for major and minor veins (Figure 2.1) as well as traits including leaf mass per area (LMA), midrib density, and plant biomass. With the exception of minor veins, which were traced using a novel deep learning neural network (Methods S2.1), all traits were measured manually. Trait correlations were examined using bivariate and multivariate analyses and genetic associations were determined using a custom GWA pipeline. See Experimental Procedures for full details.

### *Patterns of phenotypic variation and trait correlations*

Significant genotypic effects were detected for all traits measured except midrib mass fraction (Table 2.1). Table 2.1 lists the median, minimum, and maximum values

found for all traits measured, demonstrating substantial trait variation across the population. Comparing manually measured VLA to the results from the neural network analysis revealed a strong correlation (Pearson's r = 0.97), demonstrating the accuracy and validity of these computer-generated measurements (Figure S2.2).

Trait correlations were examined using both bivariate and multivariate analyses. Stomatal density and size traits from the top and the bottom of each leaf were strongly correlated with each other (Figure 2.3a; Figure S2.4; e.g., SD_Top vs. SD_Bottom, PL_Top vs. PL_Bottom); as such, stomatal sum (SD_Top + SD_Bottom) and averages of the top and bottom for other traits were used for analyses moving forward. Bivariate analysis revealed numerous significant trait correlations among stomatal and vein traits (Figure 2.2; Figure 2.3). Notably, stomatal density and length were negatively correlated (Figure 2.3b), stomatal density and VLA were positively correlated (Figure 2.3c), and stomatal length and VLA were negatively correlated (Figure S2.4). VLA was positively correlated with both average stomatal density and theoretical $g_{smax}$ (Figure 2.3d). The only traits that were significantly correlated with leaf area were second VLA and major VLA and biomass traits indicating that trait scaling with leaf size did not play a major role in observed patterns of anatomical variation. For all bivariate plots see Figure S2.4.

Multivariate trait correlations were analyzed via PCA to determine major axes of variation. Because stomatal trait values on the top and bottom of the leaf were strongly correlated, we again used an average of the top and bottom values for stomatal size traits including length, pore length, and guard cell width (Figure 2.4; see Figure S2.5 for a full

PCA including the top and bottom traits separately). The first three PCs combined to explain 62.6% of trait variation (Figure S2.6) with PC1 explaining 30.3%, PC2 explaining 22.6%, and PC3 explaining 10.0% of variation. The top three traits contributing to each of the major axes were: PC1 – stomatal density (SD_Sum), stomata per vein length (SV), and whole plant biomass (Plant Bio); PC2 – 2nd VLA, Major VLA, and leaf area; and PC3 – midrib density, midrib mass fraction, and LMA (Table 2.2). While all traits have a loading score on each PC axis, we sought to infer some functional significance for each of the major axes of variation. Given the observed trait loadings, PC1 appears to be most heavily influenced by traits related to gas exchange functioning such as stomatal density sum and stomata per vein length. In contrast, PC2 is strongly influenced by traits related to hydraulic functioning including major VLA and second VLA. Finally, PC3 is heavily influenced by traits related to cost of leaf construction including LMA and midrib traits.

*Genetic architecture of observed trait variation*

As a first step toward understanding the genetic basis of variation in leaf anatomical traits, we estimated narrow sense heritability for all traits under consideration (Table 2.3). Midrib traits and VLA (major and minor) had very low heritabilities (0.05 to 0.11) and the confidence intervals of these estimates all overlapped with zero. Stomatal traits had somewhat higher heritability, ranging from 0.08 to 0.20. Heritability values largely reflected our GWA results (see below) in that traits with the lowest heritability estimates had few significant associations.

Our GWA analyses revealed significant associations for 12 out of 24 traits and 2 of the 3 major PC axes (Table 2.3, Figure 2.5). There were suggestive associations for several other traits, as well (Figure 2.5c; Figure S2.8). Based on observed patterns of LD, we identified a total of 24 independent genomic regions with a significant effect on one or more traits (Figures 2.5c and S2.7). Trait co-localization within these regions varied. For example, there were multiple regions on chromosome 11 that associated with both aboveground plant biomass and whole plant biomass, and a region on chromosome 3 (i.e., region 03-01) was significantly associated with $g_{smax}$ while being suggestive for stomatal density and VLA. Interestingly, PC1 (traits primarily related to gas exchange) had a single significant association (on chromosome 12; region 12-01) but no suggestive associations; moreover, this single region was not suggestive for any other traits (Figure 2.5a). Stomata per vein length (SV), a top contributor to PC1, had a single significant association along with four suggestive regions, none of which corresponded to PC1 (Figure 2.5b). Similarly, PC3 had a single significant association (on chromosome 3; region 03-02) that did not correspond to any other traits.

Overall, we found somewhat limited evidence for trait colocalization despite the prevalence of significant trait-trait correlations (Figure 2.5c). Indeed, no region was significantly associated with more than 1-2 traits. However, the inclusion of suggestive associations revealed more support for a common genetic basis. Traits with the largest number of colocalizations were stomatal size and density-related traits. For example, region 13-01 had seven associations including a significant association for stomatal density (top) and suggestive associations for leaf area, pore length (top and average),

stomatal density (bottom and sum), and SV (Figure 2.5c). No significant associations were identified for VLA, although there was a suggestive association in region 03-01, which was significant for $g_{smax}$ and suggestive for stomatal density (both bottom and sum). Allelic effects in this case were consistent with observed trait correlations, with an increase in $g_{smax}$ being associated with an increase in VLA and stomatal density.

Relative effect sizes (RES) for individual associations ranged from 9% to 35% of the observed range of trait variation. Summing across regions, traits with significant associations had total RES values of ca. 12-90%. Stomatal density top had the largest amount of variation explained at 89.6% and midrib density the least with 12.3%. Significantly associated regions varied in size, ranging from a single SNP to 6.52 Mbp, though they tended to cluster at the lower end of the range with the majority being < 200 kbp (mean = 592.7 kbp, median = 77.54 kbp; Table S2.2). These regions contained anywhere from 1 to 135 genes; here again, the significant regions tended to cluster at the lower end of this range (mean = 12.3 genes, median = 2 genes; Table S2.2). The most gene-rich regions (i.e., 10-01, 12-01) were significantly associated with variation in plant biomass and PC1, respectively (Figures 2.5c, S2.4, and S2.9). A full list of gene names and annotations is available in Table S2.2.

## DISCUSSION

Stomata and leaf veins are central to plant-water relations and thus potentially important players in determining the performance of plants under water stress. Here, we

investigated patterns of variation and covariation in stomatal and vein traits across a diversity panel of inbred cultivated sunflower breeding lines with the goal of improving our understanding of covariation between these traits and their underlying genetic basis. We additionally sought to determine the extent to which observed trait correlations result from genomic co-localization which would indicate that trait relationships are genetically constrained and difficult (if not impossible) to disrupt in the interest of producing novel combinations. In quantifying variation in stomatal and vein traits, we observed numerous correlations amongst traits (Figure 2.2 and 2.3). Across traits, we identified three primary axes of variation that we interpreted as being most heavily influenced by traits involved in gas exchange, hydraulics, and leaf construction (Figure 2.2; Table 2.2). Subsequently, we performed GWA analyses to examine the genetic architecture of these traits and axes. We found somewhat limited overlap in significant genomic associations across traits, though we did identify significant associations for two of the three multi-trait axes (Figure 2.5; Table 2.3).

*Patterns of phenotypic variation and trait correlations*

Leaf anatomical traits are known to vary widely across species and environments. For example, stomatal length has been shown to vary globally between 10-80 μm with density varying between 5-1000 stomata/mm$^2$ (Shahinnia *et al.*, 2016; Hetherington and Woodward, 2003). Additionally, a global dataset of 796 species revealed broad variation in estimates of VLA, ranging from 0.1-24.4 mm/mm$^2$ (Sack and Scoffoni, 2013). In cultivated sunflower, we documented substantial variation in stomatal size and density as

well as VLA. Indeed, observed trait values covered 14% (227.5-369.3 stomata/mm$^2$) of the global range in stomatal density, 18% (26.8-39.4 µm) of the global range in stomatal length, and 23% (7.0-12.6 mm/mm$^2$) of the global range in VLA (Table 2.1). While there is a general lack of large datasets describing intraspecific variation in these sorts of traits, particularly for VLA, the ranges that we observed in cultivated sunflower appear quite wide. For example, a global collection of 62 wild accessions of *Arabidopsis thaliana,* grown under benign conditions, covered just 4.3% (17-59 stomata/mm$^2$) of the global range of stomatal densities (Delgado *et al.*, 2011) while a collection of 330 accessions from across the European range of the same species covered less than 12% (87-204 stomata/mm$^2$) of the global range (Dittberner *et al.*, 2018). The wide range of variability observed herein is perhaps even more noteworthy given that cultivated sunflower has experienced genetic bottlenecks associated with domestication and improvement that reduced levels of genetic variability as compared to its wild progenitor (Liu and Burke, 2006; Mandel *et al.*, 2011; Park and Burke, 2020).

When analyzed together, leaf anatomical traits exhibited many significant bivariate trait correlations that generally followed expectations based on the literature and their known roles in plant-water relations (Sack and Scoffoni, 2013; Doheny-Adams *et al.*, 2012; Shahinnia *et al.*, 2016; Figure 2.2). For example, our data showed that stomatal density and VLA are positively correlated. This was expected as there tends to be a balance between stomata and veins such that water use and carbon acquisition are optimized (Carins Murphy *et al.*, 2014; Brodribb *et al.*, 2007; Sack and Scoffoni, 2013). Additionally, stomatal size and density were negatively correlated, as expected, since the

total area allocated to stomata affects total stomatal conductance and thus total photosynthesis (Harrison *et al.*, 2019; Shahinnia *et al.*, 2016; Figure 2.2) both within (Doheny-Adams *et al.*, 2012) and across species (Hetherington and Woodward, 2003). Overall plant size, estimated as biomass, correlated positively with stomatal density and related traits (e.g., $g_{smax}$ and SV) but negatively with 2nd/major VLA, with larger plants tending to have higher stomatal density and lower 2nd/major VLA. Conversely, stomatal size was unrelated to plant biomass despite its correlation with other leaf traits of interest. Besides scaling with plant mass (Wang *et al.*, 2020), the potential scaling of traits with leaf area is of interest as correlations can arise as a byproduct of trait values scaling with size. Given that stomatal and vein traits were not significantly correlated with leaf area, however, it appears that observed correlations between these traits exist independently of variation in leaf size (Figure 2.2).

When compared to minor VLA, lower order vein traits (i.e., 2nd and major VLA) exhibited a distinct pattern of trait correlations. These traits were not significantly correlated with any stomatal traits; rather, they exhibited significant correlations with traits related to the investment in leaf production (i.e., LMA and leaf area; Figures 2.2 and 2.3). Contrary to expectations based on cross-species comparisons (e.g., Walls, 2011; Kawai and Okada, 2016), 2nd and major VLA were negatively correlated with LMA (Figure 2.2) suggesting that variation in LMA at this scale may be driven by other, perhaps unmeasured traits such as leaf thickness. Similarly, 2nd and major VLA were negatively correlated with leaf size. This pattern was, however, expected given that major veins are typically formed early in leaf development before being pushed apart as leaf

expansion accelerates (Sack and Scoffoni, 2013). In contrast, minor veins are expected to show no such relationship (consistent with our results) because they can be initiated throughout leaf development.

As compared to bivariate analyses, multivariate analyses provide a more holistic view of trait relationships along with possible impacts of leaf anatomical variation on 'higher level' traits such as biomass, leaf size, and LMA. When analyzed via PCA, nearly two-thirds of the observed trait variation was captured by the first three PC axes. As noted above, these axes are most heavily influenced by suites of traits involved in gas exchange, hydraulics, and leaf construction. More specifically, plants with lower stomatal density (estimated as stomatal sum) and fewer stomata per vein length (SV), which are primary players in stomatal conductance, tended to be smaller overall. In terms of hydraulic traits, and consistent with the results of our bivariate analyses, plants with greater second and major VLA tended to have smaller leaves. Interestingly, this trait combination is thought to confer greater leaf drought tolerance (Scoffoni *et al.,* 2011). Finally, in terms of leaf construction traits, plants that produced more costly leaves (i.e., leaves with higher LMA) tended to have a greater relative investment in major structural features including midrib density and midrib mass fraction (Figure 2.4; Table 2.2), likely reflecting an increase in the mechanical strength of such leaves (Méndez-Alonzo *et al.*, 2013).

*Genetic architecture of observed trait variation*

Estimates of narrow sense heritability ranged from 0.05 to 0.49 across traits. Notably, vein (including midrib) traits had low heritability estimates while stomatal traits

had higher estimates (Table 2.3). The highest estimates were for biomass-related traits, LMA, and $g_{smax}$ indicating a more substantial contribution of additive genetic effects to observed variation in these traits as compared to others (Kruijer *et al.*, 2015). Somewhat surprisingly given the highly significant effect of genotype on VLA, the heritability estimate for that trait was not significantly different from zero (Tables 2.1 and 2.3), indicating little to no contribution of additive genetic effects to observed variation. Midrib density and midrib mass fraction had similarly low heritability estimates, though the evidence of a genotypic effect on the former was less clear, and genotype had no apparent effect on the latter. Interestingly, heritability estimates for the composite trait SV (i.e., stomata per vein length) were noticeably higher than estimates for vein traits alone indicating an additive genetic component of the observed variation in this trait. Collectively, these results suggest that traits with the lowest heritability estimates have limited potential for improvement via breeding while others are likely to be more amenable to such efforts.

Consistent with our heritability estimates, the two biomass-related traits exhibited the largest number of significant associations in our GWA analyses (Table 2.3; Figure 2.5c; Figure S2.8). These traits colocalized with leaf area, midrib density, and LMA but not with any other vein or stomatal traits. Similarly, we identified significant associations for multiple stomatal traits, including stomatal density (bottom, top, and sum) and pore length (bottom), many of which colocalized with suggestive associations (i.e., SNPs with $-\log_{10}(p)$ values in the top 0.1%) for other stomatal traits. Consistent with the low heritability estimates for traits related to vein density (i.e., VLA, 2nd VLA, and major

VLA), no significant genomic associations were found for any of these traits. There was, however, one suggestive association for VLA that colocalized with a significant association for $g_{smax}$ (region 03-01) and suggestive associations for stomatal density (bottom and sum), consistent with a presumed functional relationship between these traits. Despite the lack of significant associations for vein-related traits considered on their own, we identified one significant and five suggestive associations for the composite trait SV (i.e., stomata per vein length). These regions tended to colocalize with stomatal traits suggesting that variation in stomatal characteristics is the primary driver of this trait relationship (Figure 2.5c, Table S2.1).

Taken together, our trait-by-trait analyses revealed limited evidence for colocalization between stomatal and vein traits despite the existence of widespread and significant correlations between such traits. While this result could be due, at least in part, to the high stringency of our significance threshold and thus the failure to detect true positives – a common challenge in GWA analyses (Gupta *et al.*, 2019) – the identification and inclusion of suggestive regions in our analyses should have helped to mitigate this issue. Nonetheless, observed trait correlations did not appear to be accompanied by clear patterns of genomic colocalization on a single trait basis suggesting a largely independent genetic basis of our traits of interest. However, when multivariate trait relationships were taken into account, our GWA analyses revealed significant associations for two of the three major PC axes (i.e., PC1 and PC3) and a suggestive association for the third (i.e., PC2). For PC1, which is most heavily influenced by traits related to gas exchange (i.e., stomatal density and SV) along with plant biomass, the

single significant association (i.e., region 12-01) colocalized with suggestive associations in 2nd VLA and SV. In contrast, the analysis of PC3, which had midrib density and mass fraction as well as LMA as its top three contributors, identified a novel association (i.e., region 03-02). This region was not identified as being significantly or suggestively associated with any of the individual traits analyzed herein, illustrating the potential value of employing a multivariate approach to GWA analyses (see also, e.g., Yano *et al.*, 2019; Ma *et al.*, 2021). These results also highlight the challenges associated with genetically decoupling certain traits to produce novel phenotypic combinations even though individual trait analyses revealed largely independent genetic architectures.

In terms of effect sizes, the significantly associated regions that we identified tended to have had small to moderate effects (estimated as RES) on trait values. In fact, only three trait/region combinations individually accounted for > 25% of the observed range of trait values across the population (stomatal density [top and sum] in region 05_01 and stomatal density [sum] in region 09_01; Table S2.1). This result is perhaps not surprising given the relatively low heritability estimates observed for many traits. It is worth noting, however, that the traits with the highest heritability estimates (i.e., biomass-related traits and LMA) tended to be associated with regions of relatively minor effect (i.e., RES < 15%) suggesting that they have a complex genetic basis. In contrast, stomatal traits were associated with some of the largest RES values, suggesting the presence of genes of larger effect and a simpler genetic basis overall. This result was mirrored in the multivariate analyses with the single association underlying PC1 (region 12-01), which is heavily influenced by stomatal traits, accounting for nearly 21% of the observed range of

variation in this ‘trait’ across the population. Unfortunately, most of the genes contained within the significantly associated regions identified herein did not yield obvious candidates for the traits of interest.

While many of the genes in regions of interest were annotated as hypothetical proteins or otherwise showed no clear connection with leaf anatomy, two regions did contain potential genes of interest. Region 10-01, which is significant for total biomass and suggestive aboveground biomass, leaf size, and several stomatal size traits (Figure 2.5b), includes a gene annotated as a *Putative transcription factor SSXT* (Ha412HOChr10g0435021; GO:0048366 [leaf development]; Table S2.2). Members of this gene family are thought to play a role in cell size determination in leaves in *Arabidopsis* (Nozaki *et al.*, 2020). This is, however, one of the one of the larger regions that we identified and contains 135 genes so, while this gene appears to be a promising candidate for one or more of the size-related traits that map to this region, this result should be interpreted with caution until functional evidence is available to support its effect on one or more of the associated traits. Nonetheless, it is interesting to note that epidermal cell size is also known to be negatively associated with vein and stomatal densities such that smaller epidermal cells facilitate greater stomatal and vein densities (Brodribb *et al.*, 2013; Murphy *et al.*, 2017; Simonin and Roddy, 2018). The other region containing a potential gene of interest, 11-01, contains a *Putative Epidermal Patterning Factor-like protein* (*EPF*; Ha412HOChr11g0479421; GO:0010052 [guard cell differentiation]; Table S2.2). This region is significant for MidribMF and suggestive for top stomatal length. EPFs are known to be involved in the density of guard cells and

epidermal cells (Hara *et al.*, 2009), but how this might relate to midrib mass fraction is unclear. Establishment of a (potential) role for these genes in producing variation in any of the leaf anatomical traits analyzed herein awaits further investigation. Nonetheless, the genomic regions identified during the course of this work, particularly those with larger effects, represent potential targets for future efforts aimed at modifying leaf anatomical traits in sunflower.

## METHODS

### *Plant material*

The cultivated sunflower lines analyzed in this study comprise the sunflower association mapping (SAM) population (Mandel *et al.*, 2011), which includes 288 inbred lines that capture ca. 90% of allelic diversity in crop sunflower (Mandel *et al.*, 2013). This population has since been subjected to whole genome re-sequencing, thereby enabling the identification of a genome-wide collection of single nucleotide polymorphisms (SNPs) from the full set of lines (Hübner *et al.*, 2019).

### *Experimental design*

In the summer of 2017, 239 inbred lines from the SAM population (4 four replicates each; N = 4 x 239 = 956 total individuals) were grown in the greenhouse in a randomized block design. The plants used in this study correspond to the control plants from Temme et al. (2020) and detailed plant growth methods are described therein.

Briefly, 239 of the 288 lines in the mapping population were used due to greenhouse space constraints and to remove lines with greater than expected levels of heterozygosity. Following germination, all plants were grown for one week in seedling trays to allow for establishment before being transplanted into 2.83 L pots (TP414; Stuewe & Sons, Tangent, OR) filled with a 3:1 mixture of sand and a calcined clay mixture (Turface MVP, Turface Athletics). Pots were fertilized with 40g Osmocote Plus (15-12-9 NPK; ScottsMiracle-Gro, Marysville, OH) and 5 mL each of gypsum (Performance Minerals Corporation, Birmingham, AL) and lime (Austinville Limestone, Austinville, VA) powders for supplemental $Ca^{2+}$. All pots were well-watered, and plants were allowed to grow for three additional weeks before being harvested at four weeks old. Plants were grown under typical summer temperatures and natural light levels in Georgia**.** At harvest, biomass was collected and dried in ovens at 60°C for at least 72 hours. Roots were washed and dried in the same manner. Dried samples were weighed to calculate total and aboveground biomass. During harvest, the two most recently fully expanded leaves (MRFEL) were also collected from each plant. One leaf was arbitrarily designated for use in the estimation of LMA and the other was used for leaf anatomy analyses. Due to our focus on sampling at an equivalent stage during leaf development, we chose the MRFEL at the time of harvest such that the specific leaf pair varied across the population (though generally leaves came from the top 90% of the plant with the number of underdeveloped leaves above varying)**.** The adaxial and abaxial (hereafter top and bottom) surfaces of one half of one MRFEL per plant were pressed into dental putty (President Dental Putty; Coltène/Whaledent Inc., Cuyahoga Falls, OH) to create an impression of the epidermis of

each leaf surface to allow for the visualization and analysis of stomatal traits following the general methods of (Weyers and Johansen, 1985). The other half of the same leaf was stored in Formalin-Acetic Acid-Alcohol (FAA) fixative for imaging and analysis of vein traits.

To estimate LMA, the designated MRFEL from each plant was scanned on a flatbed scanner at 300 dpi (Temme *et al.*, 2020). This image was then used to calculate leaf area using ImageJ v1.52b (Schindelin *et al.*, 2012). The leaf was then dried at 60°C for 48 hours and weighed (the petiole was not included). Using both the mass and area measurements, LMA was calculated as LMA = dry mass/unit area ($g/m^2$).

For stomatal traits, clear nail polish was applied to the epidermal impressions of the top and bottom leaf surfaces and subsequently peeled off using clear tape and placed on microscope slides (Hilu and Randall, 1984; Weyers and Johansen, 1985). Slides were imaged using a Zeiss Axioskop 2 microscope along with ZEN software (Carl Zeiss Microscopy) under the 100X objective to enable estimation of stomatal size. A second set of images (four different fields of view per impression) were taken using the 20x objective to enable estimation of stomatal density. Size estimates were based on 10 stomata per leaf, separately for the top and bottom surfaces of each leaf, for a total of 20 stomata per plant taken with the 100x objective. Stomatal length, pore length, and guard cell width were measured for each stomate using ImageJ (Figure 2.1a). Stomatal densities were estimated by counting the number of stomata in each of the four fields of view (counting partial stomata on only two sides of each image) per side of each leaf (eight

images total per plant). Stomatal ratio was then calculated as number of bottom stomata/total stomata and stomatal sum was calculated as number of top stomata + number of bottom stomata. For consistency with the literature, we used stomatal sum instead of average density of stomates (e.g., Muir, 2018; Richardson *et al.*, 2020). Finally, maximum stomatal conductance ($g_{smax}$), the theoretical maximum rate of gas exchange if all stomata were fully open (calculated as sum of top and bottom), was calculated based on stomatal density and size measurements following the approach of Dow et al. (2014). This was used instead of directly measuring $g_s$ since direct measurements were not feasible for such a large sample size.

For vein traits, the half of each leaf that was fixed in FAA was cleared and stained for analysis using a modification of established procedures (Berlyn *et al.*, 1976; Scoffoni and Sack, 2013). Leaves were cleared in 5% NaOH at 55°C for 5-7 days. Subsequently, leaves were rinsed with deionized water and run through an ethanol dilution series of 30%, 50%, and 70% to dehydrate. After dehydration, leaves were stained with a 0.01% safranin dye solution for 30 minutes to make the veins more visible. Images of the stained leaves were captured using both a flatbed scanner at 2400 dpi to image the entire leaf half and a microscope (Zeiss Axioskop 2) using the 5X objective on a small section of leaf with three to four different fields of view per leaf (Vasco *et al.*, 2014; Figure 2.1 a-b). Second-order vein length was measured by manually tracing veins that branched off the midrib (primary vein) and joined together in arches (Ellis *et al.*, 2009). Major vein length was estimated by adding the length of the midrib to the second-order vein length. Minor vein lengths were estimated from a subset of the microscopic images by manually tracing

the veins with ImageJ. The subset that was manually traced was then used to train a deep learning algorithm (see below) to process the rest of the images. The results of these analyses of minor veins were used to calculate vein length per area (VLA). Midrib density (expressed as $mg/cm^3$) was estimated from the mass of the midrib and an estimate of its volume; the latter value was calculated from the length of the midrib and its diameter at the base of the leaf and assuming a conical shape. Midrib mass fraction is the ratio of mass of the midrib to mass of the leaf. A composite trait of stomata number per vein length was also calculated as SV = average stomatal density (i.e., calculated as the average of the top and bottom density estimates) divided by VLA (Zhao *et al.*, 2017).

*Image segmentation using a neural network*

A modified version of the U-Net (Xu *et al.*, 2020; Ronneberger *et al.*, 2015) deep neural network was used to segment leaf-vein pixels from background pixels (Figures S2.1-S2.3). Network structure, hyperparameter tuning, and training details are included in Methods S2.1. Briefly, a test set of 85 images was created by randomly selecting one image from each of 85 randomly selected (without replacement) genotypes. These images were not used during training of the network or hyperparameter estimation. All remaining, manually traced (i.e., hand-segmented) images were used in the training set (747 images. Training was performed on randomly selected 572 pixels wide x 572 pixels high x 3 color (RGB) channels regions of the bright-field leaf images. Each region was normalized to a mean of 0 and a standard deviation of 1. The network was trained with a batch size of 1 (Ronneberger *et al.*, 2015) for 1900 batches with a learning rate of $10^{-4}$.

Per-pixel in-vein predictions were performed by mirror padding each full size (2584x1936 pixel) bright field image, normalizing to a mean of zero and standard deviation of one, and passing the images through the trained network. To reduce the creation of small, non-real branches during medial-axis thinning, the probabilities were filtered with a Gaussian kernel with a standard deviation of 12, about the width of a typical vein. The smoothed images were segmented with a cutoff of 0.2. The resulting segmented images were thinned to single-pixel-wide lines using the medial-axis transform (Bucksch, 2014). Vein lengths were then calculated as the sum of all pixels within the thinned line. The hand-segmented and network-segmented vein lengths of the testing set images have a Pearson correlation of 0.97 (Figure S2.2). All code can be found at https://github.com/aatemme/burke_leaf_veins/. For additional methodological details, see Methods S2.1.

*Data analysis*

All data analysis was conducted using R v3.4.3 (R Core Team, 2013). Bivariate plots were made for all pairwise comparisons using the R package *ggplot2* (Wickham, 2016) to show the range of trait variation. A two-way ANOVA with genotype and block as the main effects was performed to test for variation among genotypes and to calculate estimated marginal trait means for genotypes after removing block effects. Marginal means calculated with the R package *emmeans* (Lenth, 2020) were also used to estimate trait correlations and to create a correlation matrix using the R package *corrplot (Wei and Simko, 2017)*. A principal component analysis (PCA) was conducted using the function

prcomp() and the package *ggfortify* (Tang *et al.*, 2016; Horikoshi and Tang, 2018) to visualize multivariate correlations. Narrow sense heritabilities ($h^2$) were calculated using the package *heritability* (Kruijer *et al.*, 2019) by inputting the kinship matrix (see below) for all genotypes and individual pot-level trait data.

All traits of interest, including the first three principal components (PCs) from the PCA, were analyzed via GWA analyses to identify genomic regions that are significantly associated with each trait. These analyses were performed using a custom pipeline as described in Temme et al. (2020; https://github.com/aatemme/Sunflower-GWAS-v2). SNPs used in these analyses were called as described in Hübner et al. (2019) and reordered based on the improved HA412-HOv2 sunflower genome assembly (Todesco *et al.*, 2020). SNPs were filtered to retain those with minor allele frequency ≥ 5% and residual heterozygosity of < 10% (Temme *et al.*, 2020). The GWA analyses were performed using GEMMA v.98.1 (Zhou and Stephens, 2012) to test for associations while correcting for kinship (as calculated by GEMMA) and population structure (using the first four PCs from an analysis using a subset of independent SNPs in SNPRelate; Zheng *et al.*, 2012). The significance threshold was corrected for multiple comparisons using a modified Bonferroni correction based on the number of multi-SNP haplotypic within the genome as determined by an analysis of linkage disequilibrium (LD) across the population (Temme *et al.*, 2020); any SNPs exceeding this threshold were considered to be significantly associated with the trait of interest. Following this step, significant SNPs were grouped into significantly associated genomic regions, with all SNPs occurring within a previously identified haplotypic block being assumed to mark a single

region (see Temme et al., 2020 for details). Suggestive associations were then identified as SNPs in the top 0.1% of all SNPs that co-localized with significant associations for one or more other traits. The relative effect size (RES) of associated SNPs/regions were then estimated as the percentage of the observed range of variation in a particular trait that is explained by each association, as follows:

$$RES = |(2 * \beta/\text{range of observed trait values})| * 100$$

Here, $\beta$ represents the effect of the minor allele on the trait value and the range is based on the distribution of trait values across all genotypes (Masalia *et al.*, 2018). In cases of multi-SNP blocks, the RES value was estimated as the maximum value for all SNPs within that block. These values can also be summed to represent the total percentage variation explained by all significant associations for a particular trait.

## DATA STATEMENT

All raw data from the resequencing of the SAM population are stored in the Sequence Read Archive under Bioproject PRJNA353001. SNP set used and genome assembly as in Todesco et al. (2020). Raw phenotypic data and image files are available via Dryad at https://doi.org/10.5061/dryad.63xsj3v54.

REFERENCES

**Bergmann, D.C. and Sack, F.D.** (2007) Stomatal development. *Annu. Rev. Plant Biol.*, **58**, 163–181.

**Berlyn, G.P., Miksche, J.P., Sass, J.E. and Others** (1976) *Botanical microtechnique and cytochemistry*, Iowa State University Press.

**Bertolino, L.T., Caine, R.S. and Gray, J.E.** (2019) Impact of stomatal density and morphology on water-use efficiency in a changing world. *Front. Plant Sci.*, **10**, 225.

**Blackman, B.K., Scascitelli, M., Kane, N.C., Luton, H.H., Rasmussen, D.A., Bye, R.A., Lentz, D.L. and Rieseberg, L.H.** (2011) Sunflower domestication alleles support single domestication center in eastern North America. *Proc. Natl. Acad. Sci. U. S. A.*, **108**, 14360–14365.

**Boer, H.J. de, Eppinga, M.B., Wassen, M.J. and Dekker, S.C.** (2012) A critical transition in leaf evolution facilitated the Cretaceous angiosperm revolution. *Nat. Commun.*, **3**, 1221.

**Brodribb, T.J., Feild, T.S. and Jordan, G.J.** (2007) Leaf maximum photosynthetic rate and venation are linked by hydraulics. *Plant Physiol.*, **144**, 1890–1898.

**Brodribb, T.J., Jordan, G.J. and Carpenter, R.J.** (2013) Unified changes in cell size permit coordinated leaf evolution. *New Phytol.*, **199**, 559–570.

**Buckley, T.N.** (2019) How do stomata respond to water status? *New Phytol.*, **224**, 21–36.

**Bucksch, A.** (2014) A practical introduction to skeletons for the plant sciences. *Applications in Plant Sciences*, **2**, 1400005.

**Carins Murphy, M.R., Jordan, G.J. and Brodribb, T.J.** (2014) Acclimation to humidity modifies the link between leaf size and the density of veins and stomata. *Plant Cell Environ.*, **37**, 124–131.

**Connor, D.J. and Sadras, V.O.** (1992) Physiology of yield expression in sunflower. *Field Crops Research*, **30**, 333–389.

**Delgado, D., Alonso-Blanco, C., Fenoll, C. and Mena, M.** (2011) Natural variation in stomatal abundance of *Arabidopsis thaliana* includes cryptic diversity for different developmental processes. *Annals of Botany*, **107**, 1247–1258.

**Díaz, S., Kattge, J., Cornelissen, J.H.C., et al.** (2016) The global spectrum of plant form and function. *Nature*, **529**, 167–171.

**Dittberner, H., Korte, A. and Mettler-Altmann, T.** (2018) Natural variation in stomata size contributes to the local adaptation of water-use efficiency in *Arabidopsis thaliana*. *Molecular Ecology*, **27**, 4052–4065.

**Doheny-Adams, T., Hunt, L., Franks, P.J., Beerling, D.J. and Gray, J.E.** (2012) Genetic manipulation of stomatal density influences stomatal size, plant growth and tolerance to restricted water supply across a growth carbon dioxide gradient. *Philosophical Transactions of the Royal Society of London. Series B, Biological sciences*, **367**, 547–555.

**Dow, G.J., Bergmann, D.C. and Berry, J.A.** (2014) An integrated model of stomatal development and leaf physiology. *New Phytologist*, **201**, 1218–1226.

**Ellis, B., Daly, D.C., Hickey, L.J., Mitchell, J.D., Johnson, K.R., Wilf, P. and Wing, S.L.** (2009) *Manual of Leaf Architecture* 1 edition., Comstock Pub. Associates.

**FAO** (2018) Food Outlook - Oilcrops. *United Nations*. Available at: http://www.fao.org/fileadmin/templates/est/COMM_MARKETS_MONITORING/Oilcrops/Documents/Food_outlook_oilseeds/FO_Oilcrops.pdf [Accessed March 25, 2019].

**Faralli, M., Matthews, J. and Lawson, T.** (2019) Exploiting natural variation and genetic manipulation of stomatal conductance for crop improvement. *Curr. Opin. Plant Biol.*, **49**, 1–7.

**Fiorin, L., Brodribb, T.J. and Anfodillo, T.** (2016) Transport efficiency through uniformity: organization of veins and stomata in angiosperm leaves. *New Phytol.*, **209**, 216–227.

**Gudesblat, G.E., Schneider-Pizoń, J., Betti, C., et al.** (2012) SPEECHLESS integrates brassinosteroid and stomata signalling pathways. *Nat. Cell Biol.*, **14**, 548–554.

**Gupta, P.K., Kulwal, P.L. and Jaiswal, V.** (2019) Chapter Two - Association mapping in plants in the post-GWAS genomics era. In D. Kumar, ed. *Advances in Genetics*. Academic Press, pp. 75–154.

**Hara, K., Yokoo, T., Kajita, R., Onishi, T., Yahata, S., Peterson, K.M., Torii, K.U. and Kakimoto, T.** (2009) Epidermal cell density is autoregulated via a secretory peptide, EPIDERMAL PATTERNING FACTOR 2 in Arabidopsis leaves. *Plant Cell Physiol.*, **50**, 1019–1031.

**Harrison, E.L., Arce Cubas, L., Gray, J.E. and Hepworth, C.** (2019) The influence of stomatal morphology and distribution on photosynthetic gas exchange. *The Plant Journal*, **101**, 768–779.

**Haworth, M., Marino, G., Loreto, F. and Centritto, M.** (2021) Integrating stomatal physiology and morphology: evolution of stomatal control and development of future crops. *Oecologia*, **197**, 867–883.

**Hetherington, A.M. and Woodward, F.I.** (2003) The role of stomata in sensing and driving environmental change. *Nature*, **424**, 901–908.

**Hilu, K. and Randall, J.** (1984) Convenient method for studying grass leaf epidermis. *Taxon*, **33**, 413–415.

**Horikoshi, M. and Tang, Y.** (2018) ggfortify: Data Visualization Tools for Statistical Analysis Results. Available at: https://CRAN.R-project.org/package=ggfortify.

**Hübner, S., Bercovich, N., Todesco, M., et al.** (2019) Sunflower pan-genome analysis shows that hybridization altered gene content and disease resistance. *Nat Plants*, **5**, 54–62.

**Hussain, M., Farooq, S., Hasan, W., Ul-Allah, S., Tanveer, M., Farooq, M. and Nawaz, A.** (2018) Drought stress in sunflower: Physiological effects and its management through breeding and agronomic alternatives. *Agric. Water Manage.*, **201**, 152–166.

**IPCC** (2014) Climate Change 2014: Synthesis Report. Contribution of Working Groups I, II and III to the Fifth Assessment Report of the Intergovernmental Panel on Climate Change. *Intergovernmental Panel on Climate Change*.

**John, G.P., Scoffoni, C., Buckley, T.N., Villar, R., Poorter, H. and Sack, L.** (2017) The anatomical and compositional basis of leaf mass per area. *Ecol. Lett.*, **20**, 412–425.

**Kawai, K. and Okada, N.** (2016) How are leaf mechanical properties and water-use traits coordinated by vein traits? A case study in Fagaceae J. Watling, ed. *Funct. Ecol.*, **30**, 527–536.

**Khan, M.U., Chowdhry, M.A., Khaliq, I. and Ahmad, R.** (2003) Morphological response of various genotypes to drought conditions. *Asian J. Plant Sci.*, **2**, 392–394.

**Kruijer, W., Boer, M.P., Malosetti, M., Flood, P.J., Engel, B., Kooke, R., Keurentjes, J.J.B. and Eeuwijk, F.A. van** (2015) Marker-based estimation of heritability in immortal populations. *Genetics*, **199**, 379–398.

**Kruijer, W., Padraic Flood, W. a. C.F.I.W.C.D.C. by and Kooke., R.** (2019) heritability: Marker-Based Estimation of Heritability Using Individual Plant or Plot Data. Available at: https://CRAN.R-project.org/package=heritability.

**Lei, Z.Y., Han, J.M., Yi, X.P., Zhang, W.F. and Zhang, Y.L.** (2018) Coordinated variation between veins and stomata in cotton and its relationship with water-use efficiency under drought stress. *Photosynthetica*, **56**, 1326–1335.

**Lenth, R.** (2020) emmeans: Estimated Marginal Means, aka Least-Squares Means. Available at: https://CRAN.R-project.org/package=emmeans.

**Liu, A. and Burke, J.M.** (2006) Patterns of nucleotide diversity in wild and cultivated sunflower. *Genetics*, **173**, 321–330.

**Ma, L., Qing, C., Zhang, M., Zou, C., Pan, G. and Shen, Y.** (2021) GWAS with a PCA uncovers candidate genes for accumulations of microelements in maize seedlings. *Physiol. Plant.*, **172**, 2170–2180.

**Mandel, J.R., Dechaine, J.M., Marek, L.F. and Burke, J.M.** (2011) Genetic diversity and population structure in cultivated sunflower and a comparison to its wild progenitor, *Helianthus annuus* L. *Theor. Appl. Genet.*, **123**, 693–704.

**Mandel, J.R., Nambeesan, S., Bowers, J.E., Marek, L.F., Ebert, D., Rieseberg, L.H., Knapp, S.J. and Burke, J.M.** (2013) Association mapping and the genomic consequences of selection in sunflower. *PLoS Genet.*, **9**, e1003378.

**Masalia, R.R., Temme, A.A., Torralba, N. de L. and Burke, J.M.** (2018) Multiple genomic regions influence root morphology and seedling growth in cultivated sunflower (*Helianthus annuus* L.) under well-watered and water-limited conditions. *PLoS One*, **13**, e0204279.

**Méndez-Alonzo, R., Ewers, F.W. and Sack, L.** (2013) Ecological variation in leaf biomechanics and its scaling with tissue structure across three Mediterranean-climate plant communities. *Funct. Ecol.*, **27**, 544–554.

**Muir, C.D.** (2018) Light and growth form interact to shape stomatal ratio among British angiosperms. *New Phytol.*, **218**, 242–252.

**Muir, C.D., Pease, J.B. and Moyle, L.C.** (2014) Quantitative genetic analysis indicates natural selection on leaf phenotypes across wild tomato species (*Solanum* sect. *Lycopersicon*; Solanaceae). *Genetics*, **198**, 1629–1643.

**Murphy, Dow and Jordan** (2017) Vein density is independent of epidermal cell size in Arabidopsis mutants. *Funct. Plant Biol.*, **44**, 410–418.

**NOAA** Drought: Monitoring Economic, Environmental, and Social Impacts. *NOAA: National Centers for Environmental Information*. Available at: https://www.ncdc.noaa.gov/news/drought-monitoring-economic-environmental-and-social-impacts [Accessed May 11, 2021].

**Nozaki, M., Kawade, K., Horiguchi, G. and Tsukaya, H.** (2020) an3-Mediated Compensation Is Dependent on a Cell-Autonomous Mechanism in Leaf Epidermal Tissue. *Plant Cell Physiol.*, **61**, 1181–1190.

**Park, B. and Burke, J.M.** (2020) Phylogeography and the Evolutionary History of Sunflower (*Helianthus annuus* L.): Wild Diversity and the Dynamics of Domestication. *Genes*, **11**, 266.

**Poorter, H., Niinemets, Ü., Poorter, L. and Wright, I.J.** (2009) Causes and consequences of variation in leaf mass per area (LMA): a meta-analysis. *New*, **182**, 565–588.

**R Core Team** (2013) *R: The R project for statistical computing*, Available at: https://www.r-project.org/ [Accessed April 17, 2019].

**Reich, P.B.** (2014) The world-wide "fast–slow"plant economics spectrum: a traits manifesto. *The Journal of Ecology*, **102**, 275–301.

**Richardson, F., Jordan, G.J. and Brodribb, T.J.** (2020) Leaf hydraulic conductance is linked to leaf symmetry in bifacial, amphistomatic leaves of Sunflower. *J. Exp. Bot.*, **71**, 2808–2816.

**Ries, L.L., Purcell, L.C., Carter, T.E., Edwards, J.T. and King, C.A.** (2012) Physiological Traits Contributing to Differential Canopy Wilting in Soybean under Drought. *Crop Sci.*, **52**, 272–281.

**Ronneberger, O., Fischer, P. and Brox, T.** (2015) U-Net: Convolutional networks for biomedical image segmentation. In *Medical Image Computing and Computer-Assisted Intervention – MICCAI 2015*. Springer International Publishing, pp. 234–241.

**Sack, L. and Scoffoni, C.** (2013) Leaf venation: structure, function, development, evolution, ecology and applications in the past, present and future. *New Phytologist*, **198**, 983–1000.

**Sack, L. and Scoffoni, C.** (2012) Measurement of leaf hydraulic conductance and stomatal conductance and their responses to irradiance and dehydration using the Evaporative Flux Method (EFM). *Journal of Visualized Experiments*, e4179.

**Schindelin, J., Arganda-Carreras, I., Frise, E., et al.** (2012) Fiji: an open-source platform for biological-image analysis. *Nature Methods*, **9**, 676–682.

**Scoffoni, C., Rawls, M., McKown, A., Cochard, H. and Sack, L.** (2011) Decline of leaf hydraulic conductance with dehydration: relationship to leaf size and venation architecture. *Plant Physiol.*, **156**, 832–843.

**Scoffoni, C. and Sack, L.** (2013) Quantifying leaf vein traits. *Prometheus Wiki*. Available at: http://prometheuswiki.org/tiki-index.php?page=Quantifying+leaf+vein+traits&highlight=leaf%20clearing [Accessed March 21, 2019].

**Shahinnia, F., Le Roy, J., Laborde, B., Sznajder, B., Kalambettu, P., Mahjourimajd, S., Tilbrook, J. and Fleury, D.** (2016) Genetic association of stomatal traits and yield in wheat grown in low rainfall environments. *BMC Plant Biology*, **16**, 150.

**Shi, P., Jiao, Y., Diggle, P.J., Turner, R., Wang, R. and Niinemets, Ü.** (2021) Spatial distribution characteristics of stomata at the areole level in Michelia cavaleriei var. platypetala (Magnoliaceae). *Ann. Bot.*, **128**, 875–886.

**Simonin, K.A. and Roddy, A.B.** (2018) Genome downsizing, physiological novelty, and the global dominance of flowering plants. *PLoS Biol.*, **16**, e2003706.

**Tang, Y., Horikoshi, M. and Li, W.** (2016) ggfortify: Unified Interface to Visualize Statistical Result of Popular R Packages. *The R Journal*, **8**. Available at: https://journal.r-project.org/.

**Temme, A.A., Kerr, K.L., Masalia, R.R., Burke, J.M. and Donovan, L.A.** (2020) Key Traits and Genes Associate with Salinity Tolerance Independent from Vigor in Cultivated Sunflower. *Plant Physiol.*, **184**, 865–880.

**Todesco, M., Owens, G.L., Bercovich, N., et al.** (2020) Massive haplotypes underlie ecotypic differentiation in sunflowers. *Nature*, **584**, 602–607.

**Vasco, A., Thadeo, M., Conover, M. and Daly, D.C.** (2014) Preparation of samples for leaf architecture studies, a method for mounting cleared leaves. *Appl. Plant Sci.*, **2**, 1400038.

**Walls, R.L.** (2011) Angiosperm leaf vein patterns are linked to leaf functions in a global-scale data set. *American Journal of Botany*, **98**, 244–253.

**Wang, Y., Donovan, L.A. and Temme, A.A.** (2020) Plasticity and the role of mass-scaling in allocation, morphology, and anatomical trait responses to above- and belowground resource limitation in cultivated sunflower *(Helianthus annuus* L.). *Plant Direct*, **4**, e02924.

**Wei, T. and Simko, V.** (2017) *R package "corrplot": Visualization of a Correlation Matrix*, Available at: https://github.com/taiyun/corrplot.

**Weyers, J.D.B. and Johansen, L.G.** (1985) Accurate Estimation of Stomatal Aperture from Silicone Rubber Impressions. *New Phytol.*, **101**, 109–115.

**Wickham, H.** (2016) ggplot2: Elegant Graphics for Data Analysis. Available at: https://ggplot2.tidyverse.org.

**Wills, D.M. and Burke, J.M.** (2006) Chloroplast DNA variation confirms a single origin of domesticated sunflower (*Helianthus annuus* L.). *J. Hered.*, **97**, 403–408.

**Wright, I.J., Reich, P.B., Westoby, M., et al.** (2004) The worldwide leaf economics spectrum. *Nature*, **428**, 821–827.

**Xing, K., Niinemets, Ü., Rengel, Z., Onoda, Y., Xia, J., Chen, H.Y.H., Zhao, M., Han, W. and Li, H.** (2021) Global patterns of leaf construction traits and their covariation along climate and soil environmental gradients. *New Phytol.*, **232**, 1648–1660.

**Xiong, D. and Flexas, J.** (2020) From one side to two sides: the effects of stomatal distribution on photosynthesis. *New Phytol.*, **228**, 1754–1766.

**Xu, H., Blonder, B., Jodra, M., Malhi, Y. and Fricker, M.** (2020) Automated and accurate segmentation of leaf venation networks via deep learning. *New Phytol.*, **229**, 631–648.

**Yano, K., Morinaka, Y., Wang, F., et al.** (2019) GWAS with principal component analysis identifies a gene comprehensively controlling rice architecture. *Proc. Natl. Acad. Sci. U. S. A.*, **116**, 21262–21267.

**Zhang, S.-B., Guan, Z.-J., Sun, M., Zhang, J.-J., Cao, K.-F. and Hu, H.** (2012) Evolutionary association of stomatal traits with leaf vein density in *Paphiopedilum*, Orchidaceae. *PLoS One*, **7**, e40080.

**Zhao, W.-L., Siddiq, Z., Fu, P.-L., Zhang, J.-L. and Cao, K.-F.** (2017) Stable stomatal number per minor vein length indicates the coordination between leaf water supply and demand in three leguminous species. *Sci. Rep.*, **7**, 2211.

**Zheng, X., Levine, D., Shen, J., Gogarten, S.M., Laurie, C. and Weir, B.S.** (2012) A high-performance computing toolset for relatedness and principal component analysis of SNP data. *Bioinformatics*, **28**, 3326–3328.

**Zhou, X. and Stephens, M.** (2012) Genome-wide efficient mixed-model analysis for association studies. *Nat. Genet.*, **44**, 821–824.

FIGURES

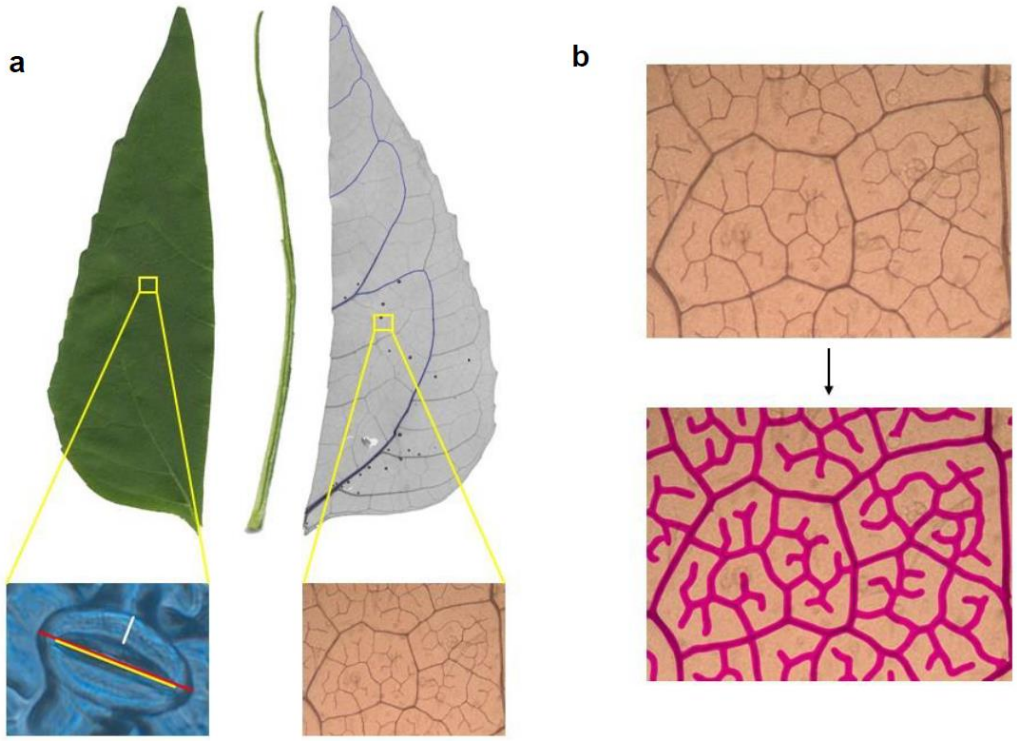


**Figure 2.1**: (a) Left: Image of dissected leaf. Right: Cleared and stained leaf showing major veins (green). Left Inset: A single stoma taken using the100x objective. Colored lines indicate measurements taken: stomate length (red), pore length (yellow), and guard cell width (white). Right Inset: A microscope image of minor veins taken using the 5x objective. (b) Top: Image of minor veins taken at 5x. Bottom: Image of computer-traced minor veins using our deep learning approach. See Methods for details.

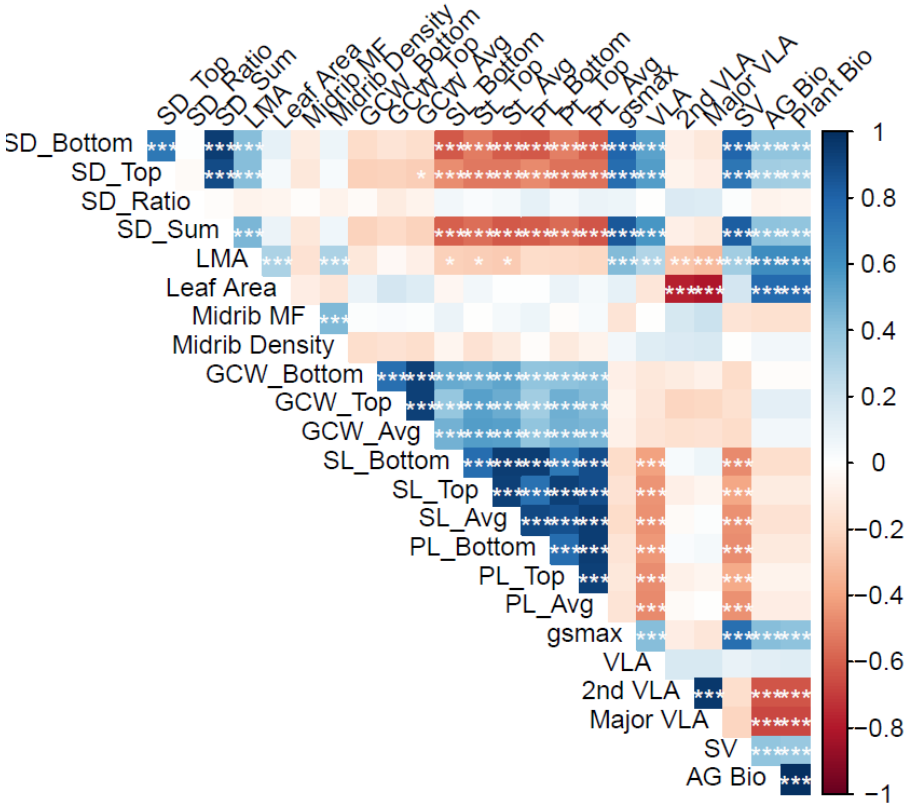


**Figure 2.2**: Correlation matrix of leaf traits. Values were calculated using genotype marginal means and significance tests were corrected for multiple comparisons using a Bonferroni correction. Positive correlations are in blue and negative correlations are in red. Shading gives a relative indication of the magnitude of the estimate. ***$P \leq 0.001$, **$P \leq 0.01$, * $P \leq 0.05$. Trait abbreviations are as defined in Table 2.1.

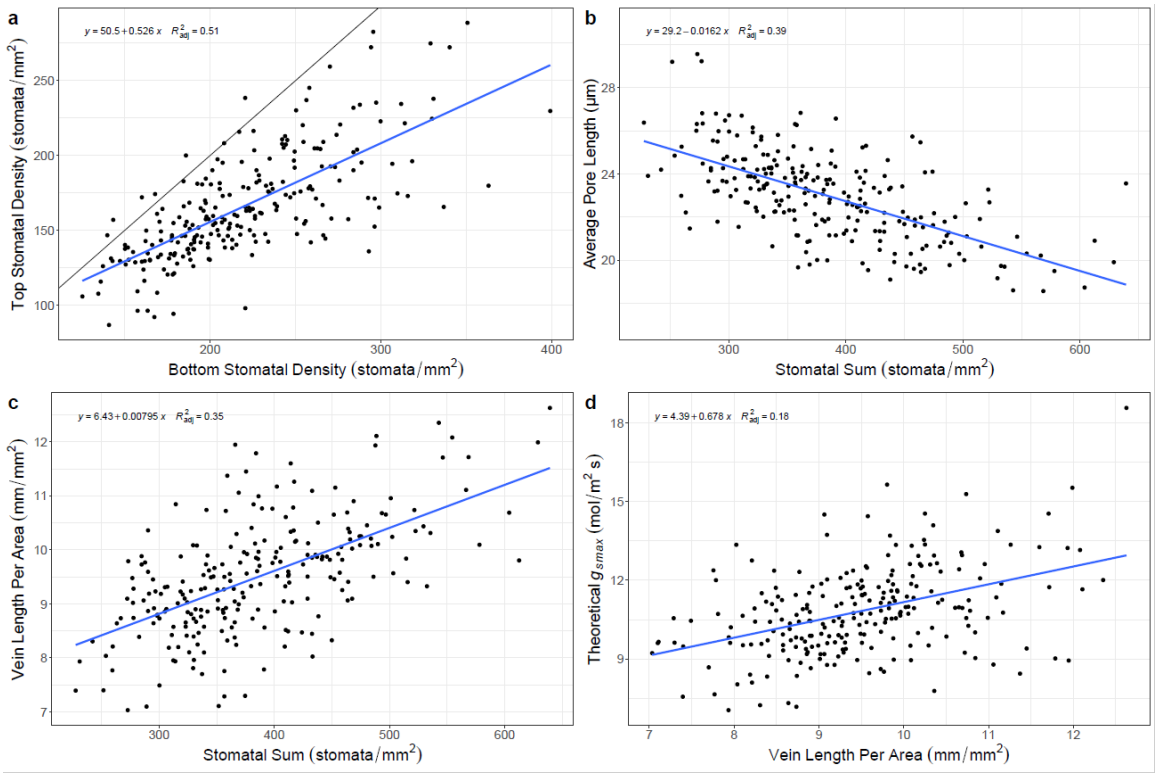


**Figure 2.3**: Example bivariate trait plots. In all panels, the blue line is the best fit. (a) Top vs. bottom stomatal density (black line is 1:1). (b) Average (top and bottom) stomatal pore length vs. stomatal sum. (c) Vein length per area vs. stomatal sum. (d) Theoretical stomatal conductance ($g_{smax}$) vs. vein length per area.

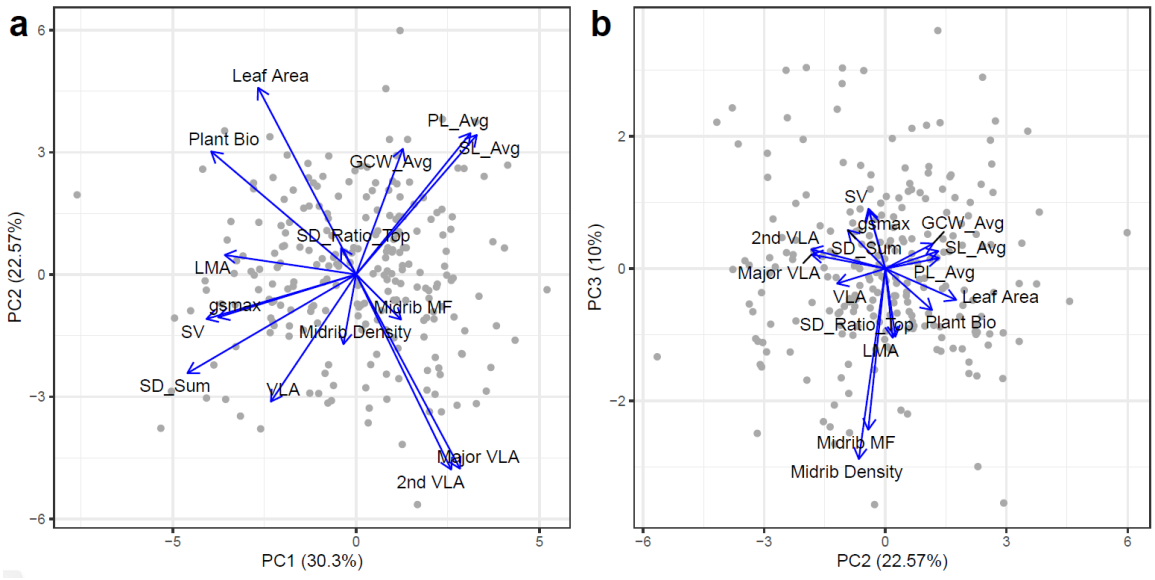


**Figure 2.4**: Principal component analysis (PCA) of leaf traits using estimated marginal means for each trait. (A) PC1 vs. PC2. (B) PC2 vs. PC3. Traits names that include _Avg (stomatal length [SL], pore length [PL], guard cell width [GCW]) are averages of the values from the top and bottom of the leaf and SD_Sum is the sum of stomatal density from the top and bottom. Trait abbreviations are as defined in Table 2.1.

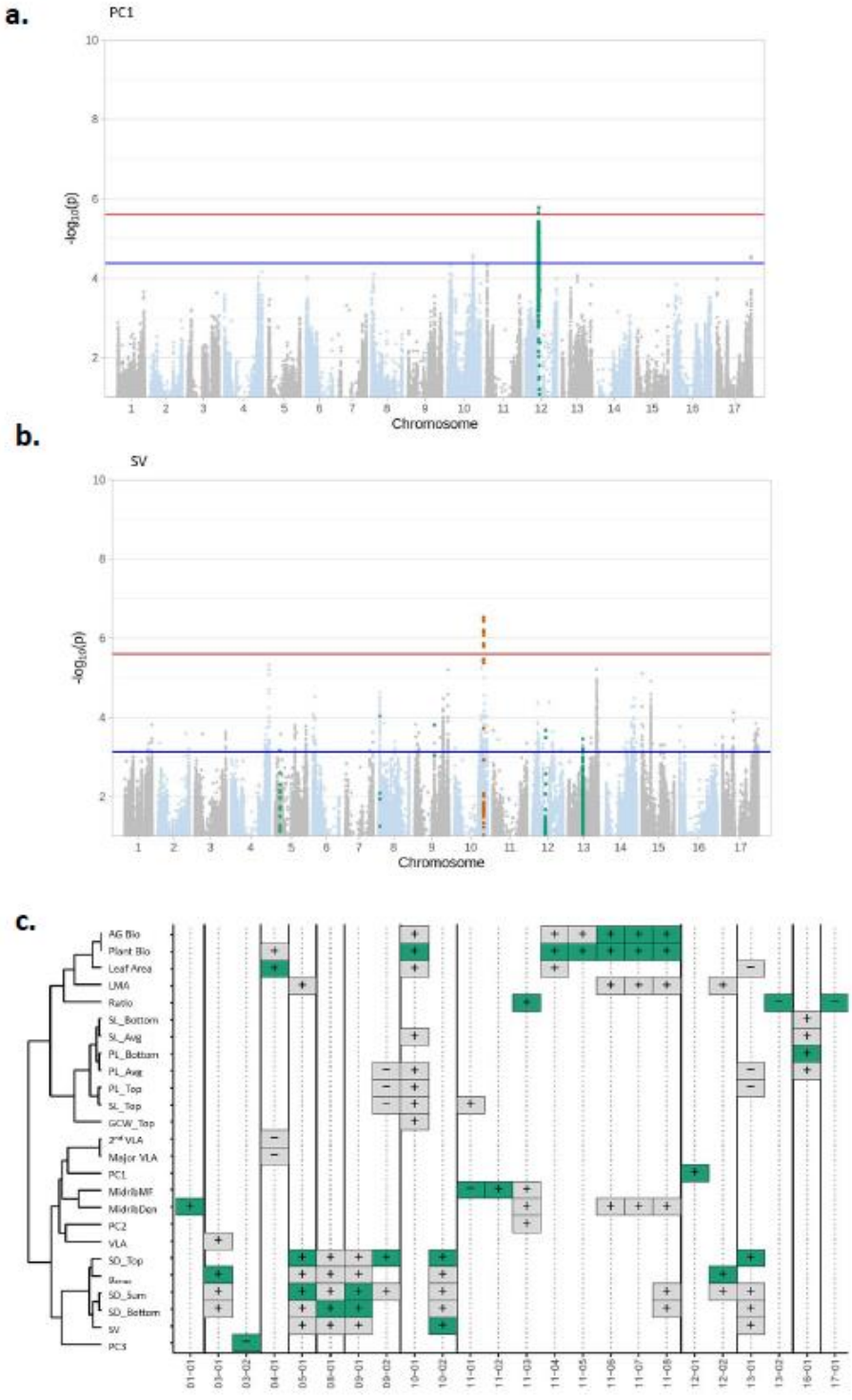
a.
PC1
-log10(p)
Chromosome
b.
SV
-log10(p)
Chromosome
c.
AG Bio
Plant Bio
Leaf Area
LMA
Ratio
SL_Bottom
SL_Avg
PL_Bottom
PL_Avg
PL_Top
SL_Top
GCW_Top
2nd VLA
Major VLA
PC1
MidribMF
MidribDen
PC2
VLA
SD_Top
SD_Sum
SD_Bottom
SV
PC3

**Figure 2.5**: Examples and summary of GWA results. (a) Manhattan plot of PC1 showing the single significantly associated region on chromosome 12. (b) Manhattan plot of stomata per vein length (SV) showing the single significantly associated region on chromosome 10 and suggestive associations on chromosomes 5, 6, 8, and 13. In both plots, the red line is the significance threshold based on the modified Bonferroni correction and the blue line is the suggestive threshold based on the top 0.1% of all SNPs. Differently colored dots represent all SNPs in a region that are significant or suggestive for at least one trait. (c) Visual summary of all GWA results highlighting colocalization within regions. The dendrogram to the left is based on hierarchical clustering of trait correlations. Green and gray boxes indicate significant or suggestive associations with a given trait, respectively. The sign (+/-) refers to the sign of β (the effect of the minor allele on the trait value). Regions are numbered numerically within chromosomes and box/region sizes are arbitrary. Ratio refers to the stomatal ratio. Trait abbreviations are otherwise as defined in Table 2.1.

TABLES

**Table 2.1**: List of all traits measured along with the median and range of trait values. Significance for genotypic effects (***P ≤ 0.001, **P ≤ 0.01, * P ≤ 0.05, ns = not significant) and adjusted R2 from the model are also presented. SD = stomatal density; LMA = leaf mass per area; MF = mass fraction; GCW = guard cell width; SL = stomatal length; PL = stomatal pore length; $g_{smax}$ = theoretical maximum stomatal conductance; VLA = vein length per area; SV = stomata per vein length; AG = aboveground; Bio = biomass.

| Trait | Median | Min | Max | Genotypic Effect | Adjusted $R^2$ |
|---|---|---|---|---|---|
| SD_Bottom (stomata/mm$^2$) | 211.20 | 125.17 | 399.17 | *** | 0.24 |
| SD_Top (stomata/mm$^2$) | 158.72 | 86.73 | 288.62 | *** | 0.21 |
| SD_Sum (stomata/mm$^2$) | 373.37 | 227.50 | 369.30 | *** | 0.25 |
| Stomatal Ratio (bottom/sum) | 0.57 | 0.48 | 0.68 | *** | 0.16 |
| LMA (g/m$^2$) | 22.56 | 12.28 | 32.03 | *** | 0.33 |
| Leaf Area (m$^2$) | 0.0096 | 0.0035 | 0.0228 | *** | 0.48 |
| Midrib MF ($g_{midrib}/g_{leaf}$) | 0.07 | 0.03 | 0.10 | ns | 0.04 |
| Midrib Density (mg/cm$^3$) | 67.49 | 33.93 | 118.86 | * | 0.10 |
| GCW_Bottom (µm) | 6.51 | 5.28 | 8.00 | ** | 0.09 |
| GCW_Top (µm) | 5.94 | 4.67 | 7.79 | *** | 0.12 |
| GCW_Avg (µm) | 6.24 | 4.98 | 7.89 | *** | 0.12 |
| SL_Bottom (µm) | 33.31 | 27.74 | 42.09 | *** | 0.18 |
| SL_Top (µm) | 30.60 | 25.62 | 36.63 | *** | 0.15 |
| SL_Avg (µm) | 32.09 | 26.81 | 39.36 | *** | 0.19 |
| PL_Bottom (µm) | 24.26 | 19.02 | 31.95 | *** | 0.21 |
| PL_Top (µm) | 21.78 | 16.90 | 29.19 | *** | 0.16 |
| PL_Avg (µm) | 23.13 | 18.57 | 29.55 | *** | 0.20 |
| $g_{smax}$ (mol/m$^2$s) | 10.73 | 7.05 | 18.56 | *** | 0.35 |
| VLA (mm/mm$^2$) | 9.48 | 7.03 | 12.63 | *** | 0.23 |
| 2nd VLA (mm/mm$^2$) | 0.07 | 0.02 | 0.14 | *** | 0.19 |
| Major VLA (mm/mm$^2$) | 0.10 | 0.05 | 0.20 | *** | 0.21 |
| SV (stomata/mm) | 19.82 | 12.99 | 31.84 | *** | 0.24 |
| AG Bio (g) | 3.78 | 0.80 | 9.45 | *** | 0.53 |
| Plant Bio (g) | 4.31 | 1.01 | 10.65 | *** | 0.53 |

**Table 2.2**: Trait loadings percentage of trait variation explained by each trait in the associated principal component) of first three principal components (PC). The top three traits per PC are highlighted in bold and with the ranking of the traits for each PC in parentheses. Trait abbreviations are as defined in Table 2.1.

| Traits | PC1 | PC2 | PC3 |
|---|---|---|---|
| **SD_Sum** | **16.08 (1)** | 4.46 (9) | 1.76 (8) |
| **SD_Ratio** | 0.13 (14) | 0.32 (14) | 5.48 (4) |
| **LMA** | 9.75 (5) | 0.17 (15) | **5.66 (3)** |
| **Leaf Area** | 5.42 (9) | **15.94 (3)** | 1.16 (9) |
| **Midrib MF** | 1.14 (13) | 0.93 (11) | **30.73 (2)** |
| **Midrib Density** | 0.09 (15) | 2.22 (10) | **42.88 (1)** |
| **GCW_Avg** | 1.23 (12) | 7.23 (7) | 0.74 (10) |
| **SL_Avg** | 8.21 (6) | 8.90 (5) | 0.36 (12) |
| **PL_Avg** | 7.38 (7) | 9.13 (4) | 0.13 (15) |
| $g_{smax}$ | 10.75 (4) | 0.84 (13) | 3.89 (6) |
| **VLA** | 4.11 (11) | 7.39 (6) | 0.26 (13) |
| **2nd VLA** | 5.10 (10) | **17.40 (1)** | 0.44 (11) |
| **Major VLA** | 6.09 (8) | **17.24 (2)** | 0.24 (14) |
| **SV** | **12.65 (2)** | 0.91 (12) | 4.25 (5) |
| **Plant Bio** | **11.87 (3)** | 6.92 (8) | 2.03 (7) |

**Table 2.3**: List of all traits measured along with estimated narrow sense heritabilities, numbers of significantly associated regions, and total relative effect sizes (RES Sum). Trait abbreviations are as defined in Table 2.1.

| Trait | $h^2$ | No. Reg. | RES Sum |
|---|---|---|---|
| SD_Bottom (stomata/mm$^2$) | 0.18 (0.10-0.26) | 2 | 45.2 |
| SD_Top (stomata/mm$^2$) | 0.13 (0.07-0.20) | 4 | 89.6 |
| SD_Sum (stomata/mm$^2$) | 0.16 (0.09-0.24) | 2 | 61.3 |
| Stomatal Ratio (bottom/sum) | 0.12 (0.05-0.19) | 3 | 53.8 |
| LMA (g/m$^2$) | 0.32 (0.22-0.41) | - | - |
| Leaf Area (m$^2$) | 0.08 (0.04-0.12) | 1 | 15.4 |
| Midrib MF ($g_{midrib}/g_{leaf}$) | 0.05 (-0.01-0.12) | 2 | 20.8 |
| Midrib Density (mg/cm$^3$) | 0.05 (-0.01-0.10) | 1 | 12.3 |
| GCW_Bottom (µm) | 0.08 (0.03-0.14) | - | - |
| GCW_Top (µm) | 0.11 (0.05-0.17) | - | - |
| GCW_Avg (µm) | 0.10 (0.04-0.16) | - | - |
| SL_Bottom (µm) | 0.17 (0.09-0.25) | - | - |
| SL_Top (µm) | 0.14 (0.08-0.21) | - | - |
| SL_Avg (µm) | 0.18 (0.10-0.25) | - | - |
| PL_Bottom (µm) | 0.20 (0.12-0.28) | 1 | 22.2 |
| PL_Top (µm) | 0.15 (0.08-0.22) | - | - |
| PL_Avg (µm) | 0.19 (0.11-0.27) | - | - |
| $g_{smax}$ (mol/m$^2$s) | 0.27 (0.18-0.36) | 2 | 39.8 |
| VLA (mm/mm$^2$) | 0.06 (0-0.11) | - | - |
| 2nd VLA (mm/mm$^2$) | 0.05 (0.02-0.09) | - | - |
| Major VLA (mm/mm$^2$) | 0.11 (0.05-0.17) | - | - |
| SV (stomata/mm) | 0.23 (0.15-0.31) | 1 | 19.1 |
| AG Bio (g) | 0.49 (0.40-0.58) | 3 | 41.0 |
| Plant Bio (g) | 0.46 (0.37-0.56) | 6 | 84.3 |

# CHAPTER 3

# LEAF TRAITS PREDICT PLANT PERFORMANCE UNDER VARYING LEVELS OF DROUGHT STRESS IN CULTIVATED SUNFLOWER (*HELIANTHUS ANNUUS* L.)[2]

[2] Earley, Ashley M, Kristen M. Nolting, John M. Burke. To be submitted to *AoB Plants.*

ABSTRACT

Drought is a major challenge for agriculture and is only expected to worsen with climate change. Exploring plant traits and how they respond to drought has the potential to improve our understanding of drought tolerance and thereby inform breeding efforts to develop more drought tolerant plants. Given their importance in plant-water relations, we explored variation and plasticity in leaf traits in response to water limitation in cultivated sunflower (*Helianthus annuus* L.). A set of four sunflower genotypes was grown under four different levels of water availability and leaf vein and stomatal traits were measured along with total biomass (as an indicator of overall performance), leaf mass per area (LMA), chlorophyll content, and various mass fraction traits related to resource allocation (e.g., leaf, root, and stem mass fraction). Traits exhibited numerous bivariate correlations within treatments that generally followed expectations based on the literature. For example, stomatal size and density were negatively correlated while stomatal density and vein length per area (VLA) were positively correlated. Most traits also exhibited substantial plasticity, as evidenced by significant shifts in trait values across environments and multivariate analyses revealed differentiation in trait space across treatment levels. This included an overall reduction in growth/productivity in response to stress, accompanied by a shift in traits relating to gas exchange and hydraulics including stomatal and vein density (increased), stomatal size (decreased), and theoretical $g_{smax}$ (increased). We found that variation in performance across treatments (estimated as total biomass) can be largely explained by a small number of putatively

size-independent traits (i.e., VLA, stomatal length and density and LMA; $R^2 = 0.74$). Moreover, on average, more extreme changes in VLA were associated with more extreme decreases in performance across environments. Taken together, these results indicate that a small number of leaf traits can predict plant performance, with plasticity in VLA being the best predictor of changes in productivity.

## INTRODUCTION

Drought is a major agricultural challenge that limits plant growth and productivity worldwide (Munns, 2011). As climate change worsens, droughts are expected to increase in frequency and severity (Foley *et al.*, 2011; Munns, 2011; IPCC, 2014). Moreover, the human population is expected to increase from a current size of 7.6 billion to 9.8 billion by 2050 (United Nations, 2017). This poses a challenge as the growing population size will increase food demand while much of our agricultural land will be increasingly impacted by environmental stresses including drought. To address this challenge, we need crop plants that are better able to withstand environmental challenges such as drought. A better understanding of the response of key traits to stress will facilitate efforts to develop more resilient crops. For example, given their influence on hydraulics and gas exchange, leaf anatomical traits such as stomatal and vein-related traits have been the subject of considerable interest in the context of drought (e.g, Bresta *et al.*, 2018; Du *et al.*, 2021; Lei *et al.*, 2018). Interestingly, associations between these sorts of traits and relevant aspects of the environment have been observed both across and within species suggesting a possible role for such traits in adaptation to drier environments (e.g., Bresta

*et al*, 2018; Lei *et al* 2018). For instance, in barley, plants with smaller and denser stomata as well as denser veins showed less dramatic changes in these traits under drought (Bresta *et al*, 2018).

When looking across species, vein density and stomatal density are positively correlated with each other (Sack and Scoffoni, 2013), while stomatal density and size are negatively correlated (Shahinnia *et al.*, 2016; Doheny-Adams *et al.*, 2012). This relationship between stomatal size/density and vein density (estimated as vein length per area; VLA) is important for optimization of water transport and transpiration (Fiorin *et al.*, 2016; Bertolino *et al.*, 2019). Consistent with a role for such traits in adaptation to dry environments, populations of plants occupying increasingly arid habitats exhibit a trend toward smaller and more dense stomata (Xie, Wang, and Li 2022; Dunlap and Stettler 2001). For example, across 19 *Protea repens* populations, stomatal density in a common garden was found to correlate negatively with summer rainfall levels. In addition to inherent differences between populations, these traits have also been shown to exhibit plastic responses to water limitation. For example, plants often shift toward increased VLA, higher stomatal density, and smaller stomata under drought vs. well-watered conditions (Sack and Scoffoni, 2013; Sun *et al.*, 2014). These changes are thought to improve gas exchange by decreasing the distance from veins to stomata, thereby improving photosynthetic efficiency by increasing leaf-level water use efficiency while limiting water loss (Brodribb *et al.*, 2007; Bertolino *et al.*, 2019). This allows for more carbon to be assimilated per unit of water used by the plant. Because smaller stomata can typically close more quickly due to faster ion fluxes, stomatal conductance can likewise

change quickly (Bertolino *et al.*, 2019; Drake *et al.*, 2013). This behavior allows plants to reduce transpiration in response to drying while still allowing them to rapidly "gear up" when water is available (Sack and Scoffoni, 2013).

Studies of leaf trait plasticity in response to drought have also found a general tendency toward increasingly large trait changes across increasing stress severity. More specifically, decreases in stomatal size and increases in stomatal density and VLA are generally more pronounced as drought severity increases (Lei *et al.*, 2018; Wang *et al.*, 2018; Stojnić *et al.*, 2015; Bresta *et al.*, 2018). For instance, there was an increase in stomatal and vein density with increased drought severity in cotton (Lei *et al.*, 2018). Similarly, more severe drought resulted in increased stomatal and vein density along with decreased stomatal size in barley (Bresta *et al.*, 2018). These observations suggest a potential role for leaf trait plasticity in mitigating the effects of drought, suggesting that the modification of leaf traits might be a reasonable strategy for breeding plants that are more drought resilient. There is, however, a paucity of research that explicitly explores the association of variation in both stomatal and vein traits with performance across multiple levels of drought severity. Here we investigate patterns of leaf trait variation, plasticity, and overall performance in response to varying levels of drought stress in cultivated sunflower (*Helianthus annuus* L.).

Cultivated sunflower is one of the world's most important oilseed crops (FAO, 2018) and an important source of confectionery seeds and ornamental flowers. Because it is often grown on non-irrigated land, sunflower productivity can be largely dependent on

natural patterns of precipitation (Meyer, 1999). While sunflower roots deeply and is able to avoid drought once established (Connor and Sadras, 1992), drought remains a major yield-limiting factor across much of the range of production (Hussain *et al.*, 2018). As such, the investigation of drought tolerance and associated traits remains a vital avenue of research. Considering the role that leaf traits play in plant-water relations (Sack and Scoffoni, 2013; Buckley, 2019), they are a potentially important consideration when developing plants that can maintain performance under drought. Previous research in sunflower has shown considerable genetic variability in leaf anatomical traits (Earley et al. 2022) as well as substantial phenotypic plasticity in their response to environmental challenges including light- and nutrient-limitation (Wang *et al.*, 2020), but little is known about the role of such traits in the response to drought in sunflower. The focus of the present study is on the impact of varying levels of water limitation on leaf anatomical traits and their relationship with overall growth/performance. More specifically, we sought to: (1) evaluate patterns of leaf trait variation and covariation within and across varying levels of water availability; (2) quantify trait plasticity in response to water limitation; and (3) determine the relationship between observed trait variation and plasticity and performance across varying levels of drought stress.

## METHODS

### *Experimental design*

In the summer of 2019, four inbred lines from the sunflower association mapping (SAM) population (Mandel *et al.*, 2011) were grown in the Botany Greenhouses at the University of Georgia under a range of watering treatments. These lines correspond to RHA 436 (SAM 33), RHA 364 (SAM 61), INRA line SF 076 (SAM 273), and INRA line SF 075 (SAM 282). These lines were chosen to cover a range of stomatal densities based on observations from Earley *et al.* (Chapter 2; 2022) The experimental design, which included four treatments with four replicates of each genotype in each treatment (N = 4 x 4 x 4 = 64 total individuals), were grown in the greenhouse in a randomized block design. Following germination, all plants were grown for one week in seedling trays to allow for establishment before being transplanted into 7.6 L plastic pots (HPP200; Haviland Plastic Products, Haviland, OH) filled with a 3:1 mixture of sand and a calcined clay mixture (Turface MVP, Turface Athletics). Greenhouse temperature generally ranged from 82-84°F during the day and 72-74°F at night. Individual pots were fertilized with 60 g Osmocote Plus (15-12-9 NPK; Scotts Miracle-Gro, Marysville, OH) and 15 mL each of gypsum (Performance Minerals Corporation, Birmingham, 136 AL) and lime (Austinville Limestone, Austinville, VA) powders for supplemental $Ca^{2+}$. Pots were randomly assigned to one of four treatments: a well-watered control treatment and three drought treatments of varying severity. These treatments were implemented based on the weight of each pot when fully watered. The well-watered control treatment was re-watered daily

to 100% of pot capacity while the drought treatments were re-watered to 60%, 40%, and 20% of their capacity based on pot weight (Figure S3.1). This was done by weighing each pot (with substrate) when fully dry (i.e., substrate before watering and after allowing to sit for three days in the greenhouse) and fully saturated (i.e., pots watered thoroughly and weighed once no longer dripping) to estimate the amount of water required to fully saturate the substrate and determine a target weight for each pot. For context, when converted to gravimetric water content (see below), these treatments correspond to an average of 23.6%, 14.1%, 9.2%, and 4.7% gravimetric water content for the well-watered, mild, moderate, and severe treatments, respectively.

Gravimetric water content = (mass of water / mass of sand mixture) * 100

Hereafter, the four treatments will be referred to as the well-watered (100%), mild (60%), moderate (40%), and severe (20%) drought treatments. Following transplantation and initial saturation of the soil, the plants were allowed to acclimate for three days before the treatments commenced. Once the treatments started, pots were re-weighed daily between 9:00-11:00 AM using a postage scale (PS-IN202; Prime Scales, Chino, CA) and allowed to dry to their target levels. Generally, pots for each treatment reached target levels around the same time. Once they dipped below their target weight, pots were individually re-watered to bring them back to their target weight. Note that, while the plants in the severe treatment experienced the most severe drought, most did not reach their target level before the end of the experiment (Figure S3.1). The drought treatments were maintained for 24 days. Throughout the experiment, plant weight was considered

negligible relative to pot/soil weight and was thus not considered when weighing. All individuals were maintained in this way until they reached five weeks of age, at which point they were harvested.

At harvest, traits were measured as described in Earley et al. (2022). Briefly, on harvest day, two of the most recent fully expanded leaves (MRFELs) were collected for analysis: one for estimation of LMA and one for anatomical characterization. Prior to removal, chlorophyll content index was measured (Apogee MC-100) on the latter ("anatomy") leaf for each plant. Following harvest, the LMA leaf was scanned on a flatbed scanner to determine leaf area, dried and weighed to determine the dry biomass of the lamina and midrib (excluding the petiole), and LMA was calculated as: dry mass/unit area ($g/m^2$). All remaining biomass was likewise collected, dried, and weighed to determine root, stem, bud, and leaf biomass, which could be summed into total and aboveground biomass. These values were then used to calculate stem, leaf, bud, and root mass fractions by dividing each by the total biomass. Note that bud biomass was not used in further analyses because only a subset of plants had produced buds at the time of sampling.

The anatomy leaf was cut in half lengthwise along the midrib and one half was dried and stored. This half was rehydrated overnight in water at a later date and the adaxial and abaxial (hereafter top and bottom) surfaces were pressed into dental putty (President Dental Putty; Coltène/Whaledent Inc., Cuyahoga Falls, OH) to produce an impression of the epidermis that could be used to visualize and analyze stomatal traits

following the general methods of Weyers and Johansen (1985). Nail polish was applied to each impression and lifted off with tape and imaged; this was done separately for the top and bottom surfaces of each leaf (Hilu and Randall, 1984; Weyers and Johansen, 1985). Traits of interest included: stomatal density sum (top + bottom), stomatal length, stomatal pore length, and guard cell width (2022). The total number of stomata was also estimated by multiplying stomatal density sum by leaf area. Imaging for stomatal density and size involved taking images of both the top and bottom impressions for stomatal density and size measurements at 5x and 100x, respectively. Maximum stomatal conductance ($g_{smax}$), the theoretical maximum rate of gas exchange if all stomata were fully open, was calculated based on stomatal density and size measurements. This was used instead of directly measuring $g_s$ since it was not feasible to measure directly for all plants. Maximum stomatal conductance was calculated using the approach of (Dow *et al.*, 2014).

The second half of the anatomy leaf was stored in Formalin-Acetic Acid-Alcohol (FAA) fixative for imaging and analysis of vein traits. Each sample was cleared, stained, and imaged as described in Earley et al. (2022). This included both scanning on a flatbed scanner and imaging four different fields of view under a microscope at 5x. Second order vein length was measured from the scanned images by manually tracing veins that branched off of the midrib (i.e., the primary vein). Major vein length was then determined by adding the length of the midrib to the sum of the second order vein lengths. Minor vein length was measured from the microscope images using a deep neural network as described in Earley et al. (2022). Finally, a composite trait of stomata number per vein

length was calculated as SV = average [top + bottom] stomatal density/VLA (Zhao et al. 2017).

*Data analysis*

All data analyses were conducted using R v3.4.3 (R Core Team, 2013) in R Studio v1.3.1093 (RStudio Team, 2015). A two-way ANOVA with genotype and block as the main effects was used to test for variation among genotypes and treatments and to calculate estimated marginal trait means (emmeans; Lenth, 2020) for each genotype after removing block effects. These values were then used to calculate the relative distance plasticity index (RDPI) of each genotype for each trait and treatment. RDPI, which was calculated as described by Valladares et al. (2006), but modified to range from -1 to -1 to show the direction of change, allows for cross-treatment comparisons and is strongly correlated with the majority of other measures of phenotypic plasticity. It was calculated for each trait and all treatments versus the well-watered control, as follows:

RDPI = (mean stress - mean control) / (mean stress + mean control)

RDPI was also calculated at the pot (i.e., individual plant) level using the same formula except it was calculated for each genotype/treatment combination separately for each block. Therefore, the same control value for each genotype within each block was used in each RDPI calculation. This resulted in 48 individual RDPI measurements.

Pot-level data were used to estimate bivariate trait correlations and to create correlation matrices per treatment using the R package *corrplot* (Wei and Simko 2017).

Mantel tests were performed using correlation matrix data and the R package *vegan* to compare correlation matrices and test for differences across treatments (Oksanen *et al.*, 2013). A principal component analysis (PCA) of traits by treatment was conducted using the function prcomp() and the package *ggfortify* (Tang et al. 2016; Horikoshi and Tang 2018) to visualize the trait-trait correlations. Differences between treatments were investigated using Hotellings $t^2$ test on the first two principal components. All graphs were made using the R package *ggplot2* (Wickham, 2016). Correlation matrices and PCA analyses were also conducted using RDPI values for traits within each level of water limitation compared to control to view how plasticity varied across treatments.

A linear mixed effects regression model using the package *brms* (Bürkner, 2017; Bürkner, 2018; Bürkner, 2021) was used to evaluate the relationship between trait variation and variation in performance within each treatment. Given the highly correlated nature of many of the traits in our dataset, we selected four leaf traits that reflect important axes of leaf trait variation in cultivated sunflower (see Earley *et al.*, 2022). Traits of interest included: stomatal length and density (important structural traits that influence gas exchange; Lawson and Blatt, 2014), VLA (a venation trait related to leaf water transport; Sack and Scoffoni, 2013), and LMA (which reflects the investment in biomass and leaf construction; Wright *et al.*, 2004). We centered and scaled all traits to have a mean of zero and standard deviation of one. Due to a few extreme LMA values, we log-transformed LMA values before centering and scaling to improve model fit. The model included the four leaf traits and the interaction of each with stress level as main effects. Block and genotype ID were included as random intercepts in the model. Default

priors were used (Bürkner, 2017; Bürkner, 2018; Bürkner, 2021) with a step size of 0.99, four chains with 2000 iterations (with 1000 iterations for a warm-up), and no thinning for a total of 4000 samples from the posterior. The model was evaluated for efficient mixing. No Rhat values greater than 1.00 were reported and there were no divergent transitions. The treatment level-specific coefficients relating each leaf trait to total biomass are reported below, as are the Bayesian marginal $R^2$ estimates (Gelman *et al.*, 2019) which estimates the variance explained by the fixed effects in the model.

A similar model was fit to evaluate the association between the plasticity of a trait (i.e., the RDPI value, compared to control) and the RDPI in biomass to investigate the association between shifts in trait values and changes in performance across treatments. The only difference in this model is that we did not include the interaction with treatment level, and instead included treatment as a random intercept to account for multiple comparisons (i.e., each trait RDPI in each of the three stress treatments was compared with the same control). We used the same model parameters and report no Rhat values greater than 1.00 and no divergent transitions.

## RESULTS

### *Leaf trait variation and covariation within and across treatments*

The median, minimum, and maximum values for all traits, along with a summary of the ANOVA results for each, are listed in Table 3.1. See also Figure 3.1 for a visual presentation of data for four representative traits. Tukey's HSD test results for all traits

across levels of treatment severity are presented in Table S3.1. In general terms, biomass decreased as severity increased while stomatal and vein density increased with increasing severity. In contrast, $g_{smax}$ remained largely constant across all but the most severe treatment. Significant genotypic effects were detected for a subset of leaf anatomical as well as higher-level (i.e., whole plant) traits. This included traits related to guard cell width, several traits related to venation, leaf size, total and aboveground biomass, and multiple mass fractions. Significant treatment effects were found for nearly all traits with the exception of guard cell width, SV, chlorophyll, and bud mass fraction. There was, however, minimal evidence of genotype-by-treatment interactions; exceptions to this included significant interactions for leaf area, midrib density, total biomass, and total stomata.

All bivariate trait correlations are presented in correlations matrices for each treatment (Figure S3.2). Mantel tests revealed that none of the matrices were significantly different from one another (i.e., the null hypothesis of a lack of correlation between matrices was rejected [$P < 0.001$] for all comparisons) suggesting that the overall correlation structure does not change appreciably across treatments. Multivariate trait relationships were analyzed via PCA to determine the major axes of variation (Figure 3.2). In the case of traits with values for the top and bottom of leaves, which are strongly correlated, averages were used to simplify the analysis and interpretation. Because overall size differences across treatments would largely obscure other trait relationships, this analysis was based on putatively size-independent traits (i.e., traits that lacked a significant correlation with size-related measures), with leaf area and both aboveground

and total biomass being excluded. Second VLA was also removed due to its redundancy with major VLA. For a full PCA including all measured traits see Figure S3.3**.** For the analysis of size-independent traits, the top three principal components accounted for 67.5% of the observed trait variation (Figure 3.2; Figure S3.4) with PC1 explaining 35.2%, PC2 explaining 16.6%, and PC3 explaining 15.7%. The top three traits contributing to each major axes were: PC1 - stomatal density sum, stomata length (SL_Avg), and stomatal pore length average (PL_Avg); PC2 - chlorophyll content, stomata per vein length (SV), and theoretical $g_{smax}$; and PC3 - leaf mass fraction, root mass fraction, and LMA (Table 3.2). Consistent with the observations of Earley et al. (2022), the first three PCs seem to be heavily influenced by traits relating gas exchange, hydraulics, and leaf construction.

*Trait plasticity in response to water limitation*

When calculated using a relative distance plasticity index (RDPI; Valladares *et al.*, 2006), estimates of trait plasticity can range from -1 to 1 with positive or negative values reflecting increases or decreases in trait values in response to the treatment, and 0 representing no plasticity. Overall, trait plasticity (as compared to control) increased with increasing drought severity for nearly all traits and was consistent across all genotypes (Figure 3.3). In general, smaller-scale leaf anatomical traits such as stomatal size and density and VLA exhibited smaller plasticity estimates than larger-scale traits related to construction and growth, such as second/major VLA, leaf area, and biomass.

Analysis of multivariate relationships for the RDPI values of putatively size-independent traits were analyzed via PCA. The top three PCs account for 68.2% of the observed variation in plasticity values with PC1 explaining 29.0%, PC2 explaining 22.2%, and PC3 explaining 17.0% (Figure 3.4). The top three plasticity values contributing to each major axes corresponded to the following traits: PC1 - stomatal density sum, stomata length (SL_Avg), and stomatal pore length average (PL_Avg); PC2 - chlorophyll content, stomata per vein length (SV), and midrib mass fraction; PC3 - theoretical $g_{smax}$, leaf mass fraction, and root mass fraction (Table 3.3). As seen for the trait PCA, the first three PCs are heavily influenced by plasticity in traits relating to hydraulics, gas exchange, and construction (Table 3.3). For a PCA of the RDPI for all traits see Figure S3.5.

*Relationship between trait variation and/or trait plasticity and performance*

Our model using four key traits selected to represent variation in major axes of leaf trait variation (i.e., vein length per area, stomatal length, stomatal density [sum], and LMA) to predict plant performance across environments (measured as total biomass) exhibited strong predictive power with an overall model marginal $R^2 = 0.74$ (Figure 3.5A). The treatment-specific estimated associations between each trait and biomass are presented in Figure 3.5B and the effect of stress on productivity (biomass) is illustrated in Figure 3.5C. For coefficients and credible intervals, see Table S3.2. Uncertainty in model estimates was evaluated using posterior credible intervals. Estimates with 95% CIs

not overlapping zero were interpreted as having strong support of the association, and those with 80% CIs with moderate support. VLA was negatively associated with biomass under control and mild stress conditions, but positively associated under severe stress (the effect estimated for moderate stress was positive, but the 80% CI overlapped with zero). Stomatal length had no clear association with biomass under control conditions, mild, or severe stress, and a positive association under moderate stress. Stomatal sum had a positive association with biomass under control and moderate stress conditions, but no association under mild and severe stress. Finally, log-LMA had a positive association with biomass under control conditions but no clear association under any of the stress conditions (Figure 3.5B).

The results of the model using plasticity estimates (i.e., RDPI values) for the same traits as above (i.e., VLA, stomatal length, stomatal density, and LMA) revealed the ability to predict plasticity in plant performance with a marginal model $R^2 = 0.25$ (Figure 3.6A). Individual coefficient estimates are presented in Figure 3.6B. For coefficients and credible intervals see Table S3.3. The RDPI of both VLA and stomatal density were associated with changes in biomass, but in different directions (negatively and positively, respectively). The resulting pattern is one in which higher VLA RDPI is associated with more extreme decreases in biomass (and vice versa), while higher stomatal density RDPI is associated with less extreme decreases in biomass (Figures 3.6C and 3.6D). In contrast, the RDPI of stomatal length and LMA had no association with the change in biomass.

## DISCUSSION

Drought is a major challenge that reduces plant growth and limits crop productivity worldwide. Stomatal and vein traits play an important role in plant-water relations and are thus of interest in the context of drought tolerance. Here, we investigated patterns of leaf trait covariation within and across treatments in cultivated sunflower. We also sought to quantify leaf trait plasticity in response to water limitation and determine the extent to which trait variation and/or plasticity predicts performance across treatments.

### *Leaf trait variation and covariation within and across treatments*

The existence of significant genotypic effects for traits related to leaf area, stomatal morphology, venation, and growth/allocation suggests the occurrence of genetic differentiation for a wide range of traits across cultivated sunflower lines. Within treatments, traits exhibited many of the predicted relationships based on the literature and their known roles in plant-water relations (Sack and Scoffoni, 2013; Doheny-Adams *et al.*, 2012; Shahinnia *et al.*, 2016; Figure S3.2). For example, stomatal density and size were negatively correlated while stomatal density and VLA were positively correlated (Figure S3.2). The former relationship indicates that the total area allocated to stomata affects total stomatal conductance and thus total photosynthesis (Harrison et al. 2019; Shahinnia et al. 2016). The latter relationship likely represents a balance between stomata and veins such that water use and carbon acquisition are optimized (Carins Murphy et al. 2014; Brodribb et al. 2007; Sack and Scoffoni 2013).

Notably, there was minimal evidence of trait variation scaling with size within treatments. The primary exception was that second and major VLA are negatively correlated with various aspects of plant size, whereas leaf size is negatively correlated with second and major VLA. This makes sense, as larger plants typically had larger leaves, and major veins are formed early in leaf development before being pushed apart as leaf expansion accelerates (Sack and Scoffoni, 2013). Minor veins are expected to show no such relationship (as seen here) because they can be initiated throughout leaf development. While total stomatal count was positively correlated with leaf size, no other stomatal or vein traits were associated with leaf size, indicating that correlations between combinations of those traits exist independent of leaf size as opposed to being a byproduct of allometric scaling.

Interestingly, the structures of the correlation matrices were largely conserved across treatments, suggesting that the observed trait relationships are quite robust to environmental perturbations. However, when viewed in a multivariate context, differences begin to emerge (Figure 3.2). For example, the trait space occupied by individuals in the severe stress treatment was significantly different from all other treatments. Similarly, the moderate and well-watered treatments were significantly different from each other, though mild was not detectably different from either of them. Across treatments, individuals separated along major axes of variation corresponding to traits involved in gas exchange, hydraulics, and construction. Interestingly, similar axes of variation were observed in a prior study of a large cultivated sunflower diversity panel

(Earley *et al.*, 2022) suggesting the existence of a persistent functional relationship amongst these traits that could mediate interactions with the environment.

*Trait plasticity in response to water limitation*

As expected, drought stress resulted in decreased biomass production, with the magnitude of the effect increasing with increased stress severity (Figure 3.1A). This decrease in biomass was presumably due to water limitation reducing the capacity for photosynthesis, thereby slowing or stopping growth (Munns, 2011; Kruger *et al*. 2006). In addition to this overall effect on growth, allocation patterns changed with root mass fraction increasing and stem and leaf mass fractions slightly decreasing (Table 3.1). For the most part, these allocation changes reflect common responses to drought stress (Eziz et al. (2017). By shifting resources into roots, plants are effectively maximizing their ability (given their decreased overall size) to find and acquire water during drought. Given that leaves are a source of water loss, decreases in leaf biomass might also help limit loss during times of limited water availability.

In general terms, we observed an increase in stomatal density and VLA along with a decrease in stomatal size in response to drought (Table 3.1; Figure 3.1). Similar phenotypic responses have been documented in response to water limitation in other plant species (e.g., Xu and Zhou 2008; Sun et al. 2014) and may play a role in increasing water use efficiency under stress (Xu and Zhou, 2008; Lei *et al.*, 2018). These trait shifts also reflect observed patterns of genetic differentiation both within (Xie *et al.*, 2022; Dunlap and Stettler, 2001) and among species (de Boer *et al.*, 2016; Strobel and Sundberg, 1983),

wherein individuals from increasingly dry habitats tend to exhibit smaller, denser stomata with an associated increase in vein density. The plastic responses of leaf anatomical traits thereby appear to parallel putatively adaptive solutions to water limitation that have evolved within and among plant species. Given that smaller stomata are able to close more quickly, this phenotypic response to stress might improve the ability of plants to rapidly adjust stomatal conductance in response to changes in water availability (e.g., (Brodribb *et al.*, 2007; Bertolino *et al.*, 2019; Sack and Scoffoni, 2013) The associated increase in VLA allows for greater hydraulic conductance and the maintenance of hydraulic function is critical for plant survival under drought (Yao *et al.*, 2021).

Looking across treatments, we found that the magnitude of plasticity for most traits increased as drought stress intensified (Figure 3.3). Overall, plasticity (RDPI) estimates were quite large for traits related to biomass production as well as traits related to leaf construction such as second and major VLA, leaf area, and LMA (Figure 3.3). In contrast, RDPI estimates for leaf anatomical traits such as measures of stomatal size, stomatal density, and VLA were much smaller. Similar trends have been documented in other species when subjected to stress. For example, in a study of plasticity in response to varying light intensities in rice (Chen *et al.*, 2021), traits related to leaf morphology and anatomy exhibited less plasticity than growth-related traits. This pattern may result from the coordination of certain trait combinations that need to maintain specific relationships to ensure proper function – e.g., stomatal and vein traits exhibit strong correlations, the maintenance of which helps ensure efficient water use (Brodribb *et al.*, 2013). In contrast,

growth-related traits are perhaps more free to vary in response to changes in resource availability without impairing function.

When viewed in a multivariate context, the extent of trait plasticity clearly varies across treatments (Figure 3.4). This is, however, largely due to an increase in the magnitude of response across traits as the severity of the drought treatment increased as opposed to novel trait shifts in response to different stress scenarios. As was the case with the PCA of trait values *per se*, the analysis of trait plasticity (RDPI) values revealed three primary axes of variation. Interestingly, these axes largely matched those observed in the trait-based, with the top contributors of the first three PCs again corresponding to (plastic responses in) traits involved in hydraulics, gas exchange, and construction (Table 3.3). It thus appears that variation in trait responses across environments is structured in much the same way as trait variation within environments.

*Relationship between trait variation and/or trait plasticity and performance*

Our results show that variation in just four size-independent leaf traits is strongly predictive ($R^2 = 0.74$) of plant performance measured as total biomass production. These four traits (VLA, stomatal length, stomatal density, and LMA) were primarily chosen to reflect the major axes of variation identified in previous work (Earley *et al.*, 2022) and documented again herein. This result suggests that these and/or closely related leaf traits are strongly associated with, and potentially impact overall plant performance. This makes logical sense and has been observed in the literature. Given the role that veins, and stomata play in gas exchange and water transport and thus photosynthetic capacity (Sack

*et al.*, 2013), the observed relationship between these traits and growth performance is perhaps not surprising.

Interestingly, the area of a single leaf was even more strongly predictive of total biomass ($R^2$ = 0.94). While not a truly size-independent trait, this result points to a single, easy to measure trait that may perform well as a proxy for total biomass in sunflower. As far as we are aware, a similar relationship has not been documented in other plant species. It is important to note that leaf area and VLA are not entirely independent, as the log-transformed values of both traits exhibit a linear relationship (Figure S3.6). Despite this relationship, we found substantial variation in VLA within each of the four treatments suggesting that this relationship is more complex than just scaling with size. In addition, it has been shown that VLA and stomatal density are coordinated independent of leaf area (Carins Murphy *et al.*, 2016).

In terms of trait plasticity, we found that VLA RDPI is negatively associated with biomass RDPI and that stomatal density RDPI is positively associated (Figure 3.6). In other words, increases in VLA are associated with a more severe drop in biomass under stress. Conversely, increases in stomatal density are associated with a less severe drop in biomass (Figure 3.6). Given the documented positive correlation between stomatal density and VLA (Earley et al. 2022 and herein), the finding that changes in these traits have opposite effects on performance seems counterintuitive. Based on previous work (Chapter 2; Earley et al. 2022), we would have expected an increase in both to increase performance, but our results here show a positive relationship with stomatal density and a

negative relationship with VLA. Ultimately, however, this finding suggests that the covariation of these traits is not strictly constrained and that decoupling them might allow for the exploration of novel phenotypic space that could improve performance under drought.

REFERENCES

**Bertolino, L.T., Caine, R.S. and Gray, J.E.** (2019) Impact of stomatal density and morphology on water-use efficiency in a changing world. *Front. Plant Sci.*, **10**, 225.

**Boer, H.J. de, Drake, P.L., Wendt, E., Price, C.A., Schulze, E.-D., Turner, N.C., Nicolle, D. and Veneklaas, E.J.** (2016) Apparent Overinvestment in Leaf Venation Relaxes Leaf Morphological Constraints on Photosynthesis in Arid Habitats. *Plant Physiol.*, **172**, 2286–2299.

**Bresta, P., Nikolopoulos, D., Stavroulaki, V., Vahamidis, P., Economou, G. and Karabourniotis, G.** (2018) How does long-term drought acclimation modify structure-function relationships? A quantitative approach to leaf phenotypic plasticity of barley. *Funct. Plant Biol.*, **45**, 1181–1194.

**Brodribb, T.J., Feild, T.S. and Jordan, G.J.** (2007) Leaf maximum photosynthetic rate and venation are linked by hydraulics. *Plant Physiol.*, **144**, 1890–1898.

**Brodribb, T.J., Jordan, G.J. and Carpenter, R.J.** (2013) Unified changes in cell size permit coordinated leaf evolution. *New Phytol.*, **199**, 559–570.

**Buckley, T.N.** (2019) How do stomata respond to water status? *New Phytol.*, **224**, 21–36.

**Bürkner, P.-C.** (2018) Advanced Bayesian Multilevel Modeling with the R Package brms. *R J.*, **10**, 395.

**Bürkner, P.-C.** (2021) Bayesian Item Response Modeling in R with brms and Stan. *J. Stat. Softw.*, **100**, 1–54. Available at: [Accessed February 21, 2022].

**Bürkner, P.-C.** (2017) brms: An R Package for Bayesian Multilevel Models Using Stan. *J. Stat. Softw.*, **80**, 1–28. Available at: [Accessed February 21, 2022].

**Carins Murphy, M.R., Jordan, G.J. and Brodribb, T.J.** (2016) Cell expansion not cell differentiation predominantly co-ordinates veins and stomata within and among herbs and woody angiosperms grown under sun and shade. *Ann. Bot.*, **118**, 1127–1138.

**Carlson, J.E., Adams, C.A. and Holsinger, K.E.** (2016) Intraspecific variation in stomatal traits, leaf traits and physiology reflects adaptation along aridity gradients in a South African shrub. *Ann. Bot.*, **117**, 195–207.

**Chen, L., Luo, W., Huang, J., Peng, S. and Xiong, D.** (2021) Leaf photosynthetic plasticity does not predict biomass responses to growth irradiance in rice. *Physiol. Plant.*, **173**, 2155–2165.

**Connor, D.J. and Sadras, V.O.** (1992) Physiology of yield expression in sunflower. *Field Crops Research*, **30**, 333–389.

**Doheny-Adams, T., Hunt, L., Franks, P.J., Beerling, D.J. and Gray, J.E.** (2012) Genetic manipulation of stomatal density influences stomatal size, plant growth and tolerance to restricted water supply across a growth carbon dioxide gradient. *Philosophical Transactions of the Royal Society of London. Series B, Biological sciences*, **367**, 547–555.

**Dow, G.J., Bergmann, D.C. and Berry, J.A.** (2014) An integrated model of stomatal development and leaf physiology. *New Phytologist*, **201**, 1218–1226.

**Drake, P.L., Froend, R.H. and Franks, P.J.** (2013) Smaller, faster stomata: scaling of stomatal size, rate of response, and stomatal conductance. *J. Exp. Bot.*, **64**, 495–505.

**Du, B., Zhu, Y., Kang, H. and Liu, C.** (2021) Spatial variations in stomatal traits and their coordination with leaf traits in *Quercus variabilis* across Eastern Asia. *Sci. Total Environ.*, **789**, 147757.

**Dunlap, J.M. and Stettler, R.F.** (2001) Variation in leaf epidermal and stomatal traits of *Populus trichocarpa* from two transects across the Washington Cascades. *Can. J. Bot.*, **79**, 528–536.

**Earley, A.M., Temme, A.A., Cotter, C.R. and Burke, J.M.** (2022) Genomic regions associate with major axes of variation driven by gas exchange and leaf construction traits in cultivated sunflower (*Helianthus annuus* L.). *Plant J.* Available at: http://dx.doi.org/10.1111/tpj.15900.

**Eziz, A., Yan, Z., Tian, D., Han, W., Tang, Z. and Fang, J.** (2017) Drought effect on plant biomass allocation: A meta-analysis. *Ecol. Evol.*, **7**, 11002–11010.

**FAO** (2018) Food Outlook - Oilcrops. *United Nations*. Available at: http://www.fao.org/fileadmin/templates/est/COMM_MARKETS_MONITORING/Oilcrops/Documents/Food_outlook_oilseeds/FO_Oilcrops.pdf [Accessed March 25, 2019].

**Fiorin, L., Brodribb, T.J. and Anfodillo, T.** (2016) Transport efficiency through uniformity: organization of veins and stomata in angiosperm leaves. *New Phytol.*, **209**, 216–227.

**Foley, J.A., Ramankutty, N., Brauman, K.A., et al.** (2011) Solutions for a cultivated planet. *Nature*, **478**, 337–342.

**Gelman, A., Goodrich, B., Gabry, J. and Vehtari, A.** (2019) R-squared for Bayesian Regression Models. *Am. Stat.*, **73**, 307–309.

**Hilu, K. and Randall, J.** (1984) Convenient method for studying grass leaf epidermis. *Taxon*, **33**, 413–415.

**Hussain, M., Farooq, S., Hasan, W., Ul-Allah, S., Tanveer, M., Farooq, M. and Nawaz, A.** (2018) Drought stress in sunflower: Physiological effects and its management through breeding and agronomic alternatives. *Agric. Water Manage.*, **201**, 152–166.

**IPCC** (2014) Climate Change 2014: Synthesis Report. Contribution of Working Groups I, II and III to the Fifth Assessment Report of the Intergovernmental Panel on Climate Change. *Intergovernmental Panel on Climate Change*.

**Kruger, E.L. and Volin, J.C.** (2006) Reexamining the empirical relation between plant growth and leaf photosynthesis. *Functional Plant Biology* **33.5**: 421-429.

**Lawson, T. and Blatt, M.R.** (2014) Stomatal size, speed, and responsiveness impact on photosynthesis and water use efficiency. *Plant Physiol.*, **164**, 1556–1570.

**Lei, Z.Y., Han, J.M., Yi, X.P., Zhang, W.F. and Zhang, Y.L.** (2018) Coordinated variation between veins and stomata in cotton and its relationship with water-use efficiency under drought stress. *Photosynthetica*, **56**, 1326–1335.

**Lenth, R.** (2020) emmeans: Estimated Marginal Means, aka Least-Squares Means. Available at: https://CRAN.R-project.org/package=emmeans.

**Mandel, J.R., Dechaine, J.M., Marek, L.F. and Burke, J.M.** (2011) Genetic diversity and population structure in cultivated sunflower and a comparison to its wild progenitor, *Helianthus annuus* L. *Theor. Appl. Genet.*, **123**, 693–704.

**Meyer, R.** (1999) High plains sunflower production handbook. Available at: https://agris.fao.org/agris-search/search.do?recordID=US201300051629 [Accessed August 1, 2022].

**Munns, R.** (2011) Chapter 1 - Plant Adaptations to Salt and Water Stress: Differences and Commonalities. In I. Turkan, ed. *Advances in Botanical Research*. Academic Press, pp. 1–32.

**Oksanen, J., Blanchet, F.G., Kindt, R., et al.** (2013) Community ecology package. *R package version*, **2**. Available at: http://sortie-admin.readyhosting.com/lme/R%20Packages/vegan.pdf.

**R Core Team** (2013) *R: The R project for statistical computing*, Available at: https://www.r-project.org/ [Accessed April 17, 2019].

**RStudio Team** (2015) *RStudio: integrated development for R*,.

**Sack, L. and Scoffoni, C.** (2013) Leaf venation: structure, function, development, evolution, ecology and applications in the past, present and future. *New Phytologist*, **198**, 983–1000.

**Sack, L., Scoffoni, C., John, G.P., Poorter, H., Mason, C.M., Mendez-Alonzo, R. and Donovan, L.A.** (2013) How do leaf veins influence the worldwide leaf economic spectrum? Review and synthesis. *J. Exp. Bot.*, **64**, 4053–4080.

**Shahinnia, F., Le Roy, J., Laborde, B., Sznajder, B., Kalambettu, P., Mahjourimajd, S., Tilbrook, J. and Fleury, D.** (2016) Genetic association of stomatal traits and yield in wheat grown in low rainfall environments. *BMC Plant Biology*, **16**, 150.

**Stojnić, S., Orlović, S., Trudić, B., Živković, U., Wuehlisch, G. von and Miljković, D.** (2015) Phenotypic plasticity of European beech (*Fagus sylvatica* L.) stomatal features under water deficit assessed in provenance trial. *Dendrobiology*, **73**, 163–173.

**Strobel, D.W. and Sundberg, M.D.** (1983) Stomatal Density in Leaves of Various Xerophytes: A Preliminary Study. *J. Minn. Acad. Sci.*, **49**, 7–9. Available at: [Accessed August 29, 2022].

**Sun, Y., Yan, F., Cui, X. and Liu, F.** (2014) Plasticity in stomatal size and density of potato leaves under different irrigation and phosphorus regimes. *J. Plant Physiol.*, **171**, 1248–1255.

**United Nations** (2017) World Population Prospects. *Department of Economics and Social Affairs*. Available at: https://population.un.org/wpp/Publications/Files/WPP2017_KeyFindings.pdf.

**Valladares, F., Sanchez-Gomez, D. and Zavala, M.A.** (2006) Quantitative estimation of phenotypic plasticity: bridging the gap between the evolutionary concept and its ecological applications. *J. Ecol.*, **94**, 1103–1116.

**Wang, X., Du, T., Huang, J., Peng, S. and Xiong, D.** (2018) Leaf hydraulic vulnerability triggers the decline in stomatal and mesophyll conductance during drought in rice. *J. Exp. Bot.*, **69**, 4033–4045.

**Wang, Y., Donovan, L.A. and Temme, A.A.** (2020) Plasticity and the role of mass-scaling in allocation, morphology, and anatomical trait responses to above- and belowground resource limitation in cultivated sunflower (*Helianthus annuus* L.). *Plant Direct*, **4**, e02924.

**Weyers, J.D.B. and Johansen, L.G.** (1985) Accurate Estimation of Stomatal Aperture from Silicone Rubber Impressions. *New Phytol.*, **101**, 109–115.

**Wickham, H.** (2016) ggplot2: Elegant Graphics for Data Analysis. Available at: https://ggplot2.tidyverse.org.

**Wright, I.J., Reich, P.B., Westoby, M., et al.** (2004) The worldwide leaf economics spectrum. *Nature*, **428**, 821–827.

**Xie, J., Wang, Z. and Li, Y.** (2022) Stomatal opening ratio mediates trait coordinating network adaptation to environmental gradients. *New Phytol.*, **235**, 907–922.

**Xu, Z. and Zhou, G.** (2008) Responses of leaf stomatal density to water status and its relationship with photosynthesis in a grass. *J. Exp. Bot.*, **59**, 3317–3325.

**Yao, G.-Q., Nie, Z.-F., Turner, N.C., Li, F.-M., Gao, T.-P., Fang, X.-W. and Scoffoni, C.** (2021) Combined high leaf hydraulic safety and efficiency provides drought tolerance in *Caragana* species adapted to low mean annual precipitation. *New Phytol.*, **229**, 230–244.

FIGURES

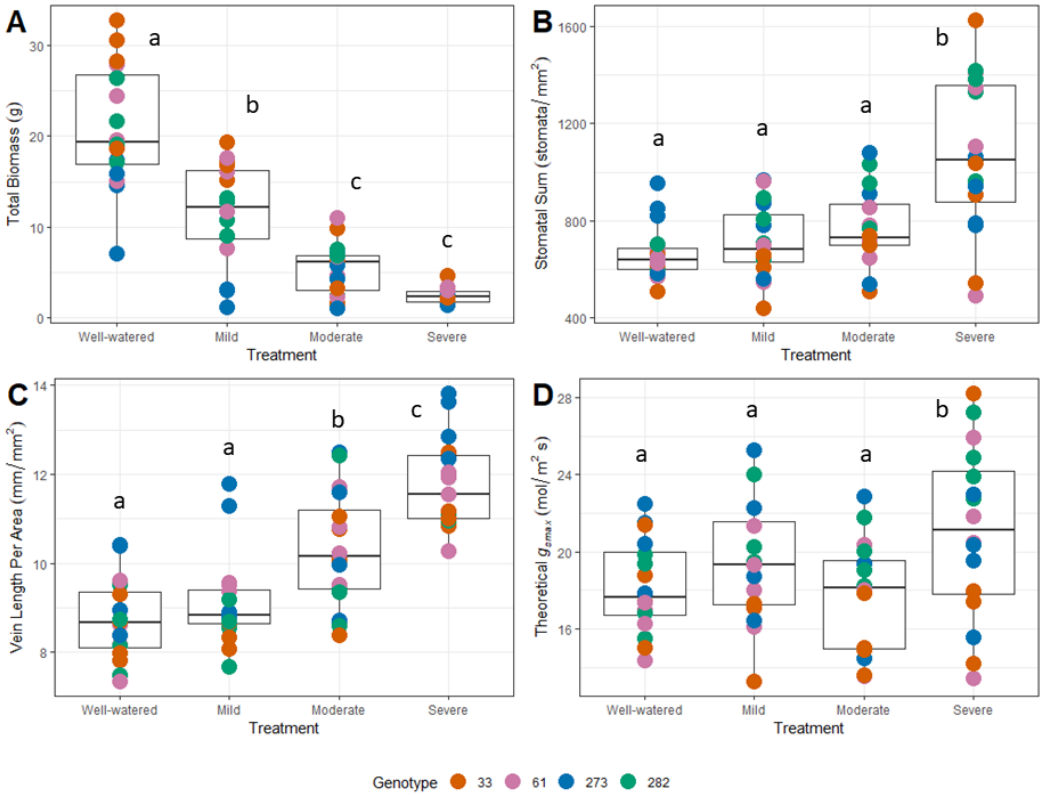


**Figure 3.1:** Boxplots of variation in representative traits across treatments. Dots are colored based on genotype, which are listed by line number in the key at the bottom. Traits of interest include: (A) total biomass; (B) stomata density sum; (C) vein length per area; and (D) theoretical $g_{smax}$. Letters indicate significant differences across treatments based on Tukey's HSD test.

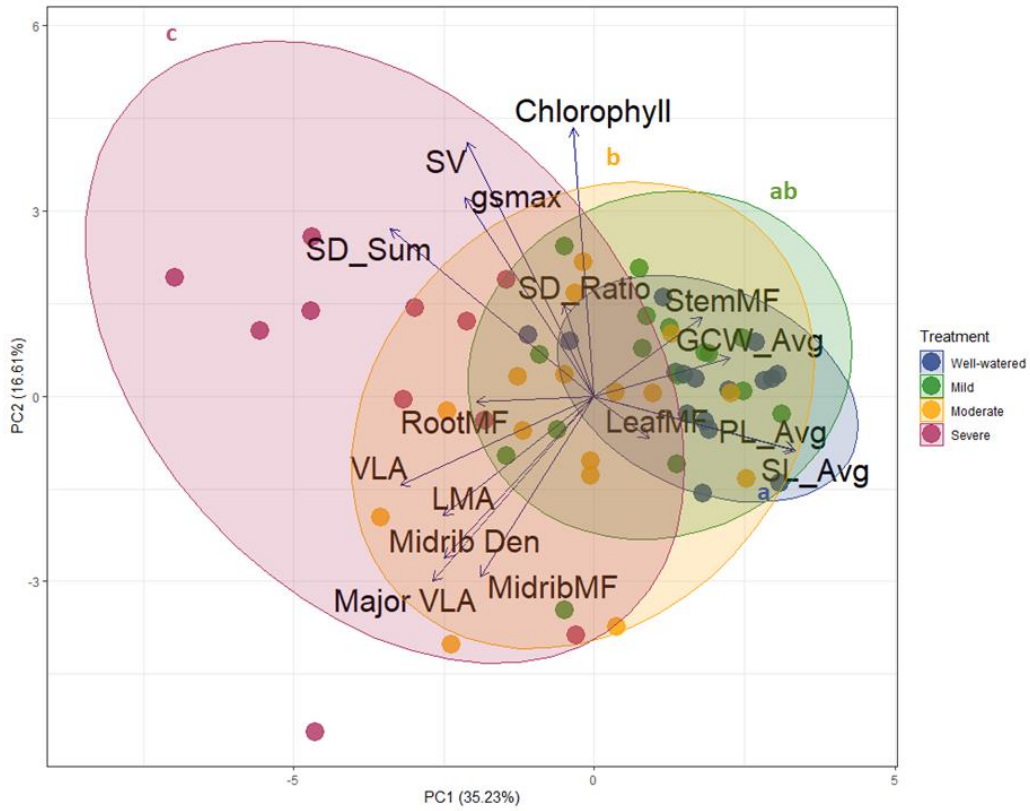


**Figure 3.2:** Principal component analysis (PCA) of putatively size-independent traits. Traits names that include _Avg (stomatal length [SL], pore length [PL], guard cell width [GCW]) are averages of the values from the top and bottom of the leaf. SD_Sum is the sum of stomatal density from the top and bottom of the leaf. Colors indicate treatment and trait abbreviations are as defined in Table 3.1. Lower-case letters associated with each of the colored ellipses indicate the results of Hotelling's $t^2$ tests for differences between treatments. P-values were adjusted for multiple comparisons using a Bonferroni correction.

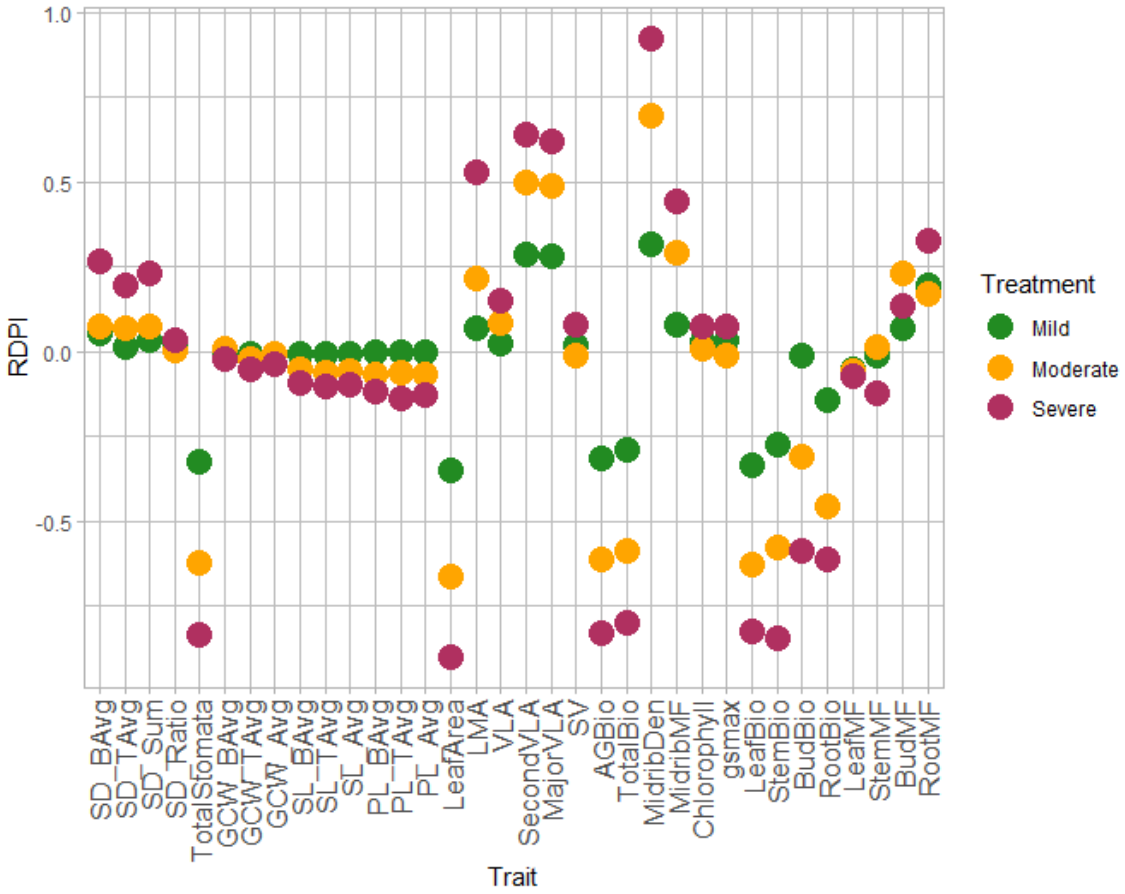


**Figure 3.3**: Relative distance plasticity index (RDPI) plot for each trait and treatment. Points indicate the average estimated marginal mean for each trait for each treatment. RDPI was calculated as each treatment versus the well-watered control. Trait abbreviations follow Table 3.1.

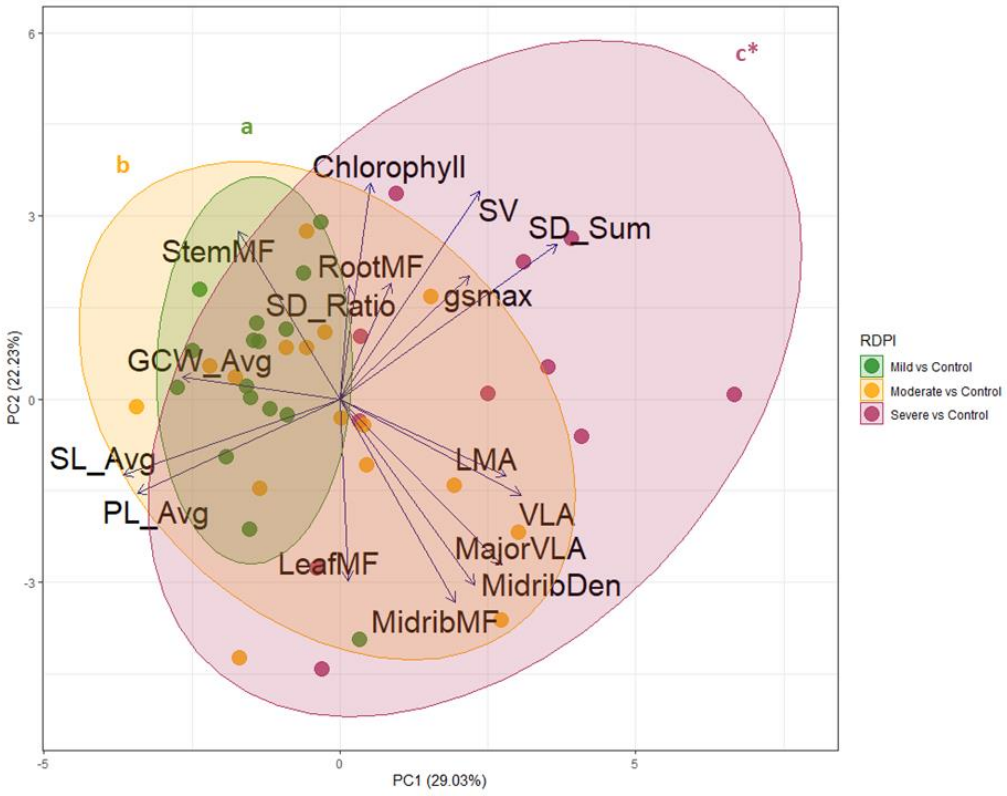


**Figure 3.4:** Principal component analysis (PCA) of trait plasticity values (estimated as RDPI) for each treatment compared to control. Trait abbreviations follow Table 3.1. Lower-case letters associated with each of the colored ellipses indicate the results of Hotelling's $t^2$ tests for differences between treatments. P-values were adjusted for multiple comparisons using a Bonferroni correction. *Severe vs. control is marginally significant following correction for multiple comparisons.

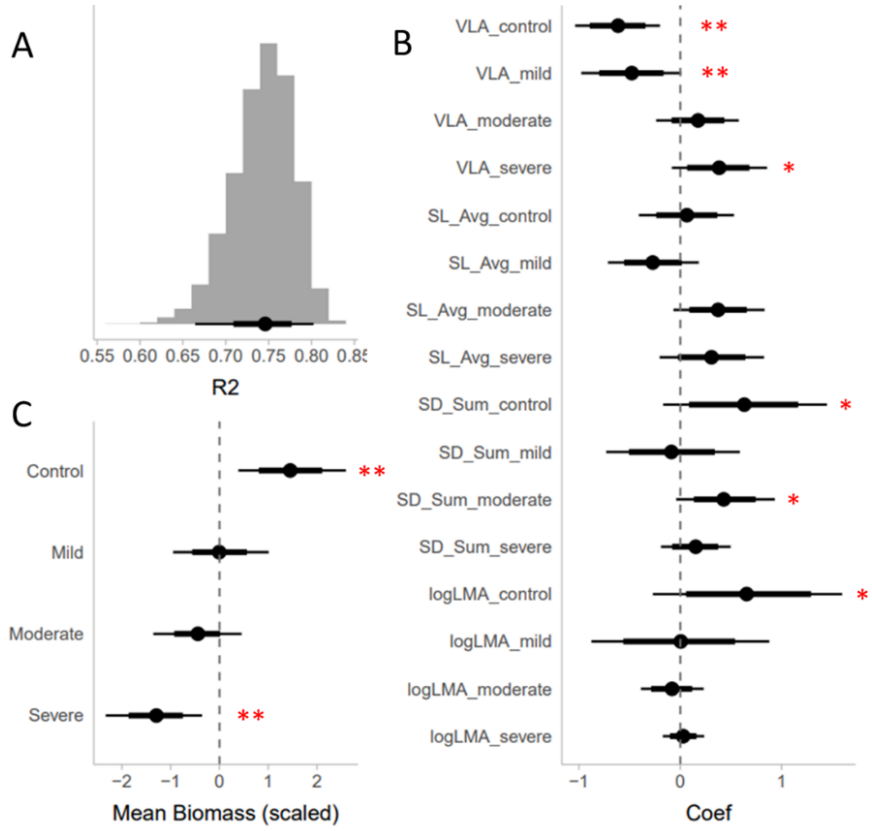


**Figure 3.5:** Results of our analysis of performance as a function of variation in VLA, average stomatal length (SL_Avg), stomatal density (SD_sum), and LMA across environments using a linear mixed effects regression model. All output reflects posterior summaries from the model. (A) Estimated Bayesian R2, for fixed effects only (full posterior distribution of the model). (B) Coefficient estimates for each trait/environment combination. LMA was log-transformed to improve model fit and all traits were scaled to a mean of zero and standard deviation of one. (C) Mean biomass for each treatment scaled to a mean of zero and a standard deviation of one. Black dot indicates the estimated value. The heavier bars indicate the 80% credible interval for each estimate, and the lighter lines indicate the 95% credible interval. Estimates with 95% CIs not

overlapping zero were interpreted as having strong support (**), and those with 80% Cis with moderate support (*).

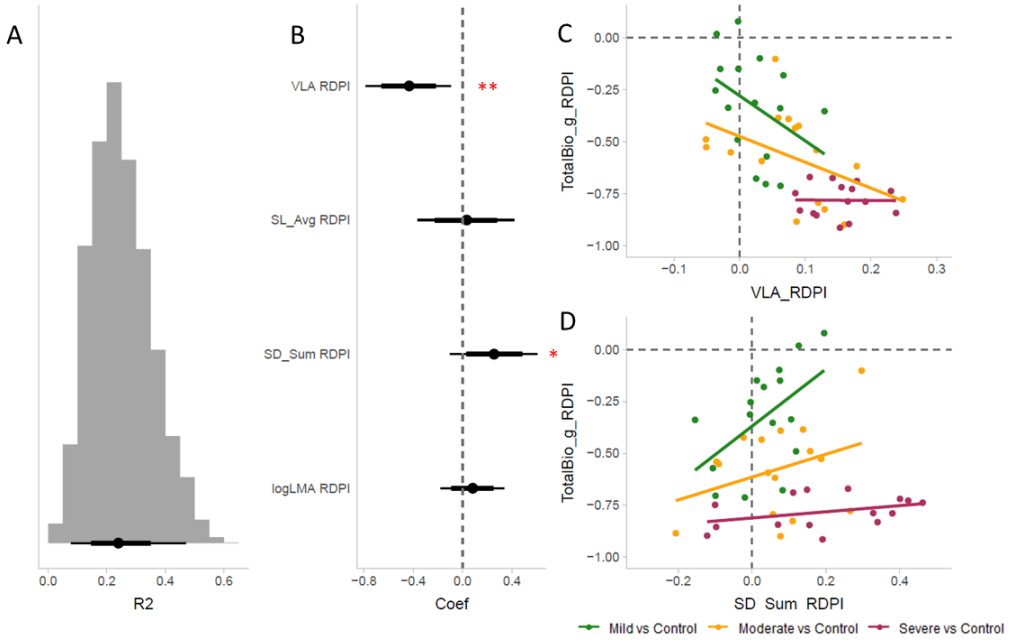


**Figure 3.6**: Results of our analysis of plasticity in performance as a function of variation in plasticity (RDPI) of VLA, average stomatal length (SL_Avg), stomatal density sum (SD_sum), and LMA using a linear mixed effects regression model. All output reflects posterior summaries from the model. (A) Estimated Bayesian R2, for fixed effects only (full posterior distribution of the model). (B) Coefficient estimates for each trait. LMA was log-transformed, and all traits were scaled to a mean of zero and standard deviation of one. Black dot indicates the estimated value. The heavier bars indicate the 80% credible interval for each estimate, and the lighter lines indicate the 95% credible interval. Estimates with 95% CIs not overlapping zero were interpreted as having strong support (**), and those with 80% Cis with moderate support (*). Plots of (C) VLA vs total biomass and (D) stomatal density sum vs total biomass. Dots represent individuals and lines are the line of best fit per treatment.

TABLES

**Table 3.1**: List of all traits measured along with the median and range of trait values. Significance for genotypic effects (***P ≤ 0.001, **P ≤ 0.01, * P ≤ 0.05, # P ≤ 0.1, ns = not significant) and adjusted R2 from the model are also presented. SD = stomatal density; LMA = leaf mass per area; MF = mass fraction; GCW = guard cell width; SL = stomatal length; PL = stomatal pore length; $g_{smax}$ = theoretical maximum stomatal conductance; VLA = vein length per area; SV = stomata per vein length; AG = aboveground; Bio = biomass.

| | Well-Watered | | | Mild | | | Moderate | | | Severe | | | | | | |
|---|---|---|---|---|---|---|---|---|---|---|---|---|---|---|---|---|
| | Median | Min | Max | Median | Min | Max | Median | Min | Max | Median | Min | Max | Genotype | Treatment | Block | GXT |
| SD_Bottom (stomata/mm$^2$) | 320.89 | 247.76 | 490.36 | 370.78 | 268.41 | 507.57 | 375.09 | 258.09 | 533.38 | 555.75 | 263.25 | 884.38 | ns | *** | ns | ns |
| SD_Top (stomata/mm$^2$) | 331.21 | 263.25 | 464.56 | 323.47 | 170.34 | 514.45 | 362.18 | 249.48 | 545.42 | 493.81 | 227.12 | 743.29 | # | *** | ns | ns |
| Stomatal Ratio (bottom/sum) | 0.5 | 0.42 | 0.55 | 0.53 | 0.47 | 0.61 | 0.51 | 0.44 | 0.56 | 0.52 | 0.45 | 0.63 | ns | * | ns | ns |
| SD_Sum (stomata/mm$^2$) | 637.47 | 511.01 | 954.92 | 681.35 | 438.75 | 966.96 | 728.66 | 507.57 | 1078.8 | 1050.41 | 490.36 | 1627.67 | ns | *** | ns | ns |
| LMA (g/m$^2$) | 38.19 | 24.73 | 45.84 | 39.88 | 29.07 | 83.07 | 42.47 | 26.16 | 215.55 | 80.11 | 28.03 | 374.46 | ns | *** | ns | ns |
| Leaf Area (m$^2$) | 0.0296 | 0.013 | 0.0514 | 0.0152 | 0.0015 | 0.0231 | 0.0062 | 0.0009 | 0.0138 | 0.0017 | 0.0004 | 0.0027 | *** | *** | ns | *** |
| Midrib MF ($g_{midrib}/g_{leaf}$) | 0.08 | 0.01 | 0.2 | 0.09 | 0.01 | 0.21 | 0.13 | 0.02 | 0.36 | 0.2 | 0.03 | 0.52 | ns | *** | ns | ns |
| Midrib Density (mg/cm$^3$) | 80.27 | 11.63 | 327.91 | 129.88 | 9.97 | 1282.15 | 208.37 | 52.75 | 2874.44 | 1256 | 20.76 | 16852.83 | * | *** | ns | ** |
| GCW_Bottom (µm) | 6.24 | 4.9 | 7.52 | 6.33 | 4.41 | 8.06 | 6.43 | 4.75 | 8.61 | 6.05 | 4.51 | 8.62 | * | ns | *** | ns |
| GCW_Top (µm) | 5.71 | 3.47 | 7.12 | 5.73 | 3.4 | 7.24 | 5.44 | 3.14 | 8.05 | 5.39 | 3.59 | 6.17 | ** | ns | *** | # |
| GCW_Avg (µm) | 6.08 | 4.18 | 7.27 | 6.05 | 3.91 | 7.48 | 6.02 | 4.34 | 8.33 | 5.63 | 4.27 | 7.29 | ** | ns | *** | # |
| SL_Bottom (µm) | 33.12 | 28.38 | 37.56 | 32.74 | 25.88 | 35.45 | 28.61 | 23.64 | 35.31 | 27.02 | 19.96 | 33.58 | ns | *** | ns | ns |
| SL_Top (µm) | 30.51 | 21.03 | 34.25 | 30.14 | 22.03 | 33.15 | 25.39 | 18.47 | 34.35 | 24.65 | 18.24 | 30.48 | # | *** | # | ns |
| SL_Avg (µm) | 32.3 | 25.04 | 34.62 | 31.66 | 23.95 | 33.01 | 26.71 | 21.05 | 33.5 | 25.26 | 19.75 | 32.03 | ns | *** | # | ns |
| PL_Bottom (µm) | 22.9 | 18.27 | 28.46 | 23.02 | 18.57 | 26.17 | 20.35 | 16.23 | 24.72 | 17.86 | 12.87 | 23.3 | ns | *** | ns | ns |
| PL_Top (µm) | 21.56 | 15.19 | 24.55 | 21.12 | 15.75 | 24.89 | 18.06 | 13.36 | 23.18 | 15.74 | 11.35 | 20.25 | # | *** | ns | ns |
| PL_Avg (µm) | 21.9 | 17.26 | 25.72 | 22.14 | 17.91 | 24.18 | 19.21 | 14.86 | 23.3 | 16.24 | 12.11 | 21.78 | ns | *** | ns | ns |
| $g_{smax}$ (mol/m$^2$s) | 17.63 | 14.35 | 22.48 | 19.32 | 13.26 | 25.3 | 18.11 | 13.57 | 22.88 | 21.14 | 13.45 | 28.25 | ** | * | ns | ns |
| VLA (mm/mm$^2$) | 8.67 | 7.34 | 10.43 | 8.83 | 7.68 | 11.78 | 10.16 | 8.39 | 12.49 | 11.54 | 10.27 | 13.83 | *** | *** | ns | ns |
| 2nd VLA (mm/mm$^2$) | 0.04 | 0.02 | 0.06 | 0.05 | 0.03 | 0.25 | 0.09 | 0.04 | 0.25 | 0.16 | 0.11 | 0.31 | * | *** | ns | ns |
| Major VLA (mm/mm$^2$) | 0.05 | 0.03 | 0.09 | 0.08 | 0.06 | 0.33 | 0.13 | 0.07 | 0.39 | 0.22 | 0.15 | 0.4 | * | *** | ns | ns |
| SV (stomata/mm) | 11.17 | 7.98 | 14.19 | 11.06 | 6.94 | 15.93 | 11.2 | 7.31 | 16.14 | 12.8 | 6.94 | 18.91 | ns | ns | ns | ns |
| AG Bio (g) | 16.87 | 6.19 | 30.12 | 9.99 | 0.66 | 15.87 | 4.64 | 0.69 | 8.61 | 1.59 | 0.89 | 3.18 | *** | *** | ns | ** |
| Total Bio (g) | 19.37 | 7.1 | 32.88 | 12.2 | 1.19 | 19.35 | 6.09 | 0.98 | 11.01 | 2.24 | 1.34 | 4.64 | *** | *** | ns | ** |
| Leaf MF ($g_{leaf}/g_{plant}$) | 0.62 | 0.55 | 0.67 | 0.54 | 0.39 | 0.76 | 0.53 | 0.4 | 0.69 | 0.51 | 0.29 | 0.8 | *** | * | ns | ns |
| Stem MF ($g_{stem}/g_{plant}$) | 0.24 | 0.2 | 0.29 | 0.23 | 0.12 | 0.3 | 0.25 | 0.17 | 0.32 | 0.19 | 0.02 | 0.29 | ** | ** | ns | ns |
| Bud MF ($g_{bud}/g_{plant}$) | 0.01 | 0 | 0.02 | 0.01 | 0 | 0.03 | 0 | 0 | 0.06 | 0 | 0 | 0.07 | ns | ns | ns | ns |
| Root MF ($g_{root}/g_{plant}$) | 0.14 | 0.08 | 0.2 | 0.18 | 0.12 | 0.44 | 0.2 | 0.09 | 0.3 | 0.27 | 0.12 | 0.49 | *** | *** | ns | ns |
| Chlorophyll (index) | 25.45 | 18.3 | 30.8 | 26 | 12.1 | 33.7 | 24.95 | 13.3 | 38.4 | 30.35 | 14.6 | 41.2 | *** | ns | ns | ns |
| TotalStomata (stomata) | 90137.07 | 37980.9 | 158232.7 | 52374.41 | 4205.652 | 74514.11 | 24686.92 | 3028.235 | 37432.9 | 9889.031 | 1583.439 | 14437.41 | *** | *** | ns | * |

**Table 3.2:** Trait loadings (percentage of trait variation explained by each trait in the associated principal component [PC]) for each of the first three PCs. The top three traits per PC are highlighted in bold. Trait abbreviations follow Table 3.1.

| Trait | PC1 | PC2 | PC3 |
|---|---|---|---|
| SD_Ratio | 0.06 | 3.48 | 1.67 |
| SD_Sum | 8.03 | 13.72 | 1.04 |
| LMA | 7.58 | 0.00 | 8.58 |
| MidribMF | 6.26 | 5.67 | 5.24 |
| MidribDen | 6.96 | 3.33 | 11.37 |
| GCW_Avg | 7.18 | 0.10 | 4.61 |
| SL_Avg | 10.95 | 4.49 | 4.04 |
| PL_Avg | 9.54 | 5.11 | 4.69 |
| gsmax | 1.74 | 9.60 | 12.05 |
| VLA | 12.25 | 0.82 | 4.01 |
| MajorVLA | 12.38 | 4.54 | 1.01 |
| SV | 1.62 | 18.62 | 4.20 |
| LeafMF | 0.14 | 4.63 | 18.52 |
| StemMF | 4.97 | 4.01 | 2.93 |
| RootMF | 0.64 | 2.19 | 11.34 |
| Chlorophyll | 0.17 | 13.87 | 2.13 |
| TotalStomata | 9.54 | 5.83 | 2.56 |

**Table 3.3:** Trait loadings (percentage of trait variation explained by each trait in the associated principal component [PC]) for each of the first three PCs of plasticity (RDPI) values. The top three traits per PC are highlighted in bold. Trait abbreviations follow Table 3.1.

| Trait | PC1 | PC2 | PC3 |
|---|---|---|---|
| SD_Ratio | 0.03 | 3.68 | 3.92 |
| SD_Sum | **14.37** | 6.79 | 1.58 |
| LMA | 8.41 | 1.69 | 6.17 |
| MidribMF | 4.05 | **11.84** | 2.27 |
| MidribDen | 5.55 | 9.86 | 6.89 |
| GCW_Avg | 7.60 | 0.14 | 7.68 |
| SL_Avg | **14.24** | 1.66 | 5.25 |
| PL_Avg | **12.51** | 2.54 | 5.28 |
| gsmax | 5.12 | 4.32 | **14.94** |
| VLA | 9.98 | 2.66 | 7.41 |
| MajorVLA | 7.96 | 7.88 | 2.96 |
| SV | 5.95 | **12.34** | 7.00 |
| LeafMF | 0.02 | 9.44 | **13.25** |
| StemMF | 3.13 | 8.03 | 1.24 |
| RootMF | 0.78 | 3.83 | **8.57** |
| Chlorophyll | 0.28 | **13.31** | 5.60 |

# CHAPTER 4

# LEAF TRAIT VARIATION, ENVIRONMENTAL ASSOCIATIONS, AND PLANT PERFORMANCE IN WILD SUNFLOWER (*HELIANTHUS ANNUUS* L.)[3]

[3] Earley, Ashley M, Kristen M. Nolting, John M. Burke. To be submitted to *Plant Direct*.

ABSTRACT

Cultivated sunflower (*Helianthus annuus* L.) exhibits a large reduction in genetic diversity relative to its wild progenitor which may limit our ability to adapt sunflower to novel environmental challenges arising from climate change. Given this, we explored leaf trait variation and covariation in wild sunflower (also *H. annuus*) sampled from across its native range in a common garden setting, investigated correlations between traits and key environmental variables, and determined the extent to which trait values can predict plant growth/performance. Most traits exhibited significant variation across populations, and bivariate correlations amongst traits were largely as expected based on presumptive functions as well as observations from the literature. For example, stomatal size and density were negatively correlated while stomatal density and vein length per area (VLA) were positively correlated. From a multivariate perspective, the two major axes of trait variation largely reflecting traits involved in gas exchange and resource allocation, respectively. When modeling trait variation as a function of home-habitat environment and accounting for population structure, we found that biomass traits tended to correlate positively with temperature-related variables. While there were few strong environmental correlations with leaf anatomical traits, we found that variation in performance can be largely explained by variation in a small number of such traits ($R^2 = 0.67$), and predictive power was even better when modeling performance as a function of variation in the first two trait principal components ($R^2 = 0.73$). Taken together, these results indicate the existence of genetic variation in numerous leaf traits across wild sunflower populations and show that leaf trait variation can be used to accurately predict plant performance.

## INTRODUCTION

Cultivated sunflower (*Helianthus annuus* L.), like most crops, exhibits a substantial reduction in genetic diversity relative to its wild progenitor due to genetic bottlenecks during domestication and improvement (Mandel *et al.*, 2011; Liu and Burke, 2006). This loss of genetic diversity potentially limits our ability to adapt sunflower, which is one of the world's most important oilseed crops, to emerging environmental challenges such as warmer temperatures and increasingly variable precipitation patterns due to climate change (Godfray *et al.*, 2010). Wild plant populations represent a possible source of additional genetic variation that can be utilized to develop more tolerant crop varieties (e.g., Dempewolf *et al.*, 2017). Common sunflower (also *H. annuus*), the wild progenitor of cultivated sunflower, occurs across a broad geographic range spanning a diversity of environments across much of North America and is thought to contain valuable trait variation for breeding purposes (Seiler and Rieseberg, 1997).

In general, variation in leaf anatomical traits plays a central role in plant-water relations with veins distributing the water throughout the leaf and stomata controlling the rate of transpiration (Sack and Scoffoni, 2013). Stomatal conductance ($g_s$), a measure of the conductance of water vapor through the stomata, is determined by the physiological control of stomatal opening and closing as well as the size and distribution of stomata (Faralli *et al.*, 2019). Similarly, vein length per area (VLA) affects leaf hydraulic conductance ($K_{leaf}$), or the ratio of water flow rate to the water potential gradient across the leaf, and thus greatly affects how long stomata can remain open without drying out

the leaf (Sack and Scoffoni, 2012). Stomatal and vein traits are thus thought to play an important role in plant adaptation to drought (e.g., Bertolino *et al.*, 2019; Sack and Scoffoni, 2013), which is an ever-increasing agricultural challenge that limits productivity worldwide (NOAA and NIDIS, 2022; FAO, 2021). Consistent with a role for such traits in adaptation to dry environments, populations within species that occur across a moisture gradient exhibit a trend toward smaller and more dense stomata in increasingly arid habitats allowing for a higher water use efficiency when water is available (Dunlap and Stettler, 2001; Xie *et al.*, 2022). This tradeoff between stomatal size and density is a general feature of plants and is typically accompanied by a positive relationship between stomatal and vein density (Sack and Scoffoni, 2013; Shahinnia *et al.*, 2016; Doheny-Adams *et al.*, 2012; see also Earley et al. 2022 and Chapter 3 of this dissertation). The observed shift toward increased VLA and stomatal density, along with decreases in stomatal size, is thought to allow plants to manage their transpiration rates to limit water loss under dry conditions, and to quickly maximize productivity when water is available (Sack and Scoffoni, 2013; Carlson *et al.*, 2016). Smaller and more dense stomata allow for faster ion fluxes and can thus close more quickly than larger stomata. This results in faster changes in stomatal conductance (Bertolino *et al.*, 2019; Drake *et al.*, 2013) which allows plants to reduce transpiration in response to dry conditions while still allowing them to rapidly re-open when water is available (Sack and Scoffoni, 2013).

In addition to its effects on water use, transpiration also allows for evaporative cooling. Stomatal closure thus helps to retain water but reduces the potential for evaporative cooling, which can increase canopy temperatures and negatively impact plant growth and productivity (Buckley, 2019; Siebert *et al.*, 2014; De la Haba *et al.*, 2014). As temperatures increase, more water is released and the amount of water vapor needed to saturate the air increases exponentially with increasing temperature which can further increase water loss (Moore *et al.*, 2021). Relative humidity (RH) values, the ratio of the water vapor pressure in the air compared to the water vapor pressure at saturation, are also predicted to decline as global temperatures continue to increase in the coming years (Driesen *et al.*, 2020)**.** This decrease in RH levels may have adverse effects on plants as stomatal closure to prevent water loss limits photosynthesis while potentially increasing canopy temperatures (Driesen *et al.*, 2020). Given the above, stomatal and vein traits are expected to interact strongly with variation in temperature and water availability.

Here, we investigate patterns of variation in leaf and growth-related traits in greenhouse-grown wild sunflower sampled from across its natural range and the association of these traits with prevailing environmental conditions in their native habitats, with a particular focus on moisture and temperature-related variables. More specifically, we seek to: (1) quantify leaf trait variation and covariation across the range of wild sunflower in a common garden setting; (2) test for putatively adaptive relationships between observed trait variation and relevant environmental variables across the range of wild sunflower; and (3) determine the extent to which leaf trait variation can be used to predict whole plant performance.

## METHODS

### *Plant material*

This work was based on a subset of the wild sunflower (*H. annuus*) populations studied by Todesco et al. (2020). Twenty-four of these populations from across the natural range of wild sunflower in the western half of the United States were chosen for inclusion in this work to provide broad coverage of the geographic range as well as climatic variables (Figure 4.1). This included populations from the high plains, south Texas, the Intermountain West, and the West. All seeds for this work were sourced from wild-collected accessions held within the USDA-GRIN oilseed collection at the North Central Regional Plant Introduction Station (NCRPIS; Ames, IA). See Table S4.1 for a summary of population information.

### *Experimental design*

Seeds were scarified and germinated on moist filter paper and after one week, seedlings were transplanted into seed trays with soil and, two days later, were transferred to the University of Georgia Botany greenhouses and allowed to establish for two weeks. Following establishment, six plants from each of the 24 populations (144 plants total) were transplanted into 7.6 L plastic pots (HPP200; Haviland Plastic Products, Haviland, OH) filled with a 3:1 mixture of sand and a calcined clay mixture (Turface MVP, Turface Athletics). Pots were fertilized with 60g Osmocote Plus (15-12-9 NPK; ScottsMiracle-Gro, Marysville, OH) and 15 mL each of gypsum (Performance Minerals Corporation,

Birmingham, 136 AL) and lime (Austinville Limestone, Austinville, VA) powders for supplemental $Ca^{2+}$. These pots were arranged in a randomized block design (6 replicated blocks x 1 individual per population x 24 populations) and maintained in the greenhouse for four additional weeks before being harvested at seven and a half weeks old. Greenhouse temperature was generally 82-84°F during the day and 72-74°F at night.

The day before harvest, gas exchange measurements were taken on a subset of plants using a Li-6800 Portable Photosynthesis System (Li-Cor, Inc. Lincoln, NE, USA). Measurements were taken from a single, most recent fully expanded leaf (MRFEL) from three blocks in twelve populations subsampled from across the range (noted in Table S4.1) in three blocks for a total of 36 plants. All measurements were taken (on the same day) between 10 AM and 1 PM and were made with the environmental chamber conditions set to an ambient $CO_2$ concentration of 400 μmol $mol^{-1}$, a fan speed of 10,000 rpm, and a light source of 2000 μmol $m^{-2}$ $s^{-1}$ PAR. Relative humidity in the chamber remained at ~ 20% greater than the ambient value for every measurement. Notably, the resulting estimates of empirical stomatal conductance correlated strongly with theoretical maximum stomatal conductance (see below) calculated as described by Earley et al. (2022; Figure S4.1).

The day-of-harvest traits were measured as described by Earley et al. (2022). Briefly, we collected biomass and separated leaves, stems, buds, and roots. Roots were gently washed to remove the growth substrate and all samples were dried in an oven at 60°C for at least 72 hours. Dried samples were weighed to determine root, stem, and leaf

biomass. Note that bud biomass was not analyzed further because only a subset of plants (45% of plants) had produced buds at the time of sampling, and buds only accounted for a mean of 1.3% of biomass; as such, they could be reasonably removed from further analyses. Mass fractions for the roots, stem, and leaves were determined by dividing each by total biomass. During harvest, one MRFEL was collected from each plant for leaf anatomy measurements. This leaf was weighed to determine fresh weight to calculate succulence. After weighing, leaves were scanned at 300 dpi to estimate leaf area using ImageJ v1.52b (Schindelin *et al.*, 2012). Half of each leaf was then pressed into dental putty for impressions to measure stomatal density and size (President Dental Putty; Coltène/Whaledent Inc., Cuyahoga Falls, OH) and then dried and weighed. The other half of the leaf was placed in Formalin-Acetic Acid-Alcohol (FAA) fixative and later cleared and stained for analyses of leaf venation (see below). Using the area estimates of the MRFEL along with the mass of the half of the leaf and midrib that were not placed in fixative we estimated the mass of the half of the leaf in fixative based on the LMA of the other half and then used that mass to calculate LMA for the whole leaf (both halves and midrib). Using LMA of the half we had weight for we estimated weight of the other half and used that to estimate LMA for the full leaf, not including petiole. LMA was calculated as LMA = dry mass/unit area ($g/m^2$). Similarly, succulence ($g/mm^2$) was calculated as (fresh weight - dry weight) / leaf area. Finally, maximum stomatal conductance ($g_{smax}$), the theoretical maximum rate of gas exchange if all stomata were fully open, was calculated based on stomatal density and size measurements using the approach of (Dow *et al.*, 2014).

Images of leaf impressions were taken and processed as described in Earley et al. (2022). Briefly this involved imaging both the top and bottom impressions for stomatal density and size measurements at 5x and 100x, respectively. Images of the stained leaves were captured using a flatbed scanner at 1200 dpi and then processed as described except that image resolution was decreased from previous work (from 2400 dpi to 1200 dip) since it decreased time to image while maintaining sufficient detail for all necessary measurements. This included both scanning on a flatbed scanner (for major and second VLA) and imaging four different fields of view under a microscope at 5x (for VLA). Second order vein length was measured from the scanned images by manually tracing veins that branched off of the midrib (i.e., the primary vein). Major vein length was then determined by adding the length of the midrib to the sum of the second order vein lengths. Minor vein length was measured from the microscope images using a deep neural network as described in Earley et al. (2022). Finally, a composite trait of stomata number per vein length was calculated as SV = average [top + bottom] stomatal density/VLA (Zhao et al. 2017).

*Data analysis*

All data analyses were conducted using R v3.4.3 (R Core Team, 2013) in R Studio v1.3.1093 (RStudio Team, 2015) and all graphs were made using the R package *ggplot2* (Wickham, 2016). A two-way ANOVA with population ID and block as the main effects was performed to test for variation among populations and to calculate estimated marginal trait means for genotypes after removing block effects. Marginal

means were estimated using the R package *emmeans* (Lenth, 2020) and these values were used for the bivariate and multivariate correlation analyses. Correlation matrices were created using the package *corrplot* (Wei and Simko, 2017). To visualize multivariate correlations, a principal component analysis (PCA) was conducted using the function prcomp() and the package *ggfortify* (Tang *et al.*, 2016; Horikoshi and Tang, 2018).

To correct for the non-independence of observations due to population structure, the file containing the full set of 1.7 million SNPs for all wild sunflower populations described by Todesco et al. (2020) was subsetted using BCFtools to get SNP info for only the individuals from 24 populations of interest (Danecek *et al.*, 2021). This subset was then filtered for minor allele frequency of >0.10 using PLINK 1.9b (Purcell *et al.*, 2007). The data was then filtered for linkage disequilibrium (LD) with an $R^2 < 0.6$, a window size of 10 kb, and a step size of 100 SNPs. After filtering, the number of markers was reduced to ca. 1.6 million. This SNP set was imported into R and converted to a genlight object using the *vcfR* package (Knaus and Grünwald, 2017) and randomly subsetted to a file with 10,000 SNPs; it was then converted into a genind object using the *adegenet* package (Jombart and Ahmed, 2011; Jombart, 2008), and finally to a hierfstat dataframe using the *hierfstat* package (Goudet, 2005). We calculated the Weir and Cockerham's (1984) pairwise $F_{ST}$ among all populations, and converted the resulting matrix into a matrix of genetic distances among populations following the approach presented in Rousset (1997). Genetic distances amongst populations can be visualized in Figure 4.1B. Lastly, we converted this genetic distance matrix to a matrix reflecting the variances and covariances among populations by first converting it into a phylo object using the *ape*

package (Paradis and Schliep, 2019) and then using the vcv.phylo function in the *ape* package. This genetic variance-covariance matrix was used in linear regression models to account for population structure.

To evaluate the relationship between traits and environmental variables from source populations we implemented a multi-level mixed effects model using the R package *brms* for Bayesian models (Bürkner, 2021; Bürkner, 2018; Bürkner, 2017). Environmental data were compiled for 26 factors from climate data collected over a 30-year period (1961-1990) for the geographical coordinates of each population site (Tables 4.1 and S4.2) using the package Climate NA (Wang *et al.*, 2016). We evaluated all pairwise trait-environment associations, with all traits as the response variable and environmental variables as predictors. All traits and environmental variables were centered to have a mean of zero and standard deviation of one prior to model fits. We included random intercepts for block (accounting for variation in traits within the greenhouse) and population ID (accounting for location-specific variation not captured in the population variance-covariance matrix), and a genetic variance-covariance matrix (which accounts for the non-independence of observations due to the genetic similarity of populations). Marginal $R^2$ values from all trait ~ environment models were visualized using a heatmap made with theR package *heatmap3* (Zhao *et al.*, 2014). Dendrograms based on observed trait-trait and environment-environment correlations were produced via hierarchical clustering and used to organize the heatmap.

Finally, to evaluate the association between traits and our measure of performance (total biomass), we fit a similar model with the same random effects structure, but with total biomass (centered and scaled) as the response, and traits as fixed effects. For these analyses, we chose traits that represented major axes of trait variation and that strongly predicted total biomass in cultivated sunflower (stomatal density sum, stomatal length, and LMA; see Earley et al 2022). Veins were excluded from these analyses because there was no detectable population effect on VLA. All models were run with four chains, 8000 iterations with a warmup of 4000 iterations, and a step-size of 0.999 (i.e., adapt delta = 0.999). We report efficient mixing of chains with no Rhat values greater than 1.00, and no instances in which there was more than one divergent transition. For each model, we report the mean estimated coefficient and 80% and 95% credible intervals, along with the marginal and full model Bayesian $R^2$ mean estimates (Gelman et al. 2018).

## RESULTS

### *Leaf trait variation and covariation in a common garden setting*

The median, minimum, and maximum values for all traits, along with a summary of the ANOVA results for each, are listed in Table 4.2. The majority of traits exhibited significant population effects (Table 4.2). Three traits (stomatal ratio, guard cell width [bottom], and pore length [average]) exhibited marginally significant population effects, while six traits (stomatal length bottom, pore length bottom, VLA, leaf area, stem mass fraction, and succulence) had no detectable population effect (Table 4.2). The bivariate

analyses revealed multiple examples of trait-trait correlations (Figure 4.2). Notably, stomatal density and stomatal length were significantly negatively correlated. There was a positive association between stomatal density and VLA, and a negative association between stomatal length and VLA, albeit not significant except for stomatal density on the top of the leaf (Figure 4.2). Leaf area was only significantly correlated with second and major VLA (Figure 4.2), indicating that patterns of variation in most leaf traits are unlikely to be driven by variation in leaf size.

Multivariate trait relationships were analyzed via PCA to determine major axes of variation. Since top and bottom stomatal traits were strongly correlated, we simplified the presentation of Figure 4.3 by using average values. For the full PCA with all traits (including top and bottom separately) see Figure S4.2A. The first three PCs combined to explain 65.5% variation with PC1 explaining 41.2%, PC2 12.7%, and PC3 11.6% (Figures 4.3 and S4.3). The top three traits contributing to each of the major axes were: PC1 – stomatal density (SD_Sum), SV, and $g_{smax}$; PC2 – midrib, leaf, and stem mass fractions; PC3 – stomatal density ratio, major VLA, and midrib mass fraction (Table 4.3). Given the observed trait loadings, PC1 appears to be most heavily influenced by traits related to gas exchange functioning such as stomatal density sum and stomata per vein length. In contrast, PC2 is strongly influenced by traits related to plant resource allocation including stem and leaf mass fractions. PC3 was not as clearly related to a set of functional traits (Table 4.3), though inspection of the scree plot (Figure S4.3) indicates that the percentage of variation explained flattens after the first two axes. Interestingly, the fact that the primary axis of variation is heavily influenced by traits related to gas

exchange is consistent with the results of Earley et al. (2022) for a survey of cultivated sunflower (see also Chapters 2 and 3 of this dissertation).

*Correlation between trait variation and environmental variables*

A multivariate visualization of the environmental data can be seen in Figure S4.2B; for a numerical summary of the median, minimum, and maximum of values across locations and ANOVA results see Table S4.2. Inspection of this figure reveals that the first two principal components explain 63.0% (PC1) and 21.3% (PC2) of the observed variation, with PC1 corresponding primarily to variables related to temperature (MAT, DD_18, and DD5) and PC2 primarily corresponding to variables related to precipitation/moisture (MAP, CMD, and CMI; Table S4.3). The results of our trait-environment analyses are summarized in Figure 4.4 and Table S4.4. In general terms, biomass-related traits were associated (albeit not significantly) with a variety of temperature-related variables, with greater biomass accumulation in the common garden in plants from warmer environments and lower biomass accumulation in plants from cooler environments. Root mass fraction and midrib density also have many significant associations across mostly temperature related variables, with greater allocation to roots in plants from warmer environments. There were many significant trait associations for PAS (precipitation as snow). This makes sense, as more snow means more snow melt to recharge the soil with moisture for plants in the spring; interestingly, our results show that an increase in PAS is associated with less biomass production, which is counter to our expectations (Nielsen 1998). Upon closer inspection, however, we find that these

associations are likely driven by a geographic artifact (Figure S4.5A): the South Texas region exhibits no variation for PAS while the Intermountain West and West show substantial variation. These results must therefore be interpreted with caution, as they likely reflect trait differentiation that correlates more with geography than environment, and which was not captured by the inclusion of population IDs as a random effect, nor in our efforts to correct for genetic non-independence. A similar pattern was evident for SHM and AHM (the summer and annual heat-moisture indices, respectively; Figure S4.5B-C). For these traits, three of the regions exhibited a very small amount of variation, with one region being much more variable. The result was an overall negative mean estimate that is driven by the West region with all other regions exhibiting a positive correlation. A review of the bivariate plots (Figure S4.4) showed that DD_0 also had a similar pattern of geographic variation (Figure S4.5D). Therefore, any associations with these variables should be interpreted with caution. Many other traits, however, did not exhibit problematic geographic distributions such as this (e.g., Eref and RH; Figure 4.5)

As for leaf anatomical traits, we overall saw fewer clear associations with environmental variables. In fact, the only variables that were significant for VLA are SHM and AHM which, as noted above, are largely driven by regional differences, and may not reflect true trait-environment associations. Size-related stomatal traits had weak environmental associations overall, with the most promising association being between stomatal length and Eref (Hargreaves reference evaporation, which estimates potential evapotranspiration based on air temperature and radiation; Figure 4.4). Stomatal density ratio exhibited significant positive associations with EXT (maximum temperature over 30

years) and TD (temperature difference between the coldest and warmest months), both of which are measures of temperature extremes. Based on these results, it appears that extreme high temperatures and broader seasonal temperature ranges result in a higher proportion of stomata on the bottom of the leaf, suggesting a possible adaptive role for this trait. Stomatal density sum and $g_{smax}$ did not have any significant associations that did not include the potential geographic artifact mentioned above, and the overall associations are weak. Succulence exhibited significant positive associations with TD and MAP (mean annual precipitation) indicating that plants from wetter climates and with broader seasonal temperature ranges are more succulent (Figure 4.4). Succulence also had significant negative associations with MAR (mean annual solar radiation) and CMD (Hargreaves climatic moisture deficit, which measures evaporative demand that exceeds available soil moisture) indicating that plants from environments with weaker solar radiation and a smaller moisture deficit had more succulent leaves.

*Relationship between trait variation and performance*

Our analysis of plant performance (measured as biomass) as a function of three key leaf traits revealed substantial predictive power. The traits of interest (i.e., stomatal length, stomatal density [sum], and LMA) were chosen to represent major axes of leaf trait variation documented by Earley et al. (2022; see also Chapters 2 and 3 of this dissertation); VLA was excluded here due to a lack of detectable variation across populations (Table 4.2). Remarkably, the resulting model was also able to predict plant performance with an overall marginal $R^2 = 0.67$ (Figure 4.6A). Uncertainty in model

estimates was evaluated using posterior credible intervals (Figure 4.6B and Table S4.5). Estimates with 95% CIs not overlapping zero were interpreted as having strong support and those with an 80% CI not overlapping zero were viewed as having moderate support. Of the traits included as predictors, stomatal density sum and LMA were both strongly associated with total biomass and performance while stomatal length showed moderate association (Figure 4.6B and Table S4.5). Predictive power was further improved by using the first two trait principal components from our multivariate analysis of size-independent traits to predict plant performance. In this case, the overall marginal $R^2$ = 0.73 (Figure 4.6C). As noted above, PC1 is most heavily influenced by traits related to gas exchange whereas PC2 is most heavily allocation-related traits (Figure 4.3, Table 4.3), and both PCs had a strong association with total biomass (Figure 4.6D; Table S4.6).

## DISCUSSION

Cultivated sunflower exhibits a large reduction in genetic diversity compared to wild sunflower (Mandel *et al.*, 2011; Liu and Burke, 2006) due to the occurrence of genetic bottlenecks during domestication and/or improvement. While this reduction in genetic variation, which is observed in most crop taxa, may limit future breeding efforts, the wild relatives of crop plants represent a possible source of variation to support ongoing improvement efforts. We thus investigated patterns of leaf trait variation and covariation across natural populations of wild sunflower and tested for trait-environment correlations, which may reflect the adaptive value of observed variation. Finally, we

sought to determine the extent to which such trait variation can be used to predict overall whole plant performance.

*Leaf trait variation and covariation in a common garden setting*

The existence of significant trait variation across wild populations when grown in a common garden setting indicates the presence of genetic variation for the majority of analyzed traits, including various aspects of leaf anatomy along with measures of growth and allocation, across the natural range of the species. Across populations, traits also exhibited many of the expected bivariate correlations based on the literature and what is known about their likely roles in plant-water relations (Sack and Scoffoni, 2013; Doheny-Adams *et al.*, 2012; Shahinnia *et al.*, 2016; Figure S4.2). For instance, stomatal density and size were negatively correlated while stomatal density and VLA were positively correlated (Figure 4.2). These associations were expected as the total area allocated to stomata affects total stomatal conductance and photosynthesis, so size and density are tightly correlated (Harrison *et al.*, 2019; Shahinnia *et al.*, 2016). In addition, a balance between veins and stomata is expected such that water use and carbon acquisition are optimized (Brodribb *et al.*, 2007), otherwise the cost in carbon to produce larger or more dense stomata or veins exceeds the photosynthetic gain (Carins Murphy *et al*., 2014). At the multivariate level, distinct patterns emerged between suites of traits (Figure 4.3; Table 4.3). Here again, these trait relationships were largely as expected. For example, the top two PCs were heavily influenced by traits related to gas exchange and allocation, respectively (Table 4.3). The predominance of traits related to gas exchange was seen in

cultivated sunflower, as well (Earley et al. 2022), suggesting the existence of a persistent functional relationship across both wild and cultivated sunflower. The existence of a second axis that is most heavily influenced by allocation-related traits suggests the existence of different growth and resource allocation strategies across the range of wild sunflower (Hernández *et al.*, 2020; Mason and Donovan, 2015).

*Correlations between trait variation and environmental variables*

Looking across populations, we found that growth/biomass-related traits correlated most strongly with temperature-related environmental variables, with plants from warmer source environments generally being larger than those from cooler environments. This result may reflect adaptation to a longer growing season in warmer climates, with plants being able to grow larger in warmer climates. It is important to note that we only tracked plants through the earlier developmental stages, prior to harvest at seven and a half weeks after initiation of germination. Consistent with this view, we also saw generally positive (if not significant) associations with variables related to the length of the growing season such as FFP (length of the frost-free period). In terms of resource allocation and leaf construction, root mass fraction and midrib density also exhibited strong correlations with a number of these temperature related traits. Again, roots grew more (at least in a relative sense) and midrib density increased with warmer weather and a longer growing season. Previous work has shown that root biomass increases in warmer climates due to an improved plant photosynthetic rate and longer growing season (Ma *et*

*al.*, 2017). At the same time, denser midribs may be helpful for larger plants to provide increased mechanical support in the leaves (Blonder *et al.*, 2020).

As noted in the Results, the numerous trait associations with environmental variables that exhibited strong geographic structuring (e.g., PAS, SHM, and AHM) should be interpreted with caution. In fact, in some cases (e.g., VLA vs. SHM and AHM; Figure S4.5), range wide estimates of a negative trait/environment association mask possible positive associations within some regions despite our best efforts to control for population identity and genetic similarity. Interestingly, Eref (i.e., potential evapotranspiration based on air temperature and radiation) exhibited numerous trait associations (similar to the number of associations detected with PAS, but without the confounding effect due to regional differences). This includes a positive correlation with numerous biomass traits, and a strongly positive association with RMF. Increased evapotranspiration from the leaf could facilitate higher levels of photosynthesis, and thus more carbon resources being available for plant growth (Running *et al.*, 1989). However, the relationship between evapotranspiration and photosynthesis is complex (Bai *et al.*, 2021), and any conclusions on this front await further validation.

In the case of leaf anatomical traits, we found many fewer environmental associations, despite significant variation across populations for most of these traits. While it could be the case that the effects are more subtle and thus difficult to detect given the experimental design and sample sizes employed herein, the magnitude of the marginal $R^2$ values is quite low for these traits. Interestingly, for these same sorts of traits,

we observed much less in the way of plasticity as compared to growth traits (Earley *et al.*, 2022; Chapter 3), which suggests the possibility that variation in these finer-scale traits may be more constrained than in higher-level, growth-related traits. By extension, this relative lack of evolutionary lability may make these traits less likely to exhibit clear environmental associations in wild sunflower. We did, however, find a positive association between stomatal density ratio and both TD and EXT which are both reflective of temperature extremes. Stomatal ratio has been found in some species to correlate with stomatal conductance (Xiong and Flexas, 2020) though no such relationship was identified herein so possible explanations for this relationship remain unclear. Similarly, succulence was positively associated with MAP and TD, suggesting that plants from wetter climates with more extreme temperature swings produce more succulent leaves. This is a somewhat surprising result, as succulence generally tends to be higher in plants from drier climates (Grace, 2019). However, when looking more closely at the raw data this pattern is only apparent in two of the four regions, and the marginal $R^2$ and is not particularly high despite the 80% credible interval not overlapping zero. Other environmental variables of potential interest based on the presumptive roles of the traits under consideration (Sack *et al.*, 2013; Buckley, 2019) – such as RH, MSP, and MWMT – show little in the way of clear associations.

*Relationship between trait variation and performance*

Despite the lack of clear correlations between leaf anatomical traits and the environment, these traits did offer substantial predictive power for overall plant

performance (i.e., growth assessed as biomass accumulation). Indeed, our use of just three key leaf traits representing previously identified axes of phenotypic variation explained nearly 70% of the observed variation in biomass accumulation, and use of the values from the first two PCs did even better, accounting for over 70% of the observed variation. From a trait-based perspective, this relationship makes sense given that stomata play a critical role in gas exchange and thus affect resources available to the whole plant for growth (Sack *et al.*, 2013). Moreover, both stomatal density and LMA were positively correlated with biomass (Figure 4.2), and this relationship held up even after accounting for genetic similarity across populations, consistent with their inferred effects from our predictive model. This finding is further bolstered by the results of our PC-based analysis, wherein PC1 (Sack *et al.*, 2013), and related traits (Figure 4.3), corresponding to an increase in growth/performance. The other major PC, corresponding largely to allocation-related traits, was negatively associated with performance. Consistent with the bivariate correlations, this result indicates that increased allocation to leaves at the expense of the stem and midrib fractions, is associated with decreased performance.

Interestingly, stomatal length exhibited a negative (albeit non-significant) bivariate correlation with biomass – consistent with its negative correlation with stomatal density – but it had a positive effect on biomass in our trait-based model (in which we were able to estimate the association of stomatal size with biomass while accounting for the effect of density on biomass, and vice versa). Thus, it may be that case that plants with more total stomatal area per unit leaf area (i.e., those with more dense and larger stomata) are more capable of higher levels of gas exchange and photosynthesis and thus

increased growth under benign conditions with ample resources. This runs counter to the view that increasing stomatal size without a concurrent decrease in density results in stomata that are too close together and carbon acquisition and water use are not optimized (de Boer *et al.*, 2016; Carins Murphy *et al.*, 2014; Brodribb *et al.*, 2007). However, the correlation between stomatal density and size – while being negative – is far from perfect. Considering this result, it may be the case that certain aspects of leaf anatomy that have traditionally been viewed as being the subject of strong constraint can be fine-tuned to improve performance.

REFERENCES

**Bai, Y., Zhang, S., Zhang, J., Wang, J., Yang, S., Magliulo, V., Vitale, L. and Zhao, Y.** (2021) Using remote sensing information to enhance the understanding of the coupling of terrestrial ecosystem evapotranspiration and photosynthesis on a global scale. *Int. J. Appl. Earth Obs. Geoinf.*, **100**, 102329.

**Bertolino, L.T., Caine, R.S. and Gray, J.E.** (2019) Impact of stomatal density and morphology on water-use efficiency in a changing world. *Front. Plant Sci.*, **10**, 225.

**Blonder, B., Both, S., Jodra, M., et al.** (2020) Linking functional traits to multiscale statistics of leaf venation networks. *New Phytol.* Available at: http://dx.doi.org/10.1111/nph.16830.

**Boer, H.J. de, Price, C.A., Wagner-Cremer, F., Dekker, S.C., Franks, P.J. and Veneklaas, E.J.** (2016) Optimal allocation of leaf epidermal area for gas exchange. *New Phytol.*, **210**, 1219–1228.

**Brodribb, T.J., Feild, T.S. and Jordan, G.J.** (2007) Leaf maximum photosynthetic rate and venation are linked by hydraulics. *Plant Physiol.*, **144**, 1890–1898.

**Buckley, T.N.** (2019) How do stomata respond to water status? *New Phytol.*, **224**, 21–36.

**Bürkner, P.-C.** (2018) Advanced Bayesian Multilevel Modeling with the R Package brms. *R J.*, **10**, 395.

**Bürkner, P.-C.** (2021) Bayesian Item Response Modeling in R with brms and Stan. *J. Stat. Softw.*, **100**, 1–54.

**Bürkner, P.-C.** (2017) brms: An R Package for Bayesian Multilevel Models Using Stan. *J. Stat. Softw.*, **80**, 1–28.

**Carins Murphy, M.R., Jordan, G.J. and Brodribb, T.J.** (2014) Acclimation to humidity modifies the link between leaf size and the density of veins and stomata. *Plant Cell Environ.*, **37**, 124–131.

**Carlson, J.E., Adams, C.A. and Holsinger, K.E.** (2016) Intraspecific variation in stomatal traits, leaf traits and physiology reflects adaptation along aridity gradients in a South African shrub. *Ann. Bot.*, **117**, 195–207.

**Danecek, P., Bonfield, J.K., Liddle, J., et al.** (2021) Twelve years of SAMtools and BCFtools. *Gigascience*, **10**. Available at: http://dx.doi.org/10.1093/gigascience/giab008.

**De la Haba, P., De la Mata, L., Molina, E. and Agüera, E.** (2014) High temperature promotes early senescence in primary leaves of sunflower (*Helianthus annuus* L.) plants. *Can. J. Plant Sci.*, **94**, 659–669.

**Dempewolf, H., Baute, G., Anderson, J., Kilian, B., Smith, C. and Guarino, L.** (2017) Past and Future Use of Wild Relatives in Crop Breeding. *Crop Sci.*, **57**, 1070–1082.

**Doheny-Adams, T., Hunt, L., Franks, P.J., Beerling, D.J. and Gray, J.E.** (2012) Genetic manipulation of stomatal density influences stomatal size, plant growth and tolerance to restricted water supply across a growth carbon dioxide gradient. *Philosophical Transactions of the Royal Society of London. Series B, Biological sciences*, **367**, 547–555.

**Dow, G.J., Bergmann, D.C. and Berry, J.A.** (2014) An integrated model of stomatal development and leaf physiology. *New Phytologist*, **201**, 1218–1226.

**Driesen, E., Van den Ende, W., De Proft, M. and Saeys, W.** (2020) Influence of Environmental Factors Light, CO2, Temperature, and Relative Humidity on Stomatal Opening and Development: A Review. *Agronomy*, **10**, 1975. Available at: [Accessed July 5, 2022].

**Dunlap, J.M. and Stettler, R.F.** (2001) Variation in leaf epidermal and stomatal traits of *Populus trichocarpa* from two transects across the Washington Cascades. *Can. J. Bot.*, **79**, 528–536.

**Earley, A.M., Temme, A.A., Cotter, C.R. and Burke, J.M.** (2022) Genomic regions associate with major axes of variation driven by gas exchange and leaf construction traits in cultivated sunflower (*Helianthus annuus* L.). *Plant J.* Available at: http://dx.doi.org/10.1111/tpj.15900.

**FAO** (2021) The State of the World's Land and Water Resources for Food and Agriculture: Systems at breaking point. Available at: https://www.fao.org/3/cb7654en/cb7654en.pdf [Accessed August 22, 2022].

**Faralli, M., Matthews, J. and Lawson, T.** (2019) Exploiting natural variation and genetic manipulation of stomatal conductance for crop improvement. *Curr. Opin. Plant Biol.*, **49**, 1–7.

**Godfray, H.C.J., Beddington, J.R., Crute, I.R., et al.** (2010) Food security: the challenge of feeding 9 billion people. *Science*, **327**, 812–818.

**Goudet, J.** (2005) hierfstat, a package for r to compute and test hierarchical F-statistics. *Mol. Ecol. Notes*, **5**, 184–186.

**Grace, O.M.** (2019) Succulent plant diversity as natural capital. *Plants People Planet*, **1**, 336–345.

**Harrison, E.L., Arce Cubas, L., Gray, J.E. and Hepworth, C.** (2019) The influence of stomatal morphology and distribution on photosynthetic gas exchange. *The Plant Journal*, **101**, 768–779.

**Hernández, F., Poverene, M., Mercer, K.L. and Presotto, A.** (2020) Genetic variation for tolerance to extreme temperatures in wild and cultivated sunflower *(Helianthus annuus*) during early vegetative phases. *Crop Pasture Sci.*, **71**, 578–591. Available at: [Accessed September 1, 2022].

**Horikoshi, M. and Tang, Y.** (2018) ggfortify: Data Visualization Tools for Statistical Analysis Results. Available at: https://CRAN.R-project.org/package=ggfortify.

**Jombart, T.** (2008) adegenet: a R package for the multivariate analysis of genetic markers. *Bioinformatics*, **24**, 1403–1405.

**Jombart, T. and Ahmed, I.** (2011) adegenet 1.3-1: new tools for the analysis of genome-wide SNP data. *Bioinformatics*, **27**, 3070–3071.

**Knaus, B.J. and Grünwald, N.J.** (2017) vcfr: a package to manipulate and visualize variant call format data in R. *Mol. Ecol. Resour.*, **17**, 44–53.

**Lenth, R.** (2020) emmeans: Estimated Marginal Means, aka Least-Squares Means. Available at: https://CRAN.R-project.org/package=emmeans.

**Liu, A. and Burke, J.M.** (2006) Patterns of nucleotide diversity in wild and cultivated sunflower. *Genetics*, **173**, 321–330.

**Mandel, J.R., Dechaine, J.M., Marek, L.F. and Burke, J.M.** (2011) Genetic diversity and population structure in cultivated sunflower and a comparison to its wild progenitor, *Helianthus annuus* L. *Theor. Appl. Genet.*, **123**, 693–704.

**Mason, C.M. and Donovan, L.A.** (2015) Evolution of the leaf economics spectrum in herbs: Evidence from environmental divergences in leaf physiology across *Helianthus* (Asteraceae). *Evolution*, **69**, 2705–2720.

**Ma, X.-X., Yan, Y., Hong, J.-T., Lu, X.-Y. and Wang, X.-D.** (2017) Impacts of warming on root biomass allocation in alpine steppe on the north Tibetan Plateau. *J. Mt. Sci.*, **14**, 1615–1623.

**Moore, C.E., Meacham-Hensold, K., Lemonnier, P., Slattery, R.A., Benjamin, C., Bernacchi, C.J., Lawson, T. and Cavanagh, A.P.** (2021) The effect of increasing temperature on crop photosynthesis: from enzymes to ecosystems. *J. Exp. Bot.*, **72**, 2822–2844.

**Nielsen, D.C. (1998).** Snow catch and soil water recharge in standing sunflower residue. *Journal of production agriculture*, **11.4**, pp.476-480.

**NOAA and NIDIS** (2022) US Crops and Livestock in Drought. *National Integrated Drought Information System*. Available at: https://www.drought.gov/sectors/agriculture [Accessed August 22, 2022].

**Paradis, E. and Schliep, K.** (2019) ape 5.0: an environment for modern phylogenetics and evolutionary analyses in R. *Bioinformatics*, **35**, 526–528.

**Purcell, S., Neale, B., Todd-Brown, K., et al.** (2007) PLINK: a tool set for whole-genome association and population-based linkage analyses. *Am. J. Hum. Genet.*, **81**, 559–575.

**R Core Team** (2013) *R: The R project for statistical computing*, Available at: https://www.r-project.org/ [Accessed April 17, 2019].

**Rousset, F.** (1997) Genetic differentiation and estimation of gene flow from F-statistics under isolation by distance. *Genetics*, **145**, 1219–1228.

**RStudio Team** (2015) *RStudio: integrated development for R*.

**Running, S.W., Nemani, R.R., Peterson, D.L., Band, L.E., Potts, D.F., Pierce, L.L. and Spanner, M.A.** (1989) Mapping regional forest evapotranspiration and photosynthesis by coupling satellite data with ecosystem simulation. *Ecology*, **70**, 1090–1101.

**Sack, L. and Scoffoni, C.** (2013) Leaf venation: structure, function, development, evolution, ecology and applications in the past, present and future. *New Phytologist*, **198**, 983–1000.

**Sack, L. and Scoffoni, C.** (2012) Measurement of leaf hydraulic conductance and stomatal conductance and their responses to irradiance and dehydration using the Evaporative Flux Method (EFM). *Journal of Visualized Experiments*, e4179.

**Sack, L., Scoffoni, C., John, G.P., Poorter, H., Mason, C.M., Mendez-Alonzo, R. and Donovan, L.A.** (2013) How do leaf veins influence the worldwide leaf economic spectrum? Review and synthesis. *J. Exp. Bot.*, **64**, 4053–4080.

**Schindelin, J., Arganda-Carreras, I., Frise, E., et al.** (2012) Fiji: an open-source platform for biological-image analysis. *Nature Methods*, **9**, 676–682.

**Seiler, G.J. and Rieseberg, L.H.** (1997) Systematics, Origin, and Germplasm Resources of the Wild and Domesticated Sunflower. In *Sunflower Technology and Production*. Agronomy Monograph. Madison, WI: American Society of Agronomy, Crop Science Society of America, Soil Science Society of America, pp. 21–65.

**Shahinnia, F., Le Roy, J., Laborde, B., Sznajder, B., Kalambettu, P., Mahjourimajd, S., Tilbrook, J. and Fleury, D.** (2016) Genetic association of stomatal traits and yield in wheat grown in low rainfall environments. *BMC Plant Biology*, **16**, 150.

**Siebert, S., Ewert, F., Rezaei, E.E., Kage, H. and Graß, R.** (2014) Impact of heat stress on crop yield—on the importance of considering canopy temperature. *Environ. Res. Lett.*, **9**, 044012.

**Tang, Y., Horikoshi, M. and Li, W.** (2016) ggfortify: Unified Interface to Visualize Statistical Result of Popular R Packages. *The R Journal*, **8**. Available at: https://journal.r-project.org/.

**Todesco, M., Owens, G.L., Bercovich, N., et al.** (2020) Massive haplotypes underlie ecotypic differentiation in sunflowers. *Nature*, **584**, 602–607.

**Wang, T., Hamann, A., Spittlehouse, D. and Carroll, C.** (2016) Locally Downscaled and Spatially Customizable Climate Data for Historical and Future Periods for North America. *PLoS One*, **11**, e0156720.

**Weir, B.S. and Cockerham, C.C.** (1984) Estimating F-Statistics for the Analysis of Population Structure. *Evolution*, **38**, 1358–1370.

**Wei, T. and Simko, V.** (2017) *R package "corrplot": Visualization of a Correlation Matrix*, Available at: https://github.com/taiyun/corrplot.

**Wickham, H.** (2016) ggplot2: Elegant Graphics for Data Analysis. Available at: https://ggplot2.tidyverse.org.

**Xie, J., Wang, Z. and Li, Y.** (2022) Stomatal opening ratio mediates trait coordinating network adaptation to environmental gradients. *New Phytol.*, **235**, 907–922.

**Xiong, D. and Flexas, J.** (2020) From one side to two sides: the effects of stomatal distribution on photosynthesis. *New Phytol.*, **228**, 1754–1766.

**Zhao, S., Guo, Y., Sheng, Q. and Shyr, Y.** (2014) Heatmap3: an improved heatmap package with more powerful and convenient features. *BMC Bioinformatics*, **15**, 1–2.

FIGURES

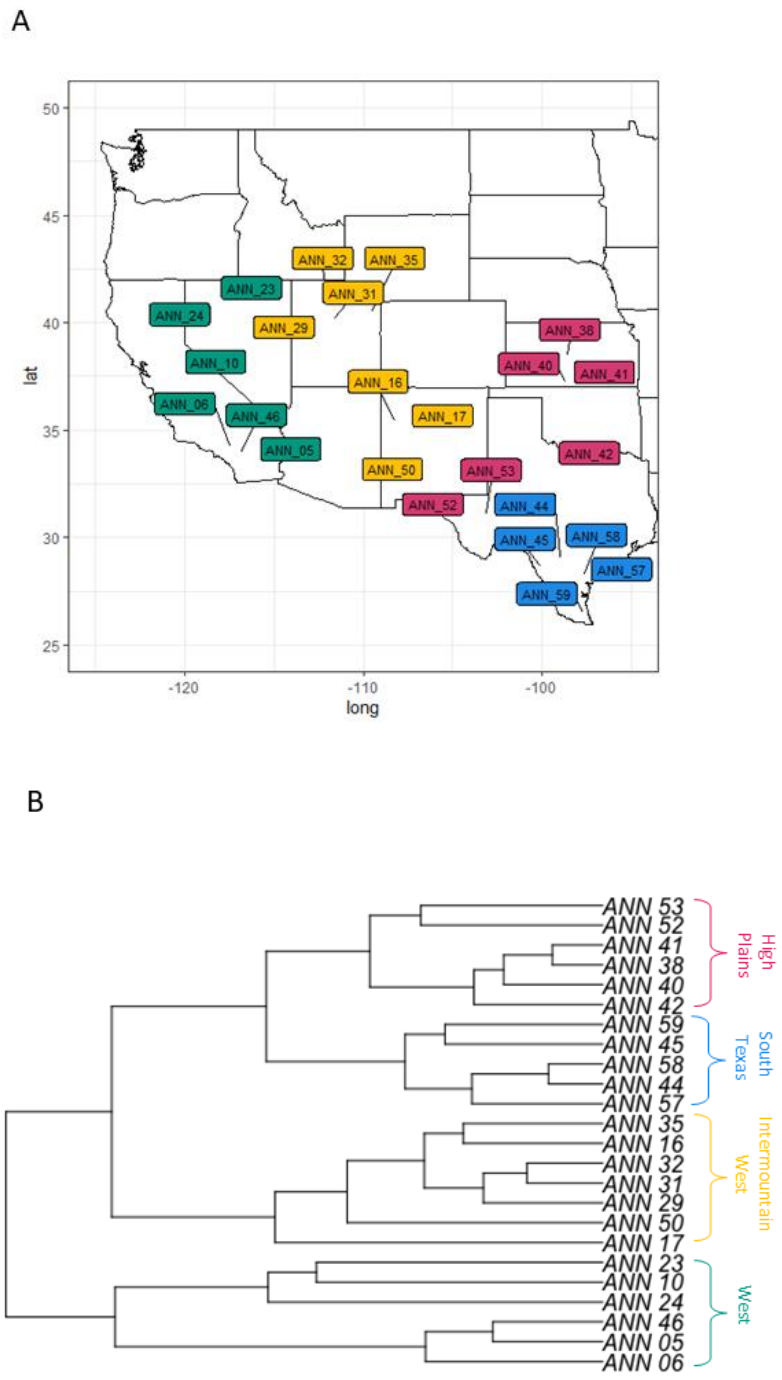


**Figure 4.1**: (A) Map of wild *Helianthus annuus* populations. Labels represent geographic locations for the 24 populations analyzed based on latitude and longitude. (B)

Dendrogram of population clustering based on genetic distances estimated from a random sampling of 10k SNPs across the genome. Broad geographic regions are indicated to the right of the dendrogram and by color-coding of the labels.

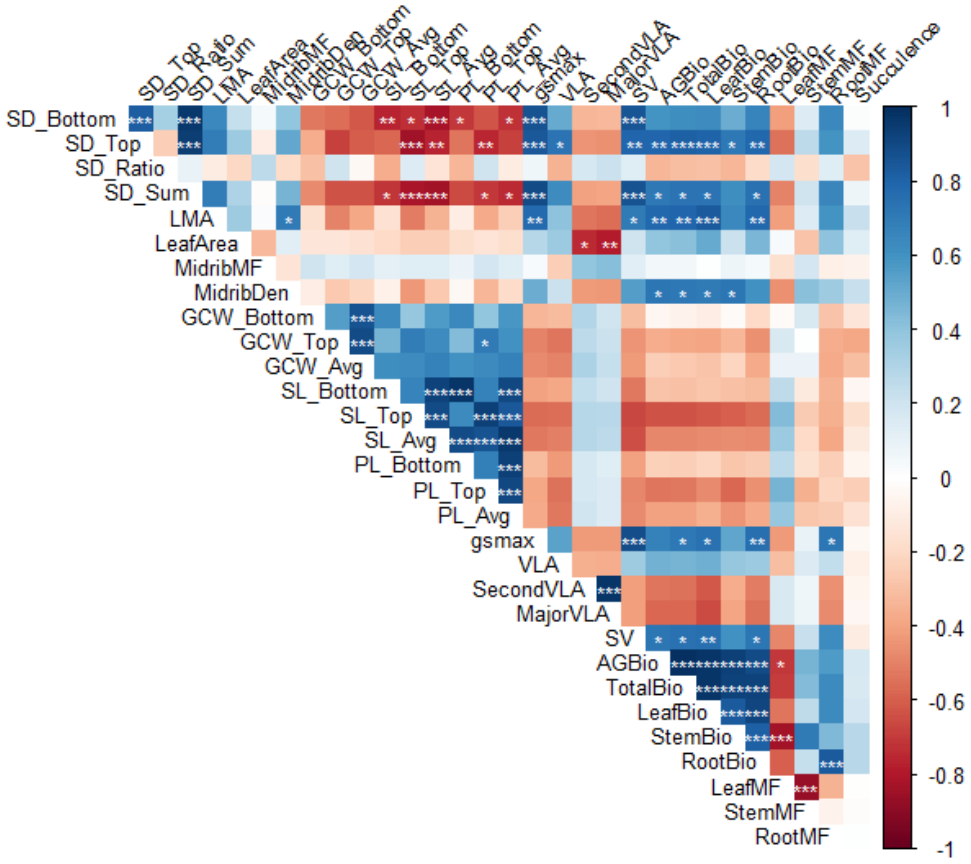


**Figure 4.2:** Correlation matrix of leaf and growth traits. Values were calculated using population marginal means and corrected for multiple comparisons using a Bonferroni correction. Positive correlations are in blue and negative correlations are in red. Shading gives a relative indication of the magnitude of the estimate. ***$P \leq 0.001$, **$P \leq 0.01$, *$P \leq 0.05$. Trait abbreviations are as defined in Table 4.1.

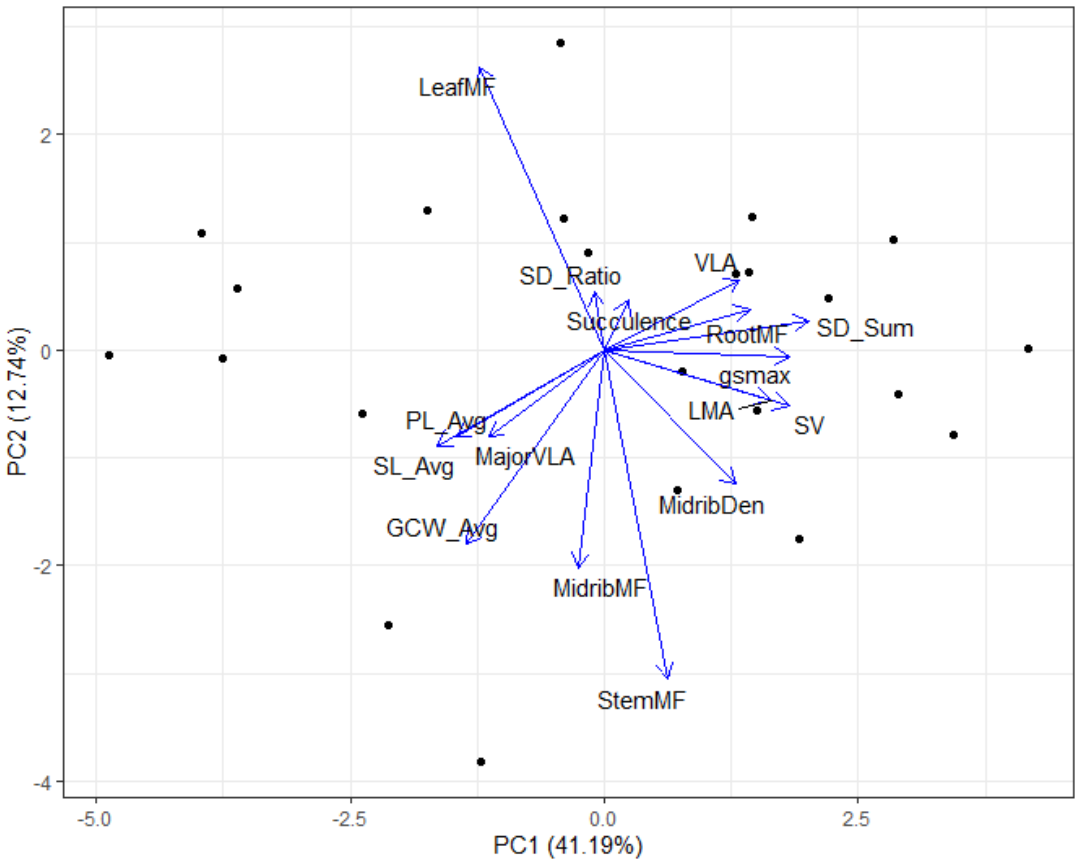


**Figure 4.3:** Principal component analysis (PCA) of putatively size-independent traits using estimated marginal means. Traits names that include _Avg (stomatal length [SL], pore length [PL], guard cell width [GCW]) are averages of the values from the top and bottom of the leaf and SD_Sum is the sum of stomatal density from the top and bottom. Trait abbreviations are as defined in Table 4.2.

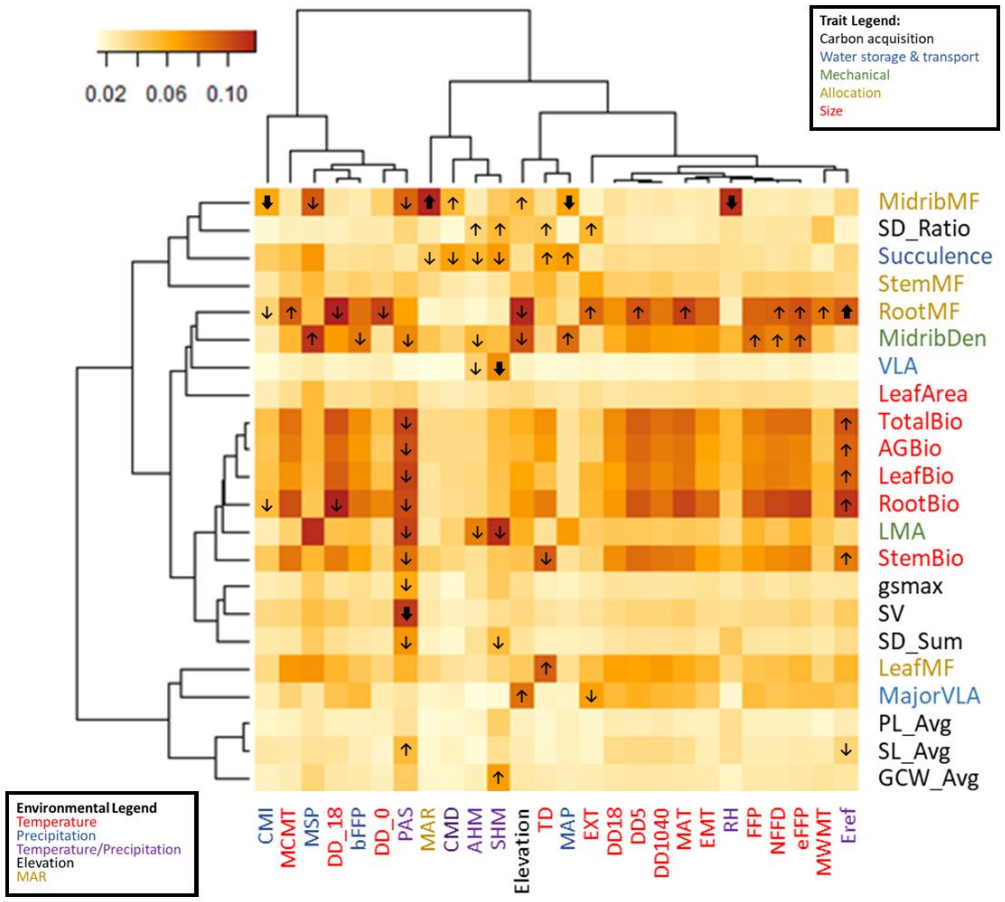


**Figure 4.4:** Heatmap of the association of traits vs. environmental variables. Dendrograms are based on hierarchical clustering of trait/trait and environment/environment correlations. Heatmap is colored based on marginal $R^2$ values of models with one trait as response variable and one environmental variable as predictor. Models are described fully in methods. All traits have been scaled to a mean of zero and a standard deviation of one. Arrows indicate models that did not overlap zero at the 80% credible interval along with the direction of association. Bold arrows indicate those that did not overlap zero at the 95% credible interval along with the direction of association. Colors of labels indicate grouping of traits and environmental variables into broad categories (see legends). Abbreviations follow Tables 4.1 and 4.2.

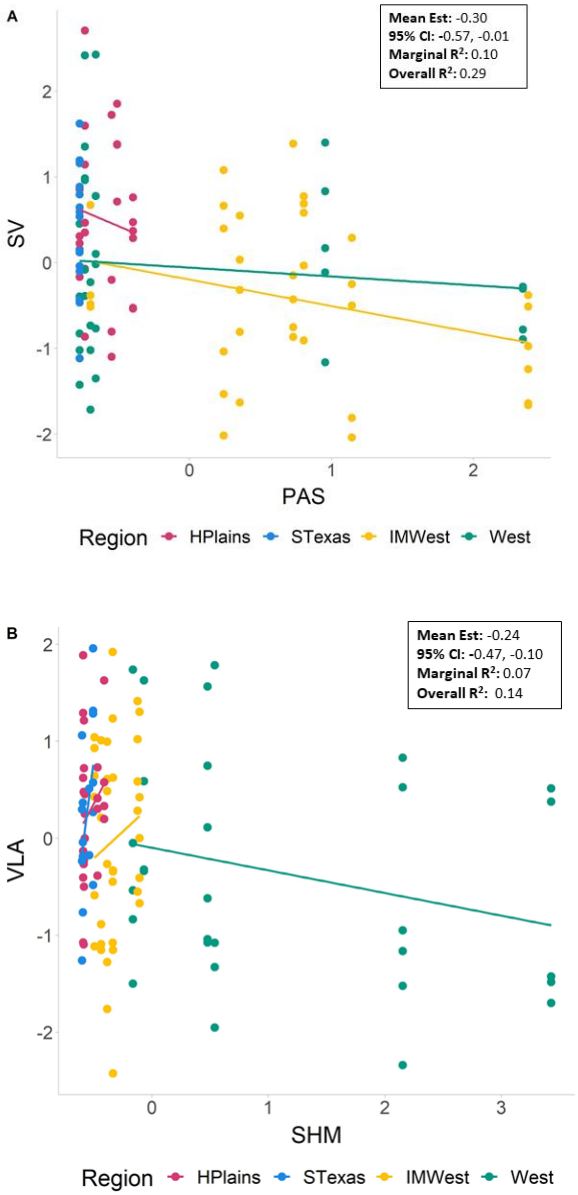


**Figure 4.5:** Example bivariate plots of traits vs. environmental variables. (A) Root MF vs. Eref, (B) Midrib MF vs. RH. All traits and environmental variables were scaled to a mean of zero and a standard deviation of one. Dots represent individual plants and lines

indicate the line of best fit per region. Text box includes results from models including mean estimate, the 95% credible interval, and marginal R2 value. HPlains = High Plains, STexas = South Texas, and IMWest = Intermountain West. Abbreviations follow Tables 4.1 and 4.2. For all bivariate plots, see Figure S4.4.

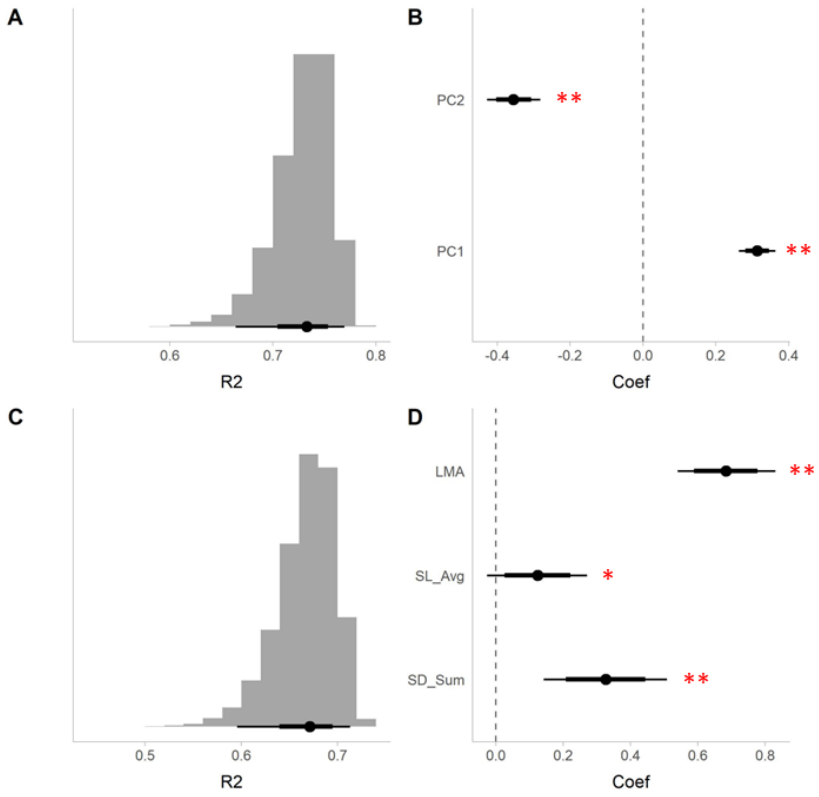


**Figure 4.6:** Results of our analysis of performance using a linear mixed effects regression model. All output reflects posterior summaries from the model. (A) Estimated Bayesian $R^2$ for fixed effects only for the model using stomatal density sum (SD_Sum), stomatal length (SL_Avg), and LMA. (B) Coefficient estimates for each trait for the traits model. (C) Estimated Bayesian $R^2$, for fixed effects only (full posterior distribution of the model) for the model using trait PCs. (D) Coefficient estimates for each trait for the PC model. All traits were scaled to a mean of zero and standard deviation of one. The black dot indicates the estimated value, the heavier bars indicate the 80% credible intervals for each estimate, and the lighter lines indicate the 95% credible intervals. Estimates with

95% CIs not overlapping zero were interpreted as having strong support (**), and those with 80% CIs with moderate support (*).

TABLES

**Table 4.1:** List of all environmental variables along with their descriptions and units.

| Enviromental Variable | Description |
|---|---|
| MAT | mean annual temperature (°C) |
| MWMT | mean temperature of the warmest month (°C) |
| MCMT | mean temperature of the coldest month (°C) |
| TD | difference between MCMT and MWMT, as a measure of continentality (°C) |
| MAP | mean annual precipitation (mm) |
| MSP | mean summer (May to Sep) precipitation (mm) |
| AHM | annual heat:moisture index (MAT+10)/(MAP/1000)) |
| SHM | summer heat:moisture index ((MWMT)/(MSP/1000)) |
| DD_0 | degree-days below 0°C, chilling degree-days |
| DD5 | degree-days above 5°C, growing degree-days |
| DD_18 | degree-days below 18°C, heating degree-days |
| DD18 | degree-days above 18°C, cooling degree-days |
| NFFD | the number of frost-free days |
| bFFP | the Julian date on which FFP begins |
| eFFP | the Julian date on which FFP ends |
| FFP | frost-free period |
| PAS | precipitation as snow (mm). For an individual year, PAS is calculated for the period between August in previous year and July in current year |
| EMT | extreme minimum temperature over 30 years. For an individual year, the EMT is estimated for a 30-year normal period (one of the nine normal periods included in the package) where the individual year is nearest to the centre of the normal period |
| EXT | extreme maximum temperature over 30 years. For an individual year, the EXT is estimated for a 30-year normal period where the individual year is nearest to the centre of the normal period |
| Eref | Hargreaves reference evaporation (mm) |
| CMD | Hargreaves climatic moisture deficit (mm) |
| MAR | mean annual solar radiation (MJ m-2 d-1) |
| RH | mean annual relative humidity (%) |

**Table 4.2:** List of all traits measured along with the median and range of trait values. Significance for population effects (***P ≤ 0.001, **P ≤ 0.01, * P ≤ 0.05, # P ≤ 0.1, ns = not significant) and adjusted $R^2$ from the model are also presented. SD = stomatal density; LMA = leaf mass per area; MF = mass fraction; GCW = guard cell width; SL = stomatal length; PL = stomatal pore length; $g_{smax}$ = theoretical maximum stomatal conductance; VLA = vein length per area; SV = stomata per vein length; AG = aboveground; Bio = biomass

| Trait | Median | Min | Max | Population Effect | Adjusted R2 |
|---|---|---|---|---|---|
| SD_Bottom (stomata/$mm^2$) | 274.19 | 189.84 | 352.84 | ** | 0.04 |
| SD_Top (stomata/$mm^2$) | 207.04 | 143.67 | 257.80 | *** | 0.09 |
| Stomatal Ratio (bottom/sum) | 0.57 | 0.54 | 0.61 | . | 0.01 |
| SD_Sum (stomata/$mm^2$) | 474.02 | 333.51 | 594.17 | *** | 0.06 |
| LMA ($g/m^2$) | 38.11 | 27.51 | 46.48 | *** | 0.10 |
| Leaf Area ($m^2$) | 0.02 | 0.01 | 0.03 | ns | 0.04 |
| Midrib MF ($g_{midrib}/g_{leaf}$) | 0.05 | 0.04 | 0.07 | ** | 0.05 |
| Midrib Density ($mg/cm^3$) | 64.21 | 43.72 | 92.57 | *** | 0.15 |
| GCW_Bottom (µm) | 7.00 | 6.45 | 7.71 | . | 0.03 |
| GCW_Top (µm) | 6.79 | 6.21 | 7.62 | *** | 0.09 |
| GCW_Avg (µm) | 6.93 | 6.48 | 7.58 | ** | 0.08 |
| SL_Bottom (µm) | 33.99 | 30.97 | 39.39 | ns | 0.01 |
| SL_Top (µm) | 32.94 | 29.76 | 36.73 | ** | 0.06 |
| SL_Avg (µm) | 33.77 | 31.04 | 37.85 | * | 0.03 |
| PL_Bottom (µm) | 24.05 | 21.14 | 28.24 | ns | 0.00 |
| PL_Top (µm) | 23.28 | 19.88 | 26.30 | * | 0.03 |
| PL_Avg (µm) | 23.68 | 21.07 | 27.05 | . | 0.01 |
| $g_{smax}$ ($mol/m^2s$) | 13.56 | 11.08 | 17.53 | *** | 0.09 |
| VLA ($mm/mm^2$) | 10.24 | 9.26 | 11.66 | ns | 0.01 |
| 2nd VLA ($mm/mm^2$) | 0.05 | 0.04 | 0.07 | ** | 0.08 |
| Major VLA ($mm/mm^2$) | 0.07 | 0.05 | 0.10 | *** | 0.09 |
| SV (stomata/mm) | 23.54 | 18.29 | 28.31 | *** | 0.09 |
| AG Bio (g) | 14.91 | 6.05 | 23.32 | *** | 0.13 |
| Plant Bio (g) | 16.95 | 6.71 | 27.77 | *** | 0.14 |
| Leaf Bio (g) | 9.67 | 4.27 | 15.32 | *** | 0.15 |
| Stem Bio (g) | 4.91 | 1.78 | 9.06 | *** | 0.13 |
| Root Bio (g) | 2.11 | 0.65 | 4.97 | *** | 0.14 |
| Leaf MF ($g_{leaf}/g_{plant}$) | 0.59 | 0.50 | 0.66 | * | 0.04 |
| Stem MF ($g_{stem}/g_{plant}$) | 0.28 | 0.23 | 0.36 | ns | 0.01 |
| Root MF ($g_{root}/g_{plant}$) | 0.12 | 0.09 | 0.18 | *** | 0.11 |
| Succulence ($g/mm^2$) | 0.00035 | 0.00027 | 0.00131 | ns | 0.00 |

**Table 4.3**: Trait loadings (percentage of trait variation explained by each trait in the associated principal component) of first three principal components (PC). The top three traits per PC are highlighted in bold. Trait abbreviations are as defined in Table 4.2.

| Traits | PC1 | PC2 | PC3 |
|---|---|---|---|
| SD_Sum | **14.07** | 0.25 | 1.99 |
| SD_Ratio | 0.04 | 1.02 | **33.73** |
| SL_Avg | 9.37 | 2.73 | 4.75 |
| PL_Avg | 7.38 | 2.21 | 3.94 |
| GCW_Avg | 6.40 | 11.25 | 0.40 |
| VLA | 6.16 | 1.48 | 2.68 |
| MajorVLA | 4.48 | 2.26 | **12.13** |
| SV | **11.41** | 0.93 | 3.31 |
| LMA | 9.31 | 0.75 | 3.59 |
| MidribDen | 5.79 | 5.38 | 8.84 |
| MidribMF | 0.22 | **14.23** | **14.06** |
| LeafMF | 5.17 | **23.93** | 0.02 |
| StemMF | 1.33 | **32.33** | 0.04 |
| RootMF | 7.12 | 0.50 | 0.18 |
| Succulence | 0.21 | 0.74 | 9.58 |
| $g_{smax}$ | **11.55** | 0.01 | 0.74 |

# CHAPTER 5

# CONCLUSIONS

The overall goal of this dissertation was to examine variation in plant traits, focusing on stomatal and venation traits, across cultivated and wild sunflower. This was done by investigating patterns of both phenotypic and genetic variation. I examined variation in these and related traits, including various measures of growth and allocation, across the cultivated sunflower gene pool and investigated the genetic architecture of these traits. Next, I focused on a subset of cultivated sunflower genotypes to analyze the response of leaf traits to varying degrees of drought stress and to test whether variation in these traits can be used to predict overall plant performance. This allows for further understanding of the role that leaf anatomy and growth-related traits play in adaptation to drought and how variation in such traits may improve performance under drought. Finally, I studied wild sunflower populations to determine the extent of the variation and covariation in these traits across the natural range of the species, and to test for trait-environment associations. The results of this work improve our understanding of the extent and nature of the variation in leaf anatomical traits, their potential role in plant adaptation to water limitation, and their ability to predict performance in a major oilseed crop and its wild progenitor. This, in turn, improves our understanding of the role of leaf

anatomical traits in plant performance and biomass accumulation and provides potential targets for breeders seeking to develop more resilient crops.

First, I investigated variation in leaf anatomical traits across cultivated sunflower and sought to identify genomic regions underlying these traits with a goal of determining the extent to which the observed trait correlations are due to a shared genetic basis. I found substantial genotypic variation for most traits, including stomatal size and density, vein length per area (VLA), midrib density, and biomass. This result indicates the presence of heritable genetic variation in these traits. I further investigated this issue by using genome-wide association (GWA) analyses to identify genomic regions underlying trait variation. I found trait associations for numerous traits, but limited evidence of genomic colocalization across traits, even in cases where strong trait-trait correlations are observed. However, when looking at the multivariate level, I identified major axes of trait variation that corresponded to traits relating to gas exchange, hydraulics, and leaf construction. When subjected to association mapping, I found significant associations for two of these PCs (relating to gas exchange and leaf construction) thereby documenting the existence of genetic associations underlying functional multi-trait axes. In addition, I was able to catalog the genes contained within all significant regions associated with either individual traits or PCs, resulting in the identification of multiple promising candidate genes. One gene of particular interest is known to play a role in cell size determination and epidermal cell size is known to influence stomatal density. Taken together, these results provide insight into the genetic basis of leaf trait variation and

covariation in sunflower and highlight potential targets for future efforts aimed at modifying leaf traits in cultivated sunflower.

Next, I sought to determine how this same core set of traits varies/covaries across differing levels of water availability. For the most part, the correlation structure across these traits was unchanged across treatments, suggesting that the observed trait relationships are quite robust to environmental perturbations. Virtually all of these traits also exhibited substantial trait plasticity, the magnitude of which increased with increasing drought stress severity for most traits. Overall, there was a marked decrease in plant performance (estimated as biomass) under stress, along with progressively increased VLA and decreased stomatal density values. It is therefore clear that this entire suite of traits can change in response to changes in water availability. Moreover, these changes occurred along the same major axes of trait variation that I had previously documented (see Chapter 2), suggesting that coordinated changes in these traits plays a key role in maintaining performance under stress and control conditions. Finally, I found that a small number of key leaf traits (VLA, LMA, stomatal length and density) could be used to predict plant performance, estimated as total biomass, with a marginal $R^2 = 0.74$, indicating that leaf traits are strong predictors of overall plant performance. Taken together, these results indicate the occurrence of substantial leaf trait plasticity in response to water limitation, with changes generally occurring in a predictable fashion – i.e., with a transition to more, smaller stomata and an increased density of minor veins under drought stress. In addition, changes in VLA and stomatal density were found to be the predictors of changes in performance. Overall, these findings, when coupled with

evidence for genetic variation underlying observed traits variation (see Chapter 2), suggests that there is potential to use these traits to breed for plants with increased productivity under stress.

Finally, I shifted focus to common sunflower to investigate patterns of variation and covariation in leaf anatomical traits and performance-related traits in the wild. As part of this effort, I also tested for associations of these traits with key environmental variables from the source populations and examined the extent to which leaf trait variation can be used to predict plant performance. I also found many of the same trait correlations that I had previously documented in cultivated sunflower including the expected associations between stomatal size and density as well as stomatal density and VLA. At the multivariate level, I once again found evidence of a major axis of trait variation relating to gas exchange; the observation of such an axis of trait variation in both cultivated and wild sunflower suggests the existence of a persistent functional relationship across both the cultivated and wild forms of this species. A second major axis relating to resource allocation was also identified. When comparing traits to environmental variables, I found that much of the observed trait variation was a result of population structure. But when genetic differentiation was accounted for, the most obvious remaining pattern was that biomass and growth-related traits tend to be associated with temperature variables. Notably, leaf anatomical traits overall did not exhibit strong or widespread environmental associations, albeit with a few exceptions – e.g., stomatal density seemingly relates to environmental variables associated with temperature extremes. The cause of this pattern (or lack thereof) remains unclear, but it

may be the case that finer-scale leaf traits are less evolutionarily labile than higher-level, growth-related traits, and thus less likely to exhibit clear environmental associations in wild sunflower. Finally, in terms of predictive power, I found that stomatal density sum, stomatal length, and LMA can be used to predict plant performance quite accurately, and that the use of the first two trait PCs instead of individual traits further increases predictive power.

Taken together, I found substantial variation across leaf anatomical traits in both cultivated and wild sunflowers. Major axes of variation were found to relate to gas exchange, hydraulics, and leaf construction with gas exchange and leaf construction showing evidence of clear genomic associations. Despite the existence of these axes, and the evidence for genetic variation underlying these trait relationships, the lack of widespread genomic colocalization suggests that it may be possible to fine-tune variation on a per-trait basis and explore novel phenotypic space despite the occurrence of a variety of seemingly strong trait-trait correlations. Interestingly, the discovery of a common, major axis of trait variation in wild sunflower suggests that certain trait relationships may persist across both cultivated and wild sunflower. A small number of leaf traits exhibited strong predictive power for performance under varying levels of drought stress in cultivated sunflower, and across the range of wild sunflower. This suggests that variation in key leaf traits plays an important role in determining overall plant performance; this result makes sense given the crucial role of these sorts of traits in plant-water relations and photosynthesis. While the identification of specific genomic regions underlying variation in a wide variety of these traits in cultivated sunflower provides targets for

future breeding efforts, more work needs to be done to gain a more complete understanding of the potential role of these leaf traits in drought adaptation. Similarly, additional work, including possible reciprocal transplants or manipulative work in the greenhouse, is required to understand the functional significance of leaf trait variation more fully in the wild. Another interesting and potentially overlooked component of the environment relates to characteristics of the soil. For example, the moisture-holding capacity of local soils, along with variation in mineral and nutrient content, will have a major impact on the ways in which plants experience other aspects of their environment. Regardless, continued exploration of the ways in which both cultivated and wild sunflower respond to and resist temperature- and moisture-related environmental challenges has the potential to inform ongoing improvement efforts aimed at developing increasingly resilient cultivated sunflower lines.

# APPENDIX A

## SUPPLEMENTARY FIGURES, TABLES, AND METHODS FROM CHAPTER 2[4]

[4] To view Figures S2.4, 2.7, and Table S2.2 see Earley et al. 2022 (https://doi.org/10.1111/tpj.15900) Figures 4, 7 and Table 2, respectively.

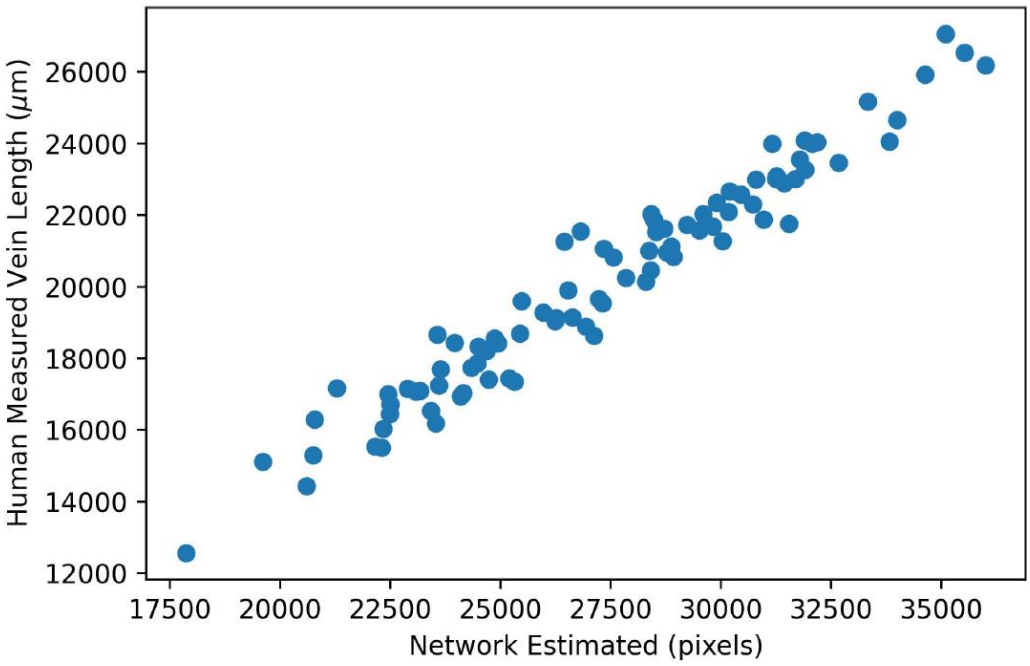


**Figure S2.1**: Comparison of human measured, and neural network estimated vein lengths on test-set images (N=85).

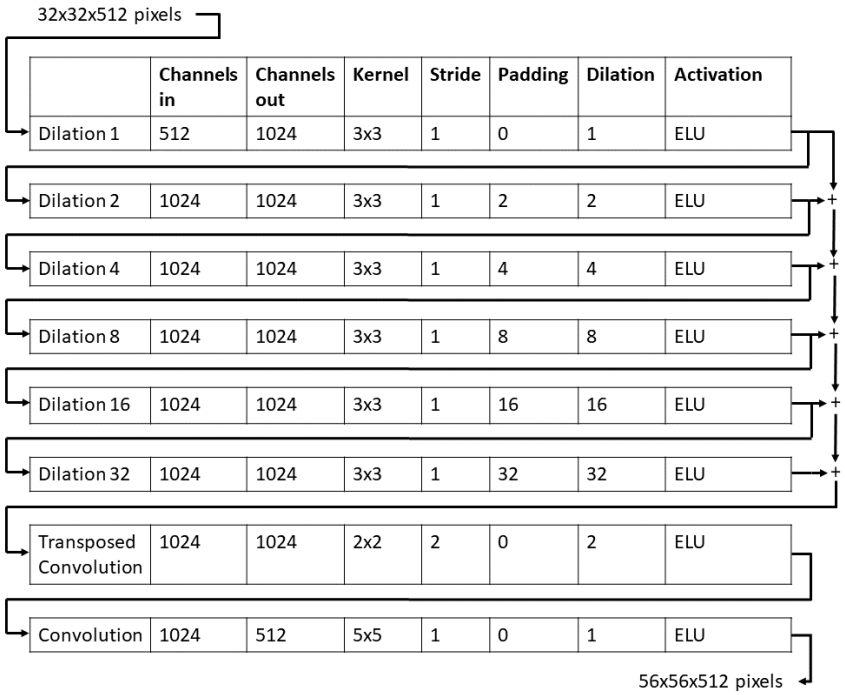


**Figure S2.2**: Network architecture used in-place of the U-Net structure after the last max pool layer through the first up convolution. The 32x32x512 input tensor represents the output of the last max-pool layer. The 56x56x512 output tensor is the same as the output size of the first up convolution. + represents element-wise addition of the output tensors.

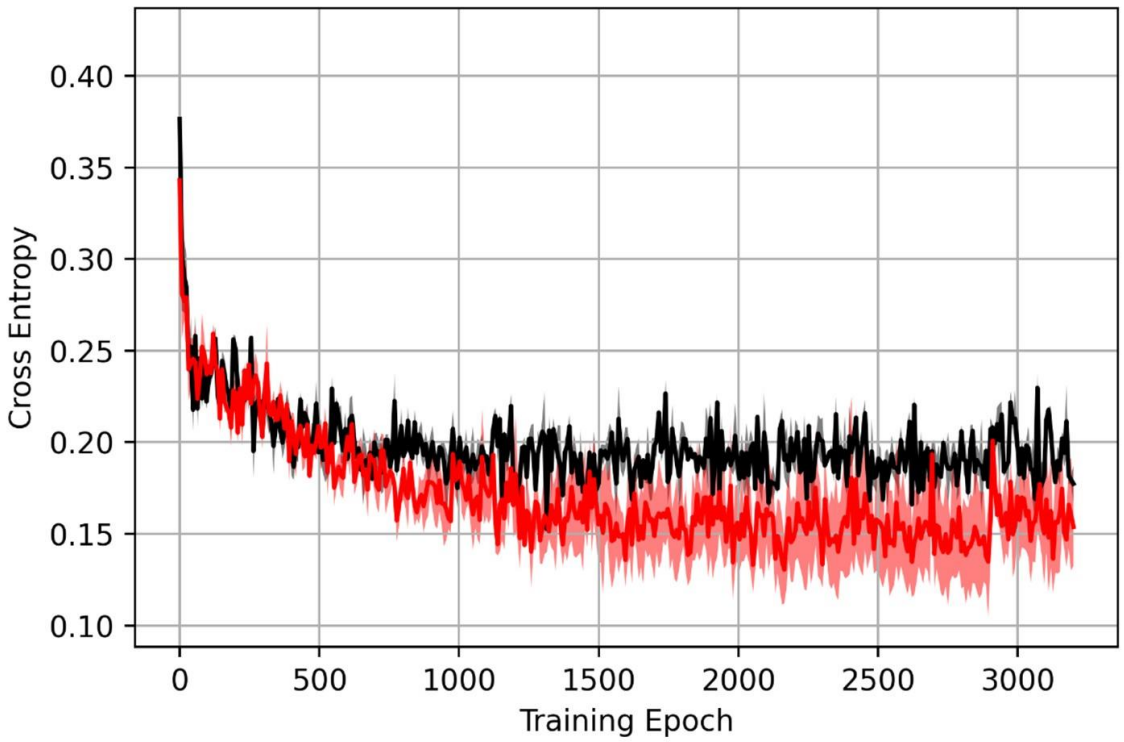


**Figure S2.3**: Cross-validated training (red) and validation (black) loss of model with final hyperparameters. Shading indicates standard error.

**Figure S2.4**: Bivariate plots for all trait correlations presented in Figure 2.2. Points represent the estimated marginal means of genotypes. Blue line represents the fitted regression line. Units for all traits are as in Table 2.1. To view figure, see Earley et al. 2022 Figure S4 (https://doi.org/10.1111/tpj.15900)

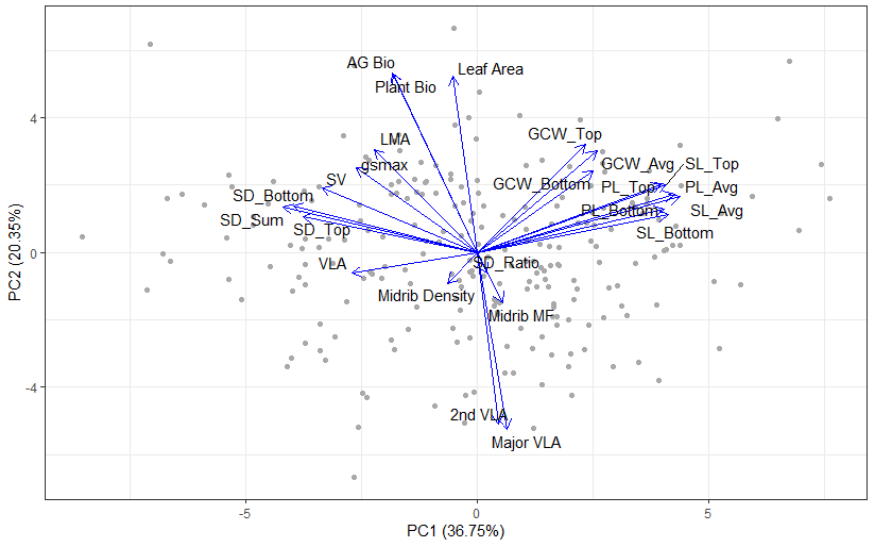


**Figure S2.5:** Principal component analysis (PCA) of all measured leaf traits using estimated marginal means for each trait. For stomatal density, length, pore length, and guard cell width, trait values are included separately for the top and bottom of the leaf.

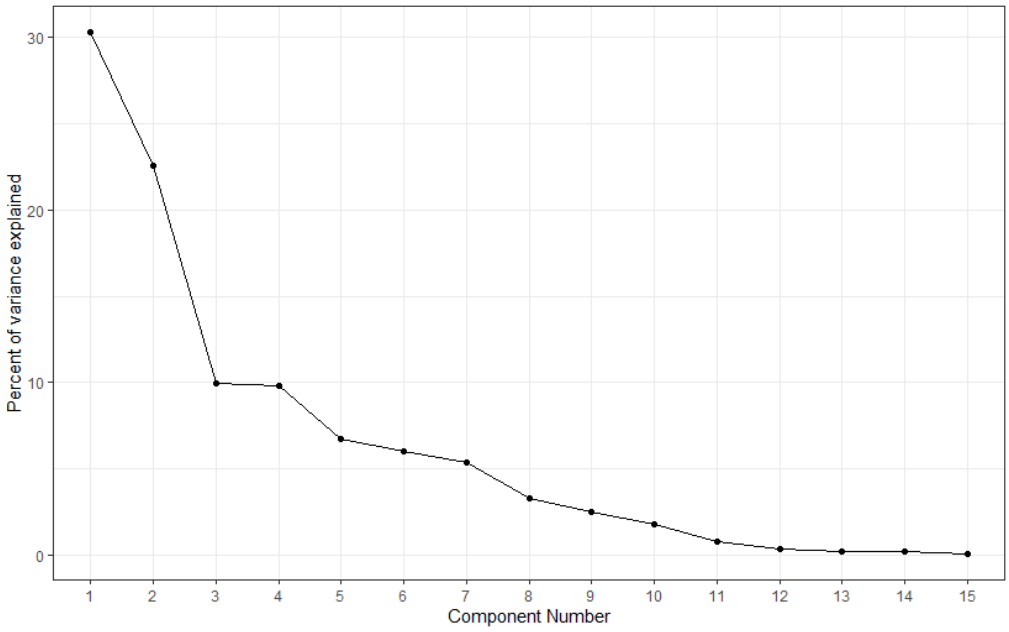


**Figure S2.6**: Scree plot showing principal components vs. percent variance explained.

**Figure S2.7**: Linkage disequilibrium heatmaps for all significant SNPs found on each chromosome. Linkage disequilibrium was estimated as R2 between all significant SNPs per chromosome. Colored blocks represent haplotypic blocks that the SNPs belong to based on the full haplotype map (Figure S2.10). Block membership is shown for both an analysis based on the full, genome-wide collection of SNPs ("genome") as well as a re-analysis based on only significant SNPs ("significant"). Colors are arbitrary. For full methodological details, see Temme et al. (2020). To view figure, see Earley et al. 2022 Figure S7 (https://doi.org/10.1111/tpj.15900).

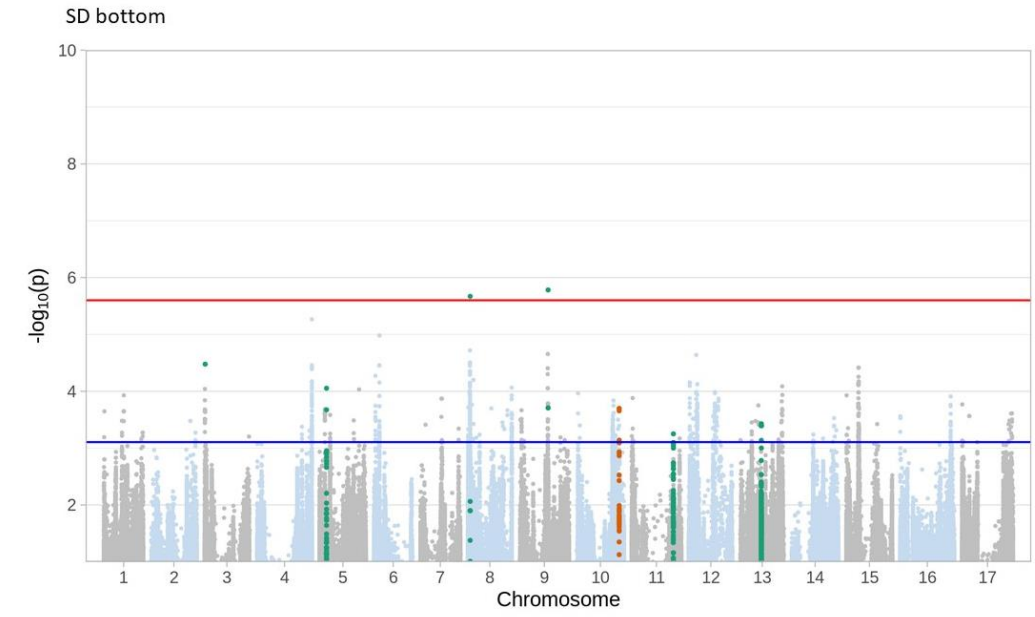
SD bottom
10
8
6
4
2
-log10(p)
1 2 3 4 5 6 7 8 9 10 11 12 13 14 15 16 17
Chromosome

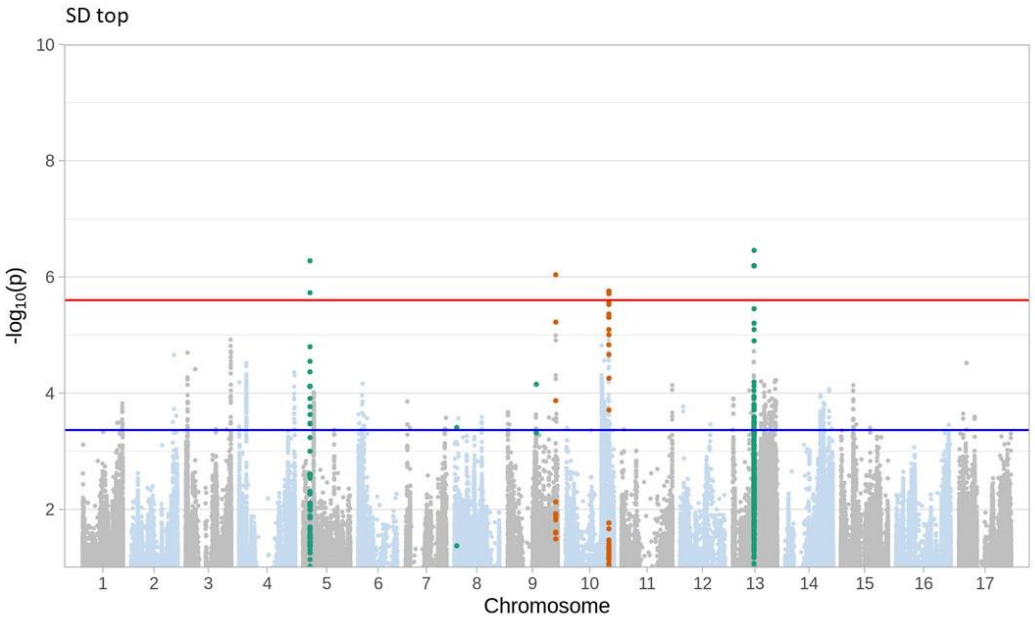
SD top
10
8
6
4
2
-log10(p)
1 2 3 4 5 6 7 8 9 10 11 12 13 14 15 16 17
Chromosome

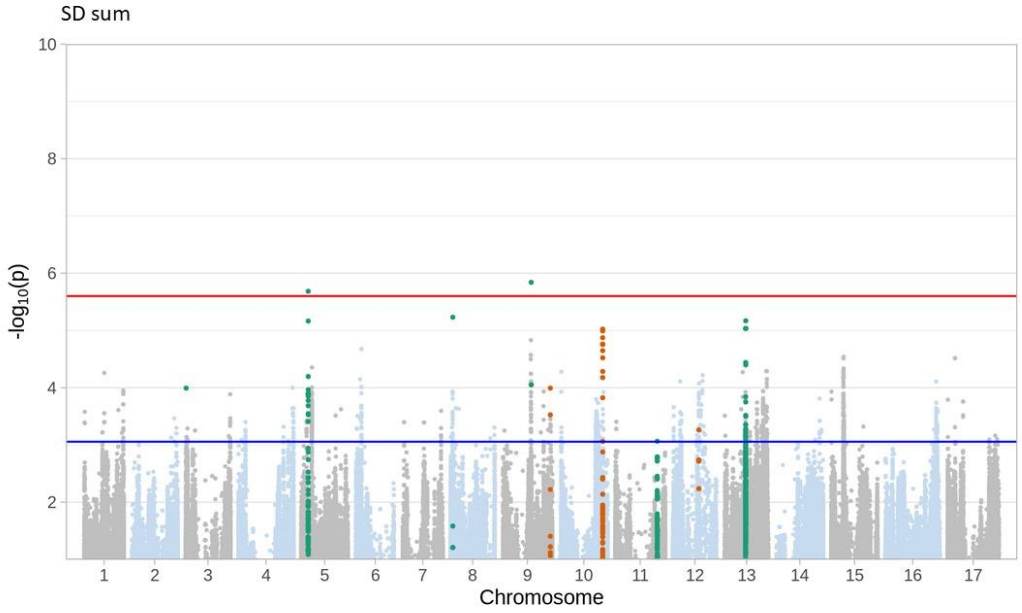
SD sum
10
8
6
4
2
-log10(p)
1
2
3
4
5
6
7
8
9
10
11
12
13
14
15
16
17
Chromosome

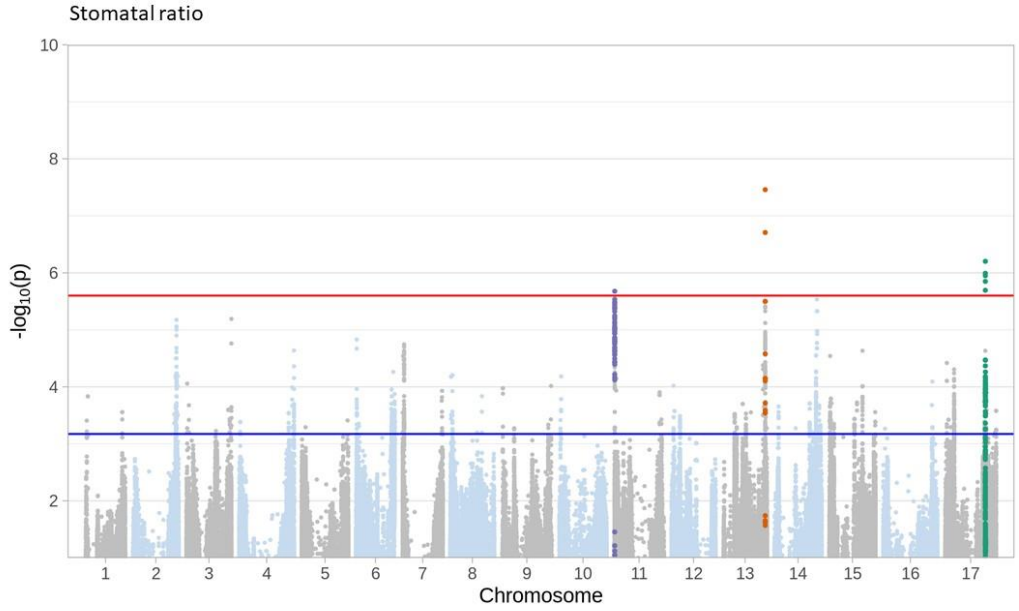
Stomatal ratio
10
8
6
4
2
-log10(p)
1
2
3
4
5
6
7
8
9
10
11
12
13
14
15
16
17
Chromosome

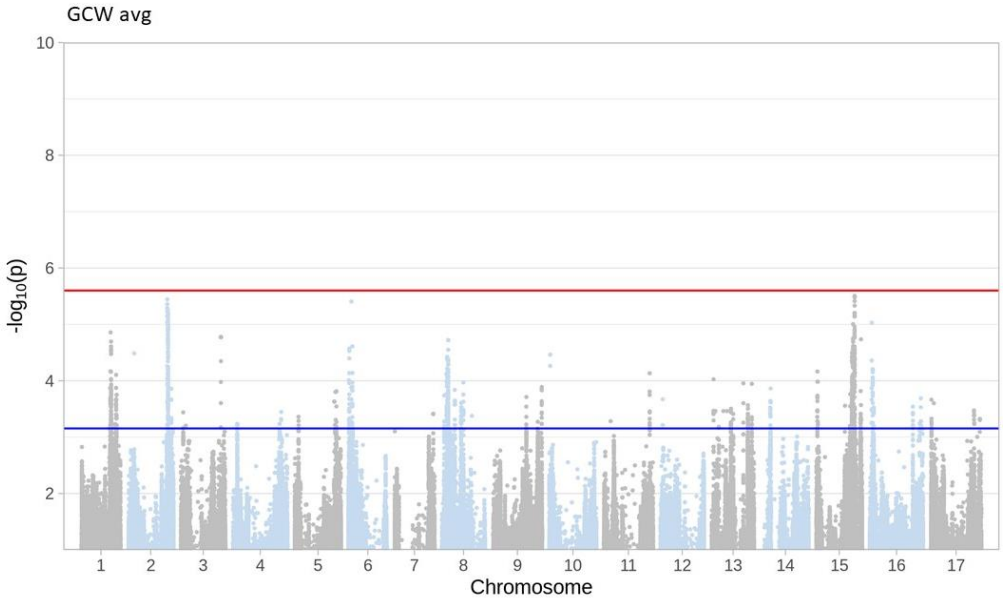
GCW avg
10
8
6
4
2
-log10(p)
1
2
3
4
5
6
7
8
9
10
11
12
13
14
15
16
17
Chromosome

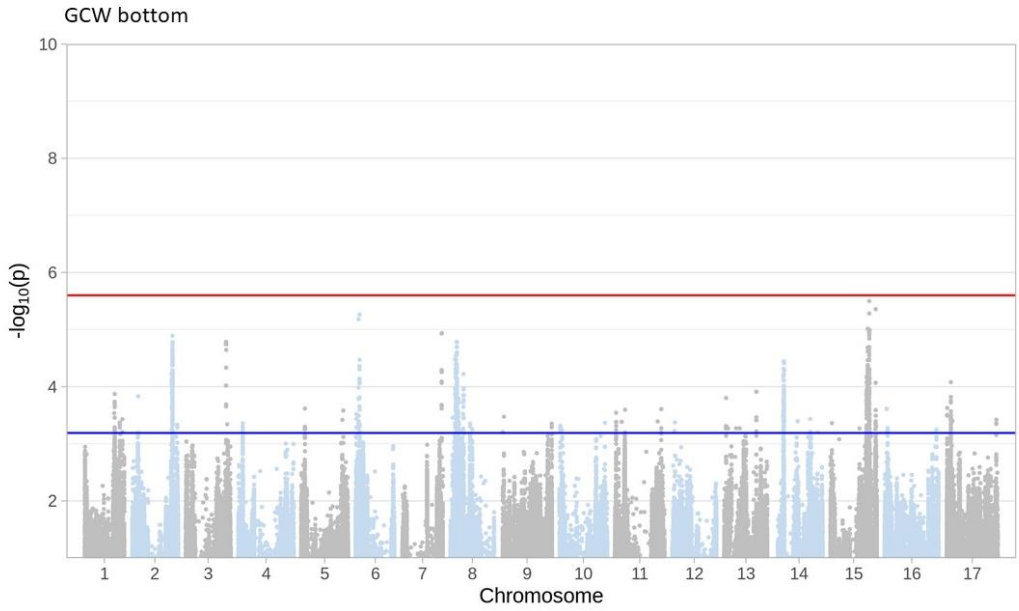
GCW bottom
10
8
6
4
2
-log10(p)
1
2
3
4
5
6
7
8
9
10
11
12
13
14
15
16
17
Chromosome

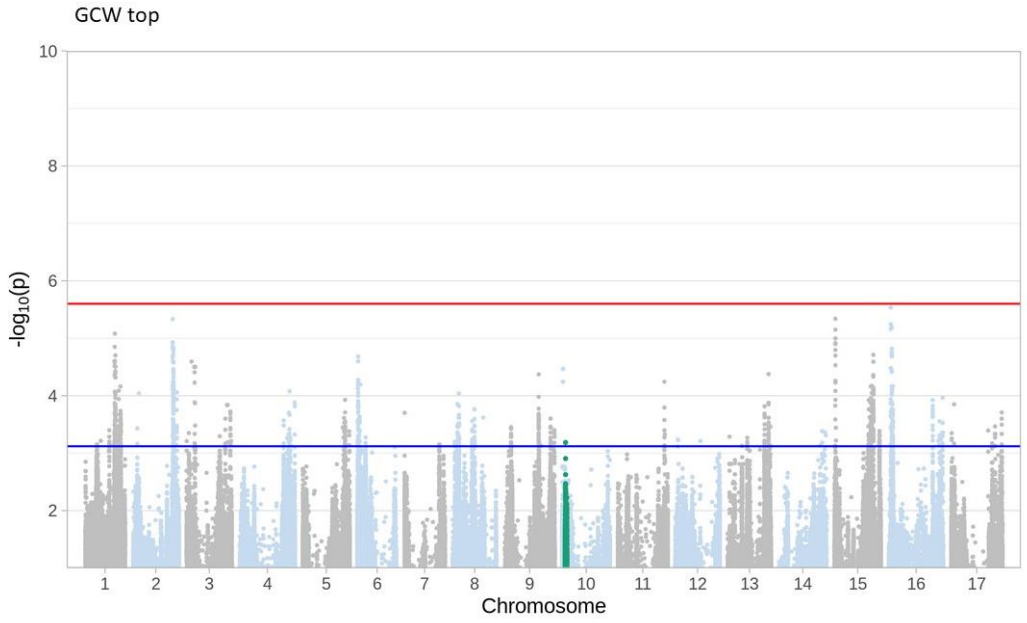
GCW top
10
8
6
4
2
-log10(p)
1
2
3
4
5
6
7
8
9
10
11
12
13
14
15
16
17
Chromosome

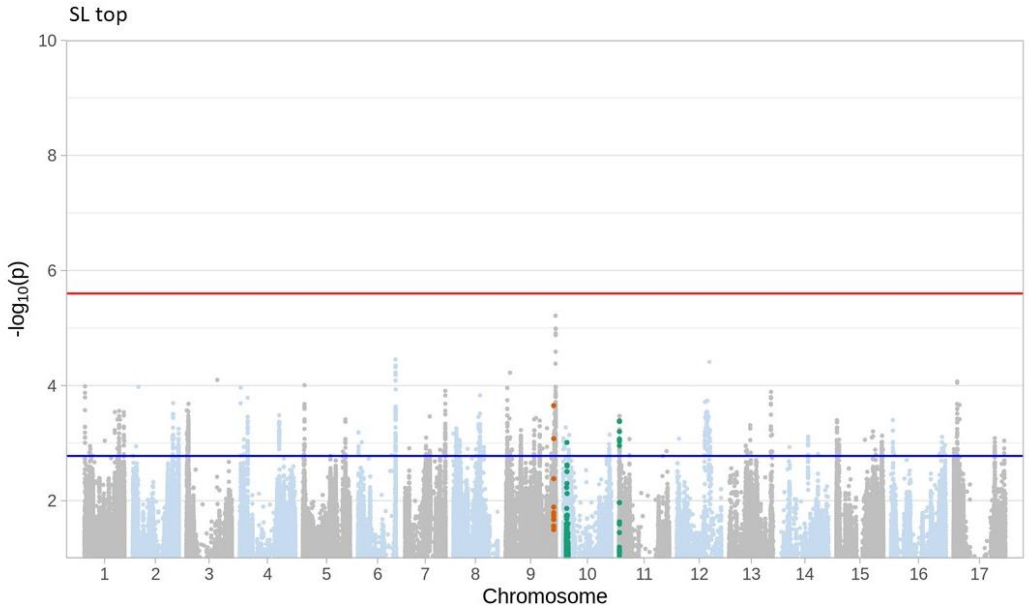
SL top
10
8
6
4
2
-log10(p)
1
2
3
4
5
6
7
8
9
10
11
12
13
14
15
16
17
Chromosome

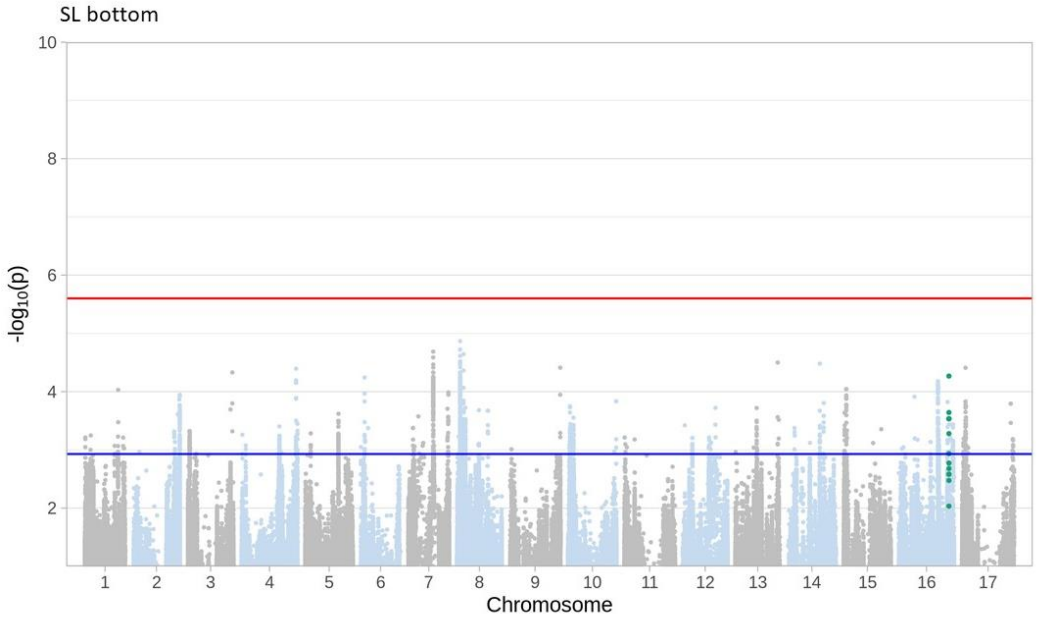
SL bottom
10
8
6
4
2
-log10(p)
1
2
3
4
5
6
7
8
9
10
11
12
13
14
15
16
17
Chromosome

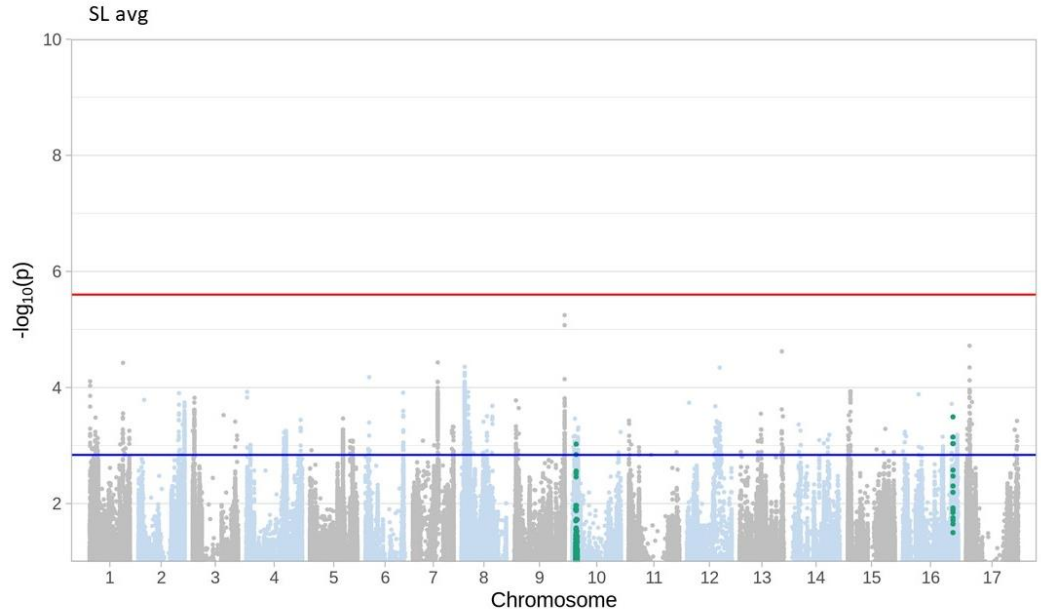
SL avg
10
8
6
4
2
-log10(p)
1
2
3
4
5
6
7
8
9
10
11
12
13
14
15
16
17
Chromosome

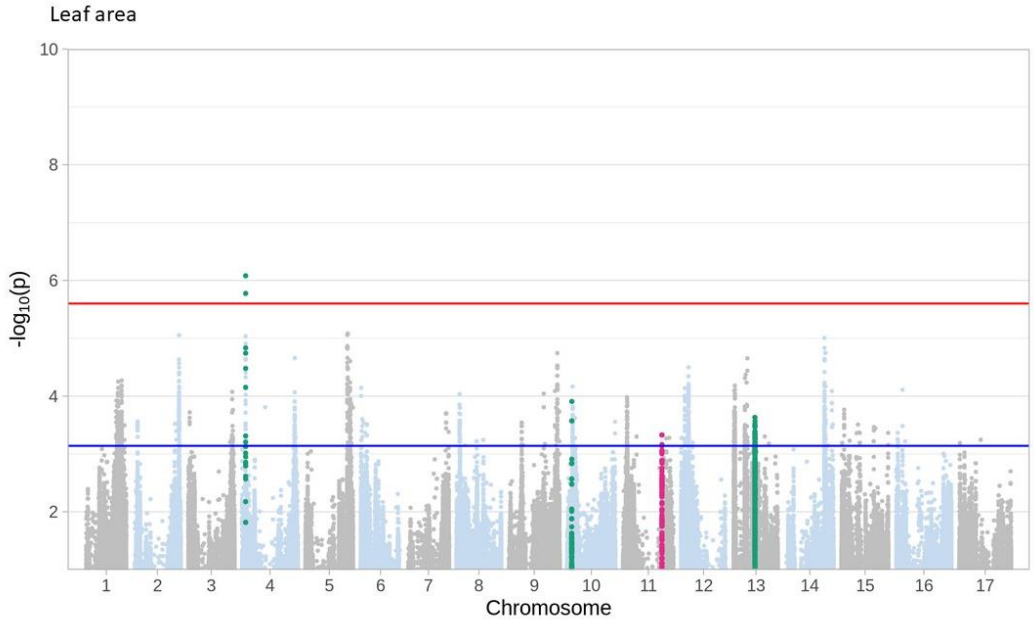
Leaf area
10
8
6
4
2
-log10(p)
1
2
3
4
5
6
7
8
9
10
11
12
13
14
15
16
17
Chromosome

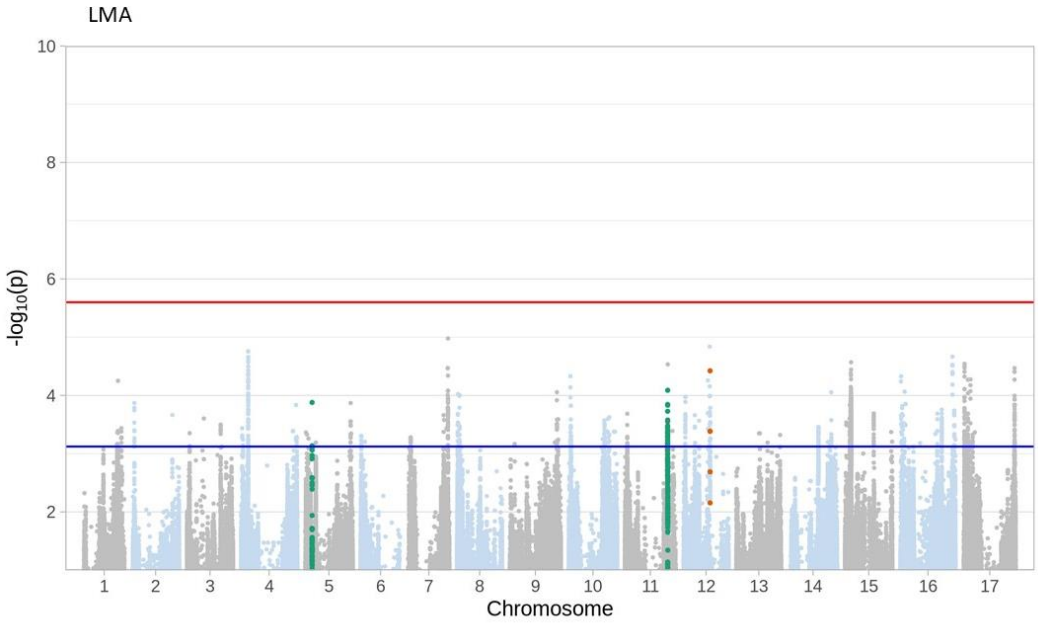
LMA
10
8
6
4
2
-log10(p)
1
2
3
4
5
6
7
8
9
10
11
12
13
14
15
16
17
Chromosome

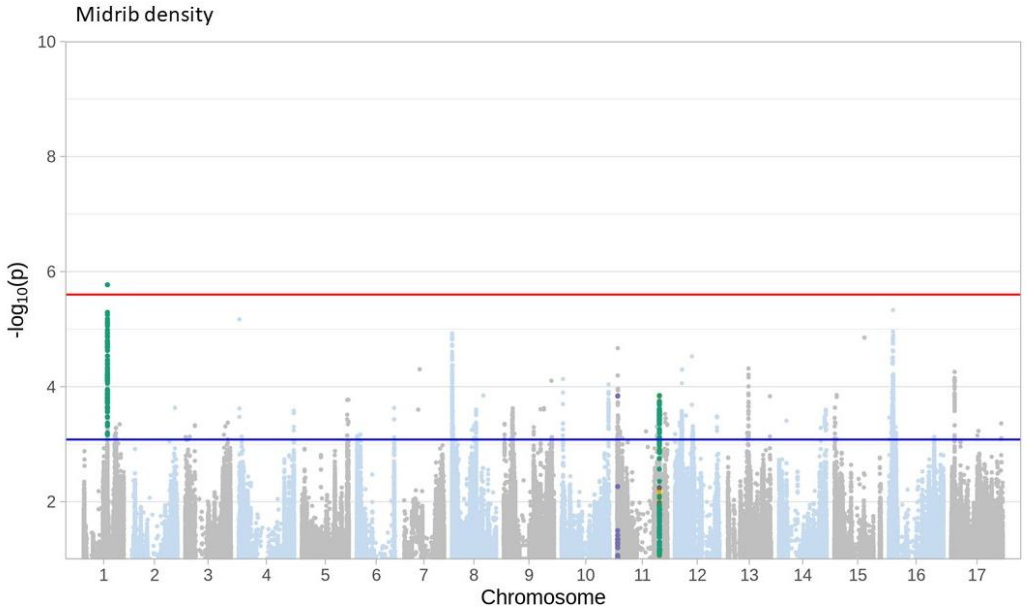
Midrib density
10
8
6
4
2
-log10(p)
1
2
3
4
5
6
7
8
9
10
11
12
13
14
15
16
17
Chromosome

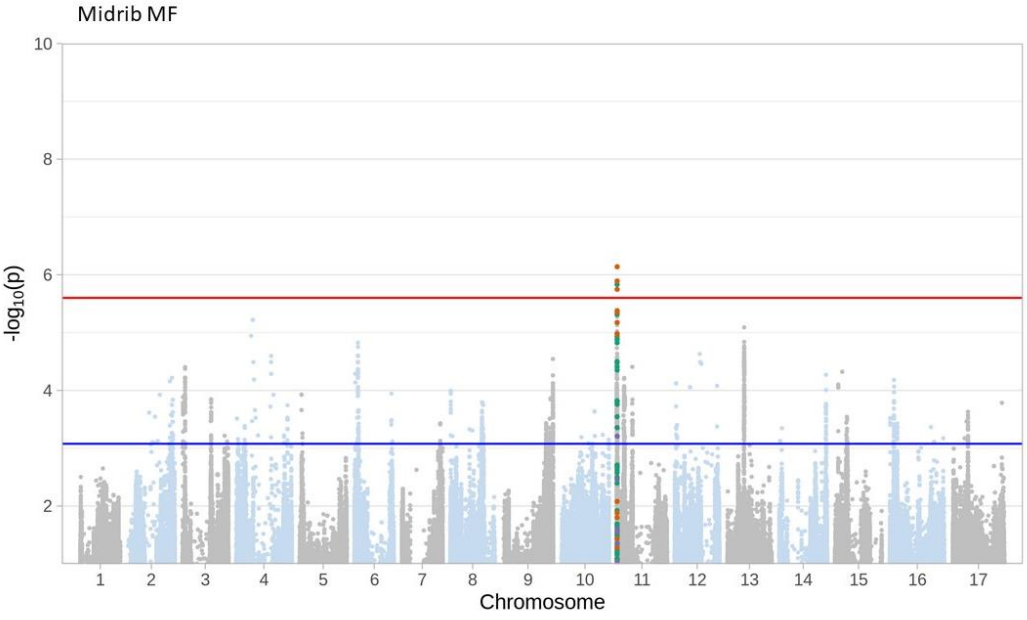
Midrib MF
10
8
6
4
2
-log10(p)
1
2
3
4
5
6
7
8
9
10
11
12
13
14
15
16
17
Chromosome

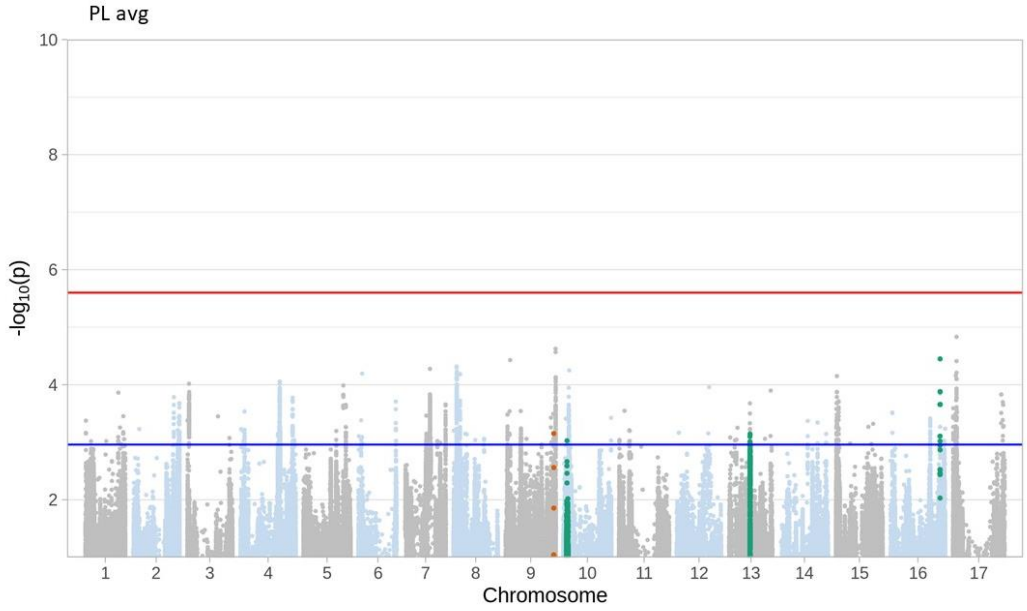
PL avg
10
8
6
4
2
-log10(p)
1 2 3 4 5 6 7 8 9 10 11 12 13 14 15 16 17
Chromosome

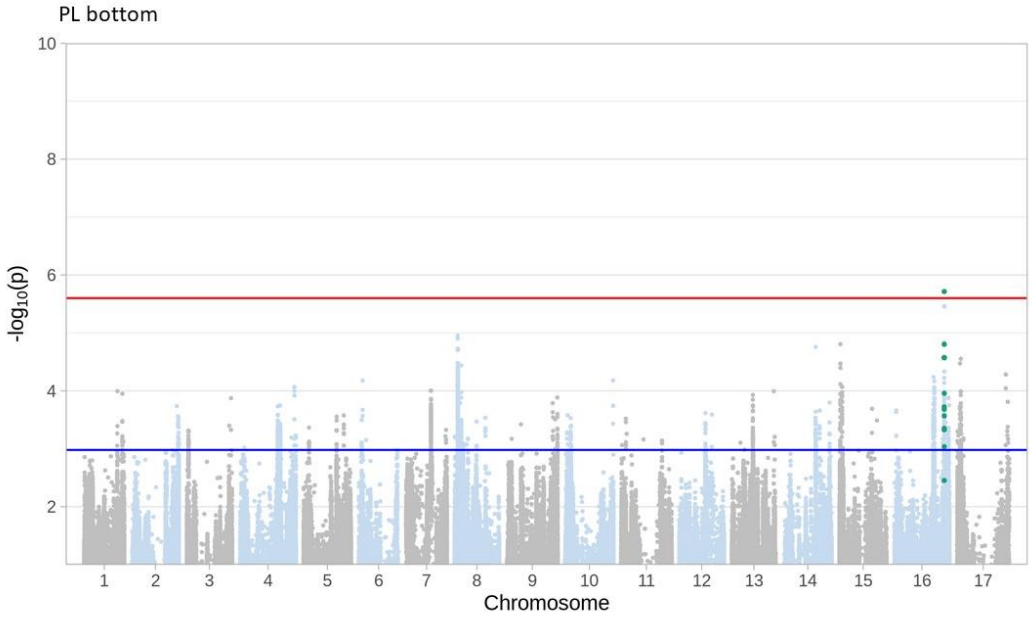
PL bottom
10
8
6
4
2
-log10(p)
1 2 3 4 5 6 7 8 9 10 11 12 13 14 15 16 17
Chromosome

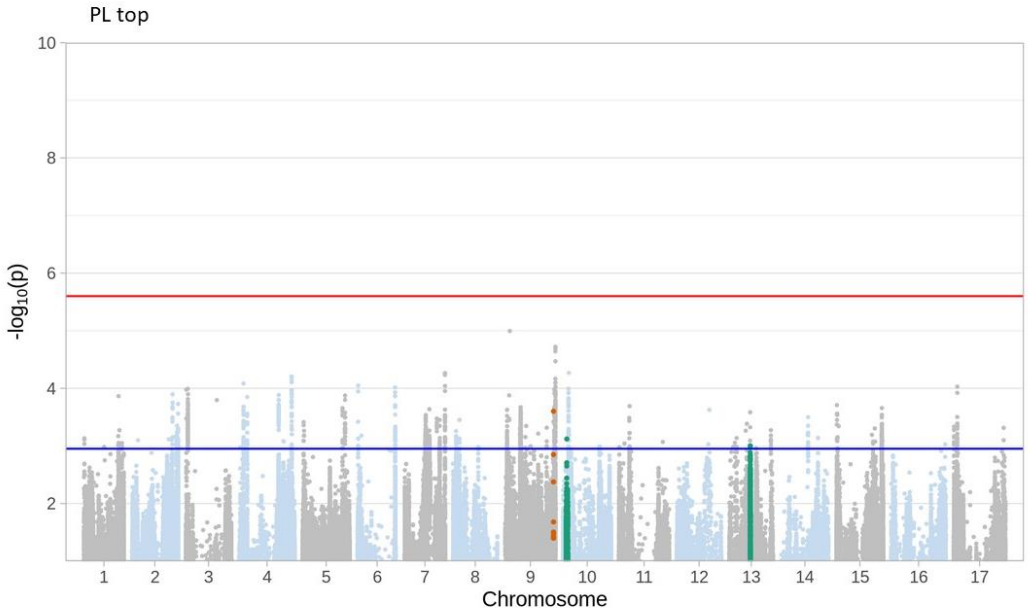
PL top
10
8
6
4
2
-log10(p)
1
2
3
4
5
6
7
8
9
10
11
12
13
14
15
16
17
Chromosome

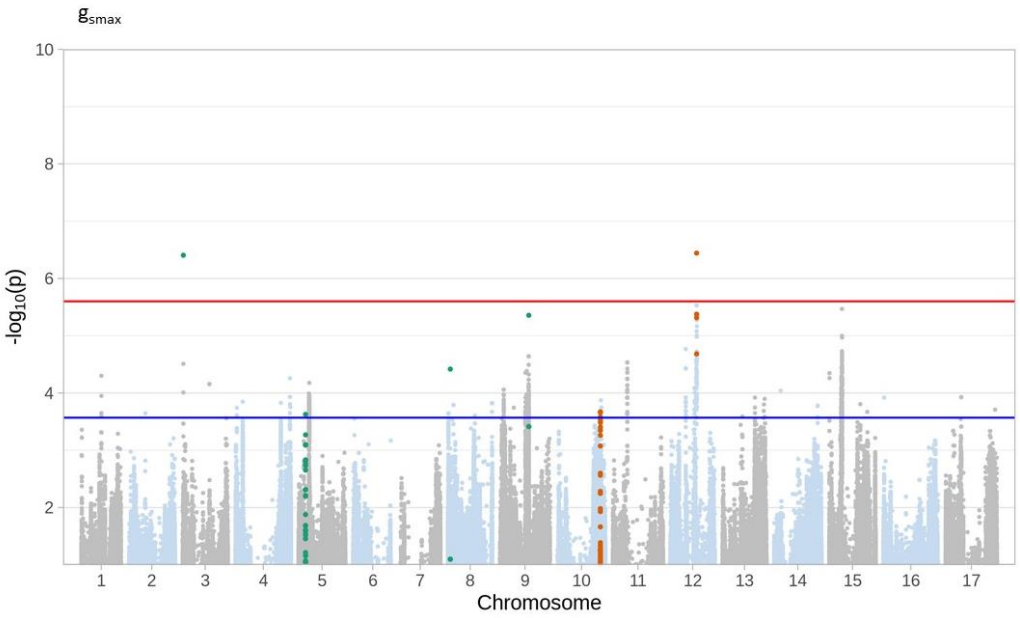
gsmax
10
8
6
4
2
-log10(p)
1
2
3
4
5
6
7
8
9
10
11
12
13
14
15
16
17
Chromosome

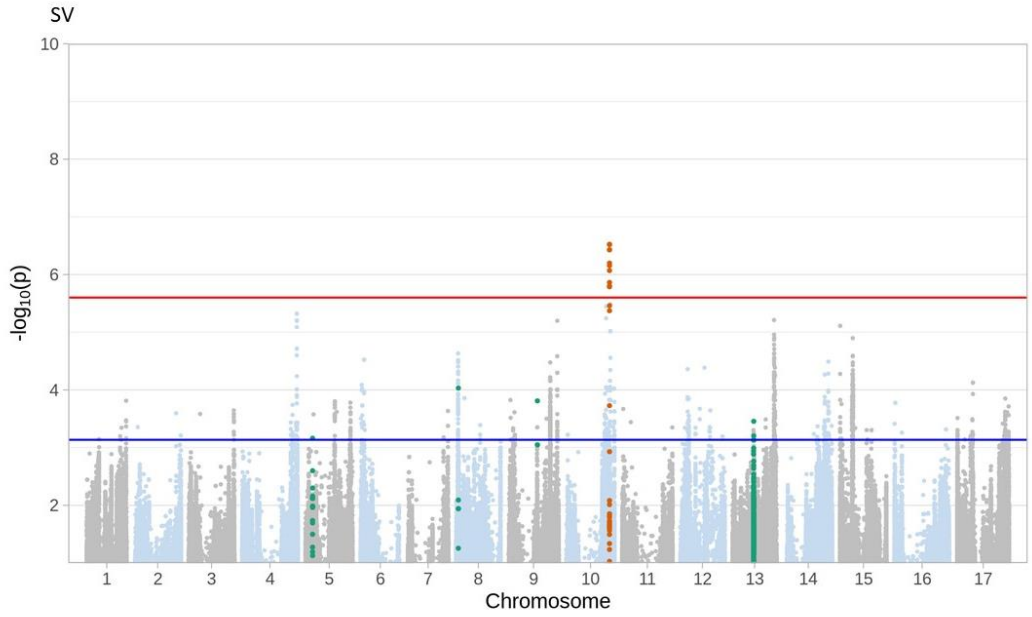
SV
10
8
6
4
2
-log10(p)
1
2
3
4
5
6
7
8
9
10
11
12
13
14
15
16
17
Chromosome

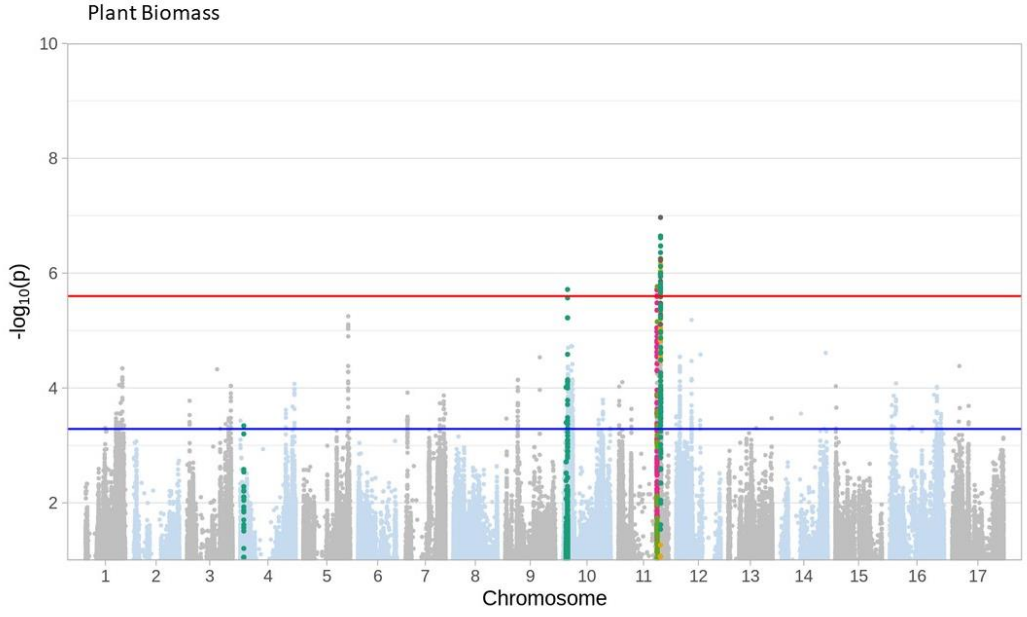
Plant Biomass
10
8
6
4
2
-log10(p)
1
2
3
4
5
6
7
8
9
10
11
12
13
14
15
16
17
Chromosome

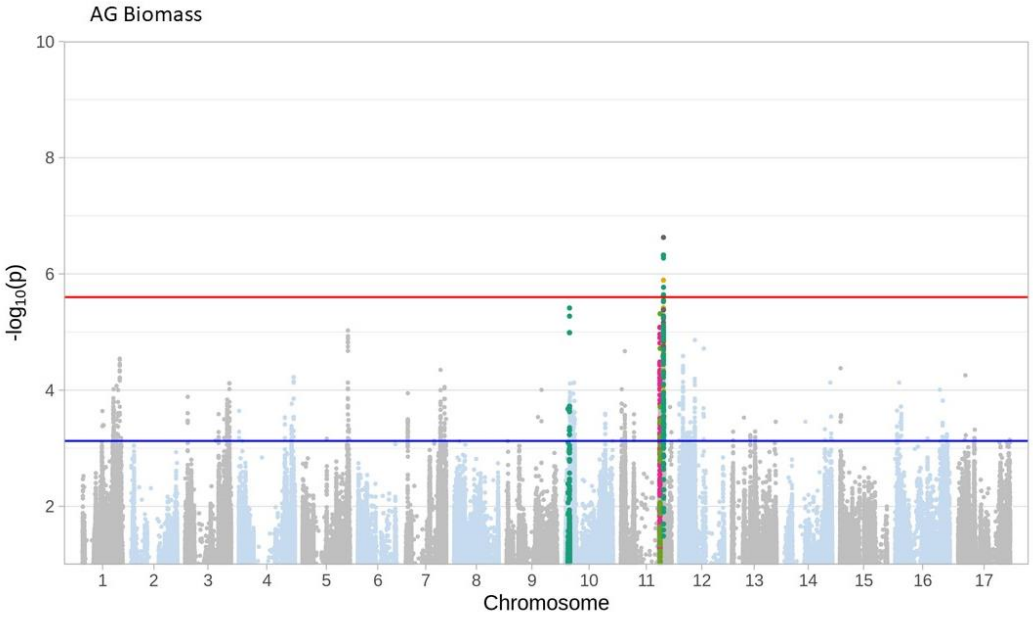
AG Biomass
10
8
6
4
2
-log10(p)
1
2
3
4
5
6
7
8
9
10
11
12
13
14
15
16
17
Chromosome

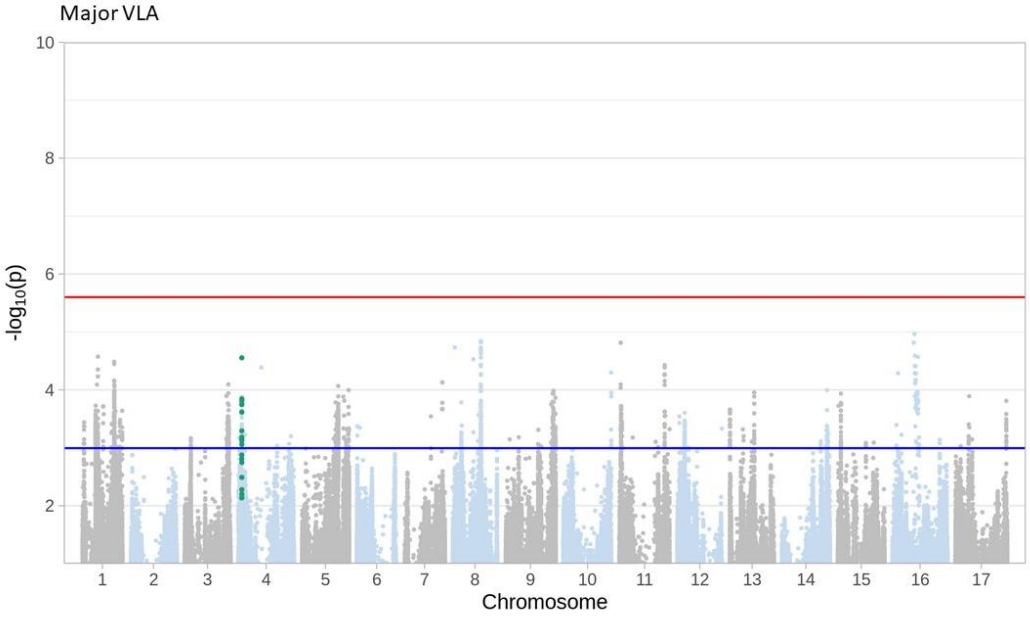
Major VLA
10
8
6
4
2
-log10(p)
1
2
3
4
5
6
7
8
9
10
11
12
13
14
15
16
17
Chromosome

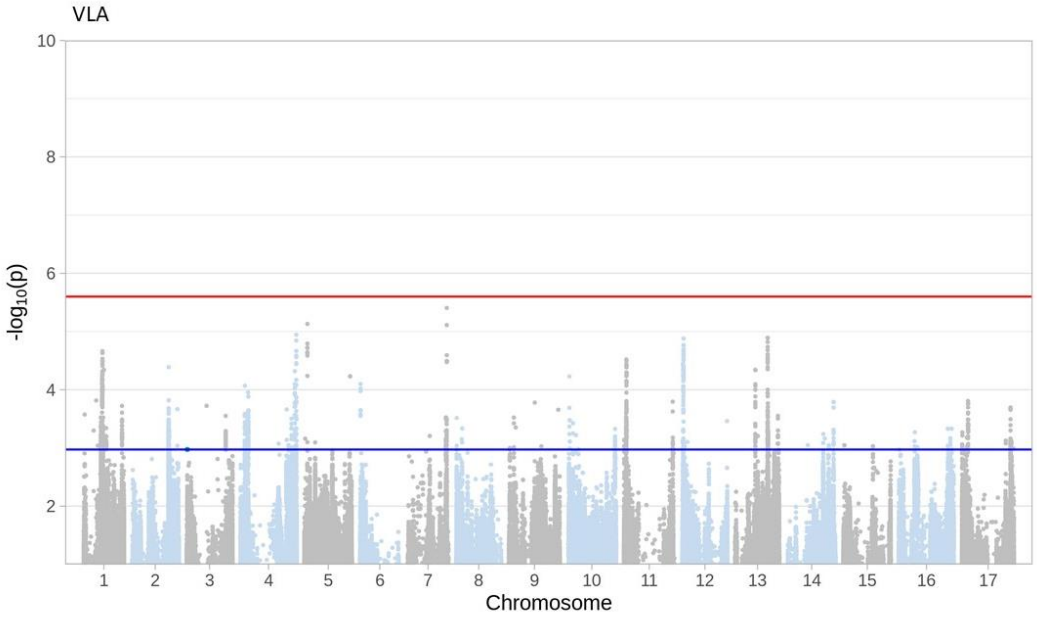
VLA
10
8
6
4
2
-log10(p)
1
2
3
4
5
6
7
8
9
10
11
12
13
14
15
16
17
Chromosome

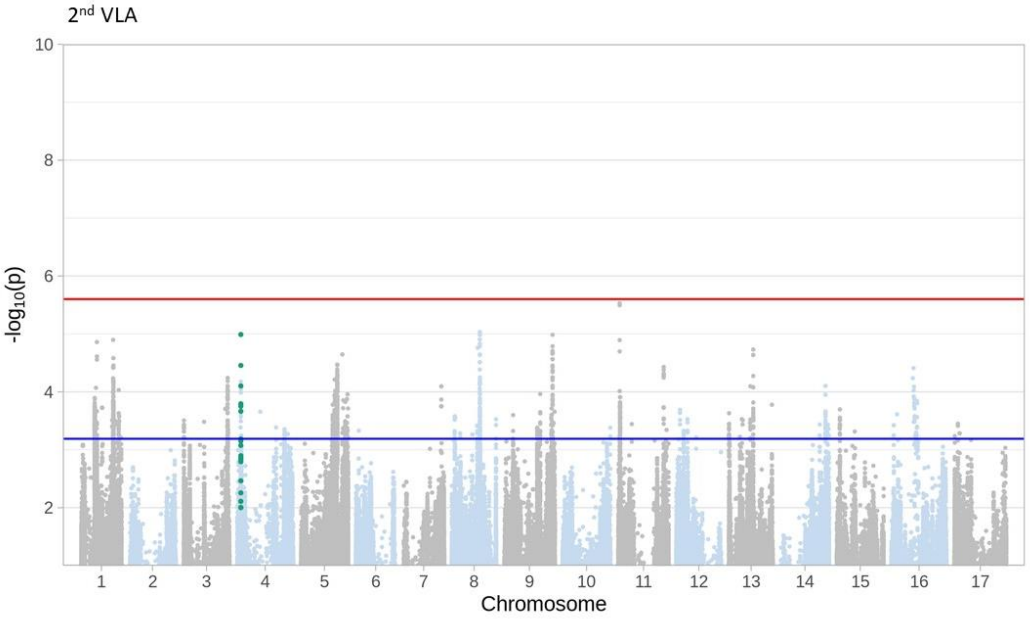
2nd VLA
10
8
6
4
2
-log10(p)
1
2
3
4
5
6
7
8
9
10
11
12
13
14
15
16
17
Chromosome

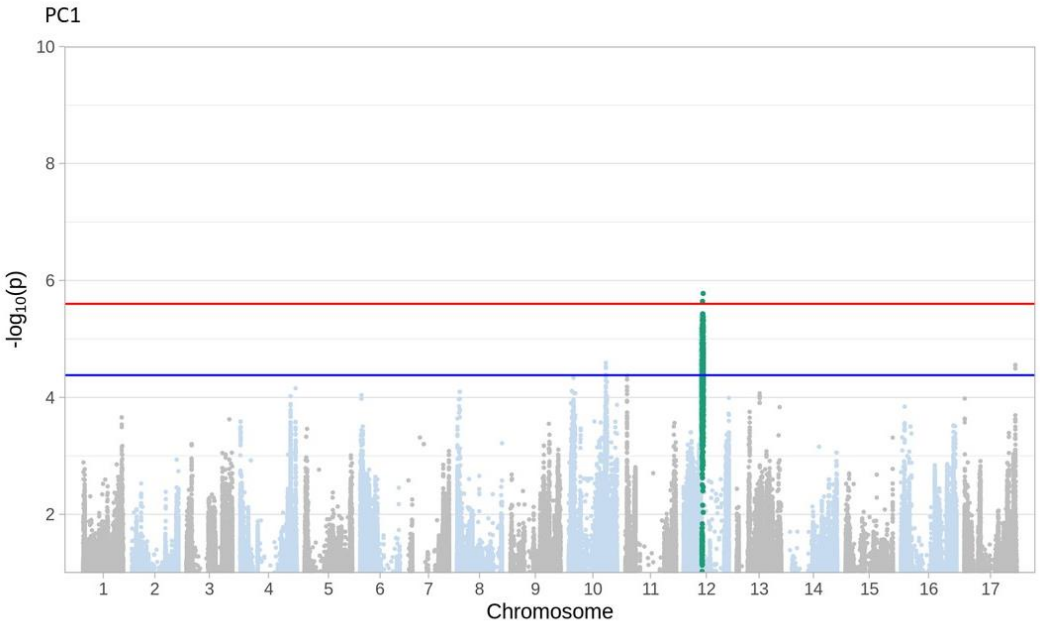
PC1
10
8
6
4
2
-log10(p)
1
2
3
4
5
6
7
8
9
10
11
12
13
14
15
16
17
Chromosome

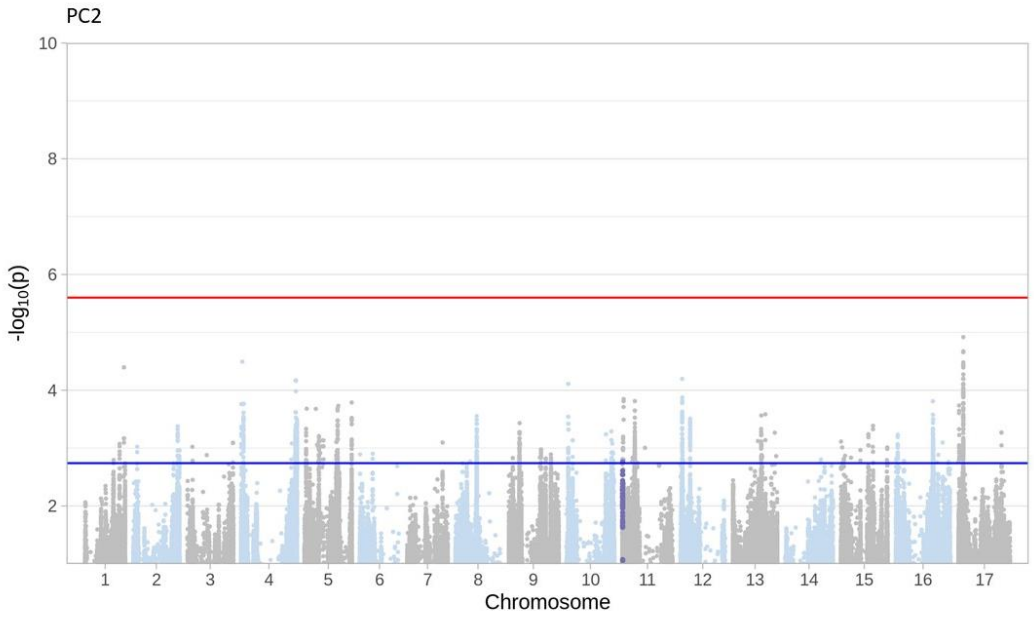
PC2
10
8
6
4
2
-log10(p)
1
2
3
4
5
6
7
8
9
10
11
12
13
14
15
16
17
Chromosome

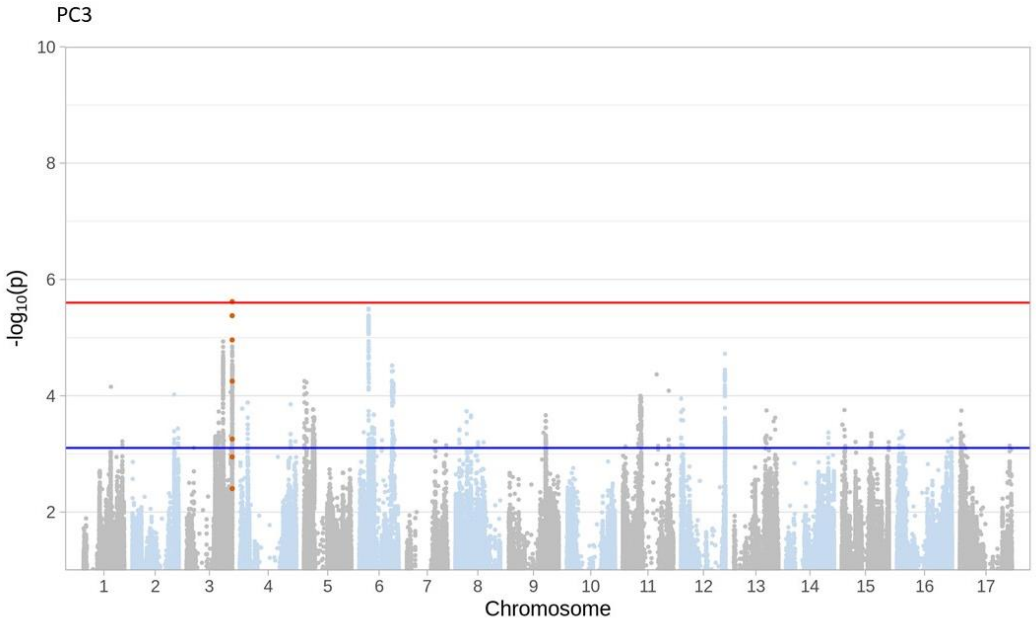


**Figure S2.8**: Manhattan plots resulting from GWA analyses for all traits. The red line is the significance threshold based on the modified Bonferroni correction (see text for details) and the blue line is the suggestive threshold based on (i.e., top 0.1% of all SNPs). Colored dots represent SNPs that are significant or suggestive for at least one trait. Color of dots is arbitrary.

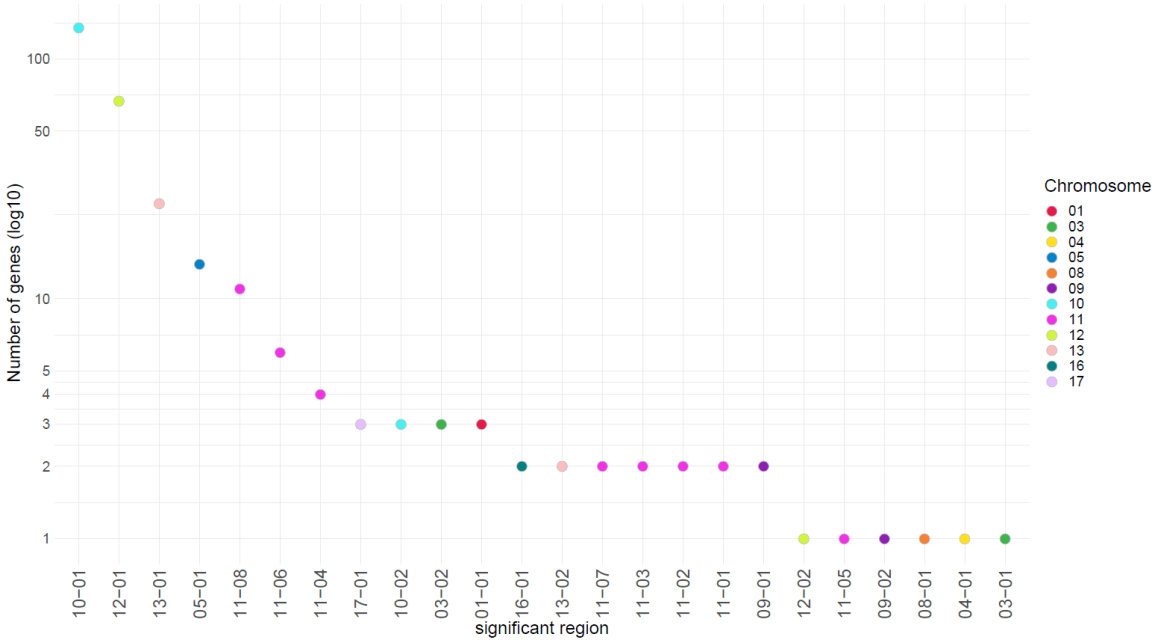


**Figure S2.9**: Distribution of the number of genes per significant region. Points represent the number of genes in each significant block. Note the log scale on the y-axis.

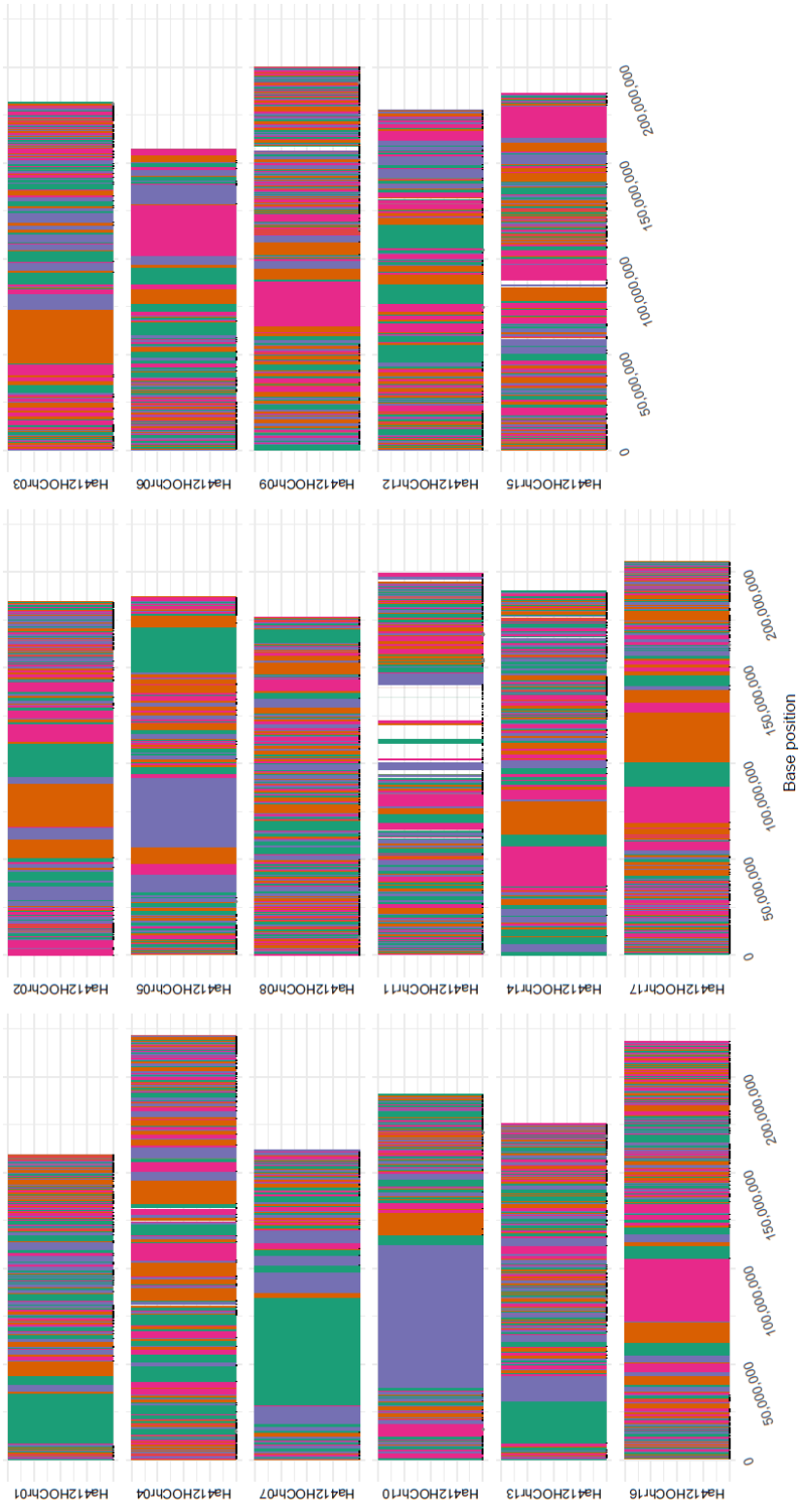
Ha412HOChr15
Ha412HOChr12
Ha412HOChr09
Ha412HOChr06
Ha412HOChr03
Ha412HOChr17
Ha412HOChr14
Ha412HOChr11
Ha412HOChr08
Ha412HOChr05
Ha412HOChr02
Ha412HOChr16
Ha412HOChr13
Ha412HOChr10
Ha412HOChr07
Ha412HOChr04
Ha412HOChr01
0
50,000,000
100,000,000
150,000,000
200,000,000
Base position

**Figure S2.10**: Visualization of haplotypic blocks across the sunflower genome. Blocks are shown for each of the 17 sunflower chromosomes. Blocks are colored in an alternating fashion and colors are arbitrary. Black dots on the x-axis indicate singleton SNPs that did not fall within blocks.

**Table S2.1:** All significant and suggestive regions that colocate with significant regions. Region refers to the genomic region determined after rerunning haplotype blocking on significant SNPs using GEMMA. Haplotype block refers to the unique block in the genome based on the full set of SNPs and NSNP gives the number of significant SNPs in that haplotype block. Beta refers to the sign and magnitude of the effect of the minor allele and RES is the relative effect size of the SNPs in the haplotype block.

| Chromosome | Region | Haplotype Block | NSNP | Trait | P Value | beta | P (most signif SNP) | RES |
|---|---|---|---|---|---|---|---|---|
| 1 | 01-01 | 1_293 | 1 | MidribDensity | significant | 5225.594 | 1.69E-06 | 0.1230674 |
| 3 | 03-01 | 3_single8 | 1 | $g_{smax}$ | significant | 1.106586 | 3.94E-07 | 0.192269 |
| 3 | 03-01 | 3_single8 | 1 | SD_Bottom | suggestive | 25.8214 | 3.33E-05 | 0.1884758 |
| 3 | 03-01 | 3_single8 | 1 | SD_Sum | suggestive | 39.14283 | 0.000102 | 0.1901099 |
| 3 | 03-01 | 3_single8 | 1 | VLA | suggestive | 0.4426898 | 0.001062 | 0.1583137 |
| 3 | 03-02 | 3_1098 | 1 | PC3 | significant | -0.5384682 | 2.41E-06 | 0.1502027 |
| 4 | 04-01 | 4_310 | 2 | LeafArea | significant | 0.001170392 | 8.31E-07 | 0.1537308 |
| 4 | 04-01 | 4_310 | 16 | 2nd VLA | suggestive | -0.004701834 | 1.02E-05 | 0.1065223 |
| 4 | 04-01 | 4_310 | 18 | MajorVLA | suggestive | -0.006228969 | 2.80E-05 | 0.1179272 |
| 4 | 04-01 | 4_310 | 1 | PlantBio | suggestive | 0.5358185 | 0.000455 | 0.1110996 |
| 5 | 05-01 | 5_482 | 2 | SD_Top | significant | 35.15059 | 5.28E-07 | 0.3482308 |
| 5 | 05-01 | 5_482 | 1 | SD_Sum | significant | 72.06399 | 2.07E-06 | 0.3500022 |
| 5 | 05-01 | 5_482 | 2 | SD_Bottom | suggestive | 37.27081 | 8.85E-05 | 0.2720475 |
| 5 | 05-01 | 5_482 | 3 | LMA | suggestive | 2.520578 | 0.000132 | 0.2683679 |
| 5 | 05-01 | 5_482 | 1 | SV | suggestive | 2.159784 | 0.000689 | 0.2292524 |
| 5 | 05-01 | 5_482 | 1 | $g_{smax}$ | suggestive | 1.240696 | 0.000236 | 0.2155706 |
| 8 | 08-01 | 8_186 | 1 | SD_Bottom | significant | 28.40094 | 2.14E-06 | 0.2073044 |
| 8 | 08-01 | 8_186 | 1 | SD_Top | suggestive | 16.34961 | 0.000391 | 0.1619727 |
| 8 | 08-01 | 8_186 | 1 | SD_Sum | suggestive | 44.22569 | 5.88E-06 | 0.2147964 |
| 8 | 08-01 | 8_186 | 1 | SV | suggestive | 1.586486 | 9.29E-05 | 0.1683991 |
| 8 | 08-01 | 8_186 | 1 | $g_{smax}$ | suggestive | 0.8760535 | 3.83E-05 | 0.1522141 |
| 9 | 09-01 | 9_346 | 1 | SD_Bottom | significant | 33.4801 | 1.65E-06 | 0.2443783 |
| 9 | 09-01 | 9_346 | 1 | SD_Sum | significant | 54.09336 | 1.45E-06 | 0.262722 |
| 9 | 09-01 | 9_346 | 1 | SD_Top | suggestive | 20.86171 | 7.04E-05 | 0.2066733 |
| 9 | 09-01 | 9_346 | 1 | SV | suggestive | 1.749626 | 0.000155 | 0.1857158 |
| 9 | 09-01 | 9_346 | 1 | $g_{smax}$ | suggestive | 1.121413 | 4.40E-06 | 0.1948452 |
| 9 | 09-02 | 9_1150 | 1 | SD_Top | significant | 16.13479 | 9.18E-07 | 0.1598446 |
| 9 | 09-02 | 9_1150 | 2 | SD_Sum | suggestive | 27.75179 | 0.000102 | 0.1347856 |
| 9 | 09-02 | 9_1150 | 2 | SD_Sum | suggestive | -0.7002668 | 0.000222 | 0.135682 |
| 9 | 09-02 | 9_1150 | 1 | PL_Top | suggestive | -0.683835 | 0.00025 | 0.1112899 |
| 9 | 09-02 | 9_1150 | 1 | PL_Avg | suggestive | -0.6227185 | 0.000705 | 0.1134071 |
| 10 | 10-01 | 10_177 | 1 | PlantBio | significant | 0.6480131 | 1.93E-06 | 0.1343627 |
| 10 | 10-01 | 10_177 | 3 | LeafArea | suggestive | 0.000880452 | 0.000124 | 0.1156473 |
| 10 | 10-01 | 10_177 | 1 | GCW_Top | suggestive | 0.1308912 | 0.000653 | 0.0839859 |
| 10 | 10-01 | 10_177 | 1 | SL_Top | suggestive | 0.654666 | 0.000973 | 0.1189437 |
| 10 | 10-01 | 10_177 | 2 | SL_Avg | suggestive | 0.6548846 | 0.000945 | 0.1043832 |
| 10 | 10-01 | 10_177 | 1 | PL_Top | suggestive | 0.6159401 | 0.000756 | 0.1002405 |
| 10 | 10-01 | 10_177 | 1 | PL_Avg | suggestive | 0.5948977 | 0.000941 | 0.1083405 |
| 10 | 10-01 | 10_177 | 16 | AGBio | suggestive | 0.5834527 | 3.86E-06 | 0.1349018 |
| 10 | 10-02 | 10_435 | 6 | SD_Top | significant | 18.98131 | 1.76E-06 | 0.1880445 |
| 10 | 10-02 | 10_435 | 13 | SV | significant | 1.796433 | 3.02E-07 | 0.1906842 |
| 10 | 10-02 | 10_435 | 10 | SD_Bottom | suggestive | 19.17107 | 0.0002 | 0.1399337 |
| 10 | 10-02 | 10_435 | 16 | SD_Sum | suggestive | 37.16124 | 9.49E-06 | 0.1804856 |
| 10 | 10-02 | 10_435 | 8 | $g_{smax}$ | suggestive | 0.7166536 | 0.000214 | 0.1245184 |

| Chromosome | Region | Haplotype Block | NSNP | Trait | P Value | beta | P (most signif SNP) | RES |
|---|---|---|---|---|---|---|---|---|
| 11 | 11-01 | 11_56 | 1 | MidribMF | significant | -0.003502418 | 1.47E-06 | 0.1025098 |
| 11 | 11-01 | 11_56 | 11 | SL_Top | suggestive | 1.014624 | 0.000417 | 0.184343 |
| 11 | 11-02 | 11_65 | 3 | MidribMF | significant | 0.00361693 | 7.27E-07 | 0.1058614 |
| 11 | 11-03 | 11_70 | 1 | Stomatal Ratio | significant | 0.02068154 | 2.10E-06 | 0.205479 |
| 11 | 11-03 | 11_70 | 1 | MidribMF | suggestive | 0.003889488 | 0.00062 | 0.1138387 |
| 11 | 11-03 | 11_70 | 1 | MidribDensity | suggestive | 5948.192 | 0.000146 | 0.1400852 |
| 11 | 11-03 | 11_70 | 1 | PC2 | suggestive | 0.7394747 | 0.001724 | 0.1270972 |
| 11 | 11-04 | 11_570 | 4 | PlantBio | significant | 0.7092267 | 1.95E-06 | 0.1470551 |
| 11 | 11-04 | 11_570 | 4 | LeafArea | suggestive | 0.000857609 | 0.00047 | 0.1126468 |
| 11 | 11-04 | 11_570 | 80 | AGBio | suggestive | 0.6508026 | 8.33E-06 | 0.150474 |
| 11 | 11-05 | 11_578 | 1 | PlantBio | significant | 0.629387 | 1.72E-06 | 0.1305006 |
| 11 | 11-05 | 11_578 | 6 | AGBio | suggestive | 0.7516597 | 4.84E-06 | 0.1737934 |
| 11 | 11-06 | 11_608 | 2 | AGBio | significant | 0.5734662 | 1.28E-06 | 0.1325928 |
| 11 | 11-06 | 11_608 | 15 | PlantBio | significant | 0.6758659 | 3.37E-07 | 0.1401378 |
| 11 | 11-06 | 11_608 | 13 | LMA | suggestive | 0.9168736 | 0.000352 | 0.0976202 |
| 11 | 11-06 | 11_608 | 17 | MidribDensity | suggestive | 4439.891 | 0.000148 | 0.1045634 |
| 11 | 11-07 | 11_609 | 4 | AGBio | significant | 0.6144799 | 2.35E-07 | 0.1420757 |
| 11 | 11-07 | 11_609 | 13 | PlantBio | significant | 0.7208257 | 1.07E-07 | 0.1494601 |
| 11 | 11-07 | 11_609 | 8 | LMA | suggestive | 0.9518446 | 0.000276 | 0.1013436 |
| 11 | 11-07 | 11_609 | 10 | MidribDensity | suggestive | 4118.071 | 0.000247 | 0.0969843 |
| 11 | 11-08 | 11_610 | 6 | AGBio | significant | 0.5967773 | 4.76E-07 | 0.1379826 |
| 11 | 11-08 | 11_610 | 15 | PlantBio | significant | 0.6991544 | 2.27E-07 | 0.1449666 |
| 11 | 11-08 | 11_610 | 1 | SD_Bottom | suggestive | 13.949 | 0.000561 | 0.1018167 |
| 11 | 11-08 | 11_610 | 1 | SD_Sum | suggestive | 21.91051 | 0.00086 | 0.1064155 |
| 11 | 11-08 | 11_610 | 18 | LMA | suggestive | 0.9833675 | 8.16E-05 | 0.1046999 |
| 11 | 11-08 | 11_610 | 58 | MidribDensity | suggestive | 4529.37 | 0.000143 | 0.1066707 |
| 12 | 12-01 | 12_640 | 3 | PC1 | significant | 1.326797 | 1.67E-06 | 0.2070592 |
| 12 | 12-02 | 12_670 | 1 | $g_{smax}$ | significant | 1.185768 | 3.61E-07 | 0.2060269 |
| 12 | 12-02 | 12_670 | 1 | SD_Sum | suggestive | 38.02738 | 0.000546 | 0.1846923 |
| 12 | 12-02 | 12_670 | 3 | LMA | suggestive | 1.855152 | 3.78E-05 | 0.1975194 |
| 13 | 13-01 | 13_275 | 9 | SD_Top | significant | 20.16487 | 3.50E-07 | 0.1997699 |
| 13 | 13-01 | 13_275 | 10 | SD_Bottom | suggestive | 18.97142 | 0.000373 | 0.1384764 |
| 13 | 13-01 | 13_275 | 27 | SD_Sum | suggestive | 55.21875 | 6.77E-06 | 0.2681878 |
| 13 | 13-01 | 13_275 | 66 | LeafArea | suggestive | -0.000977359 | 0.000233 | 0.140794 |
| 13 | 13-01 | 13_275 | 3 | PL_Top | suggestive | -0.7434031 | 0.000996 | 0.1227915 |
| 13 | 13-01 | 13_275 | 6 | PL_Avg | suggestive | -0.6986867 | 0.000723 | 0.1349041 |
| 13 | 13-01 | 13_275 | 5 | SV | suggestive | 1.336059 | 0.00035 | 0.1418173 |
| 13 | 13-02 | 13_1077 | 2 | Stomatal Ratio | significant | -0.01333152 | 3.48E-08 | 0.1402729 |
| 16 | 16-01 | 16_1310 | 1 | PL_Bottom | significant | 1.432469 | 1.93E-06 | 0.2215802 |
| 16 | 16-01 | 16_1310 | 9 | SL_Bottom | suggestive | 1.362438 | 5.42E-05 | 0.1898009 |
| 16 | 16-01 | 16_1310 | 6 | SL_Avg | suggestive | 1.071473 | 0.000321 | 0.1706915 |
| 16 | 16-01 | 16_1310 | 9 | PL_Avg | suggestive | 1.123262 | 3.55E-05 | 0.2045642 |
| 17 | 17-01 | 17_1038 | 5 | Stomatal Ratio | significant | -0.01772242 | 6.28E-07 | 0.1919132 |

**Table S2.2**: List of genes per region along with associated significant/suggestive traits. Gene names come from annotation of the sunflower HA412-HOv2 genome assembly. To view table, see Earley et al. 2022 Table S2 (https://doi.org/10.1111/tpj.15900).

**Methods S2.1:** Neural Network Architecture, Training and Prediction. The neural network followed that of the U-Net (Ronneberger *et al.*, 2015) deep neural network. High-dilation convolutions (Yu and Koltun, 2015) were integrated by replacing the U-Net architecture after the last max-pool through the first up convolution with the structure shown in Figure S2.1. In addition, all RELU activations were replaced with ELUs (Clevert *et al.*, 2015). The network architecture takes input images of size 572x572x3 pixels and outputs a segmented target image of 388x388x1 pixels that corresponds to the center of the 572x572 image. For training, input images were created by randomly selecting 388x388x3 regions from the leaf images along with the surrounding 92 pixels to create the 572x572x3 input image. As in Ronneberger et al. (2015), when surrounding data was missing at the edge of the image, the pixels were extrapolated by mirroring. The 572x572x3 bright-field leaf input images were independently normalized to have a mean of 0 and a standard deviation of 1. The network was coded using the pytorch (Paszke *et al.*, 2017) framework and trained using backpropagation using the Adam optimizer (Kingma and Ba, 2014). The loss function was weighted binary cross entropy. Non-vein pixels were given a weight of 0.05 and in-vein pixels a weight of 1. The weighting of the non-vein pixels was chosen using 3-fold cross validation of the training set of images using a grid search of 0.01, 0.05, 0.1, and 0.2 for the weight. Cross-validation training

was performed out to 3000 batches, but there was no further decrease in the loss on the validation sets past 1900 batches (Figure S2.3). Attempts at stitching 388x388 segmented tiles together to recreate the full size bright-field images resulted in incorrect segmentations at the boundaries between tiles. To avoid the boundary effects, the full-sized images (2584x1936 pixels) were mirror padded to 2876 x 2300 and passed through the network as one input. The images were normalized as described for the image tiles used in training. The resulting segmented images were cropped back to 2584x1936 pixels to remove padding pixels. The padding was used to both avoid edge effects – as done during network training – and to ensure all the convolution operations within the network were valid. The network outputs the probability a pixel is within a vein. The in-vein segmentation cutoff of 0.2 maximized the correlation between the number of pixels in the hand drawn vein lines and in that extracted with the network in a 3-way cross validation grid search of values spanning 0.2 to 0.9 with 0.1 increments.

# APPENDIX B

## SUPPLEMENTARY FIGURES, TABLES, AND METHODS FROM CHAPTER 3

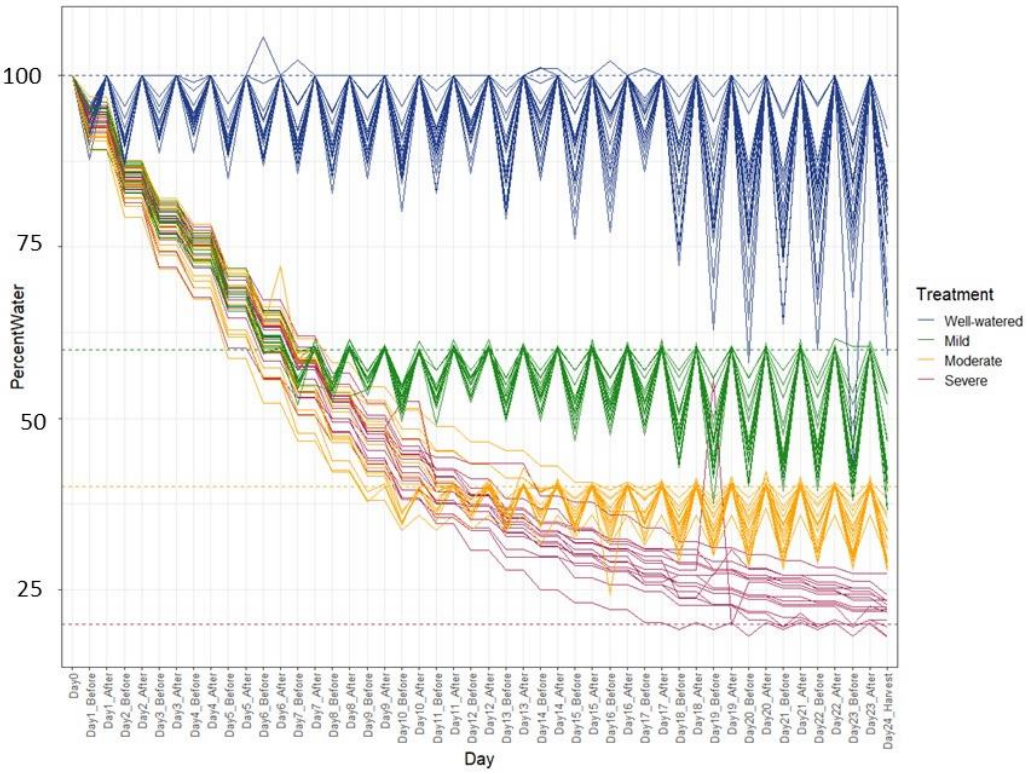


**Figure S3.1**: Watering data based on percent water compared to field capacity - before and after watering each day. Dotted lines are target levels for each treatment. Well-watered - 100%, mild - 60%, moderate - 40%, severe - 20%.

**A**

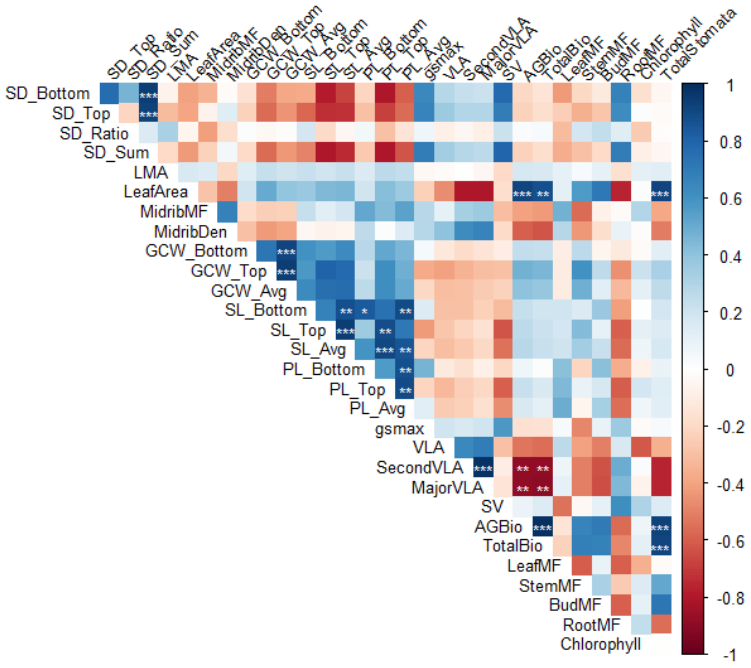
SD_Top
SD_Bottom
SD_Ratio
SD_Sum
LMA
LeafArea
MidribMF
MidribDen
GCW_Bottom
GCW_Top
GCW_Avg
SL_Bottom
SL_Top
SL_Avg
PL_Bottom
PL_Top
PL_Avg
gsmax
VLA
SecondVLA
MajorVLA
SV
AGBio
TotalBio
LeafMF
StemMF
BudMF
RootMF
Chlorophyll
TotalStomata
1
0.8
0.6
0.4
0.2
0
-0.2
-0.4
-0.6
-0.8
-1

**B**

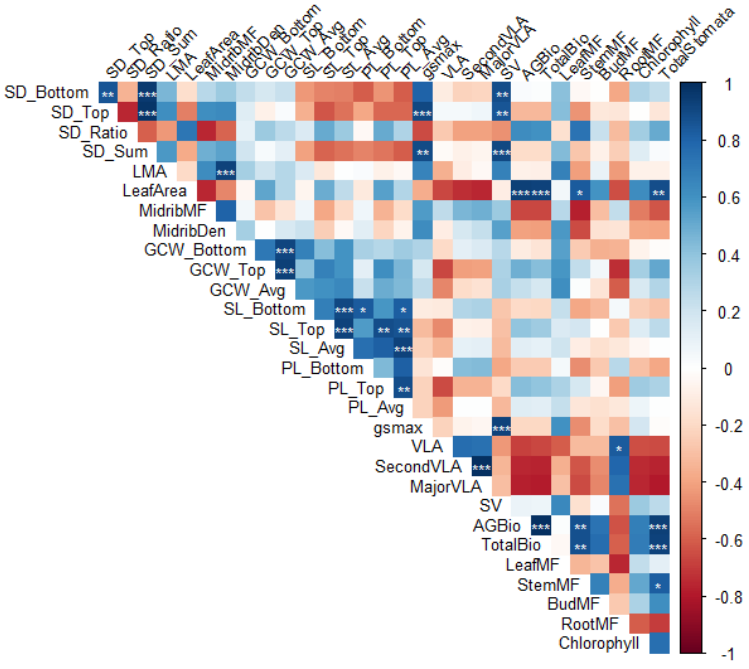
SD_Top
SD_Bottom
SD_Ratio
SD_Sum
LMA
LeafArea
MidribMF
MidribDen
GCW_Bottom
GCW_Top
GCW_Avg
SL_Bottom
SL_Top
SL_Avg
PL_Bottom
PL_Top
PL_Avg
gsmax
VLA
SecondVLA
MajorVLA
SV
AGBio
TotalBio
LeafMF
StemMF
BudMF
RootMF
Chlorophyll
TotalStomata
1
0.8
0.6
0.4
0.2
0
-0.2
-0.4
-0.6
-0.8
-1

**C**

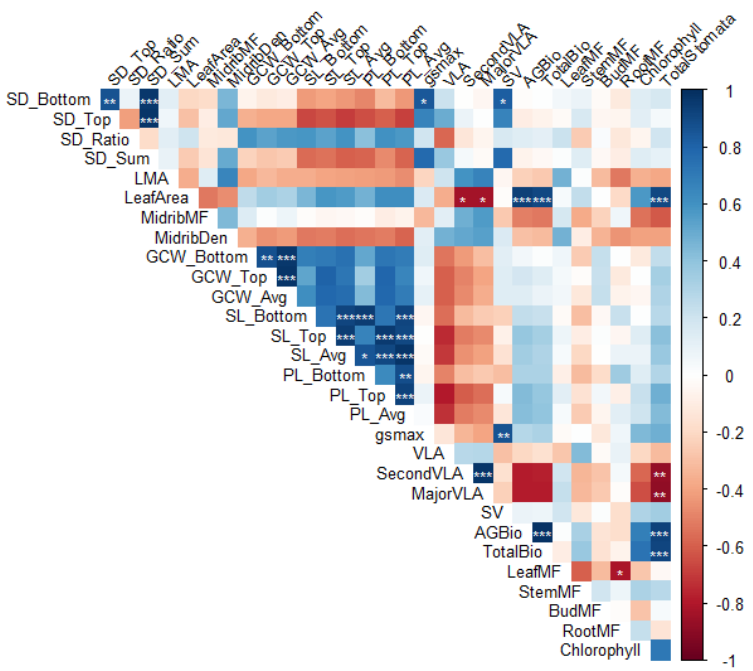
SD_Top
SD_Bottom
SD_Ratio
SD_Sum
LMA
LeafArea
MidribMF
MidribDen
GCW_Bottom
GCW_Top
GCW_Avg
SL_Bottom
SL_Top
SL_Avg
PL_Bottom
PL_Top
PL_Avg
gsmax
VLA
SecondVLA
MajorVLA
SV
AGBio
TotalBio
LeafMF
StemMF
BudMF
RootMF
Chlorophyll
TotalStomata
1
0.8
0.6
0.4
0.2
0
-0.2
-0.4
-0.6
-0.8
-1

**D**

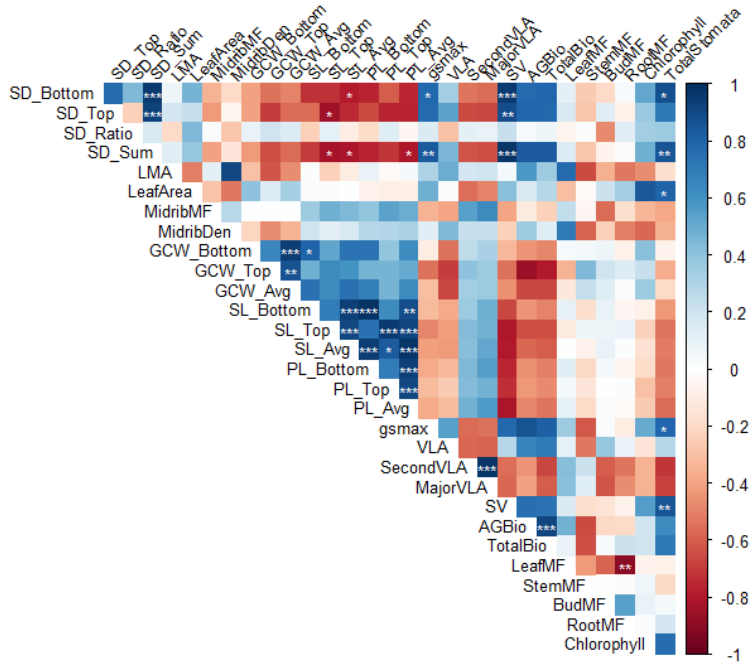
SD_Top
SD_Bottom
SD_Ratio
SD_Sum
LMA
LeafArea
MidribMF
MidribDen
GCW_Bottom
GCW_Top
GCW_Avg
SL_Bottom
SL_Top
SL_Avg
PL_Bottom
PL_Top
PL_Avg
gsmax
VLA
SecondVLA
MajorVLA
SV
AGBio
TotalBio
LeafMF
StemMF
BudMF
RootMF
Chlorophyll
TotalStomata
1
0.8
0.6
0.4
0.2
0
-0.2
-0.4
-0.6
-0.8
-1

**Figure S3.2:** Correlation matrices for each treatment (A) well-watered; (B) mild; (C) moderate; (D) severe Values were calculated using pot level data and significance tests were corrected for multiple comparisons using a Bonferroni correction. Positive correlations are in blue and negative correlations are in red. Shading gives a relative indication of the magnitude of the estimate. ***P ≤ 0.001, **P ≤ 0.01, * P ≤ 0.05. Abbreviations follow Table 3.1.

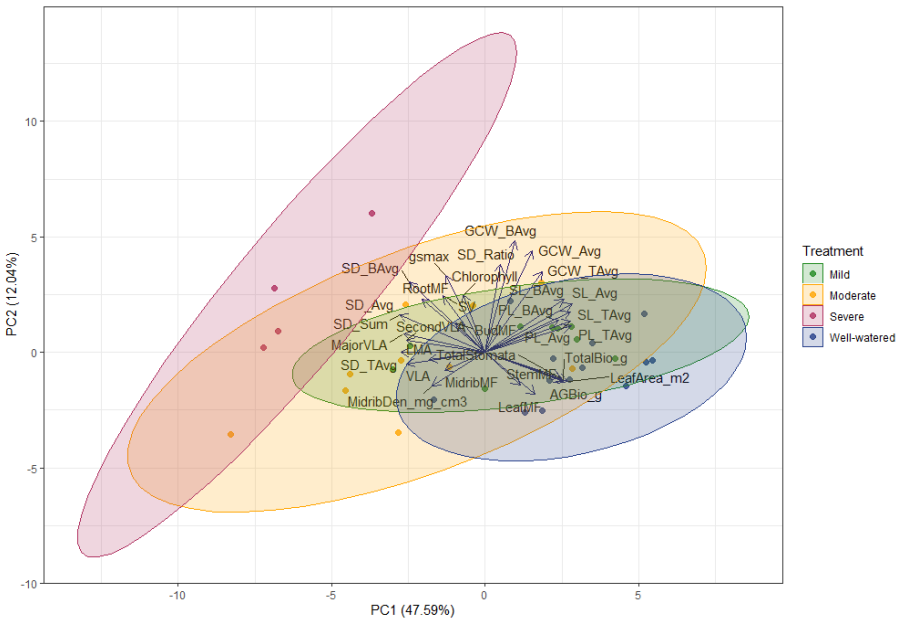


**Figure S3.3**: Principal component analysis of all traits. Colors indicate treatment as follows: blue = well-watered, green = mild, yellow = moderate, and red = severe. Abbreviations follow Table 3.1.

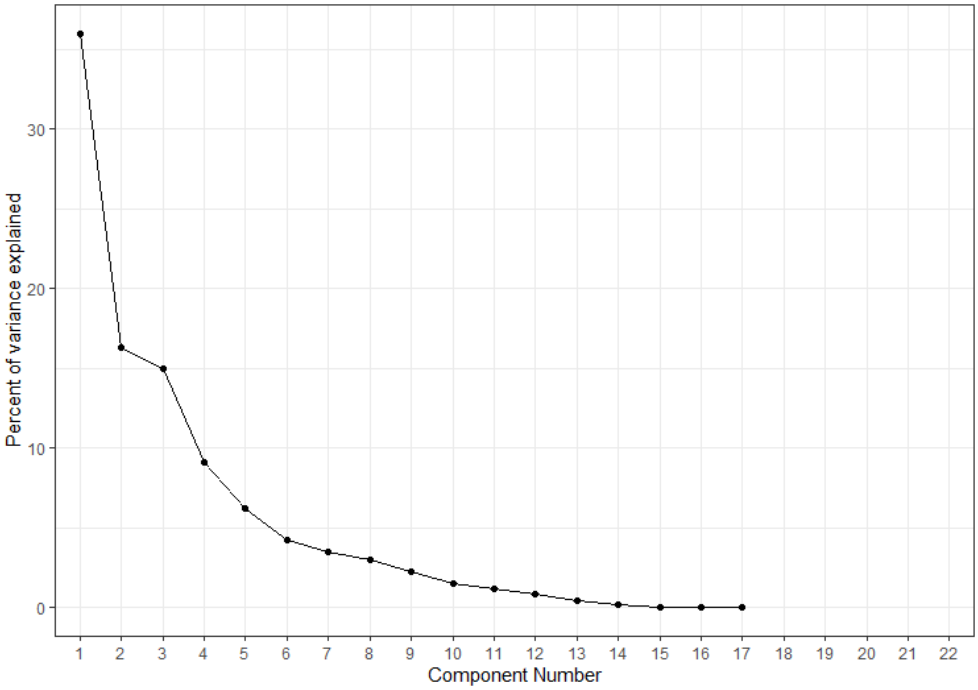


**Figure S3.4:** Scree plot showing principal components vs. percent variance explained for reduced trait PCA presented in Figure 3.2.

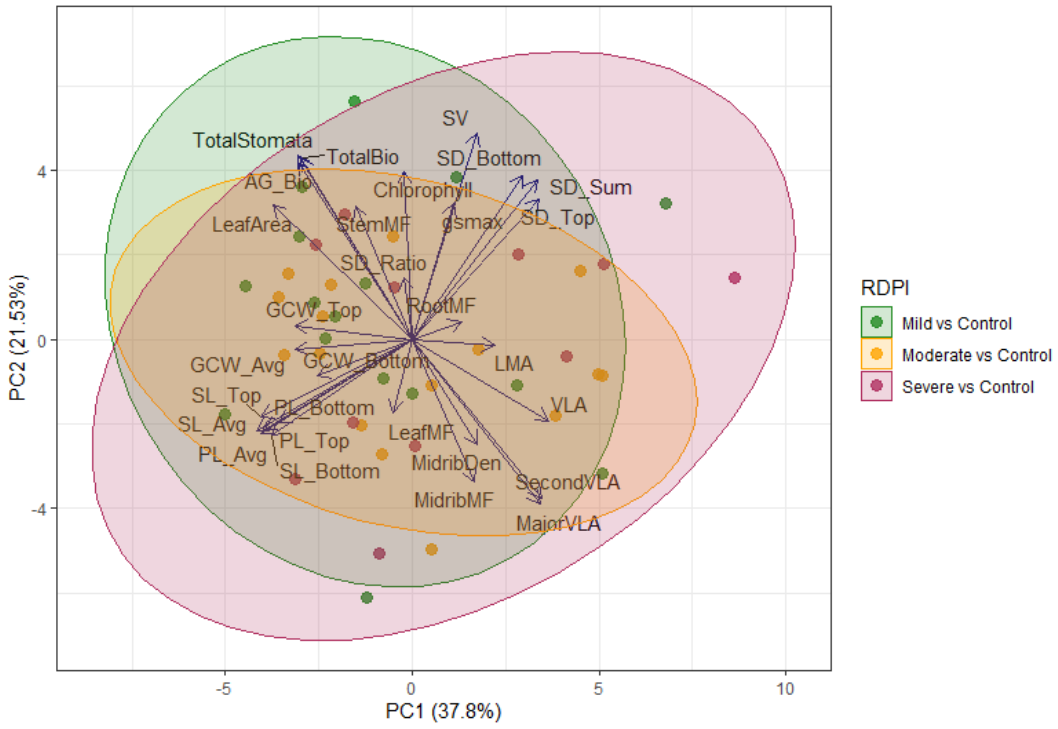


**Figure S3.5**: Principal component analysis (PCA) of trait plasticity values (estimated as RDPI) for each treatment compared to control for all traits. Abbreviations follow Table 3.1.

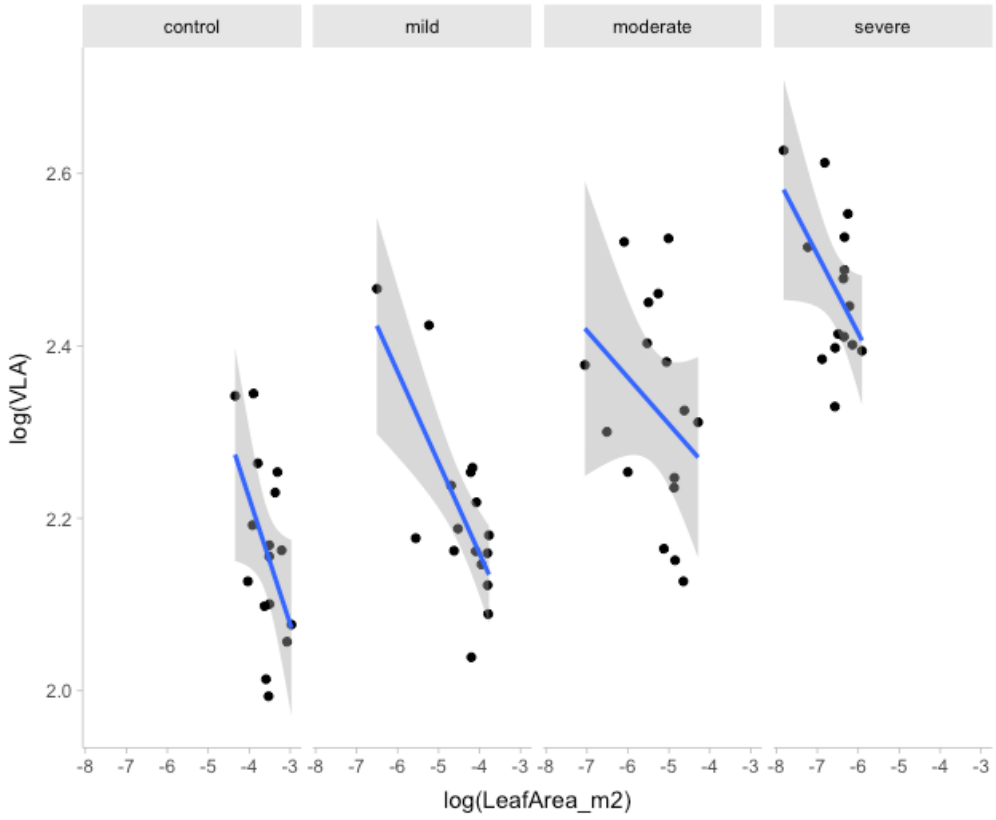


**Figure S3.6**: Relationship between log transformed VLA and log transformed leaf by treatment. Dots represent individual plants, and the blue line represents the line of best fit. The gray shading is the 95% confidence interval.

**Table S3.1**: Tukey's HSD test results for all pairwise treatment comparisons. Significance for genotypic effects (***P ≤ 0.001, **P ≤ 0.01, * P ≤ 0.05, P ≤ 0.1, ns = not significant). All traits with significant treatment effects (Table 3.1) are shown. Traits with no significant treatment effects are excluded from the table.

| Trait | Well watered-Mild | Well watered - moderate | Well watered - Severe | Moderate-Mild | Moderate-Severe | Severe-Mild |
|---|---|---|---|---|---|---|
| SD_Bottom (stomata/mm$^2$) | ns | ns | *** | ns | *** | *** |
| SD_Top (stomata/mm$^2$) | ns | ns | *** | ns | * | *** |
| SD_Sum (stomata/mm$^2$) | ns | ns | *** | ns | *** | *** |
| Stomatal Ratio (bottom/sum) | ns | ns | * | ns | . | ns |
| SL_Bottom (µm) | ns | * | *** | . | ns | *** |
| SL_Top (µm) | ns | * | *** | . | ns | *** |
| SL_Avg (µm) | ns | * | *** | * | ns | *** |
| PL_Bottom (µm) | ns | * | *** | * | ns | *** |
| PL_Top (µm) | ns | . | *** | . | * | *** |
| PL_Avg (µm) | ns | * | *** | * | . | *** |
| Leaf Area (m$^2$) | *** | *** | *** | *** | ** | *** |
| LMA (g/m$^2$) | ns | ns | *** | ns | ** | *** |
| VLA (mm/mm$^2$) | ns | *** | *** | ** | ** | *** |
| 2nd VLA (mm/mm$^2$) | ns | *** | *** | . | ** | *** |
| Major VLA (mm/mm$^2$) | ns | *** | *** | * | ** | *** |
| AG Bio (g) | *** | *** | *** | *** | . | *** |
| Total Bio (g) | *** | *** | *** | *** | . | *** |
| Midrib Density (mg/cm$^3$) | ns | ns | ** | ns | * | ** |
| Midrib MF ($g_{midrib}/g_{leaf}$) | ns | ns | *** | ns | ns | ** |
| $g_{smax}$ (mol/m$^2$s) | ns | ns | . | ns | * | ns |
| Leaf MF ($g_{leaf}/g_{plant}$) | ns | ns | * | ns | ns | ns |
| Stem MF ($g_{stem}/g_{plant}$) | ns | ns | * | ns | ** | * |
| Root MF ($g_{root}/g_{plant}$) | * | . | *** | ns | ** | * |
| TotalStomata (stomata) | *** | *** | *** | *** | . | *** |

**Table S3.2**: Mean coefficients and credible intervals for trait model shown Figure 3.5. Abbreviations follow Table 3.1.

| Trait | Probs | Control_summary | Mild_summary | Moderate_summary | Severe_summary |
|---|---|---|---|---|---|
| VLA | 95_low | -1.04 | -0.98 | -0.24 | -0.08 |
| VLA | 80_low | -0.89 | -0.80 | -0.08 | 0.07 |
| VLA | Mean | -0.61 | -0.48 | 0.18 | 0.38 |
| VLA | 80_high | -0.34 | -0.17 | 0.43 | 0.68 |
| VLA | 95_high | -0.20 | 0.01 | 0.58 | 0.86 |
| SD_Sum | 95_low | -0.17 | -0.73 | -0.04 | -0.19 |
| SD_Sum | 80_low | 0.09 | -0.51 | 0.13 | -0.08 |
| SD_Sum | Mean | 0.63 | -0.09 | 0.43 | 0.15 |
| SD_Sum | 80_high | 1.16 | 0.34 | 0.74 | 0.37 |
| SD_Sum | 95_high | 1.45 | 0.59 | 0.93 | 0.50 |
| SL_Avg | 95_low | -0.41 | -0.71 | -0.07 | -0.20 |
| SL_Avg | 80_low | -0.24 | -0.55 | 0.09 | -0.02 |
| SL_Avg | Mean | 0.07 | -0.27 | 0.37 | 0.31 |
| SL_Avg | 80_high | 0.37 | 0.02 | 0.66 | 0.64 |
| SL_Avg | 95_high | 0.53 | 0.18 | 0.83 | 0.83 |
| logLMA | 95_low | -0.27 | -0.88 | -0.39 | -0.17 |
| logLMA | 80_low | 0.06 | -0.56 | -0.29 | -0.10 |
| logLMA | Mean | 0.66 | 0.01 | -0.08 | 0.03 |
| logLMA | 80_high | 1.29 | 0.54 | 0.12 | 0.16 |
| logLMA | 95_high | 1.60 | 0.88 | 0.23 | 0.24 |
| Biomass | 95_low | 0.39 | -0.95 | -1.36 | -2.33 |
| Biomass | 80_low | 0.81 | -0.56 | -0.93 | -1.86 |
| Biomass | Mean | 1.45 | -0.01 | -0.44 | -1.29 |
| Biomass | 80_high | 2.11 | 0.56 | 0.01 | -0.75 |
| Biomass | 95_high | 2.59 | 1.01 | 0.45 | -0.36 |

**Table S3.3**: Mean coefficients and credible intervals for RDPI model shown in Figure 3.6. Abbreviations follow Table 3.1.

| Probs | VLA_summary | SD_summary | SL_summary | logLMA_summary |
|---|---|---|---|---|
| 95_low | -0.80 | -0.13 | -0.40 | -0.18 |
| 80_low | -0.66 | 0.02 | -0.24 | -0.09 |
| Mean | -0.44 | 0.25 | 0.02 | 0.08 |
| 80_high | -0.22 | 0.48 | 0.28 | 0.25 |
| 95_high | -0.10 | 0.60 | 0.43 | 0.35 |

# APPENDIX C

## SUPPLEMENTARY FIGURES, TABLES, AND METHODS FROM CHAPTER 4

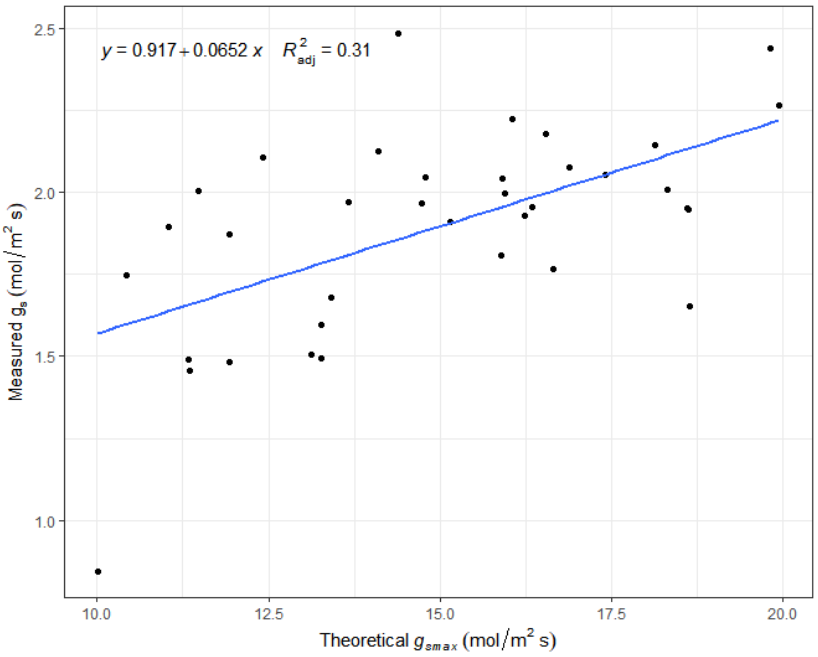


**Figure S4.1**: Bivariate plot of theoretical $g_{smax}$ versus measured stomatal conductance. Points represent pot level data for the 36 plants that had stomatal conductance measured. Blue line is the best fit.

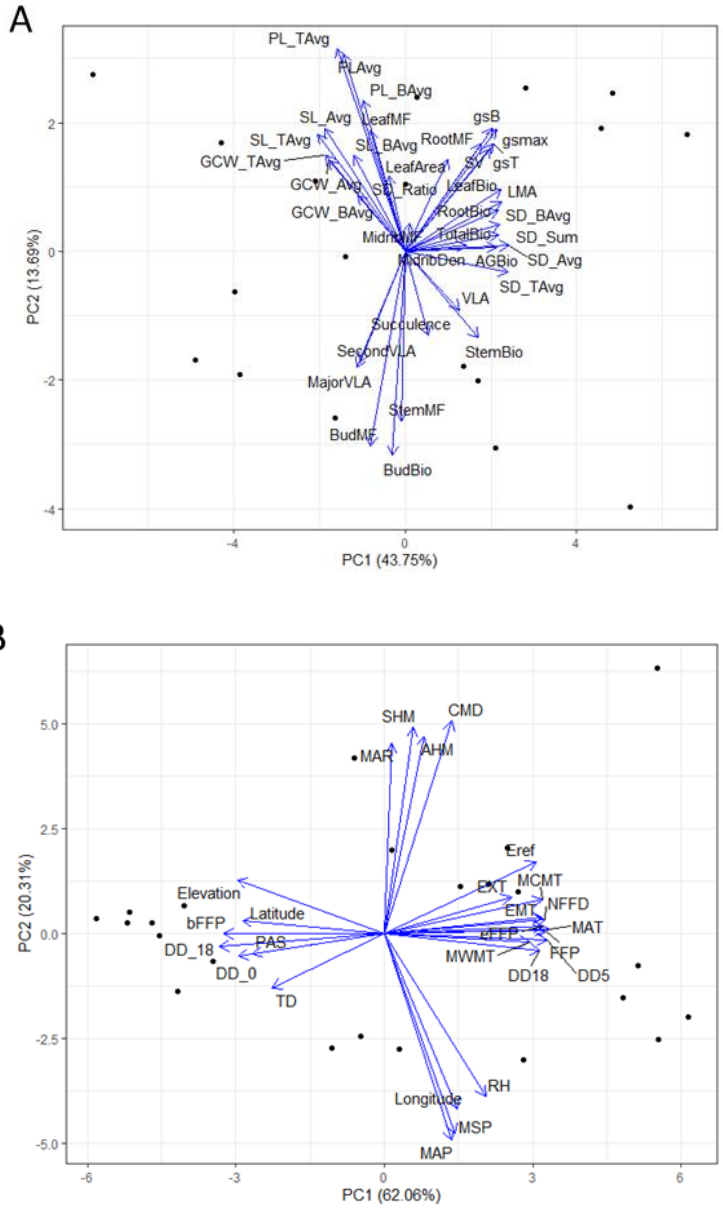


**Figure S4.2**: (A) Principal component analysis of estimated marginal means for all traits. Trait abbreviations follow Table 4.1. (B) Principal component analysis of all environmental traits. Trait abbreviations follow Table 4.2.

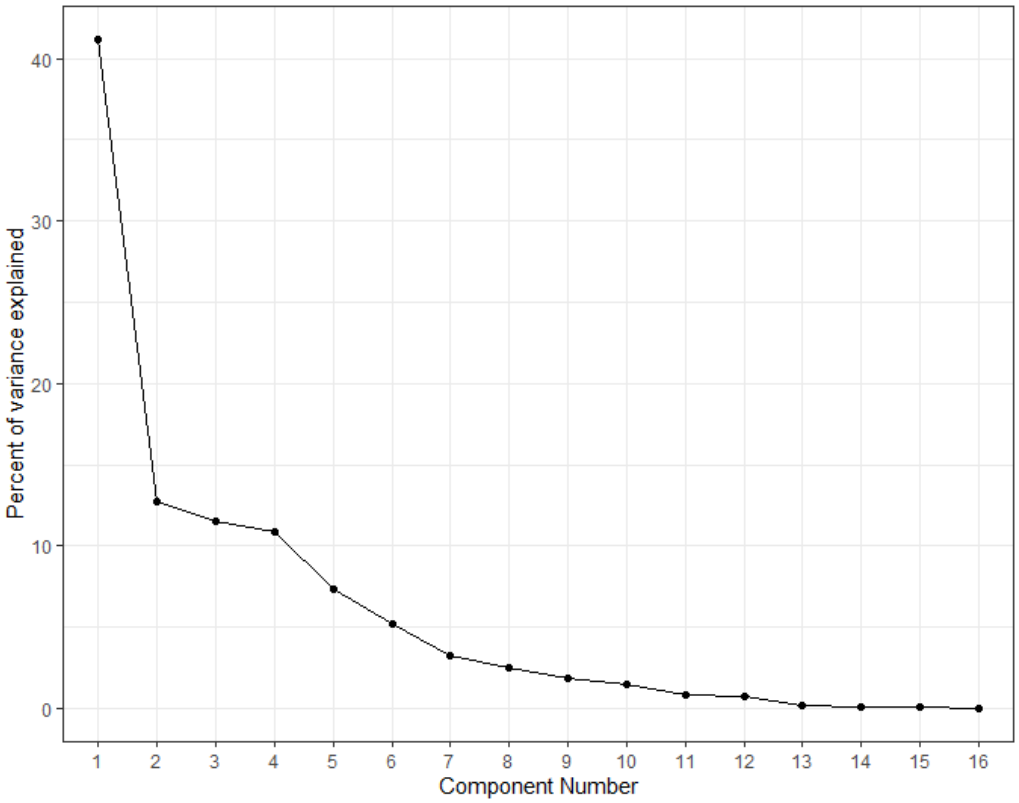


**Figure S4.3**: Scree plot for PCA presented in Figure 4.3

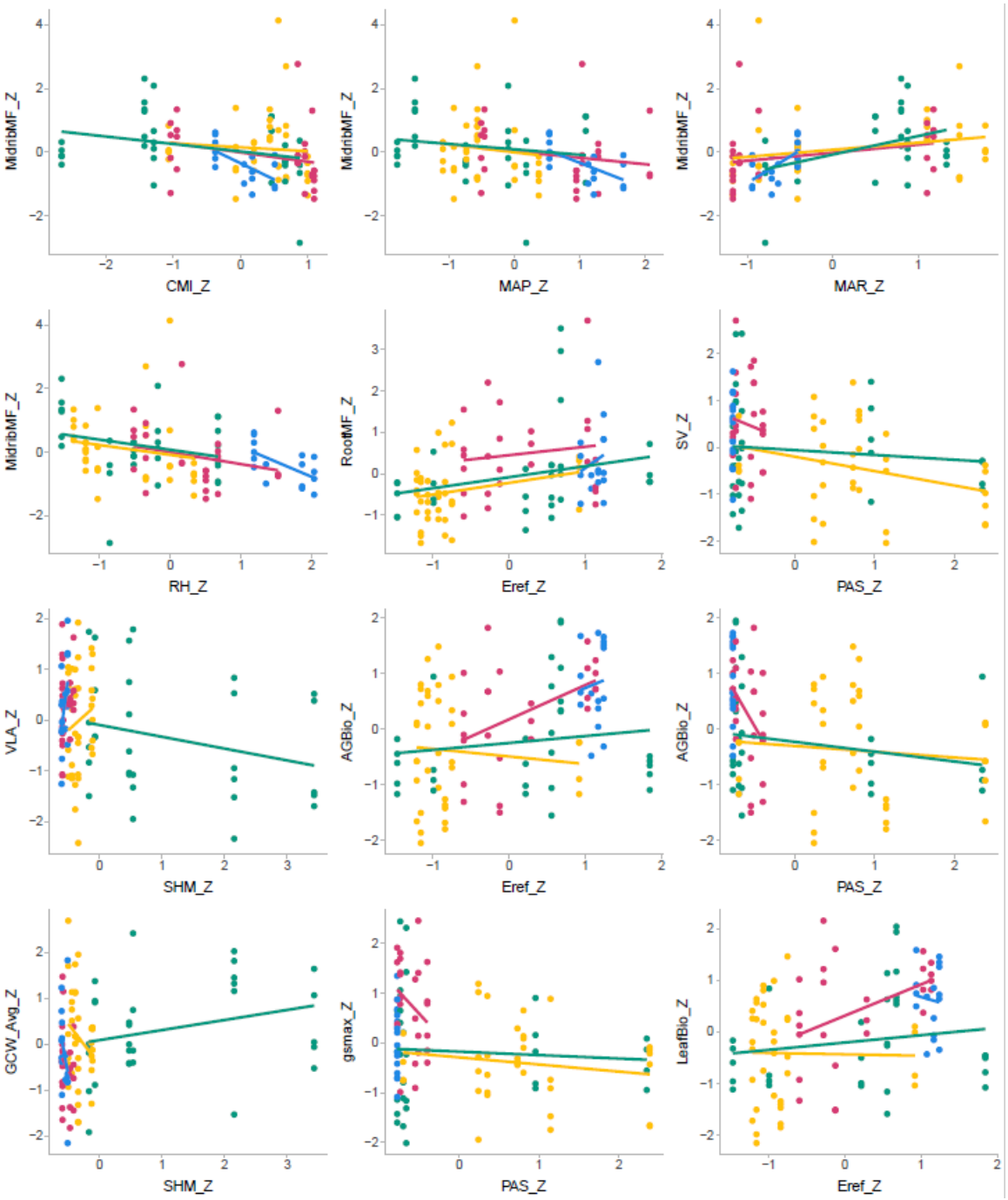
MidribMF_Z
CMI_Z
MAP_Z
MAR_Z
RH_Z
RootMF_Z
Eref_Z
SV_Z
PAS_Z
VLA_Z
SHM_Z
AGBio_Z
GCW_Avg_Z
gsmax_Z
LeafBio_Z

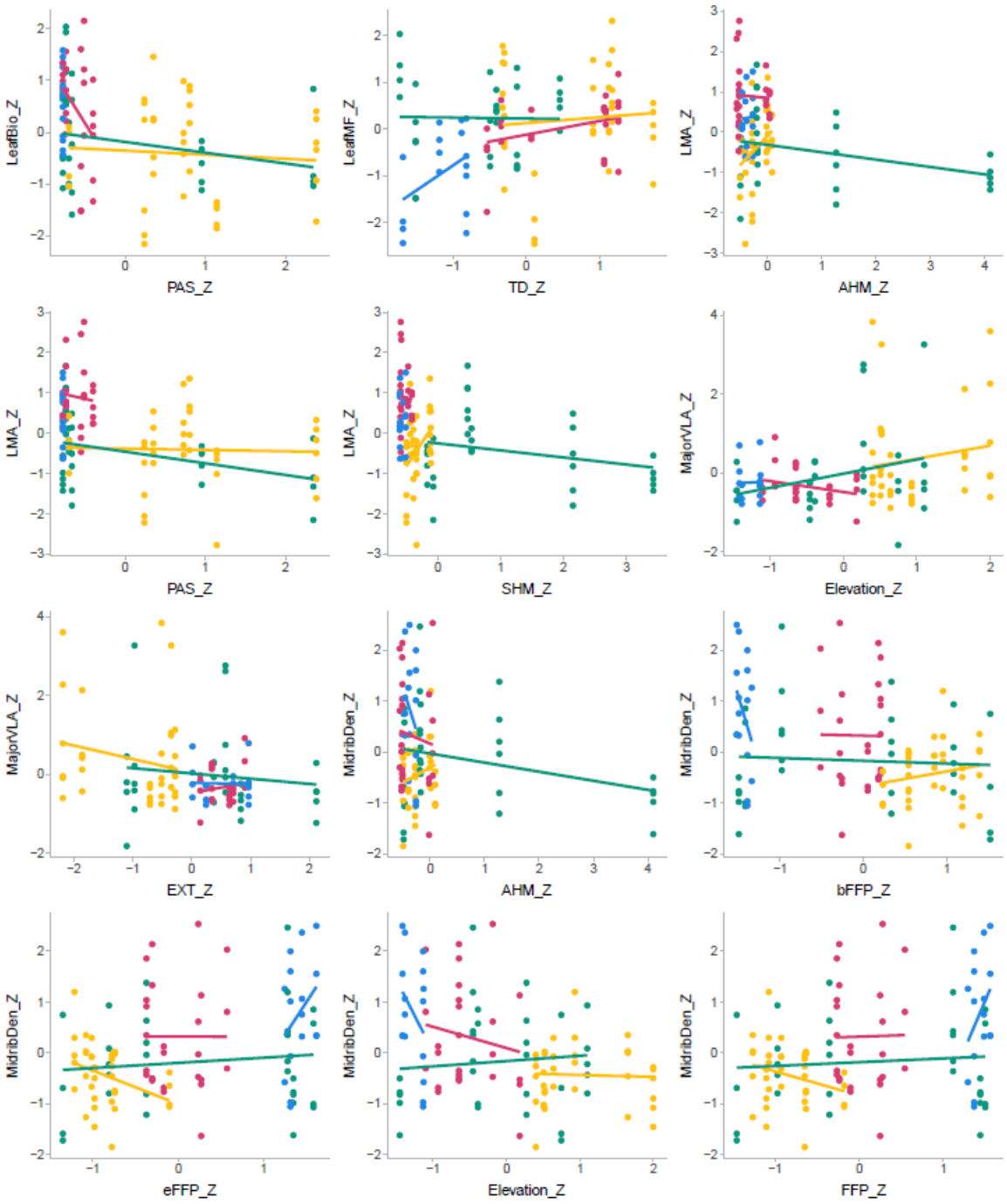
LeafBio_Z
PAS_Z
LeafMF_Z
TD_Z
LMA_Z
AHM_Z
LMA_Z
PAS_Z
LMA_Z
SHM_Z
MajorVLA_Z
Elevation_Z
MajorVLA_Z
EXT_Z
MidribDen_Z
AHM_Z
MidribDen_Z
bFFP_Z
MidribDen_Z
eFFP_Z
MidribDen_Z
Elevation_Z
MidribDen_Z
FFP_Z

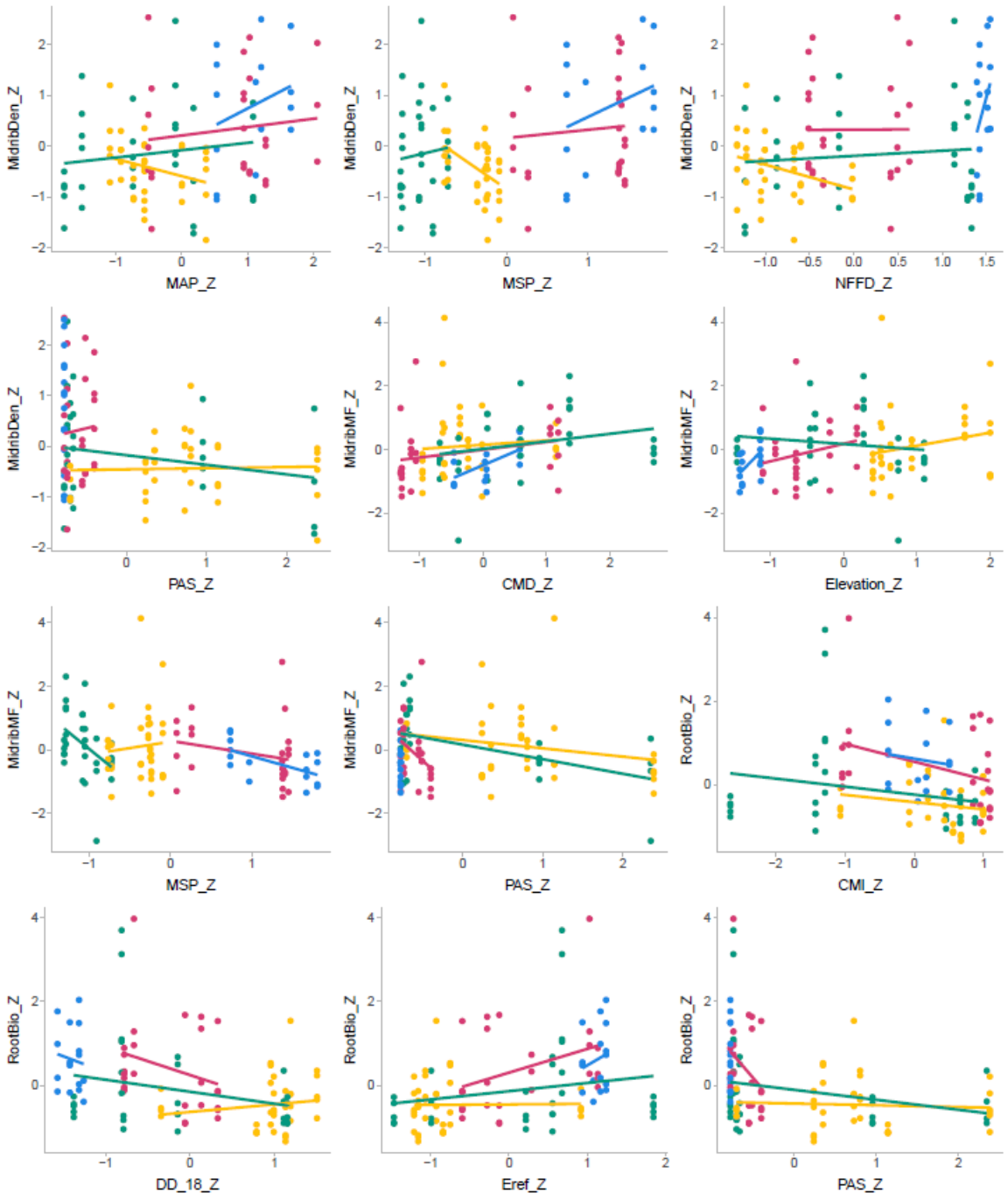
MidribDen_Z
MAP_Z
MSP_Z
NFFD_Z
PAS_Z
MidribMF_Z
CMD_Z
Elevation_Z
MSP_Z
PAS_Z
RootBio_Z
CMI_Z
DD_18_Z
Eref_Z
PAS_Z

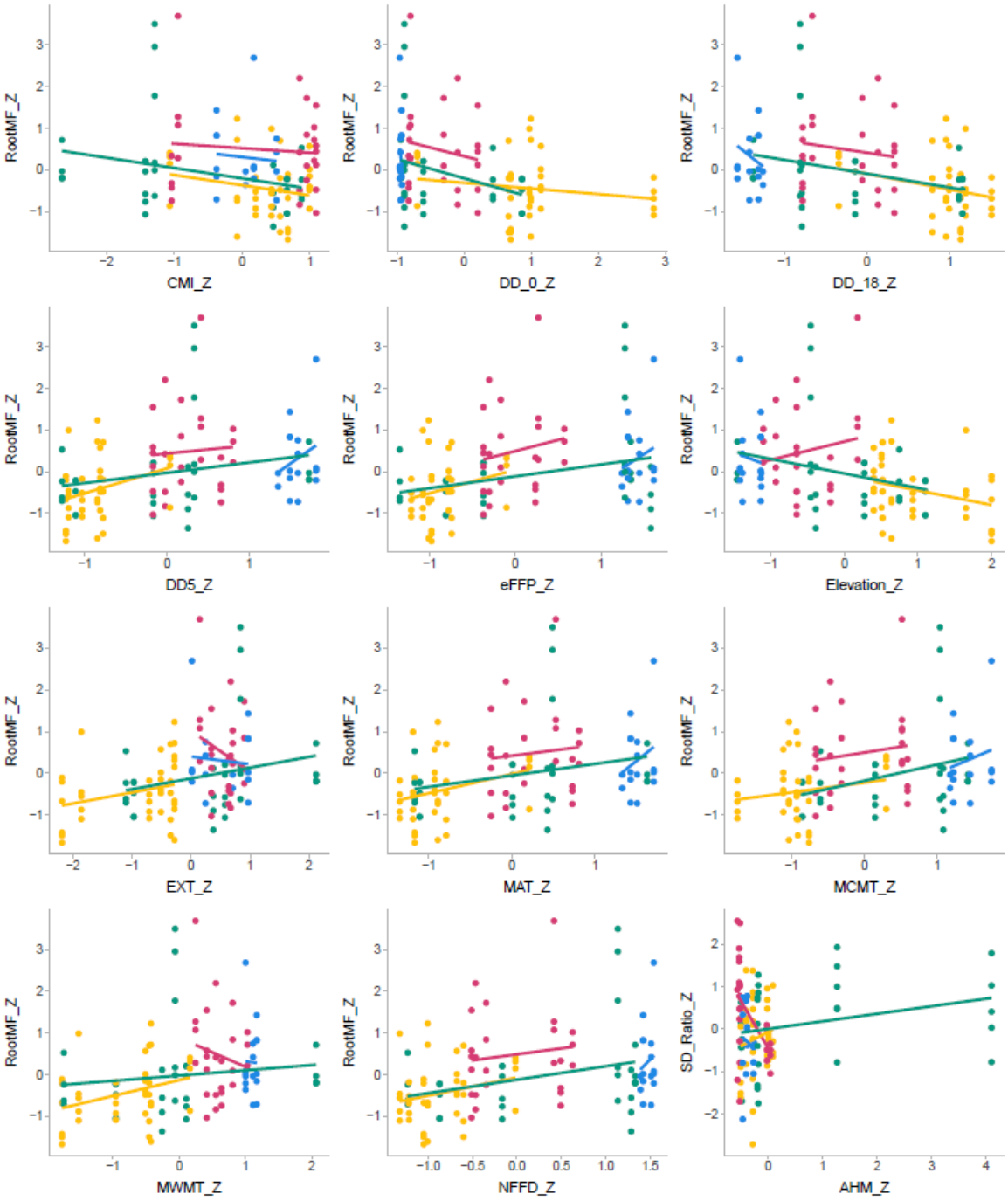
RootMF_Z
CMI_Z
DD_0_Z
DD_18_Z
DD5_Z
eFFP_Z
Elevation_Z
EXT_Z
MAT_Z
MCMT_Z
MWMT_Z
NFFD_Z
SD_Ratio_Z
AHM_Z

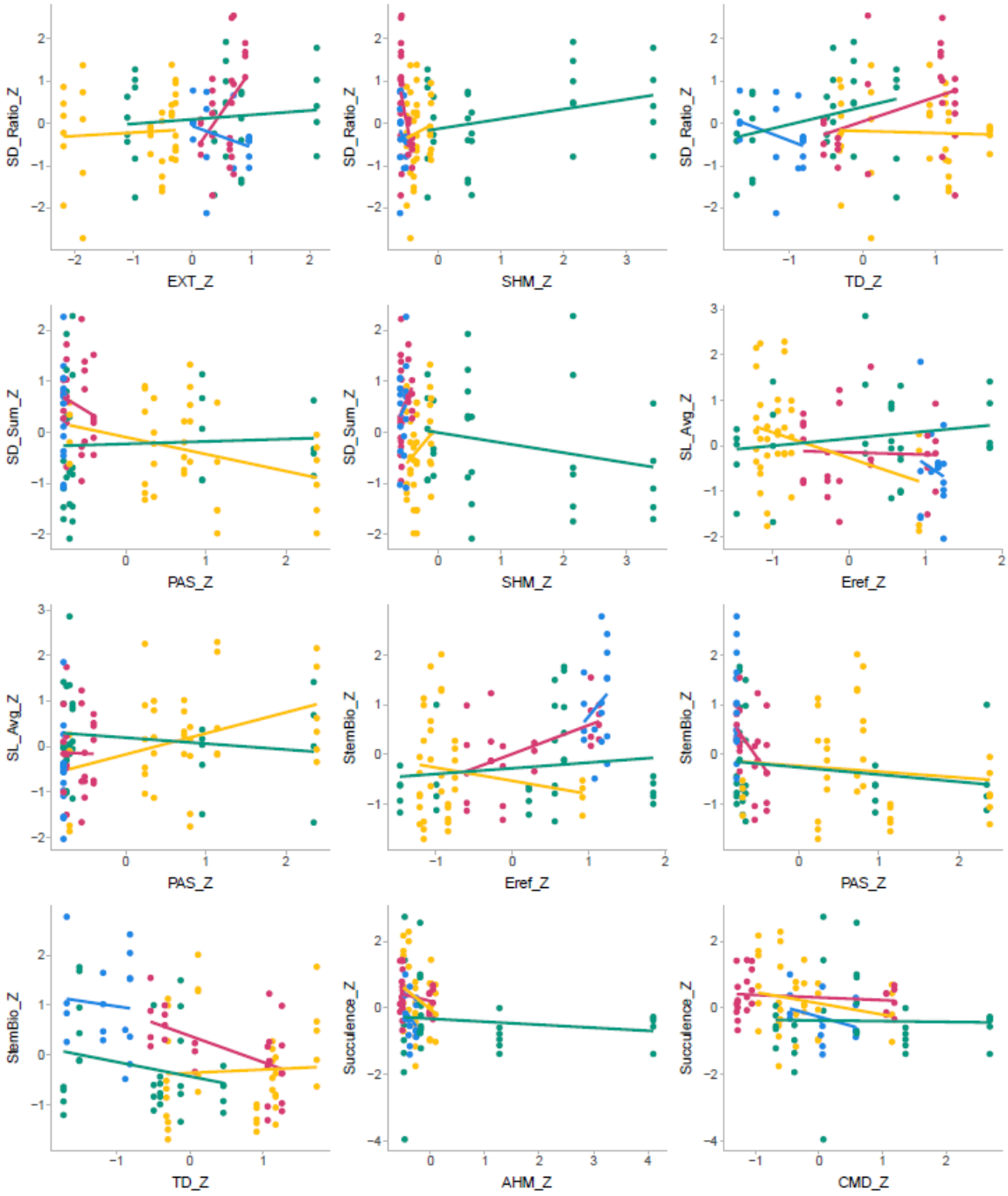
SD_Ratio_Z
EXT_Z
SD_Ratio_Z
SHM_Z
SD_Ratio_Z
TD_Z
SD_Sum_Z
PAS_Z
SD_Sum_Z
SHM_Z
SL_Avg_Z
Eref_Z
SL_Avg_Z
PAS_Z
StemBio_Z
Eref_Z
StemBio_Z
PAS_Z
StemBio_Z
TD_Z
Succulence_Z
AHM_Z
Succulence_Z
CMD_Z

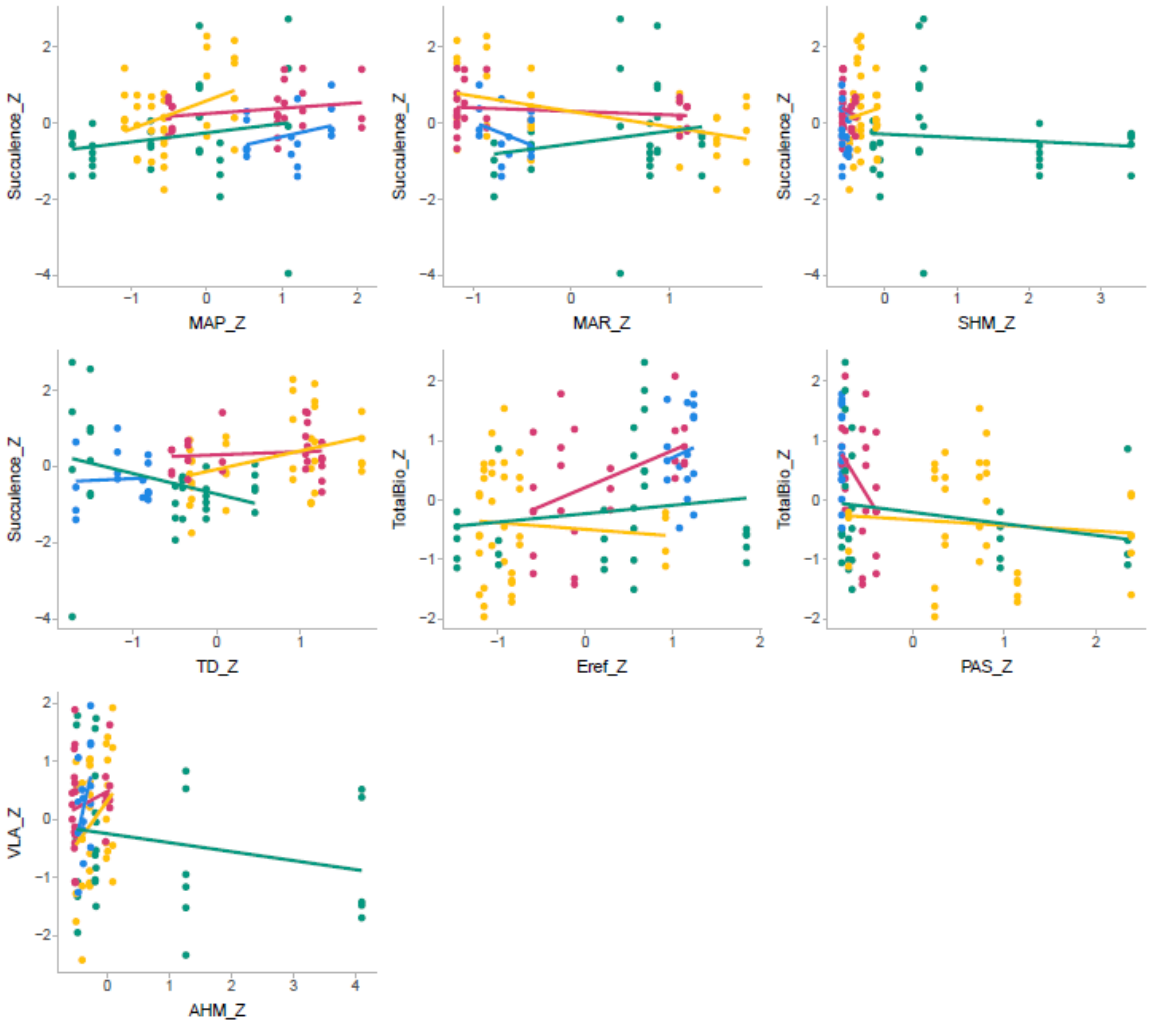


**Figure S4.4**: Bivariate plots of traits and environmental variables from all significant models. Dots represent individuals and are colored based on population region and lines represent the line of best fit per region. All traits are scaled to a mean of zero and a standard deviation of one (indicated with subscript _Z at end of trait name). Colors: Pink = High Plains, Blue = South Texas, Yellow = Intermountain West, Green = West. Trait abbreviations follow Tables 4.1 and 4.2

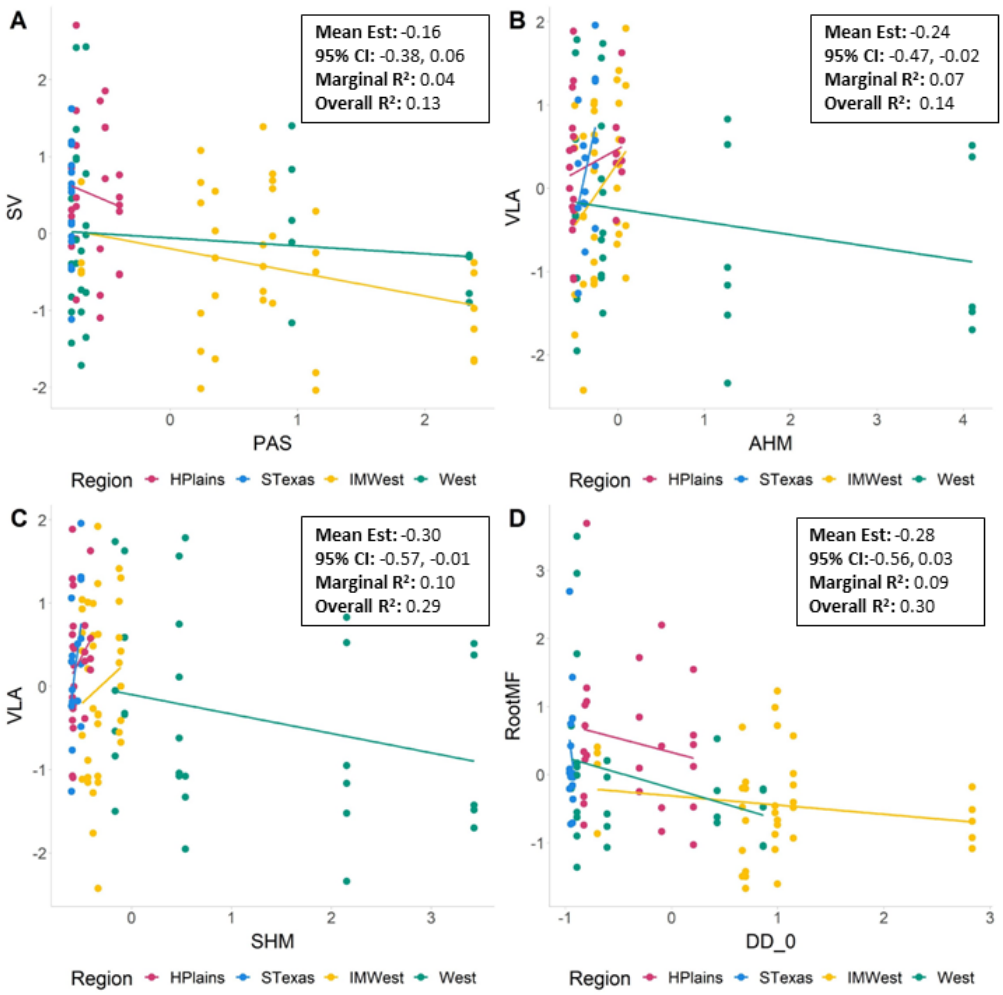


**Figure S4.5:** Example bivariate plots of trait vs environmental data with correlations across treatments driven by geographic artifact. (A) PAS vs SV, (B) AHM vs VLA, (C) SHM vs VLA, (D) DD_0 vs Root MF. All traits and environmental variables are scaled to a mean of zero and a standard deviation of one. Dots represent individual plants and lines indicate the line of best fit per region. Text box includes results from models including mean estimate, the 95% credible interval, and marginal $R^2$ value. HPlains =

High Plains, STexas = South Texas, and IMWest = Intermountain West. Abbreviations follow Tables 1 and 2. For all bivariate plots, see Figure S4.4.

**Table S4.1**: Details for the 24 wild *Helianthus annuus* populations. Data taken from Todesco et al. 2020. Table includes collection data and location, description of site, coordinates of site, estimate of population size, and number of individuals sampled.

| Population ID | Accession | Individuals | Taxon | Nr. of Individuals Sampled | Collected | Country | State or Province |
|---|---|---|---|---|---|---|---|
| ANN_05 | PI 695651 | ANN0841-0850 | *Helianthus annuus* | 30 | 1-Sep-15 | United States | California |
| ANN_06 | PI 695652 | ANN0851-0860 | *Helianthus annuus* | 29 | 2-Sep-15 | United States | California |
| ANN_10* | PI 695656 | ANN0891-0900 | *Helianthus annuus* | 30 | 12-Sep-15 | United States | California |
| ANN_16 | PI 695667 | ANN0951-0960 | *Helianthus annuus* | 30 | 15-Sep-15 | United States | New Mexico |
| ANN_17* | PI 695668 | ANN0961-0970 | *Helianthus annuus* | 29 | 15-Sep-15 | United States | New Mexico |
| ANN_23* | PI 695680 | ANN1021-1030 | *Helianthus annuus* | 27 | 18-Sep-15 | United States | Nevada |
| ANN_24* | PI 695681 | ANN1031-1040 | *Helianthus annuus* | 31 | 18-Sep-15 | United States | Nevada |
| ANN_29 | PI 695688 | ANN1081-1090 | *Helianthus annuus* | 30 | 4-Oct-15 | United States | Utah |
| ANN_31* | PI 695690 | ANN1101-1110 | *Helianthus annuus* | 30 | 4-Oct-15 | United States | Utah |
| ANN_32 | PI 695691 | ANN1111-1120 | *Helianthus annuus* | 30 | 5-Oct-15 | United States | Utah |
| ANN_35 | PI 695695 | ANN1141-1150 | *Helianthus annuus* | 35 | 11-Oct-15 | United States | Utah |
| ANN_38* | PI 695705 | ANN1171-1180 | *Helianthus annuus* | 27 | 15-Oct-15 | United States | Kansas |
| ANN_40 | PI 695710 | ANN1191-1200 | *Helianthus annuus* | 29 | 16-Oct-15 | United States | Kansas |
| ANN_41 | PI 695715 | ANN1201-1210 | *Helianthus annuus* | 30 | 17-Oct-15 | United States | Oklahoma |
| ANN_42* | PI 695719 | ANN1211-1220 | *Helianthus annuus* | 30 | 19-Oct-15 | United States | Texas |
| ANN_44 | PI 695724 | ANN1231-1240 | *Helianthus annuus* subsp. *texanus* | 30 | 21-Oct-15 | United States | Texas |
| ANN_45* | PI 695725 | ANN1241-1250 | *Helianthus annuus* subsp. *texanus* | 31 | 21-Oct-15 | United States | Texas |
| ANN_46* | PI 695726 | ANN1251-1260 | *Helianthus annuus* | 30 | 4-Nov-15 | United States | California |
| ANN_50* | PI 695734 | ANN1291-1300 | *Helianthus annuus* | 30 | 6-Nov-15 | United States | New Mexico |
| ANN_52* | PI 695748 | ANN1311-1320 | *Helianthus annuus* | 30 | 10-Nov-15 | United States | Texas |
| ANN_53 | PI 695749 | ANN1321-1330 | *Helianthus annuus* | 30 | 10-Nov-15 | United States | Texas |
| ANN_57* | PI 695774 | ANN1361-1370 | *Helianthus annuus* subsp. *texanus* | 32 | 29-Nov-15 | United States | Texas |
| ANN_58 | PI 695778 | ANN1371-1380 | *Helianthus annuus* subsp. *texanus* | 30 | 30-Nov-15 | United States | Texas |
| ANN_59 | PI 695780 | ANN1381-1390 | *Helianthus annuus* subsp. *texanus* | 30 | 3-Dec-15 | United States | Texas |

| Population ID | USA County | Location Description | Elevation (m) | Latitude | Longitude |
|---|---|---|---|---|---|
| ANN_05 | Riverside | Coachella Valley, W of Harrison Street and NE of Old California 86 | -14 | 33.69278 | -116.18411 |
| ANN_06 | San Bernardino | Cajon Canyon, roadside on Cajon Boulevard | 738 | 34.24976 | -117.45148 |
| ANN_10* | Inyo | Lone Pine, East side, roadside on California State Route 168, W of Owens River | 1205 | 37.17346 | -118.27904 |
| ANN_16 | McKinley | Thoreau, S side, roadside frontage road (New Mexico 122) along U.S. Route 40 | 2180 | 35.40041 | -108.23557 |
| ANN_17* | Cibola | Mount Taylor, W slope, roadside on New Mexico State Route 547 | 2425 | 35.24503 | -107.68594 |
| ANN_23* | Eureka | Emmigrant Pass, E end, S of Mary's Mountain, roadside on U.S. Route 80 | 1790 | 40.66257 | -116.23876 |
| ANN_24* | Washoe | Truckee River Canyon, roadside on U.S. Route 80 | 1540 | 39.48892 | -119.99511 |
| ANN_29 | Millard | Roadside on U.S. Route 6, N of Lynndyl | 1465 | 39.55006 | -112.35661 |
| ANN_31* | Utah | Utah Lake area, City of Springville, S of Hobble Creek, near intersection of N2250W and W800N | 1380 | 40.1781 | -111.65071 |
| ANN_32 | Box Elder | Perry, near intersection of Highway 91 and Interstate 15, S of U.S. Route 91 | 1295 | 41.48524 | -112.0556 |
| ANN_35 | Uintah | Vernal area, E of Steinaker Reservoir, roadside on unnamed road N of 500 E Street and E of Utah State Route 191 | 1670 | 40.51274 | -109.51947 |
| ANN_38* | Barton | Cheyenne Bottoms, intersection of Cheyenne Bottoms Road and K-156 | 555 | 38.44118 | -98.63231 |
| ANN_40 | Barber | Gypsum Hills, Cedar Creek watershed, roadside on Gypsum Hill Road | 555 | 37.23327 | -98.66459 |
| ANN_41 | Alfalfa | Salt Plains, roadside on Oklahoma State Highway 11 | 355 | 36.80874 | -98.22242 |
| ANN_42* | Tarrant | Haslet area, roadside on Fossil Springs Drive, near intersection with West Bonds Ranch Road | 235 | 32.92224 | -97.36547 |
| ANN_44 | Frio | Moore, roadside on U.S. Route 35 Frontage Road | 215 | 29.05186 | -99.01808 |
| ANN_45* | Maverick | Comanche Creek, roadside on U.S. Route 277 | 210 | 28.63085 | -100.1189 |
| ANN_46* | Riverside | City of Banning, roadside on John Street, S of U.S. Route 10, S of railroad tracks | 690 | 33.92321 | -116.86432 |
| ANN_50* | Grant | Separ area, Roadside on U.S. Route 10 Frontage Road | 1370 | 32.17943 | -108.38541 |
| ANN_52* | Reeves | Ninemile Draw, just E of junctiom between U.S. Route 10 and U.S. Route 20, near Exit 3 on U.S. Route 20, N of Interstate 20 Service Road | 1140 | 31.13312 | -104.02012 |
| ANN_53 | Pecos | Coyanosa Draw, roadside on U.S. Route 285, SE of Pecos | 880 | 31.03955 | -103.13683 |
| ANN_57* | Nueces | Intracoastal Waterway, John F. Kennedy Memorial Causeway | 0 | 27.63854 | -97.24526 |
| ANN_58 | Bee | Skidmore, S side of town, roadside on U.S. Route 181, N of intersection with County Road 612 and S of intersection with County Road 611 | 35 | 28.24166 | -97.67443 |
| ANN_59 | Willacy | Roadside on U.S. Route 77 (Interstate 69E) Frontage Road (W), S of intersection with Farm to Market Road 1762 | 12 | 26.50251 | -97.77181 |

| Population ID | Ecology | Major Associated Woody Plant Genera | Abundance and Form | Population Size Estimate |
|---|---|---|---|---|
| ANN_05 | Fallow agricultural field, with deep soil derived from alluvium | Salsola, Datura, and Ricinus. | Abundant. Annual herb, up to 3.0 m tall. | 1,000 |
| ANN_06 | Chaparral and woodland on N-facing slope, with shallow, rocky soil derived from granite parent material | Eriogonum, Artemisia, Prunus, Juglans, and Platanus. | Abundant. Annual herb, up to 2.5 m tall. | 10,000 |
| ANN_10* | Grassland on flat, with deep soil | Ericameria, Salix, Rosa, and Salsola. | Locally abundant. Annual herb, up to 1.5 m tall. | 10,000 |
| ANN_16 | Grassland and shrubland on flat, with deep soil from sedimentary parent material | Artemisia, Grindelia, and Atriplex. | Locally abundant. Annual herb, up to 2.0 m tall. | 10,000 |
| ANN_17* | Woodland and grassland in E-W trending ravine on a W-facing slope, with rocky soil from volcanic parent material | Pinus, Juniperus, and Atriplex. | Infrequent. Annual herb, up to 2.5 m tall. | 100 |
| ANN_23* | Grassland and disturbed roadside vegetation on S-facing slope, with deep soil from conglomerate parent material | Salsola and Ericameria. | Locally abundant. Annual herb, up to 1.5 m tall. | 100 |
| ANN_24* | Grassland and disturbed roadside vegetation, with deep soil from granite parent material | Pinus, Purshia, Artemisia, Ericameria, and Cercocarpus. | Locally abundant. Annual herb, up to 1.5 m tall. | 200 |
| ANN_29 | Shrubland in roadside ditch, with deep, sandy soil | Ericameria, Artemisia, Asclepias, and Salsola. | Locally abundant. Annual herb, up to 1.5 m tall. | 1,000 |
| ANN_31* | Herbaceous vegetation in recently graded vacant lot, with very rocky soil | Salsola, Chenopodium, and Polygonum. | Abundant. Annual herb, up to 2.0 m tall. | 10,000 |
| ANN_32 | Grassland on flat, with deep soil derived from alluvium | Ericameria, Grindelia, Salsola, and Tamarix. | Abundant. Annual herb, up to 1.5 m tall. | 1,000 |
| ANN_35 | Grassland on gentle, S-facing slope, with deep soil derived from sedimentary parent material | Ericameria, Salsola, and Juniperus. | Abundant. Annual herb, up to 2.0 m tall. | 1,000 |
| ANN_38* | Wetland in slough and adjacent grassland, with deep soil derived from sediment | Solidago, Rumex, Typha, and Xanthium. | Abundant. Annual herb, up to 2.0 m tall. | 1,000 |
| ANN_40 | Grassland on gentle, W-facing slope and roadside, with deep soil derived from sedimentary parent material, including gypsum | Juniperus, Celtis, Artemisia, and Andropogon. | Infrequent. Annual herb, up to 1.5 m tall. | 50 |
| ANN_41 | Herbaceous vegetation on alluvial flat between river courses, with deep soil derived from alluvium | Polygonum, Tamarix, and Sorghum. | Abundant. Annual herb, up to 4.5 m tall. | 100,000 |
| ANN_42* | Grassland on flat, with deep soil | Salsola, Xanthium, and Sorghum. | Abundant. Annual herb, up to 2.0 m tall. | 10,000 |
| ANN_44 | Grassland and savanna on flat, with rocky soil derived from limestone | Yucca, Schinus, and Acacia. | Abundant. Annual herb, up to 2.0 m tall. | 1,000 |
| ANN_45* | Grassland on banks of creek, with deep, sandy soil | Acacia and Ulmus. | Abundant. Annual herb, up to 2.0 m tall. | 100 |
| ANN_46* | Herbaceous vegetation at roadside and train-track right-of-way, on flat, with rocky soil derived from granite alluvium | Salsola. | Abundant. Annual herb, up to 3.0 m tall. | 10,000 |
| ANN_50* | Grassland on flat and shallow basin (periodically flooded), with deep soil derived from sediment | Prosopis, Salsola, and Sorghum. | Locally abundant. Annual herb, up to 2.0 m tall. | 500 |
| ANN_52* | Weedy roadside vegetation in ditch, with deep, rocky soil derived from limestone parent material | Sorghum, Prosopis, Artemisia, Conyza, and Yucca. | Abundant. Annual herb, up to 3.0 m tall. | 1,000 |
| ANN_53 | Desert scrub and riparian vegetation in shallow, rocky soil derived from limestone parent material | Larrea, Prosopis, Xanthium, Baccharis, and Acacia. | Abundant. Annual herb, up to 2.0 m tall. | 1,000 |
| ANN_57* | Weedy, disturbed roadside and shore of waterway, with rocky soil derived from silt, beach sand, and limestone road base | Not Recorded. | Infrequent. Annual herb, up to 1.5 m tall. | 200 |
| ANN_58 | Grassland on flat and roadside, with deep soil | Mimosa and Prosopis. | Abundant. Annual herb, up to 2.0 m tall. | 10,000 |
| ANN_59 | Margin of fallow Sorghum field, with deep soil | Not Recorded. | Abundant. Annual herb, up to 1.5 m tall. | 1,000 |

**Table S4.2**: Environmental traits along with the median and range of trait values for each. Significance for accession effects (***P ≤ 0.001, **P ≤ 0.01, * P ≤ 0.05, ns = not significant) and adjusted $R^2$ from the model are also presented.

| Abbreviation | Variable | Median | Min | Max | Location Effect | Adjusted R2 |
|---|---|---|---|---|---|---|
| Latitude | Latitude (°) | 34.75 | 26.50 | 41.49 | - | - |
| Longitude | Longitude (°) | -107.96 | -120.00 | -97.25 | - | - |
| Elevation | Elevation (m) | 809 | -14 | 2425 | - | - |
| MAT | mean annual temperature (°C) | 15.15 | 7.5 | 22.8 | ** | 0.33 |
| MWMT | mean warmest month temperature (°C) | 26.35 | 19.3 | 33 | * | 0.21 |
| MCMT | mean coldest month temperature (°C) | 4.4 | -8.4 | 14.3 | ** | 0.24 |
| TD | temperature difference between MWMT and MCMT, or continentality (°C) | 21.25 | 14.7 | 30.7 | ns | 0.10 |
| MAP | mean annual precipitation (mm) | 461 | 78 | 863 | ** | 0.26 |
| MSP | May to September precipitation (mm) | 185 | 24 | 464 | *** | 0.51 |
| AHM | annual heat-moisture index (MAT+10)/(MAP/1000)) | 51.7 | 32.8 | 415.4 | ns | 0.10 |
| SHM | summer heat-moisture index ((MWMT)/(MSP/1000)) | 122.85 | 62.7 | 1404.4 | ** | 0.26 |
| DD_0 | degree-days below 0°C, chilling degree-days | 61.5 | 4 | 713 | * | 0.17 |
| DD5 | degree-days above 5°C, growing degree-days | 3960 | 1938 | 6461 | ** | 0.35 |
| DD_18 | degree-days below 18°C, heating degree-days | 1993.5 | 394 | 4105 | ** | 0.32 |
| DD18 | degree-days above 18°C, cooling degree-days | 882.5 | 145 | 2204 | ** | 0.34 |
| NFFD | the number of frost-free days | 254 | 172 | 363 | ** | 0.26 |
| bFFP | the day of the year on which FFP begins | 104.5 | 34 | 159 | ** | 0.24 |
| eFFP | the day of the year on which FFP ends | 299 | 263 | 358 | ** | 0.23 |
| FFP | frost-free period | 193.5 | 104 | 323 | ** | 0.24 |
| PAS | precipitation as snow (mm) between August in previous year and July in current year | 2.5 | 0 | 84 | * | 0.15 |
| EMT | extreme minimum temperature over 30 years | -25.1 | -39.8 | -4.4 | ** | 0.23 |
| EXT | extreme maximum temperature over 30 years | 43.15 | 35.9 | 49 | ns | -0.02 |
| Eref | Hargreaves reference evaporation (mm) | 1325 | 924 | 1801 | * | 0.13 |
| CMD | Hargreaves climatic moisture deficit (mm) | 827.5 | 443 | 1724 | ns | -0.02 |
| MAR | mean annual solar radiation (MJ $m^{-2}$ $d^{-1}$) | 17 | 16 | 19.9 | ns | -0.01 |
| RH | mean annual relative humidity (%) | 53.5 | 44 | 78 | ** | 0.34 |

**Table S4.3**: Trait loadings (percentage of trait variation explained by each trait in the associated principal component) of first three principal components (PC) for PCA presented in Figure S4.2B. The top three traits per PC are highlighted in bold. Trait abbreviations are as defined in Table 4.1.

| Trait | PC1 | PC2 | PC3 |
|---|---|---|---|
| Elevation | 4.76 | 1.39 | 6.18 |
| MAT | **6.03** | 0.02 | 0.02 |
| MWMT | 4.78 | 0.06 | 10.45 |
| MCMT | 5.62 | 0.07 | 3.47 |
| TD | 2.75 | 0.34 | **26.47** |
| MAP | 0.77 | **14.35** | 0.39 |
| MSP | 0.85 | 11.32 | 0.98 |
| AHM | 0.54 | 11.31 | 9.53 |
| SHM | 0.35 | 11.31 | 5.01 |
| DD_0 | 4.69 | 0.02 | 2.50 |
| DD5 | **5.89** | 0.09 | 0.42 |
| DD_18 | **6.02** | 0.00 | 0.35 |
| DD18 | 5.37 | 0.19 | 2.38 |
| NFFD | 5.77 | 0.01 | 1.24 |
| bFFP | 5.71 | 0.10 | 0.05 |
| eFFP | 5.62 | 0.05 | 1.54 |
| FFP | 5.71 | 0.07 | 0.43 |
| PAS | 3.80 | 0.11 | 0.05 |
| EMT | 5.55 | 0.01 | 2.82 |
| EXT | 3.83 | 0.20 | **13.22** |
| Eref | 5.27 | 1.25 | 0.04 |
| CMD | 1.28 | **13.26** | 0.08 |
| MAR | 0.03 | 11.47 | **11.35** |
| RH | 2.01 | 9.62 | 0.06 |
| CMI | 1.28 | **13.25** | 0.11 |
| DD1040 | 5.71 | 0.13 | 0.86 |

**Table S4.4**: Mean coefficients and credible intervals for 80% and 95% along with marginal and total $R^2$ values for all models presented in heatmap in Figure 4.4. Trait abbreviations follow Tables 4.1 and 4.2.

| Trait | Env Var | Mean Est | Q 2.5 | Q 97.5 | Q 10 | Q 90 | R2 all | R2 marginal | Sig 95 | Sig 80 |
|---|---|---|---|---|---|---|---|---|---|---|
| MidribMF | CMI | -0.26 | -0.51 | 0.00 | -0.42 | -0.09 | 0.20 | 0.08 | yes | yes |
| MidribMF | MAP | -0.27 | -0.52 | 0.00 | -0.43 | -0.10 | 0.20 | 0.08 | yes | yes |
| MidribMF | MAR | 0.33 | 0.09 | 0.57 | 0.18 | 0.48 | 0.20 | 0.12 | yes | yes |
| MidribMF | RH | -0.33 | -0.58 | -0.08 | -0.48 | -0.17 | 0.21 | 0.11 | yes | yes |
| RootMF | Eref | 0.29 | 0.01 | 0.56 | 0.12 | 0.47 | 0.30 | 0.10 | yes | yes |
| SV | PAS | -0.30 | -0.57 | -0.01 | -0.47 | -0.12 | 0.29 | 0.10 | yes | yes |
| VLA | SHM | -0.24 | -0.47 | -0.02 | -0.39 | -0.10 | 0.14 | 0.07 | yes | yes |
| AGBio | Eref | 0.29 | -0.06 | 0.61 | 0.07 | 0.49 | 0.40 | 0.10 | no | yes |
| AGBio | PAS | -0.27 | -0.61 | 0.11 | -0.49 | -0.04 | 0.40 | 0.09 | no | yes |
| GCW_Avg | SHM | 0.23 | -0.03 | 0.48 | 0.07 | 0.39 | 0.19 | 0.06 | no | yes |
| gsmax | PAS | -0.20 | -0.49 | 0.10 | -0.39 | -0.01 | 0.24 | 0.06 | no | yes |
| LeafBio | Eref | 0.28 | -0.06 | 0.61 | 0.07 | 0.49 | 0.40 | 0.10 | no | yes |
| LeafBio | PAS | -0.28 | -0.61 | 0.09 | -0.50 | -0.05 | 0.40 | 0.10 | no | yes |
| LeafMF | TD | 0.25 | -0.12 | 0.64 | 0.02 | 0.49 | 0.45 | 0.08 | no | yes |
| LMA | AHM | -0.26 | -0.53 | 0.02 | -0.43 | -0.08 | 0.49 | 0.08 | no | yes |
| LMA | PAS | -0.27 | -0.63 | 0.11 | -0.50 | -0.03 | 0.49 | 0.10 | no | yes |
| LMA | SHM | -0.31 | -0.63 | 0.01 | -0.52 | -0.11 | 0.50 | 0.11 | no | yes |
| MajorVLA | Elevation | 0.26 | -0.05 | 0.53 | 0.07 | 0.43 | 0.19 | 0.08 | no | yes |
| MajorVLA | EXT | -0.22 | -0.47 | 0.07 | -0.39 | -0.04 | 0.19 | 0.06 | no | yes |
| MidribDen | AHM | -0.21 | -0.45 | 0.05 | -0.37 | -0.04 | 0.26 | 0.05 | no | yes |
| MidribDen | bFFP | -0.22 | -0.54 | 0.14 | -0.43 | -0.01 | 0.25 | 0.07 | no | yes |
| MidribDen | eFFP | 0.24 | -0.12 | 0.56 | 0.02 | 0.44 | 0.25 | 0.08 | no | yes |
| MidribDen | Elevation | -0.27 | -0.57 | 0.08 | -0.46 | -0.06 | 0.25 | 0.09 | no | yes |
| MidribDen | FFP | 0.23 | -0.12 | 0.55 | 0.02 | 0.44 | 0.25 | 0.08 | no | yes |
| MidribDen | MAP | 0.25 | -0.04 | 0.53 | 0.07 | 0.43 | 0.25 | 0.08 | no | yes |
| MidribDen | MSP | 0.31 | -0.03 | 0.62 | 0.11 | 0.50 | 0.25 | 0.11 | no | yes |
| MidribDen | NFFD | 0.22 | -0.13 | 0.54 | 0.01 | 0.43 | 0.25 | 0.07 | no | yes |
| MidribDen | PAS | -0.25 | -0.54 | 0.06 | -0.43 | -0.06 | 0.25 | 0.08 | no | yes |
| MidribMF | CMD | 0.24 | -0.02 | 0.49 | 0.07 | 0.40 | 0.20 | 0.07 | no | yes |
| MidribMF | Elevation | 0.22 | -0.09 | 0.54 | 0.03 | 0.42 | 0.21 | 0.06 | no | yes |
| MidribMF | MSP | -0.29 | -0.60 | 0.01 | -0.48 | -0.10 | 0.20 | 0.09 | no | yes |
| MidribMF | PAS | -0.29 | -0.65 | 0.04 | -0.52 | -0.07 | 0.22 | 0.09 | no | yes |
| RootBio | CMI | -0.22 | -0.53 | 0.10 | -0.42 | -0.02 | 0.39 | 0.06 | no | yes |
| RootBio | DD_18 | -0.26 | -0.61 | 0.15 | -0.49 | -0.02 | 0.39 | 0.10 | no | yes |
| RootBio | Eref | 0.32 | -0.02 | 0.63 | 0.11 | 0.52 | 0.39 | 0.12 | no | yes |
| RootBio | PAS | -0.27 | -0.61 | 0.10 | -0.49 | -0.04 | 0.39 | 0.10 | no | yes |
| RootMF | CMI | -0.18 | -0.45 | 0.09 | -0.35 | -0.01 | 0.30 | 0.05 | no | yes |
| RootMF | DD_0 | -0.28 | -0.56 | 0.03 | -0.46 | -0.10 | 0.30 | 0.09 | no | yes |
| RootMF | DD_18 | -0.29 | -0.58 | 0.03 | -0.48 | -0.09 | 0.30 | 0.10 | no | yes |

| | | | | | | | | | | |
|---|---|---|---|---|---|---|---|---|---|---|
| RootMF | DD5 | 0.24 | -0.12 | 0.54 | 0.03 | 0.43 | 0.30 | 0.08 | no | yes |
| RootMF | eFFP | 0.22 | -0.13 | 0.55 | 0.01 | 0.43 | 0.30 | 0.07 | no | yes |
| RootMF | Elevation | -0.27 | -0.57 | 0.08 | -0.47 | -0.07 | 0.30 | 0.09 | no | yes |
| RootMF | EXT | 0.28 | -0.03 | 0.55 | 0.09 | 0.46 | 0.30 | 0.09 | no | yes |
| RootMF | MAT | 0.26 | -0.08 | 0.56 | 0.05 | 0.46 | 0.30 | 0.09 | no | yes |
| RootMF | MCMT | 0.23 | -0.11 | 0.56 | 0.03 | 0.44 | 0.30 | 0.08 | no | yes |
| RootMF | MWMT | 0.24 | -0.12 | 0.53 | 0.03 | 0.43 | 0.30 | 0.08 | no | yes |
| RootMF | NFFD | 0.23 | -0.12 | 0.56 | 0.02 | 0.43 | 0.30 | 0.07 | no | yes |
| SD_Ratio | AHM | 0.16 | -0.08 | 0.41 | 0.01 | 0.32 | 0.15 | 0.04 | no | yes |
| SD_Ratio | EXT | 0.23 | -0.04 | 0.51 | 0.05 | 0.40 | 0.16 | 0.06 | no | yes |
| SD_Ratio | SHM | 0.21 | -0.05 | 0.48 | 0.04 | 0.38 | 0.16 | 0.05 | no | yes |
| SD_Ratio | TD | 0.20 | -0.07 | 0.48 | 0.03 | 0.37 | 0.16 | 0.05 | no | yes |
| SD_Sum | PAS | -0.23 | -0.50 | 0.06 | -0.41 | -0.04 | 0.21 | 0.07 | no | yes |
| SD_Sum | SHM | -0.18 | -0.46 | 0.10 | -0.36 | -0.01 | 0.22 | 0.05 | no | yes |
| SL_Avg | Eref | -0.17 | -0.43 | 0.08 | -0.34 | -0.01 | 0.14 | 0.04 | no | yes |
| SL_Avg | PAS | 0.18 | -0.08 | 0.45 | 0.02 | 0.35 | 0.13 | 0.05 | no | yes |
| StemBio | Eref | 0.26 | -0.09 | 0.60 | 0.04 | 0.48 | 0.41 | 0.09 | no | yes |
| StemBio | PAS | -0.24 | -0.58 | 0.13 | -0.47 | -0.01 | 0.41 | 0.08 | no | yes |
| StemBio | TD | -0.23 | -0.58 | 0.13 | -0.46 | 0.00 | 0.41 | 0.08 | no | yes |
| Succulence | AHM | -0.21 | -0.46 | 0.04 | -0.37 | -0.05 | 0.21 | 0.06 | no | yes |
| Succulence | CMD | -0.22 | -0.48 | 0.03 | -0.39 | -0.06 | 0.21 | 0.06 | no | yes |
| Succulence | MAP | 0.24 | -0.05 | 0.54 | 0.06 | 0.43 | 0.22 | 0.07 | no | yes |
| Succulence | MAR | -0.18 | -0.47 | 0.10 | -0.37 | 0.00 | 0.21 | 0.05 | no | yes |
| Succulence | SHM | -0.25 | -0.53 | 0.03 | -0.43 | -0.07 | 0.21 | 0.07 | no | yes |
| Succulence | TD | 0.21 | -0.10 | 0.51 | 0.02 | 0.40 | 0.21 | 0.06 | no | yes |
| TotalBio | Eref | 0.30 | -0.06 | 0.63 | 0.08 | 0.51 | 0.42 | 0.11 | no | yes |
| TotalBio | PAS | -0.28 | -0.61 | 0.09 | -0.49 | -0.05 | 0.42 | 0.10 | no | yes |
| VLA | AHM | -0.16 | -0.38 | 0.06 | -0.30 | -0.01 | 0.13 | 0.04 | no | yes |
| AGBio | AHM | -0.11 | -0.43 | 0.21 | -0.32 | 0.09 | 0.40 | 0.03 | no | no |
| AGBio | bFFP | -0.12 | -0.52 | 0.38 | -0.39 | 0.17 | 0.40 | 0.06 | no | no |
| AGBio | CMD | 0.15 | -0.19 | 0.48 | -0.06 | 0.36 | 0.40 | 0.04 | no | no |
| AGBio | CMI | -0.20 | -0.52 | 0.13 | -0.40 | 0.01 | 0.40 | 0.06 | no | no |
| AGBio | DD_0 | -0.07 | -0.47 | 0.38 | -0.33 | 0.21 | 0.40 | 0.04 | no | no |
| AGBio | DD_18 | -0.20 | -0.56 | 0.25 | -0.44 | 0.06 | 0.40 | 0.07 | no | no |
| AGBio | DD1040 | 0.17 | -0.33 | 0.55 | -0.12 | 0.42 | 0.40 | 0.07 | no | no |
| AGBio | DD18 | 0.15 | -0.33 | 0.53 | -0.14 | 0.40 | 0.40 | 0.06 | no | no |
| AGBio | DD5 | 0.19 | -0.28 | 0.56 | -0.08 | 0.44 | 0.40 | 0.07 | no | no |
| AGBio | eFFP | 0.15 | -0.33 | 0.54 | -0.12 | 0.41 | 0.40 | 0.06 | no | no |
| AGBio | Elevation | -0.05 | -0.48 | 0.50 | -0.34 | 0.27 | 0.40 | 0.05 | no | no |
| AGBio | EMT | 0.09 | -0.41 | 0.49 | -0.20 | 0.36 | 0.40 | 0.05 | no | no |

| | | | | | | | | | | |
|---|---|---|---|---|---|---|---|---|---|---|
| AGBio | EXT | 0.11 | -0.30 | 0.48 | -0.14 | 0.35 | 0.40 | 0.04 | no | no |
| AGBio | FFP | 0.14 | -0.36 | 0.53 | -0.15 | 0.40 | 0.40 | 0.06 | no | no |
| AGBio | MAP | -0.04 | -0.44 | 0.34 | -0.29 | 0.20 | 0.40 | 0.03 | no | no |
| AGBio | MAR | 0.11 | -0.24 | 0.46 | -0.11 | 0.33 | 0.41 | 0.03 | no | no |
| AGBio | MAT | 0.18 | -0.28 | 0.56 | -0.09 | 0.43 | 0.40 | 0.07 | no | no |
| AGBio | MCMT | 0.18 | -0.27 | 0.56 | -0.08 | 0.43 | 0.40 | 0.07 | no | no |
| AGBio | MSP | 0.11 | -0.40 | 0.52 | -0.20 | 0.38 | 0.40 | 0.05 | no | no |
| AGBio | MWMT | 0.05 | -0.43 | 0.45 | -0.25 | 0.32 | 0.40 | 0.04 | no | no |
| AGBio | NFFD | 0.18 | -0.26 | 0.56 | -0.08 | 0.43 | 0.40 | 0.07 | no | no |
| AGBio | RH | -0.18 | -0.60 | 0.24 | -0.45 | 0.09 | 0.40 | 0.06 | no | no |
| AGBio | SHM | -0.15 | -0.51 | 0.21 | -0.38 | 0.08 | 0.40 | 0.05 | no | no |
| AGBio | TD | -0.17 | -0.52 | 0.20 | -0.39 | 0.06 | 0.40 | 0.05 | no | no |
| GCW_Avg | AHM | 0.09 | -0.17 | 0.34 | -0.08 | 0.25 | 0.18 | 0.02 | no | no |
| GCW_Avg | bFFP | 0.00 | -0.36 | 0.33 | -0.22 | 0.21 | 0.19 | 0.03 | no | no |
| GCW_Avg | CMD | -0.07 | -0.34 | 0.20 | -0.24 | 0.10 | 0.19 | 0.02 | no | no |
| GCW_Avg | CMI | 0.09 | -0.18 | 0.37 | -0.08 | 0.27 | 0.19 | 0.02 | no | no |
| GCW_Avg | DD_0 | -0.02 | -0.35 | 0.28 | -0.22 | 0.18 | 0.19 | 0.02 | no | no |
| GCW_Avg | DD_18 | 0.03 | -0.32 | 0.35 | -0.19 | 0.23 | 0.19 | 0.02 | no | no |
| GCW_Avg | DD1040 | -0.04 | -0.36 | 0.31 | -0.24 | 0.17 | 0.19 | 0.03 | no | no |
| GCW_Avg | DD18 | -0.05 | -0.35 | 0.28 | -0.24 | 0.16 | 0.19 | 0.02 | no | no |
| GCW_Avg | DD5 | -0.04 | -0.35 | 0.32 | -0.24 | 0.18 | 0.19 | 0.03 | no | no |
| GCW_Avg | eFFP | 0.01 | -0.32 | 0.37 | -0.20 | 0.23 | 0.19 | 0.02 | no | no |
| GCW_Avg | Elevation | 0.00 | -0.38 | 0.32 | -0.23 | 0.21 | 0.19 | 0.03 | no | no |
| GCW_Avg | EMT | 0.04 | -0.29 | 0.41 | -0.17 | 0.26 | 0.19 | 0.03 | no | no |
| GCW_Avg | Eref | -0.10 | -0.38 | 0.18 | -0.28 | 0.07 | 0.19 | 0.03 | no | no |
| GCW_Avg | EXT | -0.08 | -0.37 | 0.21 | -0.26 | 0.10 | 0.19 | 0.02 | no | no |
| GCW_Avg | FFP | 0.00 | -0.33 | 0.37 | -0.21 | 0.23 | 0.19 | 0.03 | no | no |
| GCW_Avg | MAP | 0.09 | -0.21 | 0.41 | -0.11 | 0.29 | 0.19 | 0.03 | no | no |
| GCW_Avg | MAR | -0.03 | -0.32 | 0.25 | -0.22 | 0.15 | 0.19 | 0.02 | no | no |
| GCW_Avg | MAT | -0.03 | -0.35 | 0.31 | -0.24 | 0.17 | 0.19 | 0.03 | no | no |
| GCW_Avg | MCMT | 0.03 | -0.29 | 0.38 | -0.17 | 0.24 | 0.19 | 0.02 | no | no |
| GCW_Avg | MSP | -0.11 | -0.42 | 0.29 | -0.32 | 0.12 | 0.18 | 0.04 | no | no |
| GCW_Avg | MWMT | -0.09 | -0.38 | 0.22 | -0.28 | 0.11 | 0.19 | 0.03 | no | no |
| GCW_Avg | NFFD | -0.01 | -0.34 | 0.34 | -0.22 | 0.20 | 0.19 | 0.02 | no | no |
| GCW_Avg | PAS | 0.15 | -0.14 | 0.44 | -0.03 | 0.34 | 0.19 | 0.04 | no | no |
| GCW_Avg | RH | 0.03 | -0.26 | 0.33 | -0.16 | 0.22 | 0.19 | 0.02 | no | no |
| GCW_Avg | TD | -0.09 | -0.40 | 0.20 | -0.28 | 0.10 | 0.19 | 0.03 | no | no |
| gsmax | AHM | -0.13 | -0.37 | 0.11 | -0.28 | 0.03 | 0.24 | 0.03 | no | no |
| gsmax | bFFP | 0.06 | -0.30 | 0.46 | -0.17 | 0.30 | 0.25 | 0.03 | no | no |
| gsmax | CMD | 0.02 | -0.25 | 0.28 | -0.15 | 0.18 | 0.24 | 0.02 | no | no |

| | | | | | | | | | | |
|---|---|---|---|---|---|---|---|---|---|---|
| gsmax | CMI | -0.09 | -0.35 | 0.17 | -0.26 | 0.08 | 0.24 | 0.02 | no | no |
| gsmax | DD_0 | -0.03 | -0.34 | 0.31 | -0.24 | 0.18 | 0.24 | 0.03 | no | no |
| gsmax | DD_18 | -0.03 | -0.37 | 0.34 | -0.25 | 0.20 | 0.24 | 0.03 | no | no |
| gsmax | DD1040 | -0.05 | -0.44 | 0.30 | -0.29 | 0.18 | 0.25 | 0.03 | no | no |
| gsmax | DD18 | -0.07 | -0.44 | 0.26 | -0.31 | 0.15 | 0.25 | 0.03 | no | no |
| gsmax | DD5 | -0.03 | -0.41 | 0.33 | -0.26 | 0.21 | 0.24 | 0.03 | no | no |
| gsmax | eFFP | -0.02 | -0.42 | 0.33 | -0.26 | 0.21 | 0.24 | 0.03 | no | no |
| gsmax | Elevation | 0.06 | -0.30 | 0.46 | -0.18 | 0.31 | 0.25 | 0.03 | no | no |
| gsmax | EMT | -0.05 | -0.44 | 0.30 | -0.28 | 0.18 | 0.24 | 0.03 | no | no |
| gsmax | Eref | 0.08 | -0.22 | 0.37 | -0.11 | 0.26 | 0.24 | 0.03 | no | no |
| gsmax | EXT | 0.03 | -0.29 | 0.33 | -0.17 | 0.23 | 0.24 | 0.02 | no | no |
| gsmax | FFP | -0.05 | -0.45 | 0.31 | -0.30 | 0.18 | 0.24 | 0.03 | no | no |
| gsmax | MAP | -0.03 | -0.33 | 0.27 | -0.22 | 0.16 | 0.24 | 0.02 | no | no |
| gsmax | MAR | 0.09 | -0.18 | 0.37 | -0.08 | 0.27 | 0.27 | 0.03 | no | no |
| gsmax | MAT | -0.01 | -0.40 | 0.34 | -0.25 | 0.22 | 0.24 | 0.03 | no | no |
| gsmax | MCMT | 0.00 | -0.37 | 0.34 | -0.23 | 0.22 | 0.24 | 0.03 | no | no |
| gsmax | MSP | 0.10 | -0.30 | 0.45 | -0.14 | 0.34 | 0.24 | 0.04 | no | no |
| gsmax | MWMT | -0.04 | -0.39 | 0.29 | -0.26 | 0.18 | 0.24 | 0.03 | no | no |
| gsmax | NFFD | 0.00 | -0.37 | 0.35 | -0.23 | 0.22 | 0.24 | 0.03 | no | no |
| gsmax | RH | -0.10 | -0.41 | 0.19 | -0.30 | 0.09 | 0.25 | 0.03 | no | no |
| gsmax | SHM | -0.16 | -0.43 | 0.11 | -0.34 | 0.02 | 0.25 | 0.04 | no | no |
| gsmax | TD | -0.03 | -0.33 | 0.28 | -0.22 | 0.16 | 0.24 | 0.02 | no | no |
| LeafArea | AHM | -0.06 | -0.37 | 0.26 | -0.26 | 0.14 | 0.33 | 0.03 | no | no |
| LeafArea | bFFP | 0.02 | -0.36 | 0.44 | -0.22 | 0.27 | 0.33 | 0.03 | no | no |
| LeafArea | CMD | 0.06 | -0.26 | 0.38 | -0.14 | 0.27 | 0.33 | 0.03 | no | no |
| LeafArea | CMI | -0.08 | -0.40 | 0.24 | -0.28 | 0.12 | 0.32 | 0.03 | no | no |
| LeafArea | DD_0 | 0.11 | -0.26 | 0.53 | -0.14 | 0.37 | 0.32 | 0.04 | no | no |
| LeafArea | DD_18 | 0.03 | -0.34 | 0.45 | -0.20 | 0.28 | 0.32 | 0.03 | no | no |
| LeafArea | DD1040 | -0.06 | -0.47 | 0.32 | -0.31 | 0.18 | 0.32 | 0.03 | no | no |
| LeafArea | DD18 | -0.07 | -0.45 | 0.29 | -0.31 | 0.16 | 0.33 | 0.03 | no | no |
| LeafArea | DD5 | -0.04 | -0.45 | 0.32 | -0.29 | 0.19 | 0.32 | 0.03 | no | no |
| LeafArea | eFFP | -0.02 | -0.46 | 0.36 | -0.27 | 0.23 | 0.32 | 0.03 | no | no |
| LeafArea | Elevation | -0.04 | -0.42 | 0.35 | -0.28 | 0.20 | 0.33 | 0.03 | no | no |
| LeafArea | EMT | -0.02 | -0.46 | 0.36 | -0.28 | 0.22 | 0.32 | 0.03 | no | no |
| LeafArea | Eref | 0.05 | -0.29 | 0.39 | -0.16 | 0.27 | 0.32 | 0.03 | no | no |
| LeafArea | EXT | 0.12 | -0.22 | 0.45 | -0.10 | 0.33 | 0.32 | 0.04 | no | no |
| LeafArea | FFP | -0.02 | -0.45 | 0.36 | -0.27 | 0.22 | 0.32 | 0.03 | no | no |
| LeafArea | MAP | 0.01 | -0.32 | 0.34 | -0.20 | 0.22 | 0.33 | 0.02 | no | no |
| LeafArea | MAR | -0.07 | -0.41 | 0.26 | -0.28 | 0.14 | 0.31 | 0.03 | no | no |
| LeafArea | MAT | -0.05 | -0.47 | 0.32 | -0.31 | 0.19 | 0.33 | 0.03 | no | no |

| | | | | | | | | | | |
|---|---|---|---|---|---|---|---|---|---|---|
| LeafArea | MCMT | -0.03 | -0.47 | 0.34 | -0.29 | 0.21 | 0.32 | 0.03 | no | no |
| LeafArea | MSP | -0.16 | -0.58 | 0.23 | -0.41 | 0.08 | 0.32 | 0.05 | no | no |
| LeafArea | MWMT | -0.05 | -0.41 | 0.31 | -0.27 | 0.17 | 0.32 | 0.03 | no | no |
| LeafArea | NFFD | 0.01 | -0.38 | 0.39 | -0.22 | 0.25 | 0.32 | 0.03 | no | no |
| LeafArea | PAS | 0.13 | -0.23 | 0.51 | -0.10 | 0.37 | 0.32 | 0.04 | no | no |
| LeafArea | RH | -0.11 | -0.44 | 0.22 | -0.32 | 0.10 | 0.32 | 0.03 | no | no |
| LeafArea | SHM | -0.08 | -0.45 | 0.27 | -0.31 | 0.14 | 0.32 | 0.03 | no | no |
| LeafArea | TD | -0.01 | -0.35 | 0.35 | -0.23 | 0.21 | 0.32 | 0.03 | no | no |
| LeafBio | AHM | -0.11 | -0.43 | 0.22 | -0.32 | 0.10 | 0.40 | 0.03 | no | no |
| LeafBio | bFFP | -0.14 | -0.53 | 0.32 | -0.40 | 0.13 | 0.40 | 0.06 | no | no |
| LeafBio | CMD | 0.14 | -0.18 | 0.46 | -0.07 | 0.35 | 0.40 | 0.04 | no | no |
| LeafBio | CMI | -0.20 | -0.52 | 0.12 | -0.41 | 0.01 | 0.40 | 0.06 | no | no |
| LeafBio | DD_0 | -0.09 | -0.48 | 0.35 | -0.35 | 0.18 | 0.40 | 0.05 | no | no |
| LeafBio | DD_18 | -0.21 | -0.58 | 0.23 | -0.45 | 0.05 | 0.40 | 0.08 | no | no |
| LeafBio | DD1040 | 0.15 | -0.34 | 0.53 | -0.13 | 0.41 | 0.40 | 0.06 | no | no |
| LeafBio | DD18 | 0.12 | -0.36 | 0.51 | -0.17 | 0.38 | 0.40 | 0.05 | no | no |
| LeafBio | DD5 | 0.18 | -0.29 | 0.56 | -0.09 | 0.43 | 0.40 | 0.07 | no | no |
| LeafBio | eFFP | 0.15 | -0.31 | 0.53 | -0.12 | 0.40 | 0.40 | 0.06 | no | no |
| LeafBio | Elevation | -0.11 | -0.52 | 0.39 | -0.38 | 0.19 | 0.40 | 0.06 | no | no |
| LeafBio | EMT | 0.09 | -0.39 | 0.49 | -0.20 | 0.35 | 0.40 | 0.05 | no | no |
| LeafBio | EXT | 0.19 | -0.19 | 0.55 | -0.04 | 0.42 | 0.40 | 0.06 | no | no |
| LeafBio | FFP | 0.15 | -0.34 | 0.54 | -0.12 | 0.40 | 0.40 | 0.06 | no | no |
| LeafBio | MAP | -0.02 | -0.41 | 0.36 | -0.27 | 0.22 | 0.40 | 0.03 | no | no |
| LeafBio | MAR | 0.08 | -0.28 | 0.43 | -0.15 | 0.30 | 0.41 | 0.03 | no | no |
| LeafBio | MAT | 0.18 | -0.28 | 0.56 | -0.09 | 0.43 | 0.40 | 0.07 | no | no |
| LeafBio | MCMT | 0.16 | -0.30 | 0.55 | -0.11 | 0.41 | 0.40 | 0.06 | no | no |
| LeafBio | MSP | 0.08 | -0.43 | 0.50 | -0.23 | 0.36 | 0.40 | 0.05 | no | no |
| LeafBio | MWMT | 0.12 | -0.32 | 0.50 | -0.15 | 0.37 | 0.40 | 0.05 | no | no |
| LeafBio | NFFD | 0.18 | -0.25 | 0.56 | -0.08 | 0.43 | 0.40 | 0.07 | no | no |
| LeafBio | RH | -0.16 | -0.58 | 0.23 | -0.43 | 0.10 | 0.40 | 0.05 | no | no |
| LeafBio | SHM | -0.15 | -0.51 | 0.20 | -0.38 | 0.08 | 0.40 | 0.05 | no | no |
| LeafBio | TD | -0.11 | -0.48 | 0.26 | -0.34 | 0.12 | 0.40 | 0.04 | no | no |
| LeafMF | AHM | 0.04 | -0.30 | 0.39 | -0.18 | 0.27 | 0.45 | 0.03 | no | no |
| LeafMF | bFFP | 0.04 | -0.50 | 0.46 | -0.27 | 0.32 | 0.45 | 0.04 | no | no |
| LeafMF | CMD | -0.07 | -0.42 | 0.28 | -0.30 | 0.15 | 0.45 | 0.03 | no | no |
| LeafMF | CMI | 0.09 | -0.27 | 0.46 | -0.14 | 0.33 | 0.45 | 0.04 | no | no |
| LeafMF | DD_0 | 0.06 | -0.35 | 0.45 | -0.20 | 0.31 | 0.45 | 0.04 | no | no |
| LeafMF | DD_18 | 0.14 | -0.31 | 0.55 | -0.12 | 0.40 | 0.45 | 0.05 | no | no |
| LeafMF | DD1040 | -0.19 | -0.57 | 0.24 | -0.44 | 0.07 | 0.45 | 0.06 | no | no |
| LeafMF | DD18 | -0.19 | -0.56 | 0.23 | -0.43 | 0.07 | 0.45 | 0.06 | no | no |

| | | | | | | | | | | |
|---|---|---|---|---|---|---|---|---|---|---|
| LeafMF | DD5 | -0.17 | -0.57 | 0.27 | -0.43 | 0.09 | 0.45 | 0.06 | no | no |
| LeafMF | eFFP | -0.11 | -0.53 | 0.35 | -0.37 | 0.17 | 0.45 | 0.05 | no | no |
| LeafMF | Elevation | 0.00 | -0.54 | 0.44 | -0.32 | 0.29 | 0.45 | 0.04 | no | no |
| LeafMF | EMT | -0.11 | -0.53 | 0.35 | -0.38 | 0.16 | 0.45 | 0.05 | no | no |
| LeafMF | Eref | -0.17 | -0.54 | 0.20 | -0.40 | 0.07 | 0.45 | 0.05 | no | no |
| LeafMF | EXT | 0.11 | -0.28 | 0.52 | -0.14 | 0.37 | 0.45 | 0.04 | no | no |
| LeafMF | FFP | -0.07 | -0.50 | 0.42 | -0.35 | 0.22 | 0.45 | 0.05 | no | no |
| LeafMF | MAP | 0.02 | -0.36 | 0.43 | -0.23 | 0.28 | 0.45 | 0.03 | no | no |
| LeafMF | MAR | -0.09 | -0.51 | 0.30 | -0.36 | 0.16 | 0.45 | 0.04 | no | no |
| LeafMF | MAT | -0.16 | -0.56 | 0.28 | -0.42 | 0.10 | 0.45 | 0.06 | no | no |
| LeafMF | MCMT | -0.19 | -0.59 | 0.23 | -0.44 | 0.07 | 0.45 | 0.06 | no | no |
| LeafMF | MSP | -0.21 | -0.61 | 0.24 | -0.47 | 0.06 | 0.45 | 0.07 | no | no |
| LeafMF | MWMT | 0.03 | -0.38 | 0.49 | -0.24 | 0.31 | 0.45 | 0.04 | no | no |
| LeafMF | NFFD | -0.09 | -0.50 | 0.37 | -0.35 | 0.17 | 0.45 | 0.04 | no | no |
| LeafMF | PAS | 0.15 | -0.24 | 0.54 | -0.09 | 0.40 | 0.45 | 0.05 | no | no |
| LeafMF | RH | 0.03 | -0.36 | 0.47 | -0.24 | 0.30 | 0.45 | 0.04 | no | no |
| LeafMF | SHM | 0.09 | -0.29 | 0.47 | -0.15 | 0.33 | 0.45 | 0.04 | no | no |
| LMA | bFFP | 0.00 | -0.46 | 0.51 | -0.31 | 0.31 | 0.49 | 0.05 | no | no |
| LMA | CMD | -0.08 | -0.40 | 0.23 | -0.28 | 0.12 | 0.49 | 0.03 | no | no |
| LMA | CMI | 0.00 | -0.32 | 0.32 | -0.20 | 0.21 | 0.49 | 0.02 | no | no |
| LMA | DD_0 | 0.06 | -0.34 | 0.48 | -0.20 | 0.32 | 0.49 | 0.04 | no | no |
| LMA | DD_18 | -0.02 | -0.47 | 0.47 | -0.32 | 0.29 | 0.49 | 0.04 | no | no |
| LMA | DD1040 | -0.11 | -0.59 | 0.36 | -0.42 | 0.20 | 0.49 | 0.05 | no | no |
| LMA | DD18 | -0.15 | -0.61 | 0.31 | -0.45 | 0.15 | 0.49 | 0.05 | no | no |
| LMA | DD5 | -0.05 | -0.54 | 0.42 | -0.36 | 0.26 | 0.49 | 0.05 | no | no |
| LMA | eFFP | 0.04 | -0.45 | 0.51 | -0.26 | 0.34 | 0.49 | 0.05 | no | no |
| LMA | Elevation | -0.03 | -0.50 | 0.50 | -0.35 | 0.31 | 0.49 | 0.05 | no | no |
| LMA | EMT | -0.10 | -0.59 | 0.37 | -0.40 | 0.21 | 0.49 | 0.05 | no | no |
| LMA | Eref | 0.07 | -0.31 | 0.45 | -0.18 | 0.31 | 0.49 | 0.04 | no | no |
| LMA | EXT | 0.10 | -0.31 | 0.49 | -0.16 | 0.35 | 0.49 | 0.05 | no | no |
| LMA | FFP | 0.02 | -0.49 | 0.49 | -0.29 | 0.32 | 0.49 | 0.05 | no | no |
| LMA | MAP | 0.16 | -0.19 | 0.52 | -0.07 | 0.39 | 0.49 | 0.05 | no | no |
| LMA | MAR | -0.03 | -0.37 | 0.32 | -0.24 | 0.19 | 0.50 | 0.03 | no | no |
| LMA | MAT | -0.05 | -0.55 | 0.43 | -0.37 | 0.26 | 0.49 | 0.05 | no | no |
| LMA | MCMT | -0.07 | -0.55 | 0.38 | -0.36 | 0.22 | 0.49 | 0.04 | no | no |
| LMA | MSP | 0.27 | -0.23 | 0.71 | -0.03 | 0.56 | 0.49 | 0.11 | no | no |
| LMA | MWMT | -0.03 | -0.49 | 0.44 | -0.33 | 0.27 | 0.49 | 0.04 | no | no |
| LMA | NFFD | 0.01 | -0.47 | 0.47 | -0.29 | 0.31 | 0.49 | 0.04 | no | no |
| LMA | RH | -0.11 | -0.47 | 0.25 | -0.34 | 0.12 | 0.49 | 0.04 | no | no |
| LMA | TD | 0.03 | -0.37 | 0.42 | -0.22 | 0.28 | 0.49 | 0.03 | no | no |

| | | | | | | | | | | |
|---|---|---|---|---|---|---|---|---|---|---|
| MajorVLA | AHM | -0.03 | -0.28 | 0.21 | -0.19 | 0.13 | 0.20 | 0.01 | no | no |
| MajorVLA | bFFP | 0.16 | -0.20 | 0.46 | -0.04 | 0.36 | 0.19 | 0.05 | no | no |
| MajorVLA | CMD | -0.08 | -0.33 | 0.18 | -0.24 | 0.08 | 0.20 | 0.02 | no | no |
| MajorVLA | CMI | 0.09 | -0.17 | 0.34 | -0.07 | 0.26 | 0.20 | 0.02 | no | no |
| MajorVLA | DD_0 | -0.02 | -0.38 | 0.30 | -0.25 | 0.20 | 0.20 | 0.03 | no | no |
| MajorVLA | DD_18 | 0.15 | -0.20 | 0.44 | -0.06 | 0.34 | 0.19 | 0.05 | no | no |
| MajorVLA | DD1040 | -0.18 | -0.47 | 0.15 | -0.37 | 0.02 | 0.19 | 0.05 | no | no |
| MajorVLA | DD18 | -0.18 | -0.46 | 0.15 | -0.36 | 0.02 | 0.19 | 0.05 | no | no |
| MajorVLA | DD5 | -0.19 | -0.48 | 0.13 | -0.38 | 0.01 | 0.19 | 0.06 | no | no |
| MajorVLA | eFFP | -0.14 | -0.44 | 0.22 | -0.34 | 0.07 | 0.19 | 0.04 | no | no |
| MajorVLA | EMT | -0.11 | -0.42 | 0.26 | -0.32 | 0.11 | 0.19 | 0.04 | no | no |
| MajorVLA | Eref | -0.17 | -0.43 | 0.12 | -0.34 | 0.01 | 0.19 | 0.04 | no | no |
| MajorVLA | FFP | -0.16 | -0.46 | 0.19 | -0.35 | 0.05 | 0.19 | 0.05 | no | no |
| MajorVLA | MAP | -0.02 | -0.30 | 0.29 | -0.21 | 0.18 | 0.20 | 0.02 | no | no |
| MajorVLA | MAR | 0.06 | -0.21 | 0.34 | -0.11 | 0.24 | 0.20 | 0.02 | no | no |
| MajorVLA | MAT | -0.17 | -0.45 | 0.18 | -0.36 | 0.04 | 0.19 | 0.05 | no | no |
| MajorVLA | MCMT | -0.11 | -0.41 | 0.25 | -0.31 | 0.11 | 0.19 | 0.04 | no | no |
| MajorVLA | MSP | -0.01 | -0.36 | 0.39 | -0.23 | 0.23 | 0.20 | 0.03 | no | no |
| MajorVLA | MWMT | -0.18 | -0.44 | 0.13 | -0.35 | 0.01 | 0.19 | 0.05 | no | no |
| MajorVLA | NFFD | -0.15 | -0.44 | 0.19 | -0.34 | 0.06 | 0.19 | 0.04 | no | no |
| MajorVLA | PAS | 0.08 | -0.24 | 0.38 | -0.12 | 0.27 | 0.19 | 0.03 | no | no |
| MajorVLA | RH | 0.02 | -0.27 | 0.32 | -0.17 | 0.21 | 0.20 | 0.02 | no | no |
| MajorVLA | SHM | 0.02 | -0.26 | 0.29 | -0.16 | 0.19 | 0.19 | 0.02 | no | no |
| MajorVLA | TD | 0.00 | -0.32 | 0.29 | -0.21 | 0.19 | 0.20 | 0.02 | no | no |
| MidribDen | CMD | -0.12 | -0.39 | 0.15 | -0.29 | 0.05 | 0.26 | 0.03 | no | no |
| MidribDen | CMI | 0.06 | -0.22 | 0.34 | -0.11 | 0.24 | 0.25 | 0.02 | no | no |
| MidribDen | DD_0 | -0.06 | -0.39 | 0.31 | -0.28 | 0.17 | 0.25 | 0.03 | no | no |
| MidribDen | DD_18 | -0.20 | -0.52 | 0.17 | -0.41 | 0.02 | 0.25 | 0.06 | no | no |
| MidribDen | DD1040 | 0.19 | -0.21 | 0.51 | -0.05 | 0.40 | 0.25 | 0.06 | no | no |
| MidribDen | DD18 | 0.15 | -0.25 | 0.48 | -0.10 | 0.38 | 0.25 | 0.05 | no | no |
| MidribDen | DD5 | 0.21 | -0.18 | 0.53 | -0.02 | 0.42 | 0.25 | 0.07 | no | no |
| MidribDen | EMT | 0.19 | -0.17 | 0.51 | -0.03 | 0.40 | 0.25 | 0.06 | no | no |
| MidribDen | Eref | 0.07 | -0.26 | 0.39 | -0.13 | 0.28 | 0.25 | 0.03 | no | no |
| MidribDen | EXT | 0.10 | -0.24 | 0.41 | -0.12 | 0.30 | 0.25 | 0.03 | no | no |
| MidribDen | MAR | -0.18 | -0.46 | 0.10 | -0.36 | 0.00 | 0.26 | 0.05 | no | no |
| MidribDen | MAT | 0.19 | -0.21 | 0.51 | -0.04 | 0.40 | 0.25 | 0.06 | no | no |
| MidribDen | MCMT | 0.15 | -0.22 | 0.48 | -0.07 | 0.37 | 0.25 | 0.05 | no | no |
| MidribDen | MWMT | 0.12 | -0.27 | 0.46 | -0.12 | 0.34 | 0.25 | 0.04 | no | no |
| MidribDen | RH | 0.19 | -0.13 | 0.47 | -0.01 | 0.38 | 0.25 | 0.06 | no | no |
| MidribDen | SHM | -0.18 | -0.47 | 0.10 | -0.37 | 0.00 | 0.26 | 0.05 | no | no |

| | | | | | | | | | | |
|---|---|---|---|---|---|---|---|---|---|---|
| MidribDen | TD | -0.11 | -0.42 | 0.21 | -0.31 | 0.09 | 0.25 | 0.03 | no | no |
| MidribMF | AHM | 0.10 | -0.18 | 0.37 | -0.08 | 0.27 | 0.20 | 0.03 | no | no |
| MidribMF | bFFP | 0.07 | -0.28 | 0.41 | -0.14 | 0.28 | 0.20 | 0.03 | no | no |
| MidribMF | DD_0 | -0.12 | -0.50 | 0.21 | -0.35 | 0.10 | 0.20 | 0.04 | no | no |
| MidribMF | DD_18 | -0.01 | -0.40 | 0.33 | -0.25 | 0.21 | 0.20 | 0.03 | no | no |
| MidribMF | DD1040 | -0.12 | -0.43 | 0.21 | -0.32 | 0.08 | 0.20 | 0.04 | no | no |
| MidribMF | DD18 | -0.14 | -0.45 | 0.19 | -0.34 | 0.06 | 0.20 | 0.04 | no | no |
| MidribMF | DD5 | -0.09 | -0.43 | 0.25 | -0.30 | 0.12 | 0.20 | 0.03 | no | no |
| MidribMF | eFFP | -0.05 | -0.39 | 0.32 | -0.27 | 0.17 | 0.20 | 0.03 | no | no |
| MidribMF | EMT | -0.07 | -0.41 | 0.28 | -0.28 | 0.14 | 0.20 | 0.03 | no | no |
| MidribMF | Eref | 0.16 | -0.15 | 0.49 | -0.04 | 0.37 | 0.20 | 0.04 | no | no |
| MidribMF | EXT | 0.05 | -0.25 | 0.37 | -0.14 | 0.25 | 0.20 | 0.02 | no | no |
| MidribMF | FFP | -0.06 | -0.41 | 0.30 | -0.28 | 0.16 | 0.20 | 0.03 | no | no |
| MidribMF | MAT | -0.04 | -0.37 | 0.32 | -0.26 | 0.18 | 0.20 | 0.03 | no | no |
| MidribMF | MCMT | 0.01 | -0.32 | 0.39 | -0.20 | 0.24 | 0.20 | 0.03 | no | no |
| MidribMF | MWMT | -0.07 | -0.38 | 0.24 | -0.27 | 0.13 | 0.20 | 0.03 | no | no |
| MidribMF | NFFD | -0.03 | -0.38 | 0.33 | -0.25 | 0.19 | 0.20 | 0.03 | no | no |
| MidribMF | SHM | 0.18 | -0.11 | 0.45 | -0.01 | 0.36 | 0.20 | 0.05 | no | no |
| MidribMF | TD | -0.07 | -0.40 | 0.25 | -0.28 | 0.14 | 0.20 | 0.03 | no | no |
| PL_Avg | AHM | 0.07 | -0.17 | 0.31 | -0.08 | 0.23 | 0.12 | 0.02 | no | no |
| PL_Avg | bFFP | -0.05 | -0.39 | 0.25 | -0.26 | 0.14 | 0.13 | 0.02 | no | no |
| PL_Avg | CMD | -0.10 | -0.35 | 0.15 | -0.26 | 0.07 | 0.13 | 0.02 | no | no |
| PL_Avg | CMI | 0.11 | -0.14 | 0.37 | -0.06 | 0.27 | 0.13 | 0.03 | no | no |
| PL_Avg | DD_0 | -0.08 | -0.40 | 0.20 | -0.27 | 0.10 | 0.13 | 0.02 | no | no |
| PL_Avg | DD_18 | -0.01 | -0.33 | 0.29 | -0.20 | 0.18 | 0.13 | 0.02 | no | no |
| PL_Avg | DD1040 | -0.03 | -0.31 | 0.29 | -0.21 | 0.17 | 0.13 | 0.02 | no | no |
| PL_Avg | DD18 | -0.03 | -0.31 | 0.28 | -0.22 | 0.16 | 0.12 | 0.02 | no | no |
| PL_Avg | DD5 | -0.02 | -0.31 | 0.30 | -0.21 | 0.18 | 0.13 | 0.02 | no | no |
| PL_Avg | eFFP | 0.05 | -0.25 | 0.40 | -0.14 | 0.26 | 0.13 | 0.02 | no | no |
| PL_Avg | Elevation | -0.04 | -0.39 | 0.26 | -0.25 | 0.15 | 0.13 | 0.02 | no | no |
| PL_Avg | EMT | 0.07 | -0.23 | 0.43 | -0.13 | 0.28 | 0.13 | 0.03 | no | no |
| PL_Avg | Eref | -0.11 | -0.38 | 0.15 | -0.28 | 0.05 | 0.13 | 0.03 | no | no |
| PL_Avg | EXT | -0.01 | -0.29 | 0.27 | -0.18 | 0.16 | 0.13 | 0.02 | no | no |
| PL_Avg | FFP | 0.06 | -0.25 | 0.42 | -0.14 | 0.27 | 0.13 | 0.03 | no | no |
| PL_Avg | MAP | 0.11 | -0.17 | 0.42 | -0.07 | 0.31 | 0.13 | 0.03 | no | no |
| PL_Avg | MAR | -0.02 | -0.29 | 0.24 | -0.19 | 0.15 | 0.13 | 0.02 | no | no |
| PL_Avg | MAT | -0.01 | -0.31 | 0.33 | -0.20 | 0.20 | 0.13 | 0.02 | no | no |
| PL_Avg | MCMT | 0.02 | -0.28 | 0.35 | -0.17 | 0.22 | 0.13 | 0.02 | no | no |
| PL_Avg | MSP | -0.07 | -0.37 | 0.29 | -0.27 | 0.13 | 0.13 | 0.03 | no | no |
| PL_Avg | MWMT | 0.01 | -0.26 | 0.30 | -0.17 | 0.19 | 0.13 | 0.02 | no | no |

| | | | | | | | | | | |
|---|---|---|---|---|---|---|---|---|---|---|
| PL_Avg | NFFD | 0.03 | -0.27 | 0.36 | -0.16 | 0.23 | 0.13 | 0.02 | no | no |
| PL_Avg | PAS | 0.13 | -0.15 | 0.42 | -0.05 | 0.31 | 0.13 | 0.03 | no | no |
| PL_Avg | RH | 0.13 | -0.16 | 0.46 | -0.06 | 0.33 | 0.14 | 0.03 | no | no |
| PL_Avg | SHM | 0.15 | -0.10 | 0.40 | -0.01 | 0.31 | 0.13 | 0.04 | no | no |
| PL_Avg | TD | -0.02 | -0.31 | 0.26 | -0.20 | 0.16 | 0.13 | 0.02 | no | no |
| RootBio | AHM | -0.12 | -0.43 | 0.19 | -0.32 | 0.08 | 0.39 | 0.03 | no | no |
| RootBio | bFFP | -0.18 | -0.54 | 0.29 | -0.42 | 0.09 | 0.39 | 0.07 | no | no |
| RootBio | CMD | 0.14 | -0.17 | 0.46 | -0.06 | 0.35 | 0.39 | 0.04 | no | no |
| RootBio | DD_0 | -0.20 | -0.55 | 0.20 | -0.43 | 0.04 | 0.39 | 0.07 | no | no |
| RootBio | DD1040 | 0.17 | -0.29 | 0.54 | -0.10 | 0.42 | 0.39 | 0.07 | no | no |
| RootBio | DD18 | 0.12 | -0.36 | 0.51 | -0.17 | 0.39 | 0.39 | 0.06 | no | no |
| RootBio | DD5 | 0.20 | -0.26 | 0.57 | -0.06 | 0.44 | 0.39 | 0.07 | no | no |
| RootBio | eFFP | 0.20 | -0.22 | 0.58 | -0.05 | 0.44 | 0.39 | 0.07 | no | no |
| RootBio | Elevation | -0.13 | -0.52 | 0.38 | -0.40 | 0.16 | 0.39 | 0.06 | no | no |
| RootBio | EMT | 0.17 | -0.28 | 0.55 | -0.10 | 0.42 | 0.39 | 0.06 | no | no |
| RootBio | EXT | 0.19 | -0.20 | 0.54 | -0.05 | 0.43 | 0.39 | 0.07 | no | no |
| RootBio | FFP | 0.19 | -0.27 | 0.55 | -0.07 | 0.43 | 0.38 | 0.07 | no | no |
| RootBio | MAP | 0.00 | -0.37 | 0.36 | -0.23 | 0.24 | 0.39 | 0.03 | no | no |
| RootBio | MAR | 0.09 | -0.25 | 0.43 | -0.12 | 0.31 | 0.39 | 0.03 | no | no |
| RootBio | MAT | 0.22 | -0.21 | 0.57 | -0.03 | 0.46 | 0.39 | 0.08 | no | no |
| RootBio | MCMT | 0.23 | -0.18 | 0.58 | -0.01 | 0.46 | 0.39 | 0.08 | no | no |
| RootBio | MSP | 0.09 | -0.39 | 0.51 | -0.20 | 0.36 | 0.39 | 0.05 | no | no |
| RootBio | MWMT | 0.11 | -0.34 | 0.49 | -0.17 | 0.37 | 0.39 | 0.05 | no | no |
| RootBio | NFFD | 0.22 | -0.19 | 0.58 | -0.02 | 0.45 | 0.38 | 0.08 | no | no |
| RootBio | RH | -0.15 | -0.54 | 0.24 | -0.40 | 0.11 | 0.39 | 0.05 | no | no |
| RootBio | SHM | -0.15 | -0.50 | 0.20 | -0.37 | 0.07 | 0.38 | 0.04 | no | no |
| RootBio | TD | -0.20 | -0.55 | 0.16 | -0.42 | 0.03 | 0.39 | 0.06 | no | no |
| RootMF | AHM | -0.04 | -0.30 | 0.24 | -0.21 | 0.13 | 0.30 | 0.02 | no | no |
| RootMF | bFFP | -0.20 | -0.52 | 0.17 | -0.41 | 0.01 | 0.30 | 0.07 | no | no |
| RootMF | CMD | 0.10 | -0.18 | 0.38 | -0.08 | 0.28 | 0.30 | 0.03 | no | no |
| RootMF | DD1040 | 0.21 | -0.15 | 0.52 | -0.01 | 0.41 | 0.30 | 0.07 | no | no |
| RootMF | DD18 | 0.18 | -0.19 | 0.50 | -0.04 | 0.39 | 0.30 | 0.06 | no | no |
| RootMF | EMT | 0.21 | -0.15 | 0.54 | -0.01 | 0.42 | 0.30 | 0.07 | no | no |
| RootMF | FFP | 0.21 | -0.16 | 0.54 | -0.01 | 0.42 | 0.30 | 0.07 | no | no |
| RootMF | MAP | 0.07 | -0.25 | 0.39 | -0.13 | 0.27 | 0.30 | 0.03 | no | no |
| RootMF | MAR | 0.01 | -0.28 | 0.32 | -0.17 | 0.20 | 0.30 | 0.02 | no | no |
| RootMF | MSP | 0.14 | -0.25 | 0.51 | -0.10 | 0.37 | 0.30 | 0.05 | no | no |
| RootMF | PAS | -0.21 | -0.51 | 0.13 | -0.41 | 0.00 | 0.30 | 0.06 | no | no |
| RootMF | RH | -0.04 | -0.37 | 0.29 | -0.25 | 0.17 | 0.30 | 0.02 | no | no |
| RootMF | SHM | -0.06 | -0.37 | 0.24 | -0.25 | 0.14 | 0.30 | 0.02 | no | no |

| | | | | | | | | | | |
|---|---|---|---|---|---|---|---|---|---|---|
| RootMF | TD | -0.14 | -0.46 | 0.18 | -0.34 | 0.06 | 0.30 | 0.04 | no | no |
| SD_Ratio | bFFP | 0.11 | -0.21 | 0.43 | -0.09 | 0.31 | 0.15 | 0.03 | no | no |
| SD_Ratio | CMD | 0.03 | -0.23 | 0.29 | -0.14 | 0.20 | 0.15 | 0.02 | no | no |
| SD_Ratio | CMI | -0.07 | -0.34 | 0.19 | -0.24 | 0.10 | 0.15 | 0.02 | no | no |
| SD_Ratio | DD_0 | -0.05 | -0.35 | 0.24 | -0.24 | 0.13 | 0.15 | 0.02 | no | no |
| SD_Ratio | DD_18 | 0.03 | -0.31 | 0.34 | -0.17 | 0.22 | 0.15 | 0.02 | no | no |
| SD_Ratio | DD1040 | 0.00 | -0.30 | 0.35 | -0.20 | 0.21 | 0.15 | 0.02 | no | no |
| SD_Ratio | DD18 | 0.03 | -0.26 | 0.38 | -0.16 | 0.23 | 0.15 | 0.02 | no | no |
| SD_Ratio | DD5 | -0.01 | -0.31 | 0.33 | -0.21 | 0.19 | 0.15 | 0.02 | no | no |
| SD_Ratio | eFFP | -0.14 | -0.46 | 0.18 | -0.33 | 0.06 | 0.15 | 0.04 | no | no |
| SD_Ratio | Elevation | -0.11 | -0.46 | 0.19 | -0.32 | 0.08 | 0.15 | 0.03 | no | no |
| SD_Ratio | EMT | -0.12 | -0.44 | 0.19 | -0.32 | 0.07 | 0.15 | 0.03 | no | no |
| SD_Ratio | Eref | 0.05 | -0.22 | 0.35 | -0.13 | 0.24 | 0.15 | 0.02 | no | no |
| SD_Ratio | FFP | -0.12 | -0.44 | 0.19 | -0.32 | 0.07 | 0.15 | 0.03 | no | no |
| SD_Ratio | MAP | -0.06 | -0.35 | 0.22 | -0.24 | 0.12 | 0.15 | 0.02 | no | no |
| SD_Ratio | MAR | -0.10 | -0.36 | 0.16 | -0.26 | 0.07 | 0.15 | 0.03 | no | no |
| SD_Ratio | MAT | -0.01 | -0.32 | 0.34 | -0.20 | 0.20 | 0.15 | 0.02 | no | no |
| SD_Ratio | MCMT | -0.08 | -0.38 | 0.24 | -0.27 | 0.11 | 0.15 | 0.03 | no | no |
| SD_Ratio | MSP | 0.01 | -0.33 | 0.36 | -0.19 | 0.22 | 0.15 | 0.02 | no | no |
| SD_Ratio | MWMT | 0.15 | -0.13 | 0.45 | -0.03 | 0.34 | 0.15 | 0.04 | no | no |
| SD_Ratio | NFFD | -0.13 | -0.46 | 0.17 | -0.33 | 0.06 | 0.15 | 0.04 | no | no |
| SD_Ratio | PAS | -0.13 | -0.43 | 0.16 | -0.31 | 0.06 | 0.15 | 0.03 | no | no |
| SD_Ratio | RH | -0.13 | -0.40 | 0.14 | -0.31 | 0.04 | 0.15 | 0.03 | no | no |
| SD_Sum | AHM | -0.12 | -0.38 | 0.13 | -0.29 | 0.04 | 0.22 | 0.03 | no | no |
| SD_Sum | bFFP | 0.05 | -0.30 | 0.47 | -0.18 | 0.30 | 0.22 | 0.03 | no | no |
| SD_Sum | CMD | 0.08 | -0.19 | 0.35 | -0.09 | 0.25 | 0.22 | 0.02 | no | no |
| SD_Sum | CMI | -0.14 | -0.42 | 0.13 | -0.31 | 0.03 | 0.22 | 0.03 | no | no |
| SD_Sum | DD_0 | 0.02 | -0.31 | 0.39 | -0.19 | 0.25 | 0.22 | 0.03 | no | no |
| SD_Sum | DD_18 | -0.03 | -0.37 | 0.36 | -0.25 | 0.20 | 0.22 | 0.03 | no | no |
| SD_Sum | DD1040 | 0.00 | -0.40 | 0.34 | -0.25 | 0.23 | 0.22 | 0.03 | no | no |
| SD_Sum | DD18 | -0.02 | -0.41 | 0.32 | -0.26 | 0.21 | 0.22 | 0.03 | no | no |
| SD_Sum | DD5 | 0.01 | -0.38 | 0.35 | -0.23 | 0.23 | 0.22 | 0.03 | no | no |
| SD_Sum | eFFP | -0.04 | -0.45 | 0.31 | -0.28 | 0.19 | 0.22 | 0.03 | no | no |
| SD_Sum | Elevation | 0.05 | -0.31 | 0.47 | -0.19 | 0.31 | 0.22 | 0.03 | no | no |
| SD_Sum | EMT | -0.07 | -0.47 | 0.27 | -0.32 | 0.16 | 0.22 | 0.03 | no | no |
| SD_Sum | Eref | 0.15 | -0.16 | 0.43 | -0.04 | 0.33 | 0.22 | 0.04 | no | no |
| SD_Sum | EXT | 0.06 | -0.25 | 0.37 | -0.13 | 0.26 | 0.22 | 0.02 | no | no |
| SD_Sum | FFP | -0.05 | -0.46 | 0.31 | -0.29 | 0.18 | 0.22 | 0.03 | no | no |
| SD_Sum | MAP | -0.08 | -0.41 | 0.24 | -0.29 | 0.13 | 0.22 | 0.03 | no | no |
| SD_Sum | MAR | 0.07 | -0.22 | 0.36 | -0.11 | 0.25 | 0.22 | 0.02 | no | no |

| | | | | | | | | | | |
|---|---|---|---|---|---|---|---|---|---|---|
| SD_Sum | MAT | 0.01 | -0.39 | 0.35 | -0.23 | 0.24 | 0.22 | 0.03 | no | no |
| SD_Sum | MCMT | -0.01 | -0.40 | 0.33 | -0.25 | 0.21 | 0.22 | 0.03 | no | no |
| SD_Sum | MSP | 0.12 | -0.30 | 0.46 | -0.13 | 0.35 | 0.21 | 0.05 | no | no |
| SD_Sum | MWMT | -0.01 | -0.37 | 0.32 | -0.24 | 0.21 | 0.22 | 0.03 | no | no |
| SD_Sum | NFFD | 0.00 | -0.39 | 0.34 | -0.24 | 0.22 | 0.22 | 0.03 | no | no |
| SD_Sum | RH | -0.18 | -0.51 | 0.14 | -0.38 | 0.03 | 0.23 | 0.05 | no | no |
| SD_Sum | TD | -0.01 | -0.31 | 0.31 | -0.20 | 0.19 | 0.22 | 0.02 | no | no |
| SL_Avg | AHM | 0.04 | -0.20 | 0.29 | -0.12 | 0.20 | 0.13 | 0.02 | no | no |
| SL_Avg | bFFP | 0.00 | -0.33 | 0.29 | -0.20 | 0.19 | 0.13 | 0.02 | no | no |
| SL_Avg | CMD | -0.12 | -0.38 | 0.13 | -0.28 | 0.04 | 0.14 | 0.03 | no | no |
| SL_Avg | CMI | 0.15 | -0.10 | 0.41 | -0.01 | 0.31 | 0.14 | 0.03 | no | no |
| SL_Avg | DD_0 | 0.00 | -0.30 | 0.28 | -0.19 | 0.18 | 0.13 | 0.02 | no | no |
| SL_Avg | DD_18 | 0.07 | -0.24 | 0.36 | -0.12 | 0.25 | 0.13 | 0.02 | no | no |
| SL_Avg | DD1040 | -0.09 | -0.36 | 0.22 | -0.26 | 0.10 | 0.13 | 0.03 | no | no |
| SL_Avg | DD18 | -0.09 | -0.36 | 0.21 | -0.27 | 0.09 | 0.13 | 0.03 | no | no |
| SL_Avg | DD5 | -0.08 | -0.36 | 0.23 | -0.26 | 0.10 | 0.13 | 0.03 | no | no |
| SL_Avg | eFFP | -0.01 | -0.30 | 0.33 | -0.20 | 0.19 | 0.13 | 0.02 | no | no |
| SL_Avg | Elevation | 0.02 | -0.32 | 0.32 | -0.18 | 0.21 | 0.13 | 0.02 | no | no |
| SL_Avg | EMT | 0.01 | -0.28 | 0.35 | -0.18 | 0.22 | 0.13 | 0.02 | no | no |
| SL_Avg | EXT | -0.08 | -0.35 | 0.19 | -0.25 | 0.09 | 0.13 | 0.02 | no | no |
| SL_Avg | FFP | -0.01 | -0.30 | 0.33 | -0.19 | 0.19 | 0.13 | 0.02 | no | no |
| SL_Avg | MAP | 0.10 | -0.18 | 0.42 | -0.09 | 0.30 | 0.14 | 0.03 | no | no |
| SL_Avg | MAR | -0.05 | -0.32 | 0.20 | -0.22 | 0.12 | 0.14 | 0.02 | no | no |
| SL_Avg | MAT | -0.08 | -0.36 | 0.24 | -0.26 | 0.12 | 0.13 | 0.03 | no | no |
| SL_Avg | MCMT | -0.04 | -0.33 | 0.27 | -0.23 | 0.15 | 0.13 | 0.02 | no | no |
| SL_Avg | MSP | -0.10 | -0.39 | 0.25 | -0.29 | 0.10 | 0.13 | 0.03 | no | no |
| SL_Avg | MWMT | -0.07 | -0.34 | 0.22 | -0.25 | 0.10 | 0.13 | 0.02 | no | no |
| SL_Avg | NFFD | -0.03 | -0.31 | 0.31 | -0.21 | 0.17 | 0.13 | 0.02 | no | no |
| SL_Avg | RH | 0.12 | -0.16 | 0.44 | -0.07 | 0.32 | 0.14 | 0.03 | no | no |
| SL_Avg | SHM | 0.12 | -0.15 | 0.38 | -0.05 | 0.29 | 0.13 | 0.03 | no | no |
| SL_Avg | TD | 0.00 | -0.28 | 0.28 | -0.18 | 0.18 | 0.13 | 0.02 | no | no |
| StemBio | AHM | -0.09 | -0.41 | 0.22 | -0.29 | 0.11 | 0.41 | 0.03 | no | no |
| StemBio | bFFP | -0.10 | -0.52 | 0.43 | -0.38 | 0.21 | 0.41 | 0.05 | no | no |
| StemBio | CMD | 0.15 | -0.18 | 0.47 | -0.06 | 0.36 | 0.41 | 0.04 | no | no |
| StemBio | CMI | -0.19 | -0.52 | 0.14 | -0.40 | 0.02 | 0.41 | 0.05 | no | no |
| StemBio | DD_0 | -0.04 | -0.43 | 0.41 | -0.30 | 0.24 | 0.41 | 0.04 | no | no |
| StemBio | DD_18 | -0.19 | -0.58 | 0.27 | -0.44 | 0.08 | 0.41 | 0.07 | no | no |
| StemBio | DD1040 | 0.19 | -0.29 | 0.57 | -0.08 | 0.44 | 0.41 | 0.07 | no | no |
| StemBio | DD18 | 0.16 | -0.32 | 0.55 | -0.13 | 0.42 | 0.41 | 0.06 | no | no |
| StemBio | DD5 | 0.19 | -0.28 | 0.58 | -0.09 | 0.44 | 0.41 | 0.07 | no | no |

| | | | | | | | | | | |
|---|---|---|---|---|---|---|---|---|---|---|
| StemBio | eFFP | 0.14 | -0.34 | 0.55 | -0.14 | 0.41 | 0.41 | 0.06 | no | no |
| StemBio | Elevation | 0.03 | -0.44 | 0.59 | -0.29 | 0.38 | 0.41 | 0.05 | no | no |
| StemBio | EMT | 0.11 | -0.39 | 0.52 | -0.18 | 0.38 | 0.41 | 0.05 | no | no |
| StemBio | EXT | 0.00 | -0.41 | 0.38 | -0.25 | 0.25 | 0.41 | 0.03 | no | no |
| StemBio | FFP | 0.12 | -0.40 | 0.53 | -0.18 | 0.39 | 0.41 | 0.06 | no | no |
| StemBio | MAP | -0.08 | -0.47 | 0.31 | -0.33 | 0.17 | 0.41 | 0.04 | no | no |
| StemBio | MAR | 0.14 | -0.21 | 0.50 | -0.09 | 0.37 | 0.41 | 0.04 | no | no |
| StemBio | MAT | 0.18 | -0.30 | 0.58 | -0.09 | 0.44 | 0.41 | 0.07 | no | no |
| StemBio | MCMT | 0.19 | -0.24 | 0.57 | -0.06 | 0.44 | 0.41 | 0.07 | no | no |
| StemBio | MSP | 0.12 | -0.38 | 0.54 | -0.19 | 0.40 | 0.41 | 0.06 | no | no |
| StemBio | MWMT | -0.02 | -0.48 | 0.40 | -0.31 | 0.26 | 0.41 | 0.04 | no | no |
| StemBio | NFFD | 0.16 | -0.32 | 0.55 | -0.11 | 0.42 | 0.41 | 0.06 | no | no |
| StemBio | RH | -0.17 | -0.61 | 0.25 | -0.45 | 0.11 | 0.41 | 0.06 | no | no |
| StemBio | SHM | -0.13 | -0.49 | 0.23 | -0.36 | 0.09 | 0.41 | 0.04 | no | no |
| StemMF | AHM | 0.01 | -0.32 | 0.32 | -0.20 | 0.21 | 0.42 | 0.02 | no | no |
| StemMF | bFFP | 0.03 | -0.39 | 0.51 | -0.25 | 0.32 | 0.42 | 0.04 | no | no |
| StemMF | CMD | 0.05 | -0.28 | 0.38 | -0.16 | 0.26 | 0.42 | 0.03 | no | no |
| StemMF | CMI | -0.04 | -0.39 | 0.30 | -0.25 | 0.18 | 0.42 | 0.03 | no | no |
| StemMF | DD_0 | 0.08 | -0.30 | 0.47 | -0.16 | 0.33 | 0.42 | 0.04 | no | no |
| StemMF | DD_18 | -0.03 | -0.44 | 0.40 | -0.29 | 0.24 | 0.42 | 0.04 | no | no |
| StemMF | DD1040 | 0.12 | -0.29 | 0.52 | -0.13 | 0.37 | 0.42 | 0.05 | no | no |
| StemMF | DD18 | 0.12 | -0.28 | 0.50 | -0.13 | 0.37 | 0.42 | 0.05 | no | no |
| StemMF | DD5 | 0.10 | -0.33 | 0.50 | -0.16 | 0.35 | 0.42 | 0.04 | no | no |
| StemMF | eFFP | 0.03 | -0.44 | 0.46 | -0.25 | 0.30 | 0.42 | 0.04 | no | no |
| StemMF | Elevation | 0.10 | -0.33 | 0.59 | -0.18 | 0.40 | 0.42 | 0.05 | no | no |
| StemMF | EMT | 0.03 | -0.42 | 0.45 | -0.25 | 0.30 | 0.42 | 0.04 | no | no |
| StemMF | Eref | 0.06 | -0.31 | 0.42 | -0.17 | 0.28 | 0.42 | 0.03 | no | no |
| StemMF | EXT | -0.20 | -0.57 | 0.16 | -0.43 | 0.03 | 0.42 | 0.06 | no | no |
| StemMF | FFP | 0.00 | -0.48 | 0.43 | -0.29 | 0.27 | 0.42 | 0.04 | no | no |
| StemMF | MAP | -0.09 | -0.46 | 0.27 | -0.33 | 0.14 | 0.42 | 0.03 | no | no |
| StemMF | MAR | 0.10 | -0.27 | 0.47 | -0.13 | 0.34 | 0.42 | 0.04 | no | no |
| StemMF | MAT | 0.07 | -0.37 | 0.49 | -0.19 | 0.33 | 0.42 | 0.04 | no | no |
| StemMF | MCMT | 0.09 | -0.32 | 0.51 | -0.16 | 0.36 | 0.42 | 0.04 | no | no |
| StemMF | MSP | 0.12 | -0.37 | 0.55 | -0.16 | 0.39 | 0.42 | 0.05 | no | no |
| StemMF | MWMT | -0.09 | -0.47 | 0.29 | -0.33 | 0.15 | 0.42 | 0.04 | no | no |
| StemMF | NFFD | 0.00 | -0.48 | 0.42 | -0.29 | 0.27 | 0.42 | 0.04 | no | no |
| StemMF | PAS | -0.13 | -0.53 | 0.25 | -0.38 | 0.11 | 0.42 | 0.04 | no | no |
| StemMF | RH | -0.02 | -0.43 | 0.35 | -0.28 | 0.22 | 0.42 | 0.03 | no | no |
| StemMF | SHM | -0.01 | -0.38 | 0.36 | -0.24 | 0.23 | 0.42 | 0.03 | no | no |
| StemMF | TD | -0.18 | -0.56 | 0.19 | -0.42 | 0.05 | 0.42 | 0.06 | no | no |

| | | | | | | | | | | |
|---|---|---|---|---|---|---|---|---|---|---|
| Succulence | bFFP | -0.05 | -0.45 | 0.32 | -0.30 | 0.18 | 0.21 | 0.03 | no | no |
| Succulence | CMI | 0.16 | -0.11 | 0.44 | -0.01 | 0.34 | 0.21 | 0.04 | no | no |
| Succulence | DD_0 | 0.11 | -0.23 | 0.43 | -0.10 | 0.31 | 0.21 | 0.03 | no | no |
| Succulence | DD_18 | 0.06 | -0.31 | 0.42 | -0.17 | 0.29 | 0.20 | 0.03 | no | no |
| Succulence | DD1040 | -0.09 | -0.45 | 0.27 | -0.31 | 0.13 | 0.21 | 0.03 | no | no |
| Succulence | DD18 | -0.11 | -0.46 | 0.23 | -0.33 | 0.11 | 0.21 | 0.03 | no | no |
| Succulence | DD5 | -0.07 | -0.44 | 0.29 | -0.30 | 0.15 | 0.21 | 0.03 | no | no |
| Succulence | eFFP | 0.01 | -0.37 | 0.42 | -0.23 | 0.26 | 0.21 | 0.03 | no | no |
| Succulence | Elevation | -0.07 | -0.43 | 0.29 | -0.30 | 0.16 | 0.21 | 0.03 | no | no |
| Succulence | EMT | -0.07 | -0.43 | 0.31 | -0.30 | 0.16 | 0.21 | 0.03 | no | no |
| Succulence | Eref | -0.13 | -0.44 | 0.18 | -0.33 | 0.06 | 0.21 | 0.04 | no | no |
| Succulence | EXT | 0.06 | -0.26 | 0.37 | -0.14 | 0.25 | 0.21 | 0.02 | no | no |
| Succulence | FFP | 0.04 | -0.34 | 0.43 | -0.20 | 0.28 | 0.21 | 0.03 | no | no |
| Succulence | MAT | -0.09 | -0.45 | 0.28 | -0.32 | 0.14 | 0.21 | 0.03 | no | no |
| Succulence | MCMT | -0.16 | -0.52 | 0.20 | -0.38 | 0.06 | 0.21 | 0.05 | no | no |
| Succulence | MSP | 0.24 | -0.14 | 0.66 | -0.01 | 0.50 | 0.21 | 0.07 | no | no |
| Succulence | MWMT | 0.02 | -0.30 | 0.33 | -0.18 | 0.23 | 0.21 | 0.02 | no | no |
| Succulence | NFFD | 0.00 | -0.36 | 0.39 | -0.23 | 0.24 | 0.21 | 0.03 | no | no |
| Succulence | PAS | 0.07 | -0.25 | 0.41 | -0.13 | 0.28 | 0.21 | 0.03 | no | no |
| Succulence | RH | 0.12 | -0.19 | 0.43 | -0.08 | 0.32 | 0.21 | 0.03 | no | no |
| SV | AHM | -0.08 | -0.35 | 0.20 | -0.25 | 0.10 | 0.30 | 0.02 | no | no |
| SV | bFFP | 0.00 | -0.36 | 0.44 | -0.24 | 0.26 | 0.30 | 0.03 | no | no |
| SV | CMD | 0.06 | -0.23 | 0.34 | -0.12 | 0.24 | 0.30 | 0.02 | no | no |
| SV | CMI | -0.14 | -0.43 | 0.14 | -0.32 | 0.04 | 0.30 | 0.04 | no | no |
| SV | DD_0 | -0.07 | -0.40 | 0.30 | -0.29 | 0.16 | 0.30 | 0.03 | no | no |
| SV | DD_18 | -0.10 | -0.45 | 0.30 | -0.33 | 0.15 | 0.30 | 0.04 | no | no |
| SV | DD1040 | 0.06 | -0.36 | 0.40 | -0.19 | 0.29 | 0.30 | 0.03 | no | no |
| SV | DD18 | 0.04 | -0.36 | 0.39 | -0.21 | 0.27 | 0.30 | 0.03 | no | no |
| SV | DD5 | 0.07 | -0.35 | 0.42 | -0.18 | 0.30 | 0.30 | 0.04 | no | no |
| SV | eFFP | 0.05 | -0.37 | 0.40 | -0.20 | 0.28 | 0.30 | 0.03 | no | no |
| SV | Elevation | 0.00 | -0.38 | 0.44 | -0.25 | 0.27 | 0.30 | 0.03 | no | no |
| SV | EMT | 0.01 | -0.40 | 0.37 | -0.23 | 0.25 | 0.30 | 0.03 | no | no |
| SV | Eref | 0.15 | -0.17 | 0.45 | -0.04 | 0.35 | 0.30 | 0.04 | no | no |
| SV | EXT | 0.07 | -0.27 | 0.39 | -0.14 | 0.27 | 0.30 | 0.03 | no | no |
| SV | FFP | 0.02 | -0.40 | 0.39 | -0.23 | 0.27 | 0.30 | 0.03 | no | no |
| SV | MAP | -0.07 | -0.41 | 0.26 | -0.28 | 0.14 | 0.30 | 0.03 | no | no |
| SV | MAR | 0.09 | -0.22 | 0.39 | -0.11 | 0.28 | 0.31 | 0.03 | no | no |
| SV | MAT | 0.08 | -0.33 | 0.42 | -0.17 | 0.31 | 0.30 | 0.04 | no | no |
| SV | MCMT | 0.07 | -0.32 | 0.40 | -0.16 | 0.29 | 0.30 | 0.03 | no | no |
| SV | MSP | 0.15 | -0.26 | 0.50 | -0.09 | 0.38 | 0.30 | 0.05 | no | no |

| | | | | | | | | | | |
|---|---|---|---|---|---|---|---|---|---|---|
| SV | MWMT | 0.04 | -0.34 | 0.38 | -0.20 | 0.27 | 0.30 | 0.03 | no | no |
| SV | NFFD | 0.05 | -0.36 | 0.41 | -0.20 | 0.28 | 0.30 | 0.03 | no | no |
| SV | RH | -0.11 | -0.46 | 0.23 | -0.33 | 0.11 | 0.30 | 0.03 | no | no |
| SV | SHM | -0.10 | -0.41 | 0.21 | -0.30 | 0.10 | 0.30 | 0.03 | no | no |
| SV | TD | -0.07 | -0.39 | 0.26 | -0.27 | 0.14 | 0.30 | 0.03 | no | no |
| TotalBio | AHM | -0.12 | -0.44 | 0.21 | -0.32 | 0.09 | 0.41 | 0.04 | no | no |
| TotalBio | bFFP | -0.14 | -0.54 | 0.37 | -0.40 | 0.16 | 0.42 | 0.06 | no | no |
| TotalBio | CMD | 0.15 | -0.18 | 0.48 | -0.06 | 0.36 | 0.41 | 0.04 | no | no |
| TotalBio | CMI | -0.21 | -0.53 | 0.12 | -0.41 | 0.00 | 0.41 | 0.06 | no | no |
| TotalBio | DD_0 | -0.10 | -0.50 | 0.36 | -0.36 | 0.18 | 0.42 | 0.05 | no | no |
| TotalBio | DD_18 | -0.22 | -0.58 | 0.23 | -0.46 | 0.04 | 0.42 | 0.08 | no | no |
| TotalBio | DD1040 | 0.17 | -0.30 | 0.56 | -0.11 | 0.42 | 0.42 | 0.07 | no | no |
| TotalBio | DD18 | 0.15 | -0.34 | 0.54 | -0.14 | 0.40 | 0.42 | 0.06 | no | no |
| TotalBio | DD5 | 0.20 | -0.28 | 0.58 | -0.08 | 0.45 | 0.41 | 0.07 | no | no |
| TotalBio | eFFP | 0.16 | -0.30 | 0.55 | -0.11 | 0.42 | 0.41 | 0.06 | no | no |
| TotalBio | Elevation | -0.07 | -0.49 | 0.48 | -0.35 | 0.25 | 0.41 | 0.05 | no | no |
| TotalBio | EMT | 0.11 | -0.40 | 0.52 | -0.18 | 0.38 | 0.41 | 0.05 | no | no |
| TotalBio | EXT | 0.13 | -0.28 | 0.50 | -0.12 | 0.37 | 0.42 | 0.05 | no | no |
| TotalBio | FFP | 0.15 | -0.35 | 0.55 | -0.13 | 0.42 | 0.42 | 0.06 | no | no |
| TotalBio | MAP | -0.04 | -0.43 | 0.34 | -0.28 | 0.20 | 0.41 | 0.03 | no | no |
| TotalBio | MAR | 0.11 | -0.24 | 0.47 | -0.11 | 0.34 | 0.42 | 0.04 | no | no |
| TotalBio | MAT | 0.20 | -0.28 | 0.57 | -0.07 | 0.45 | 0.41 | 0.07 | no | no |
| TotalBio | MCMT | 0.19 | -0.25 | 0.57 | -0.07 | 0.44 | 0.41 | 0.07 | no | no |
| TotalBio | MSP | 0.10 | -0.41 | 0.51 | -0.20 | 0.38 | 0.41 | 0.05 | no | no |
| TotalBio | MWMT | 0.06 | -0.41 | 0.48 | -0.23 | 0.34 | 0.41 | 0.05 | no | no |
| TotalBio | NFFD | 0.19 | -0.27 | 0.57 | -0.08 | 0.44 | 0.42 | 0.07 | no | no |
| TotalBio | RH | -0.19 | -0.60 | 0.22 | -0.46 | 0.08 | 0.41 | 0.06 | no | no |
| TotalBio | SHM | -0.16 | -0.51 | 0.19 | -0.38 | 0.07 | 0.41 | 0.05 | no | no |
| TotalBio | TD | -0.18 | -0.54 | 0.19 | -0.41 | 0.05 | 0.41 | 0.06 | no | no |
| VLA | bFFP | 0.10 | -0.18 | 0.41 | -0.08 | 0.29 | 0.12 | 0.03 | no | no |
| VLA | CMD | -0.01 | -0.24 | 0.24 | -0.16 | 0.15 | 0.12 | 0.01 | no | no |
| VLA | CMI | 0.01 | -0.24 | 0.25 | -0.15 | 0.17 | 0.12 | 0.01 | no | no |
| VLA | DD_0 | 0.10 | -0.17 | 0.39 | -0.07 | 0.29 | 0.13 | 0.03 | no | no |
| VLA | DD_18 | 0.08 | -0.20 | 0.38 | -0.10 | 0.26 | 0.12 | 0.02 | no | no |
| VLA | DD1040 | -0.06 | -0.38 | 0.21 | -0.25 | 0.12 | 0.12 | 0.02 | no | no |
| VLA | DD18 | -0.05 | -0.36 | 0.22 | -0.24 | 0.13 | 0.12 | 0.02 | no | no |
| VLA | DD5 | -0.06 | -0.36 | 0.22 | -0.25 | 0.12 | 0.12 | 0.02 | no | no |
| VLA | eFFP | -0.11 | -0.43 | 0.18 | -0.30 | 0.07 | 0.13 | 0.03 | no | no |
| VLA | Elevation | 0.08 | -0.20 | 0.39 | -0.10 | 0.27 | 0.12 | 0.02 | no | no |

| | | | | | | | | | | |
|---|---|---|---|---|---|---|---|---|---|---|
| VLA | EMT | -0.12 | -0.44 | 0.16 | -0.31 | 0.06 | 0.13 | 0.03 | no | no |
| VLA | Eref | 0.02 | -0.24 | 0.28 | -0.14 | 0.18 | 0.12 | 0.02 | no | no |
| VLA | EXT | -0.03 | -0.28 | 0.23 | -0.19 | 0.14 | 0.12 | 0.02 | no | no |
| VLA | FFP | -0.11 | -0.42 | 0.18 | -0.29 | 0.08 | 0.13 | 0.03 | no | no |
| VLA | MAP | 0.00 | -0.27 | 0.25 | -0.17 | 0.17 | 0.12 | 0.02 | no | no |
| VLA | MAR | -0.01 | -0.26 | 0.24 | -0.17 | 0.15 | 0.12 | 0.01 | no | no |
| VLA | MAT | -0.07 | -0.38 | 0.20 | -0.26 | 0.11 | 0.12 | 0.02 | no | no |
| VLA | MCMT | -0.10 | -0.41 | 0.18 | -0.29 | 0.08 | 0.12 | 0.03 | no | no |
| VLA | MSP | 0.07 | -0.28 | 0.34 | -0.13 | 0.25 | 0.12 | 0.03 | no | no |
| VLA | MWMT | -0.06 | -0.34 | 0.20 | -0.24 | 0.11 | 0.12 | 0.02 | no | no |
| VLA | NFFD | -0.08 | -0.38 | 0.20 | -0.26 | 0.10 | 0.12 | 0.02 | no | no |
| VLA | PAS | 0.01 | -0.25 | 0.27 | -0.16 | 0.18 | 0.12 | 0.02 | no | no |
| VLA | RH | -0.09 | -0.37 | 0.17 | -0.26 | 0.08 | 0.13 | 0.02 | no | no |
| VLA | TD | 0.07 | -0.19 | 0.34 | -0.09 | 0.24 | 0.12 | 0.02 | no | no |

**Table S4.5**: Mean coefficients and credible intervals for biomass model shown in Figure 4.6A-B. Trait abbreviations follow Table 4.2.

| Probs | SD_Sum_summary | SL_Avg_summary | LMA_summary |
|---|---|---|---|
| 95_low | 0.14 | -0.03 | 0.54 |
| 80_low | 0.21 | 0.03 | 0.59 |
| Mean | 0.33 | 0.12 | 0.68 |
| 80_high | 0.44 | 0.22 | 0.78 |
| 95_high | 0.51 | 0.27 | 0.83 |

**Table S4.6**: Mean coefficients and credible intervals for biomass model shown in Figure 6C-D Trait abbreviations follow Table 2.2.

| Probs | PC1_summary | PC2_summary |
|---|---|---|
| 95_low | 0.26 | -0.43 |
| 80_low | 0.28 | -0.40 |
| Mean | 0.31 | -0.36 |
| 80_high | 0.35 | -0.31 |
| 95_high | 0.36 | -0.28 |